REPORT DOCUMENTATION PAGE

Form Approved
OMB NO. 0704-0188

1. AGENCY USE ONLY (Leave Blank)	2. REPORT DATE 9/29/03	3. REPORT TYPE AND DATES COVERED Final Report 10/1/00 to 6/30/03

4. TITLE AND SUBTITLE
Optimal Subband Coding of Cyclostationary Signals

5. FUNDING NUMBERS
DAAD19-00-1-0534

6. AUTHOR(S)
Soura Dasgupta

7. PERFORMING ORGANIZATION NAME(S) AND ADDRESS(ES)
University of Iowa, Iowa City, IA52242

8. PERFORMING ORGANIZATION REPORT NUMBER

9. SPONSORING / MONITORING AGENCY NAME(S) AND ADDRESS(ES)
U. S. Army Research Office
P.O. Box 12211
Research Triangle Park, NC 27709-2211

10. SPONSORING / MONITORING AGENCY REPORT NUMBER
39188-CI

11. SUPPLEMENTARY NOTES
The views, opinions and/or findings contained in this report are those of the author(s) and should not be construed as an official Department of the Army position, policy or decision, unless so designated by other documentation.

12 a. DISTRIBUTION / AVAILABILITY STATEMENT
Approved for public release; except for paper on bitloading as we are planning to file a patent application

12 b. DISTRIBUTION CODE

13. ABSTRACT (Maximum 200 words)

The purpose of the award was to study the subband coding of cyclostationary signals. We have completely solved the problem of subband coding with uniform filter banks. We have also shown that our approach applies also to optimization of Discrete Multitone Transmission Systems. In the coming year we shall address the issue of nonuniform filter banks.

14. SUBJECT TERMS
Subband Coding. Majorization. OFDM

15. NUMBER OF PAGES
156

16. PRICE CODE

17. SECURITY CLASSIFICATION OR REPORT	18. SECURITY CLASSIFICATION ON THIS PAGE	19. SECURITY CLASSIFICATION OF ABSTRACT	20. LIMITATION OF ABSTRACT
UNCLASSIFIED	UNCLASSIFIED	UNCLASSIFIED	UL

NSN 7540-01-280-5500

Standard Form 298 (Rev.2-89)
Prescribed by ANSI Std. 239-18
298-102

Report on US ARMY AWARD DAAD19-00-1-0534
Optimal Subband Coders for Cyclostationary Signals
PI: Soura Dasgupta
University of Iowa

The purpose of the award was to study the subband coding of cyclostationary signals. Accomplishement to date are listed below.

- We had proposed to study subband coding of cyclostationary signals with uniform filter banks, under two bit rate constraints. (i) When the bit allocation among the subband signals is static, and (ii) when the bit allocation is periodic but the bit budget across the subband signals is constant at each instant of time. Problem (i) was solved before the award was received. We have solved (ii). In addition we have also proposed a third criteria in which the bit budget is defined as a fixed *average* over a period of the signal cycle. We show that though the optimizing filter bank is the same for all three, and have characterized this filter bank, the new criteria leads to a higher coding gain.

  Figure 1 shows the coding gains under the last two schemes, for an input with 2-periodic statistics. The crosses are the second scheme and the circles the third. Observe that the last scheme leads to *higher coding gains times better*.

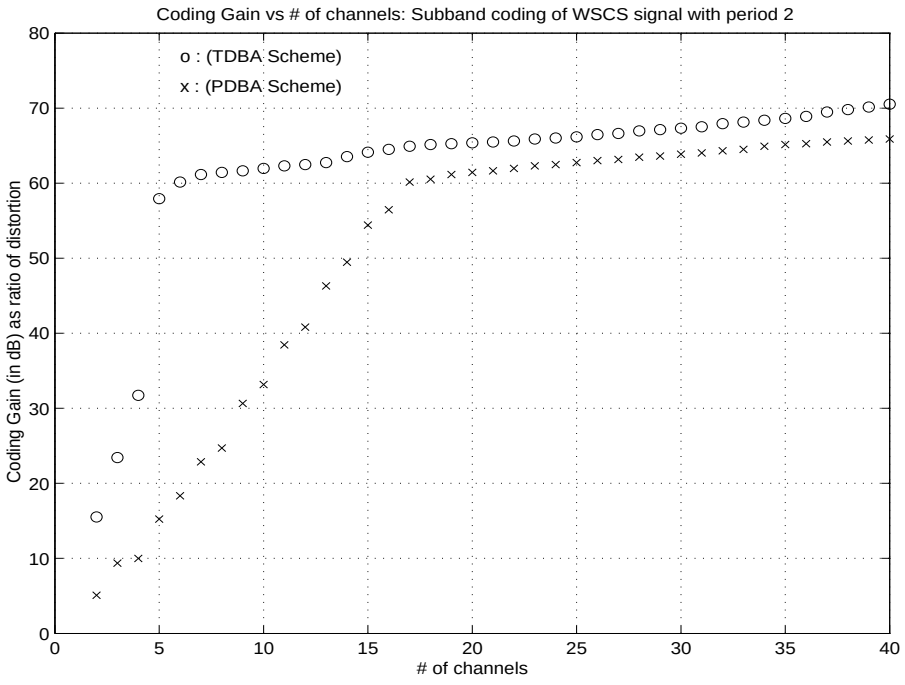

Figure 1: Coding gain plots.

- Realization of these optimizing filter banks requires the notion of compaction filters in the case of stationary signals. We have introduced the concept of energy compaction for cyclostationary signals as well. We have also generalized the notion of M-band filters to cyclostationary case. We have studied the theory and design of cyclostationary energy compaction filters and showed how they relate to the optmizing filter banks.

- We had proposed to study the use of nonuniform filter banks for subband coding for both the stationary and cyclostationary signals. *En route* to such a study, we have showed that every biorthogonal dyadic filter bank has a tree structured decomposition. This permits the optimization of such filter banks to be conducted in a tree structured framework, making the underlying task much simpler.

- A common occurrence of cyclostationarity is in Orthogonal Frequency Division Multiplexed (OFDM) communications. We have shown that certain channel resource allocation problems for OFDM systems are dual problems of subband coding. We have solved the optimum resource allocation problem for OFDM in the multiuser environment. Specifically, we have considered in turn a variety of settings culminating in one in which each user is assigned different number of subchannels and different bit rates and is required to achieve differing symbol error rates and supports potentially different modulation schemes. Our goal is to select the input and output block transforms, the linear redundancy removal scheme at the receiver, the number of bits/symbol assigned to each subchannel, and the subchannel assignment to each user, in order to achieve the QoS specifications under a zero ISI condition with minimum transmitted power. We assume knowledge of the equalized channel and the second-order statistics of the noise at the receiver input.

  (A) The optimum input/output block transforms are orthonormal.

  (B) The selection of the optimum input/output transforms and redundancy removal schemes depends only on the channel/interference conditions, and does not depend on such service requirements as the required bit rates and symbol error rates. Thus there is a conceptual separation between the selection of these variables, and the remaining tasks of bit loading and subchannel selection. In practical terms this considerably simplifies the optimzation problem.

  Figure 2 compares the transmitting power of the DFT based DMT under no optimum bit allocation and optimum bit allocation with an optimum unitary transceiver. We assume the equalized-channel to be $C(z) = 1 + 0.5z^{-1}$, and a noise source $v(n)$ whose power spectral density is shown in fig. 1. We assume the DMT system supports two user services. Both services employ QAM modulation schemes, and the target rates for the two users are 600 Kbps and 1 Mbps respectively. The (i, j) on the x-axis of the plot indicates that user 1 and 2 were respectively allocated i, j number of channels.

The plot shows that there is a 10 dB saving in transmit power with our design over the DFT based DMT under optimum bit allocation, and a 14 dB improvement over the conventional DMT with no optimum bit allocation.

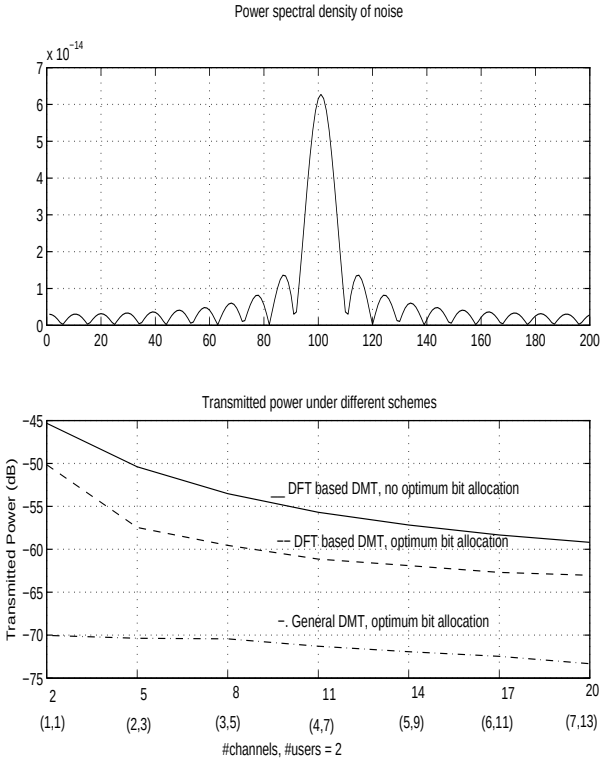

Figure 2: Comparison of transmit power levels.

- For optimum coding over transmission channels it is imoportant that the transmitter be aware of the channel it transmits over. While in recent years many algorithms have been proposed that assume such channel knowledge at the transmitter, no method for making exists for making the transmitter channel aware. We have proposed a new feedback scheme that permits the transmitter to directly estimate the channel.

- In both subband coding and DMT bit loading is an important problem. Specifically, for an N-subchannel system in these problems reduce to general problem:

$$\mathrm{M}inimize P(b_1, .., b_N) = \sum_{k=1}^{N} \phi_k(b_k) \tag{1}$$

subject to

$$Constraint : \sum_{k=1}^{N} b_k = B, b_k \in \{0, 1, ...B\}, \tag{2}$$

where ϕ_k is a convex function nonnegative integers b_k, and B is a positive integer. In subband coding

$$\phi_k(b_k) = \alpha_k 2^{-2b_k} \tag{3}$$

where α_k is determined by the signal variance in the k-th subchannel, and $P(b_1, .., b_N)$ is the average distortion variance. In multicarrier systems

$$\phi_k(b_k) = \alpha_k 2^{b_k} \tag{4}$$

where α_k reflect target symbol error rates (SER), and channel and interference conditions experienced in the the k-th subchannel, and $P(b_1, .., b_N)$ is the total transmitted power. Higher values of α_k reflects more adverse subchannel conditions and/or lower target SER; b_k is the the number of bits assigned to each symbol in the cognizant subchannel.

The complexity of most existing algorithms for such *discrete bit loading* grows with B. We have formulated a new bit loading scheme whose complexity is independent of B and yet like existing schemes depends as $O(N \log N)$ in the number of subchannels.

A comparison of the performance of the algorithms of [2] and [1] and the proposed algorithm with respect to the number of computations required is shown in the figures 3 and 4, for the cases where $N = 32$ and $N = 64$, respectively. In implementing [1], which is a suboptimal algorithm, the maximum number of bits, B^* that any channel can be assigned is kept at B.

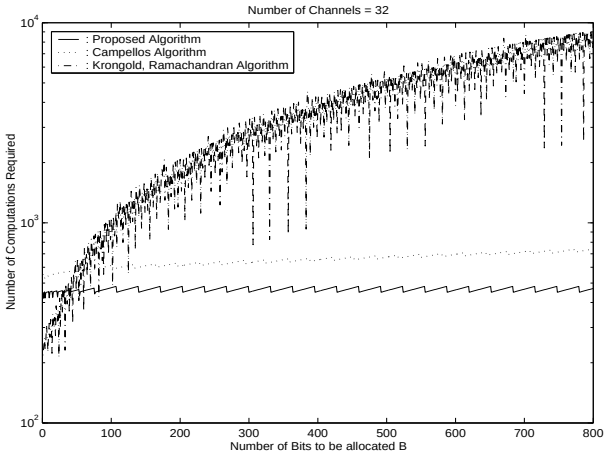

Figure 3: Runtime comparisions of the three algorithms for N=32

Number of computations needed for each algorithm to converge to the optimal solution was calculated by assuming that addition, subtraction, div, mod, multiplication or division of two numbers would need one computation as would the logical comparisons between two decimal numbers. The results show that the algorithm described

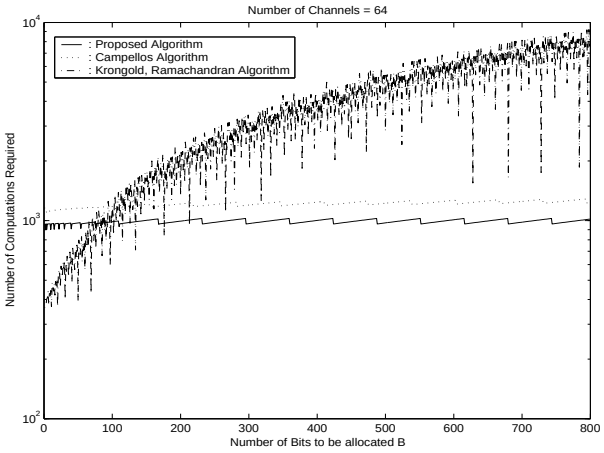

Figure 4: Runtime comparisions of the three algorithms for N=64

in [1] is linear with respect to B while the algorithm in [2] needs large number of computations to converge as B grows. The number of computations needed for the proposed algorithm is independent of the change in B the minor variations whose source is discussed in the paper referenced below. The improvement in performance is very significant if B is large when compared to N.

Collaboration with DOD Labs: We are currently part of a team that is initiating collaboration with TACOM on research on digital humans. Many of the resource allocation ideas implicit in this work are crucial to that project.

Below we list publications acknowledging this award.

List of Publications

1. A. Pandharipande and S. Dasgupta, "Subband Coding of Cyclostationary Signals", *IEEE Transactions on Circuits and Systems I, IEEE Transactions on Circuits and Systems -I*, pp 1884-1887, December 2002.

2. A. Pandharipande, S. Dasgupta and D. Kula, "Filter Banks for Optimum Subband Coding of Cyclostationary Signals with Dynamic Bit Allocation", in *Proceedings of ASILOMAR*, November 2001.

3. A. Pandharipande and S. Dasgupta, "Optimal transceivers in DMT based multiuser communications", in *Proceedings of ICASSP*, 2001.

4. A. Pandharipande and S. Dasgupta, "Optimal DMT based transceivers in multiuser communications". To appear in *IEEE Transactions on Communications.*

5. A. Pandharipande and S. Dasgupta, "Optimum compaction filters for cyclostationary signals", in *Proceeedings of ICASSP*, Orlando, Florida, May 2002. Journal version under preparation.

6. A. Pandharipande and S. Dasgupta, "Optimality in multiuser DMT, multiple description coding and the subband coding of cyclostationary signals", in *Proceedings of IFAC Workshop on Periodic Control*, Como, Italy, August 2001.

7. A. Pandharipande and S. Dasgupta, "On Biorthogonal Nonuniform Filter Banks and Tree Structures", *IEEE Transactions on Circuits and Systems -I*, pp 1457-1467, October 2002.

8. H. Xu, S. Dasgupta, and Z. Ding, "A Novel Channel Identification Method for Fast Wireless Communication Systems", Submitted to *IEEE Transactions on Communications*.

9. A. Pandharipande and S. Dasgupta, "Subband Coding of Cyclostationary Signals with Overdecimated Filter Banks", in *Proceedings of Eusipco*, Toulouse, France, September 2002. Journal version in progress.

10. M. Vemulapalli, S. Dasgupta and A. Pandharipande, "A new algorithm for optimum bit loading", Submitted to the *International Conference on Communications*. Journal version awaiting Patent Application.

11. Pandharipande, A. and Dasgupta, S., "Channel and flow adaptive multiuser DMT", in *Proceedings of 35th Asilomar Conference on Signals, Systems and Computers*, November, 2002.

12. Pandharipande, A. and Dasgupta, S., "Optimum multiuser DMT with unequal subchannel assignments", in *Proceedings of ICC*, May 2003, to appear.

13. H. Xu, S. Dasgupta, and Z. Ding, "An Improved Feedback Scheme for Dual Channel Identification in Wireless Communication Systems", in *Proceedings of ICASSP*, Hong Kong, April 2003.

14. A. Pandharipande and S. Dasgupta, "Optimum biorthogonal DMT systems for multiservice communication", in *Proceedings of ICASSP*, Hong Kong, April 2003.

15. A. Pandharipande and S. Dasgupta, "Optimum channel and multiflow-adaptive biorthogonal DMT systems", Submitted to *IEEE Transcations on Signal Provessing*.

16. Dasgupta, S. and Pandharipande, A., "Complete Characterization of Channel Resistant DMT with Cyclic Prefix", *IEEE Signal Processing Letters*, May 2003.

List of Personnel apart from the PI

1. A. Pandharipande. Ph.D. December 2002.
2. H. Xu. Ph.D. August 2003.
3. T. Tigrek. MS, March 2002.
4. X. Song. Current Ph. D. Student.
5. M. Vemulapalli. Current Ph. D. Student.

Patents

We are planning to file a patent application on the bitloading algorithm.

References

[1] J. Campello, "Practical bit loading for DMT", *IEEE International Conference on Communications*, pp 801-805, 1999.

[2] B. S. Krongold, K. Ramchandran and D. L. Jones, "An efficient algorithm for optimal margin maximization in multicarrier communication systems", *IEEE Global Telecommunications Conference*, pp 899-903, 1999.

Subband Coding of Cyclostationary Signals

Ashish Pandharipande and Soura Dasgupta

October 24, 2001

Abstract

We consider optimal orthonormal filter banks for subband coding of wide sense cyclostationary signals, with N-periodic second order statistics. An M-channel uniform filter bank, with N-periodic analysis and synthesis filters, is used as the subband coder. Dynamic schemes involving N-periodic bit allocation are employed. An average variance condition is used to measure the output distortion. We show that for at least three potential bit allocation strategies, the optimum filter bank is a principal component filter bank.

Index Terms: Subband coding, Filter bank, Bit allocation, Dynamic schemes, Majorization theory.

Author Information

Manuscript received _____

Affiliation of Authors: Department of Electrical and Computer Engineering, The University of Iowa, Iowa City, IA-52242, USA.

Email: pashish@engineering.uiowa.edu and dasgupta@engineering.uiowa.edu.

Contact Author: Soura Dasgupta.

Supported in part by US Army contract, DAAD19-00-1-0534, and NSF grants ECS-9970105 and CCR-9973133.

List of Figures

1 Introduction

Wide sense cyclostationary (WSCS) signals arise in many applications, [1], [2]. We consider optimum orthonormal subband coding of zero mean WSCS signals with N-periodic second order statistics, i.e. signals that obey for all k, l: $\mathcal{E}[x(k)x^*(l)] = \mathcal{E}[x(k+N)x^*(l+N)]$ where $\mathcal{E}[\cdot]$ denotes the expectation operator. The subband coder itself is an M-channel maximally decimated uniform filter bank (UFB), (see fig. 1), with N-periodic linear analysis and synthesis filters, $H_i(k,z)$ and $F_i(k,z)$, respectively. Each subband signal $v_i(k)$, is quantized at the kth instant, by a $b_i(k)$ bit quantizer, Q_i. Subject to bit rate and orthonormality constraints, we wish to allocate bits $b_i(k)$, and select, $H_i(k,z)$ and $F_i(k,z)$ to minimize the *average* variance of $\hat{x}(k) - x(k)$.

Among many possible bit rate constraints one can adopt, three are of interest here. The first called static bit allocation (SBA) involves constant $b_i(k)$, and has been studied in [6]. The second and third, both assume N-periodic bit allocation:

$$b_i(k+N) = b_i(k). \tag{1.1}$$

In the second, the average bit rate over all the channels is constant *at each time instant*, i.e. given b and all k,

$$b = \left(\sum_{i=0}^{M-1} b_i(k) \right) / M. \tag{1.2}$$

The third assumes a fixed average bit rate over periods of length N:

$$b = \frac{1}{MN} \sum_{k=0}^{N-1} \sum_{i=0}^{M-1} b_i(k). \tag{1.3}$$

Among these, (1.1) requires the least computation and (1.3) is the most general. On the other hand, (1.2) is preferred over (1.3) in applications, such as control over networks, where the bit rate constraint must be enforced at every time instant.

Recent studies, [4, 5] have established that the optimum UFB subband coder for Wide Sense Stationary (WSS) signals is a principal component filter bank (PCFB), [3]. In [6] we have likewise shown that for SBA also the optimum UFB is a PCFB. The principal contribution of this paper is to show that even under (1.2) and (1.3), optimality is attained through PCFB's, despite the differing bit allocation constraints. This suggests the universality of PCFB based solutions for problems such as these.

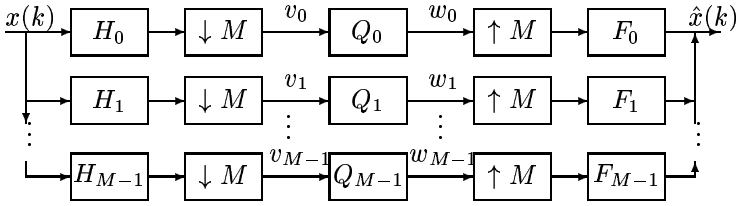

Figure 1: An M-channel filter bank as subband coder.

2 Optimum Bit Allocation

For any zero mean signal $x(k)$, define $\sigma_x^2(k) = \mathcal{E}[x^2(k)]$. All subband signals $v_i(k)$ have N-periodic second order statistics. As in [4], [5], we assume that the quantizers are modeled by additive zero mean noise sources, independent of the $v_i(k)$, with variances of the form

$$\sigma_{q_i}^2(k) = c2^{-2b_i(k)}\sigma_{v_i}^2(k), \tag{2.4}$$

with c a distribution dependent constant. Note that under (1.1), $\sigma_{q_i}^2(k)$ are N-periodic.

Observe that the overall filter bank is MN-periodic. Let $\tilde{E}(z)$ and $\tilde{R}(z)$ be the transfer functions of MN-fold blocked versions of the analysis and synthesis banks respectively. Define the WSS vectors,

$$\begin{aligned}\tilde{x}(k) &= [x_0(Nk), \ldots, x_0(NK-N+1), \ldots, x_{M-1}(Nk), \ldots, x_{M-1}(Nk-N+1)]^T,\\ \tilde{v}(k) &= [v_0(Nk), \ldots, v_0(NK-N+1), \ldots, v_{M-1}(Nk), \ldots, v_{M-1}(Nk-N+1)]^T,\end{aligned} \tag{2.5}$$

with power spectral density (PSD) matrices $S_{\tilde{x}}(\omega)$ and $S_{\tilde{v}}(\omega)$ respectively. We assume $S_{\tilde{x}}(\omega)$ is known. We assume the perfect reconstruction and orthonormality conditions,

$$\tilde{E}^\dagger(z)\tilde{E}(z) = I = \tilde{R}^\dagger(z)\tilde{R}(z), \text{ and } \tilde{R}(z) = \tilde{E}^\dagger(z). \tag{2.6}$$

We propose to minimize the *average* variance of $\hat{q}(k) = \hat{x}(k) - x(k)$ and under (1.2) and (2.6), obtain

$$\frac{1}{MN}\sum_{k=0}^{MN-1}\sigma_{\hat{q}}^2(k) = \frac{1}{MN}\sum_{k=0}^{N-1}\sum_{l=0}^{M-1}\sigma_{q_l}^2(k) = \frac{c}{MN}\sum_{k=0}^{N-1}\sum_{l=0}^{M-1}2^{-2b_l(k)}\sigma_{v_l}^2(k) \tag{2.7}$$

$$\geq \frac{c2^{-2b}}{N}\sum_{k=0}^{N-1}\left(\prod_{l=0}^{M-1}\sigma_{v_l}^2(k)\right)^{1/M}, \tag{2.8}$$

with equality holding iff for each i, l, k

$$2^{-2b_i(k)}\sigma_{v_i}^2(k) = 2^{-2b_l(k)}\sigma_{v_l}^2(k). \tag{2.9}$$

Likewise under (1.3), (2.7) is lower bounded by

$$c2^{-2b}\left(\prod_{k=0}^{N-1}\prod_{l=0}^{M-1}\sigma_{v_l}^2(k)\right)^{1/MN}, \tag{2.10}$$

with the bound met iff for each i, l, k_1, k_2

$$2^{-2b_i(k_1)}\sigma_{v_i}^2(k_1) = 2^{-2b_l(k_2)}\sigma_{v_l}^2(k_2). \tag{2.11}$$

Observe, the *optimum bit allocation* scheme (2.11) is more stringent than (2.9).

Consequently UFB selection reduces to the following problem:

Problem 2.1 *Consider the $MN \times MN$ system $\tilde{E}(z)$ with WSS input vector $\tilde{x}(k)$ with given Hermitian PSD matrix $S_{\tilde{x}}(\omega)$. Suppose $\tilde{v}(k)$ in (2.5) is the output of $\tilde{E}(z)$. For (1.2) (resp. (1.3)) find $\tilde{E}(z)$ such that J_1 (resp. J_2) is minimized subject to (2.6).*

$$J_1 = \sum_{k=0}^{N-1}\Big(\prod_{l=0}^{M-1}\sigma_{v_l}^2(k)\Big)^{1/M} \text{ and } J_2 = \prod_{k=0}^{N-1}\prod_{l=0}^{M-1}\sigma_{v_l}^2(k). \tag{2.12}$$

While J_2 is similar to the corresponding cost function in the WSS case, [5], J_1 is more complicated. The difference stems from the fact that implicit in (1.2) are N- bit budgets. Both in turn are different from the cost function for (1.1) considered in [6]. Finally, while J_2 does not change by permuting the subband variances, J_1 does. Indeed given a set of subband variances at different time instants we need consider only the arrangements that lead to the minimum value of J_1. Such optimal arrangements are characterized below.

Optimum Arrangement: Among the various permutations of $\sigma^2_{v_i}(j)$, ones that minimize J_1 obeys, [7]:

$$\sigma^2_{v_m}(k_1) \geq \sigma^2_{v_n}(k_2) \Rightarrow \prod_{i\neq m}^{M-1} \sigma^2_{v_i}(k_1) \leq \prod_{i\neq n}^{M-1} \sigma^2_{v_i}(k_2) \tag{2.13}$$

For a 2-channel filter bank, $M = 2$, this requires that the largest be paired with the smallest, the second largest with the second smallest etc..

3 Optimum Subband Coder

We now characterize the optimum selection of $\tilde{E}(z)$, by introducing the notions of majorization and Schur concavity, [7].

Definition 3.1 *Consider two sequences $x = \{x_i\}_{i=1}^n$ and $y = \{y_i\}_{i=1}^n$ with $x_i \geq x_{i+1}$ and $y_i \geq y_{i+1}$. Then we say that y majorizes x, denoted as $x \prec y$, if the following holds with equality at $k = n$*

$$\sum_{i=1}^{k} x_i \leq \sum_{i=1}^{k} y_i, \quad 1 \leq k \leq n.$$

Fact 1 *If H is an $n \times n$ Hermitian matrix with diagonal elements $h_1, \ldots, h_n$, and eigenvalues $\lambda_1, \ldots, \lambda_n$, then $h \prec \lambda$ on R^n.*

Definition 3.2 *A real valued function $\phi(z) = \phi(z_1, \ldots, z_n)$ defined on a set $\mathcal{A} \subset R^n$ is said to be Schur concave on $\mathcal{A}$ if*

$$x \prec y \quad on\, \mathcal{A} \quad \Rightarrow \quad \phi(x) \geq \phi(y).$$

ϕ is strictly Schur concave on $\mathcal{A}$ if strict inequality $\phi(x) > \phi(y)$ holds when x is not a permutation of y.

We will now state a theorem that results in a test for strict Schur concavity. We denote

$$\phi_{(k)}(z) = \frac{\partial \phi(z)}{\partial z_k}, \quad \phi_{(i,j)}(z) = \frac{\partial^2 \phi(z)}{\partial z_i \partial z_j}, \quad J_1(k,l) = \frac{\partial J_1}{\partial \sigma^2_{v_l}(k)}, \text{ and } J_1(k,l,m,n) = \frac{\partial^2 J_1}{\partial \sigma^2_{v_l}(k) \partial \sigma^2_{v_n}(m)}.$$

Theorem 3.1 *Let $\phi(z)$ be a scalar real valued function defined and continuous on $\mathcal{D} = \{(z_1, \ldots, z_n) : z_1 \geq \ldots \geq z_n\}$, and twice differentiable on the interior of $\mathcal{D}$. Then $\phi(z)$ is strictly Schur concave on $\mathcal{D}$ iff:(i) ϕ is symmetric in its arguments, (ii) $\phi_{(k)}(z)$ is increasing in k, and (iii) $\phi_{(k)}(z) = \phi_{(k+1)}(z) \Rightarrow \phi_{(k,k)}(z) - \phi_{(k,k+1)}(z) - \phi_{(k+1,k)}(z) + \phi_{(k+1,k+1)}(z) < 0$.*

It is known, that J_2 is Schur Concave, [7]. We also have the following lemma.

Lemma 3.1 *The real valued function J_1 as defined in (2.12) is strictly Schur concave under (2.13).*

Proof: Clearly J_1 is symmetric in its arguments $\sigma^2_{v_l}(k)$, satisfying (i) of Theorem 3.1. Note that

$$J_1(k,l) = \frac{1}{M}\frac{\left(\prod_{i=0}^{M-1}\sigma^2_{v_i}(k)\right)^{1/M}}{\sigma^2_{v_l}(k)}. \tag{3.14}$$

If $\sigma^2_{v_{l_1}}(k_1) \geq \sigma^2_{v_{l_1}}(k_1)$, then under (2.13) $J_1(k_1,l_1) \leq J_1(k_2,l_2)$, satisfying condition (ii).

To establish (iii), note that

$$J_1(k,l) = J_1(m,n) \Leftrightarrow \frac{\left(\prod_{i=0}^{M-1}\sigma^2_{v_i}(k)\right)^{1/M}}{\sigma^2_{v_l}(k)} = \frac{\left(\prod_{i=0}^{M-1}\sigma^2_{v_i}(m)\right)^{1/M}}{\sigma^2_{v_n}(m)}, \tag{3.15}$$

$$J_1(k,l,m,n) = \begin{cases} \frac{1-M}{M^2}\frac{\left(\prod_{i=0}^{M-1}\sigma^2_{v_i}(k)\right)^{1/M}}{\left(\sigma^2_{v_l}(k)\right)^2} & \text{if } k=m, l=n, \\ \frac{1}{M^2}\frac{\left(\prod_{i=0}^{M-1}\sigma^2_{v_i}(k)\right)^{1/M}}{\sigma^2_{v_l}(k)\sigma^2_{v_n}(k)} & \text{if } k=m, l\neq n, \\ 0 & \text{if } k\neq m, l=n, \end{cases}$$

and hence, under (3.15)

$$J_1(k,l,k,l) - J_1(k,l,m,n) - J_1(m,n,k,l) + J_1(m,n,m,n) < 0.$$

■

Note that

$$S_{\tilde{v}}(\omega) = \tilde{E}(\omega)S_{\tilde{x}}(\omega)\tilde{E}^\dagger(\omega). \tag{3.16}$$

Since $S_{\tilde{x}}(\omega)$ is Hermitian, we may write

$$S_{\tilde{x}}(\omega) = \tilde{U}(\omega)\tilde{\Lambda}(\omega)\tilde{U}^\dagger(\omega), \tag{3.17}$$

with $\tilde{U}(\omega)$ unitary and $\tilde{\Lambda}(\omega) =$ diag $\{\tilde{\lambda}_0(\omega), \tilde{\lambda}_1(\omega), \ldots, \tilde{\lambda}_{MN-1}(\omega)\}$, with $\tilde{\lambda}_i(\omega) \geq \tilde{\lambda}_{i+1}(\omega) > 0$ at all ω. Then, [7], $\{2\pi\sigma^2_{v_i}(k)\}_{k=0,i=0}^{N-1,M-1} \prec \{\int_0^{2\pi}\tilde{\lambda}_i(\omega)d\omega\}_{i=0}^{MN-1}$. We then have the following result.

Theorem 3.2 *Consider Problem 2.1 and all quantities defined therein. Then optimality is attained iff $\tilde{E}(\omega) = P\tilde{U}^\dagger(\omega)$, where for (1.3), P is any constant permutation matrix, and for (1.2), P is any constant permutation matrix that leads to an optimum arrangement for J_1 in (2.12), when the subband variances are the normalized integrals of $\tilde{\lambda}_i(\omega)$. In this case, $S_{\tilde{v}}(\omega) = P\tilde{\Lambda}(\omega)P^\dagger$.*

Figure 2 shows the coding gains under the two schemes, for an input with 5-periodic statistics. As expected, (1.3) leads to higher coding gains. Its disadvantage is that while the overall bit rate averaged over N samples is the same as in (1.2), it could lead to time instants in which the bit rate is significantly lower than the target. In certain time critical applications this may not be desirable.

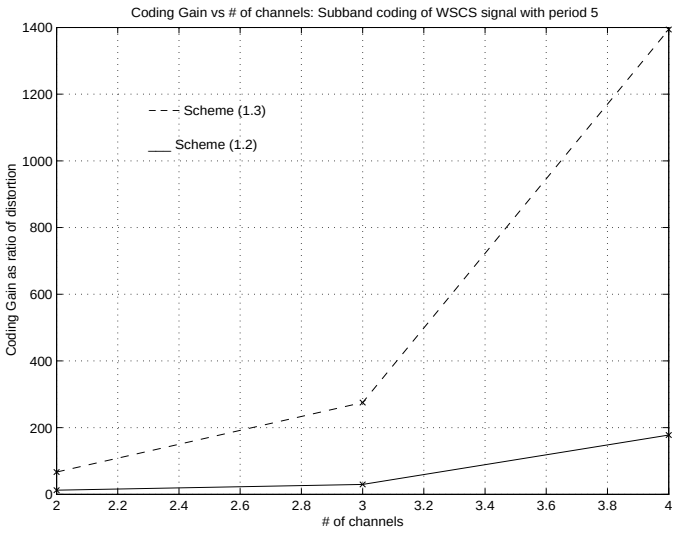

Figure 2: Coding gain plots.

4 Conclusions

We have derived conditions for the optimal orthonormal subband coding of N-WSCS signals, using an M-channel uniform filter bank as subband coder with N-periodic filters and two periodic bit allocation schemes. As with the results of [6], where a static bit allocation scheme was considered, the optimum filter bank in each case is a PCFB.

References

[1] W. A. Gardner "Exploitation of spectral redundancy in cyclostationary signals", *IEEE Signal Processing Magazine*, pp 14-37, April 1991.

[2] G. Giannakis,"Cyclostationary Signal Analysis", Chapter 17, *CRC DSP Handbook.*

[3] M. K. Tstatsanis and G. B. Giannakis, "Principal component filter banks for optimum multiresolution analysis", *IEEE Transactions on Signal Processing* , pp 1766- 1777 August 1995.

[4] M. K. Mihcak, P. Moulin, M. Anitescu, K. Ramchandran, "Rate-distortion-optimal subband coding without perfect-reconstruction constraints", *IEEE Transactions on Signal Processing*, pp 542-557, March 2001.

[5] P.P. Vaidyanathan, "Theory of optimal orthonormal subband coders", *IEEE Transactions on Signal Processing*, pp 1528-1543, June 1998.

[6] A. Pandharipande and S. Dasgupta, "Subband coding of cyclostationary signals with static bit allocation", *IEEE Signal Processing Letters*, pp 284-286, Nov 1999.

[7] A. W. Marshall and I. Olkin, *Inequalities: Theory of Majorization and its applications*, Academic Press, 1979.

SUBBAND CODING OF CYCLOSTATIONARY SIGNALS WITH OVERDECIMATED FILTER BANKS

Soura Dasgupta, Ashish Pandharipande

Department of Electrical & Computer Engineering
The University of Iowa
Iowa City, IA-52242, USA.
Email: {dasgupta, pashish}@engineering.uiowa.edu

ABSTRACT

We consider optimal orthonormal filter banks for subband coding of wide sense cyclostationary signals, with N-periodic second order statistics. An L-channel over decimated uniform filter bank, with N-periodic analysis and synthesis filters, is used as the subband coder. An average variance condition is used to measure the output distortion. We show that for at least three potential bit allocation strategies, the optimum filter bank is a principal component filter bank. This is in the same vein as our earlier results on subband coding with maximally decimated filter banks.

1. INTRODUCTION

Wide sense cyclostationary (WSCS) signals arise in many applications, [1], [2]. We consider optimum orthonormal subband coding of zero mean WSCS signals with N-periodic second order statistics, i.e. signals that obey for all k, l: $\mathcal{E}[x(k)x^*(l)] = \mathcal{E}[x(k+N)x^*(l+N)]$ where $\mathcal{E}[\cdot]$ denotes the expectation operator.

The subband coder itself is an L-channel *over decimated* uniform filter bank (UFB), (see fig. 1), with

$$M > L,$$

and N-periodic linear analysis and synthesis filters, $H_i(k,z)$ and $F_i(k,z)$, respectively. Each subband signal $v_i(k)$, is quantized at the kth instant, by a $b_i(k)$ bit quantizer, Q_i. Subject to bit rate and orthonormality constraints, we wish to allocate bits $b_i(k)$, and select, $H_i(k,z)$ and $F_i(k,z)$ to minimize the *average* variance of $\hat{x}(k) - x(k)$.

Among many possible bit rate constraints one can adopt, three are of interest here. The first called static bit allocation (SBA) involves constant $b_i(k)$, and a bit rate constraint

$$b = \left(\sum_{i=0}^{L-1} b_i\right)/L. \tag{1.1}$$

Supported by ARO contract DAAD19-00-1-0534 and NSF grants ECS-9970105 and CCR-9973133.

The second and third, both assume N-periodic bit allocation:

$$b_i(k+N) = b_i(k). \tag{1.2}$$

In the second, the average bit rate over all the channels is constant *at each time instant*, i.e. given b and all k,

$$b = \left(\sum_{i=0}^{L-1} b_i(k)\right)/L. \tag{1.3}$$

The third assumes a fixed average bit rate over periods of length N:

$$b = \frac{1}{LN}\sum_{k=0}^{N-1}\sum_{i=0}^{L-1} b_i(k). \tag{1.4}$$

Among these, (1.2) requires the least computation and (1.4) is the most general. On the other hand, (1.3) is preferred over (1.4) in applications, such as control over networks, where the bit rate constraint must be enforced at every time instant.

Subband coding under these three constraints, with *maximally decimated* filter banks (i.e. $L = M$) has been studied in [6] and [7]. These references show that, while the optimum bit allocation schemes differ among (1.1 - 1.4), the optimizing $H_i(k,z)$ and $F_i(k,z)$ can be chosen as the same regardless of the allocation scheme. In fact a Principal Component Filter Bank (PCFB), represents the common optimizing solution.

Recent studies, [4, 5] have established that the optimum UFB subband coder for Wide Sense Stationary (WSS) signals is a PCFB, [3]. The principal contribution of this paper is to show that even on the over decimated case, optimality is attained through PCFB's, despite the differing bit allocation constraints, reinforcing the universality of PCFB based solutions for problems such as these.

2. OPTIMUM BIT ALLOCATION

For any zero mean signal $x(k)$, define $\sigma_x^2(k) = \mathcal{E}[x^2(k)]$. All subband signals $v_i(k)$ have N-periodic second order statistics. As in [4], [5], we assume that the quantizers are modeled by additive zero mean noise sources, independent of the

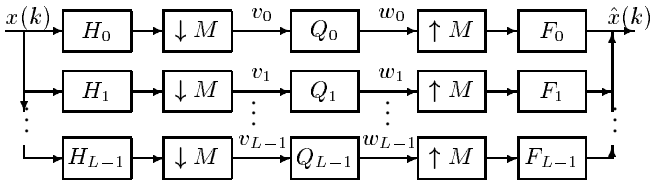

Fig. 1. An L-channel over decimated filter bank as subband coder.

$v_i(k)$, with variances of the form

$$\sigma^2_{q_i}(k) = c2^{-2b_i(k)}\sigma^2_{v_i}(k), \tag{2.5}$$

with c a distribution dependent constant. Note that under (1.2), $\sigma^2_{q_i}(k)$ are N-periodic.

Observe that the overall filter bank is MN-periodic. Let $\tilde{E}(z)$ and $\tilde{R}(z)$ be the transfer functions of MN-fold blocked versions of the analysis and synthesis banks respectively. In particular, $\tilde{E}(z)$ is $LN \times MN$ and $\tilde{R}(z)$ is $MN \times LN$. *A key difference between the over decimated and the maximally decimated cases is that these transfer functions are no longer square.*

Define $x_i(k) = x(Mk - i)$, $x_i(k) = x(Mk - i)$and the WSS vectors,

$$\begin{aligned}\tilde{x}(k) = \quad & [x_0(Nk), \ldots, x_0(NK - N + 1), \ldots, x_{M-1}(Nk), \\ & \ldots, x_{M-1}(Nk - N + 1)]^T,\end{aligned}$$

$$\begin{aligned}\tilde{v}(k) = \quad & [v_0(Nk), \ldots, v_0(NK - N + 1), \ldots, v_{L-1}(Nk), \\ & \ldots, v_{L-1}(Nk - N + 1)]^T,\end{aligned} \tag{2.6}$$

with power spectral density (PSD) matrices $S_{\tilde{x}}(\omega)$ and $S_{\tilde{v}}(\omega)$ respectively. Observe,

$$\tilde{v}(k) = \tilde{E}(z)\tilde{x}(k).$$

We assume $S_{\tilde{x}}(\omega)$ is known. We assume the perfect reconstruction and orthonormality conditions,

$$\tilde{E}(z)\tilde{E}^\dagger(z) = I = \tilde{R}^\dagger(z)\tilde{R}(z), \text{ and } \tilde{R}(z) = \tilde{E}^\dagger(z). \tag{2.7}$$

We propose to minimize the *average* variance of $\hat{q}(k) = \hat{x}(k) - x(k)$ and under (1.3) and (2.7), obtain

$$\begin{aligned}\frac{1}{LN}\sum_{k=0}^{LN-1}\sigma^2_{\hat{q}}(k) &= \frac{1}{LN}\sum_{k=0}^{N-1}\sum_{l=0}^{L-1}\sigma^2_{q_l}(k) \\ &= \frac{c}{LN}\sum_{k=0}^{N-1}\sum_{l=0}^{L-1}2^{-2b_l(k)}\sigma^2_{v_l}(k) \\ &\geq \frac{c2^{-2b}}{N}\sum_{k=0}^{N-1}\left(\prod_{l=0}^{L-1}\sigma^2_{v_l}(k)\right)^{1/L}\end{aligned} \tag{2.8}$$

with equality holding iff for each i, l, k

$$2^{-2b_i(k)}\sigma^2_{v_i}(k) = 2^{-2b_l(k)}\sigma^2_{v_l}(k). \tag{2.9}$$

Likewise under (1.4), the lower bounded becomes

$$\frac{c2^{-2b}}{N}\left(\prod_{k=0}^{N-1}\prod_{l=0}^{L-1}\sigma^2_{v_l}(k)\right)^{1/LN}, \tag{2.10}$$

with the bound met iff for each i, l, k_1, k_2

$$2^{-2b_i(k_1)}\sigma^2_{v_i}(k_1) = 2^{-2b_l(k_2)}\sigma^2_{v_l}(k_2). \tag{2.11}$$

On the other hand under the static bit allocation strategy of (1.1), as shown in [6], the lower bounded becomes

$$\frac{c2^{-2b}}{N}\prod_{l=0}^{L-1}\left(\sum_{k=0}^{N-1}\sigma^2_{v_l}(k)\right), \tag{2.12}$$

with the bound met iff for each i, l

$$2^{-2b_i}\left(\sum_{k=0}^{N-1}\sigma^2_{v_i}(k)\right) = 2^{-2b_l}\left(\sum_{k=0}^{N-1}\sigma^2_{v_l}(k)\right). \tag{2.13}$$

Observe, the *optimum bit allocation* scheme (2.11) is the most stringent among (2.9), (2.11) and (2.13).

Consequently UFB selection reduces to the following problem:

Problem 2.1 *Consider the $LN \times MN$ system $\tilde{E}(z)$ with WSS input vector $\tilde{x}(k)$ with given Hermitian PSD matrix $S_{\tilde{x}}(\omega)$. Suppose $\tilde{v}(k)$ in (2.6) is the output of $\tilde{E}(z)$. For (1.3) (resp. (1.4)), (resp. (1.1)) find $\tilde{E}(z)$ such that J_1 (resp. J_2) (resp. J_3) is minimized subject to (2.7).*

$$J_1 = \sum_{k=0}^{N-1}(\prod_{l=0}^{L-1}\sigma^2_{v_l}(k))^{1/L} \tag{2.14}$$

$$J_2 = \left(\prod_{k=0}^{N-1}\prod_{l=0}^{L-1}\sigma^2_{v_l}(k)\right)^{1/LN} \tag{2.15}$$

$$J_3 = \prod_{l=0}^{L-1}\left(\sum_{k=0}^{N-1}\sigma^2_{v_l}(k)\right) \tag{2.16}$$

Observe all three of (2.14) - (2.16) are quite different from one another. While J_2 is similar to the corresponding cost function in the WSS case, [5], J_1 and J_3 are more complicated. Further while J_2 does not change by permuting the subband variances, J_1 and J_3 do. Indeed given a set of subband variances at different time instants we need consider only the arrangements that lead to the minimum value of J_1, J_3. Such optimal arrangements are characterized below.

Optimum Arrangement for J_1: Among the various permutations of $\sigma^2_{v_i}(j)$, ones that minimize J_1 obeys, [8]:

$$\sigma^2_{v_m}(k_1) \geq \sigma^2_{v_n}(k_2) \Rightarrow \prod_{i\neq m}^{L-1} \sigma^2_{v_i}(k_1) \leq \prod_{i\neq n}^{L-1} \sigma^2_{v_i}(k_2) \quad (2.17)$$

For a 2-channel filter bank, $L = 2$, this requires that the largest be paired with the smallest, the second largest with the second smallest etc..

Optimum Arrangement for J_3: Among the various permutations of $\sigma^2_{v_i}(j)$, ones that minimize J_1 obeys, [6]: for each l, one partial sum equals the sum of the N largest among the $\sigma^2_{v_i}(j)$, another equals the sum of the next N largest, etc.

3. OPTIMUM SUBBAND CODER

We now characterize the optimum selection of $\tilde{E}(z)$, by introducing the notions of majorization and Schur concavity, [8].

Definition 3.1 *Consider two sequences $x = \{x_i\}_{i=1}^n$ and $y = \{y_i\}_{i=1}^n$ with $x_i \geq x_{i+1}$ and $y_i \geq y_{i+1}$. Then we say that y majorizes x, denoted as $x \prec y$, if the following holds with equality at $k = n$*

$$\sum_{i=1}^{k} x_i \leq \sum_{i=1}^{k} y_i, \quad 1 \leq k \leq n.$$

Definition 3.2 *Consider two sequences $x = \{x_i\}_{i=1}^l$ and $y = \{y_i\}_{i=1}^l$ with $x_i \geq x_{i+1}$ and $y_i \geq y_{i+1}$. Then we say that y weakly supermajorizes x, denoted as $x \prec^w y$, if*

$$\sum_{i=k}^{l} x_i \geq \sum_{i=k}^{l} y_i, \quad 1 \leq k \leq l.$$

We also have the following Fact from [8].

Fact 1 *Consider any $NM \times NM$ Hermitian matrix R with eigenvalues $\lambda_1 \geq \lambda_2 \geq \ldots \geq \lambda_{NM}$, and an $LM \times LM$ matrix $A = \Psi R \Psi^\dagger$, with the $LM \times NM$ matrix Ψ obeying $\Psi\Psi^\dagger = I$. Then the diagonal elements $A_{i,i}$ of A obey*

$$\{A_{i,i}\}_{i=1}^{LM} \prec^w \{\lambda_{NM-LM-1}, \ldots, \lambda_{NM}\}. \quad (3.18)$$

Further if $M = N$,

$$\{A_{i,i}\}_{i=1}^{M} \prec \{\lambda_1, \ldots, \lambda_{NM}\}. \quad (3.19)$$

Definition 3.3 *A real valued function $\phi(z) = \phi(z_1, \ldots, z_n)$ defined on a set $\mathcal{A} \subset R^n$ is said to be Schur concave on $\mathcal{A}$ if*

$$x \prec y \quad on\ \mathcal{A} \quad \Rightarrow \quad \phi(x) \geq \phi(y).$$

ϕ is strictly Schur concave on $\mathcal{A}$ if strict inequality $\phi(x) > \phi(y)$ holds when x is not a permutation of y.

Further we note the following result from [8].

Theorem 3.1 *Let ϕ be a real-valued strictly Schur concave function defined and continuous on $\mathcal{D}$ as in Theorem 3.1. Then*

$$x \prec^w y \Rightarrow \phi(x) \geq \phi(y),$$

with equality holding only if x is a permutation of y.

We will now state a theorem that results in a test for strict Schur concavity. We denote

$$\phi_{(k)}(z) = \frac{\partial \phi(z)}{\partial z_k}, \quad \phi_{(i,j)}(z) = \frac{\partial^2 \phi(z)}{\partial z_i \partial z_j},$$

and

$$J_1(k,l) = \frac{\partial J_1}{\partial \sigma^2_{v_l}(k)}, \text{ and } J_1(k,l,m,n) = \frac{\partial^2 J_1}{\partial \sigma^2_{v_l}(k) \partial \sigma^2_{v_n}(m)}.$$

Theorem 3.2 *Let $\phi(z)$ be a scalar real valued function defined and continuous on $\mathcal{D} = \{(z_1, \ldots, z_n) : z_1 \geq \ldots \geq z_n\}$, and twice differentiable on the interior of $\mathcal{D}$. Then $\phi(z)$ is strictly Schur concave on $\mathcal{D}$ iff: (i) $\phi_{(k)}(z)$ is increasing in k, and (ii)*

$$\begin{aligned} \phi_{(k)}(z) = \phi_{(k+1)}(z) \quad &\Rightarrow \quad \phi_{(k,k)}(z) - \phi_{(k,k+1)}(z) \\ &- \quad \phi_{(k+1,k)}(z) + \phi_{(k+1,k+1)}(z) < 0. \end{aligned}$$

If only (i) holds then $\phi(z)$ is only Schur concave.

It is known, that J_2 is strictly Schur concave, [8]. We also have the following lemma.

Lemma 3.1 *The real valued function J_1 as defined in (2.14) is strictly Schur concave under (2.17).*

Proof: Clearly J_1 is symmetric in its arguments $\sigma^2_{v_l}(k)$, satisfying (i) of Theorem 3.2. Note that

$$J_1(k,l) = \frac{1}{L} \frac{\left(\prod_{i=0}^{L-1} \sigma^2_{v_i}(k)\right)^{1/L}}{\sigma^2_{v_l}(k)}. \quad (3.20)$$

If $\sigma^2_{v_{l_1}}(k_1) \geq \sigma^2_{v_{l_1}}(k_1)$, then under (2.17)

$$J_1(k_1, l_1) \leq J_1(k_2, l_2),$$

satisfying condition (ii).

To establish (iii), note that

$$\begin{aligned} J_1(k,l) = J_1(m,n) \Leftrightarrow \quad & \frac{\left(\prod_{i=0}^{L-1} \sigma^2_{v_i}(k)\right)^{1/L}}{\sigma^2_{v_l}(k)} \\ &= \frac{\left(\prod_{i=0}^{L-1} \sigma^2_{v_i}(m)\right)^{1/L}}{\sigma^2_{v_n}(m)}, \quad (3.21) \end{aligned}$$

$$J_1(k,l,m,n) = \begin{cases} \frac{1-L}{L^2}\frac{\left(\prod_{i=0}^{L-1}\sigma^2_{v_i}(k)\right)^{1/L}}{\left(\sigma^2_{v_l}(k)\right)^2} & \text{if } k=m, l=n, \\ \frac{1}{L^2}\frac{\left(\prod_{i=0}^{L-1}\sigma^2_{v_i}(k)\right)^{1/L}}{\sigma^2_{v_l}(k)\sigma^2_{v_n}(k)} & \text{if } k=m, l\neq n, \\ 0 & \text{if } k\neq m, l=n, \end{cases}$$

and hence, under (3.21)

$$\begin{aligned} J_1(k,l,k,l) - J_1(k,l,m,n) &- J_1(m,n,k,l) \\ &+ J_1(m,n,m,n) < 0. \end{aligned}$$

■

Finally we note that under the pertinent optimum arrangement, J_3 is also Schur concave, but not in the strict sense. This follows from a slight variation of the fact that J_2 is strictly Schur convcave, see also [6]. Note that

$$S_{\tilde{v}}(\omega) = \tilde{E}(\omega)S_{\tilde{x}}(\omega)\tilde{E}^{\dagger}(\omega). \tag{3.22}$$

Now suppose the NM eigenvalues of $S_{\tilde{x}}(\omega)$, are

$$\{\tilde{\lambda}_0(\omega), \tilde{\lambda}_1(\omega), \ldots, \tilde{\lambda}_{LN-1}(\omega)\},$$

with $\tilde{\lambda}_i(\omega) \geq \tilde{\lambda}_{i+1}(\omega) > 0$ at all ω. Define the $NM \times LM$ matrix whose columns are the unit eigenvectors corresponding to the smallest LN eigenvalues of $S_{\tilde{x}}(\omega)$. Observe

$$\tilde{U}^{\dagger}(\omega)\tilde{U}(\omega) = I.$$

Then, because of Fact 1

$$\{2\pi\sigma^2_{v_i}(k)\}_{k=0,i=0}^{N-1,L-1} \prec^W \{\int_0^{2\pi}\tilde{\lambda}_i(\omega)d\omega\}_{i=MN-LN}^{MN-1}.$$

Note the number of diagonal elements of $S_{\tilde{v}}(\omega)$ is less than the number of eigenvalues of $S_{\tilde{x}}(\omega)$, as the overdecimated condition forces $\tilde{E}(z)$ to be rectangular. Consequently, unlike [6] and [7], where maximal decimation forced a square $\tilde{E}(z)$, weak super majorization, rather than majorization must be used.

We then have the following result.

Theorem 3.3 *Consider Problem 2.1 and all quantities defined therein. Then optimality is attained if for a suitable frequency inavriant permutation matrix P, $\tilde{E}(\omega) = P\tilde{U}^{\dagger}(\omega)$.*

We note that for J_2 this solution is unique to within an arbitrary permutation matrix P. For J_1 too this solution is unique to any permutation matrix P that enforces an optimum arrangement. This is so because both J_1 and J_2 are strictly Schur concave. For J_3, on the other hand, even though P must enforce an optimum arrangement, the solution is by no means unique, as J_3 is not strictly Schur concave. Nonetheless it is intriguing that despite the difference between the J_i, a common $\tilde{E}$ optimizes all three.

4. CONCLUSIONS

We have derived conditions for the optimal orthonormal subband coding of N-WSCS signals, using an over decimated L-channel uniform filter bank as subband coder with N-periodic filters three bit allocation schemes. As with the results of [6], [7] an optimum filter bank in each case is the same PCFB.

5. REFERENCES

[1] W. A. Gardner "Exploitation of spectral redundancy in cyclostationary signals", *IEEE Signal Processing Magazine*, pp 14-37, April 1991.

[2] G. Giannakis,"Cyclostationary Signal Analysis", Chapter 17, *CRC DSP Handbook.*

[3] M. K. Tstatsanis and G. B. Giannakis, "Principal component filter banks for optimum multiresolution analysis", *IEEE Transactions on Signal Processing* , pp 1766- 1777 August 1995.

[4] M. K. Mihcak, P. Moulin, M. Anitescu, K. Ramchandran, "Rate-distortion-optimal subband coding without perfect-reconstruction constraints", *IEEE Transactions on Signal Processing*, pp 542-557, March 2001.

[5] P.P. Vaidyanathan, "Theory of optimal orthonormal subband coders", *IEEE Transactions on Signal Processing*, pp 1528-1543, June 1998.

[6] A. Pandharipande and S. Dasgupta, "Subband coding of cyclostationary signals with static bit allocation", *IEEE Signal Processing Letters*, pp 284-286, Nov 1999.

[7] A. Pandharipande and S. Dasgupta, "Subband coding of cyclostationary signals", Submitted to *IEEE IEEE Transactions on Circuits and Systems*.

[8] A. W. Marshall and I. Olkin, *Inequalities: Theory of Majorization and its applications*, Academic Press, 1979.

OPTIMALITY IN MULTICARRIER COMMUNICATION, MULTIPLE DESCRIPTION CODING AND THE SUBBAND CODING OF CYCLOSTATIONARY SIGNALS

Soura Dasgupta *Ashish Pandharipande**

ABSTRACT

This paper considers three different problems in signal processing/communications. The first involves Multiuser Discrete Multitone Transmission (DMT). The other two problems concerns variants of subband coding, specifically subband coding of cyclostationary signals and the multiple description coding. We show that underlying each is the same optimization problem that can be solved using the theory of majorization.

1. INTRODUCTION

This paper considers three different problems in signal processing/communications. The first involves Multiuser Discrete Multitone Transmission (DMT), [1], also variously known as multicarrier modulation or Orthogonal frequency Division Multiplexed (OFDM) communication. The other two problems concerns variants of subband coding, specifically subband coding of cyclostationary signals and the multiple description coding. The paper demonstrates that despite the different antecedents of these three applications, underlying each is the same optimization problem. We show how this problem can be solved through the use of the theory of majorization, [8]. We begin by motivating the three problems in question.

1.1. Multiuser DMT:

DMT has been adopted as the signaling standard in Asymmetric Digital Subscriber Lines (ADSL), [12] and has been proposed as the modulation scheme of choice in the Mill Bahama and Magic Wand wireless ATM systems, [13]. Indeed in advocating DMT over CDMA, the following point is made in [14]: "A spreading factor of 85 (13 kb/s voice) or 128 (8kb/s voice) (for CDMA) is used with IS-95 to provide about 20 dB of processing gain. At much higher bit rates, CDMA systems must either reduce the processing gain or expand the bandwidth, but neither may be an attractive alternative."

We consider DMT in a multiuser environment. Thus the DMT system studied here supports multiple users, with varying quality of service (QoS) requirements, quantified by their respective bit rate and symbol error rate (SER) specifications. Specifically, consider the DMT system as in fig. 1 which depicts an M-subchannel filter bank model of a DMT system. We consider an overinterpolated ($N > M$) filter bank as the transceiver. We assume that the channel $C(z)$ is FIR of length κ (preequalization is assumed to have been done), and $v(n)$ is additive colored noise with known spectrum. Thus for example $v(n)$ could represent cochannel interference. Note, [10] provides models for cochannel interference in a variety of settings. To mitigate intersymbol interference (ISI), a form of redundancy is incorporated by choosing $N = M + \kappa$. The transmitting filter, $F_k(z) = \sum_{i=0}^{M-1} z^{-i} G_{ik}$, and $H_k(z) = \sum_{i=0}^{N-1} z^i S_{ki}$, act as modulating and demodulating transforms respectively. In a DFT based DMT implementation [1], the IDFT and DFT are used as the modulating and demodulating transforms respectively.

In this paper, as in [5] we will consider more general transformations leading to a *generalized DMT* system. To capture a multiuser environment, we assume that there are r-users each having been assigned L subchannels, i.e. $M = Lr$. Further the k-th user requires a bit rate of t_k, and an SER of no more than η_k. Our goal is to select F_i and H_i, and distribute the bit rates among the various sub-channels to achieve the above specifications with the *minimum possible transmitted power*, given the knowledge of $C(z)$ and the spectrum of $v(n)$. The problem addressed here thus directly generalizes that in [5], who also address the same power minmization issue, but assuming a single user subject to only one bit rate and SER constraint. The multiuser setting renders the optimization problem highly nontrivial in comparison to the single user case as will be shown.

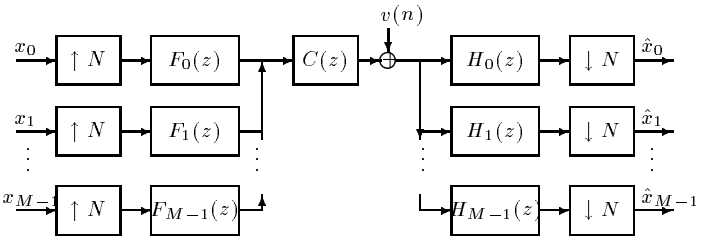

Figure 1. Filter bank based DMT model.

*Department of Electrical and Computer Engineering, The University of Iowa, Iowa City, IA-52242, USA, dasgupta@eng.uiowa.edu and pashish@icaen.uiowa.edu. Supported by ARO contract DAAD19-00-1-0534

1.2. Multiple Description Coding (MDC)

Multiple description coding is a variant of subband coding in which different parts of the signal to be coded have different bit budget requirements. Specifically in fig. 2 assume $M = Lr$ the Q_i are b_i bit quantizers that are subject to r separate average bit rate constraints. The goal in MDC is to have essentially r redundant coders as insurance against failure of one or more. Thus, channels $\{L(j-1)+1, \cdots, L(j-1)+L-1\}$ represent the j-th coder. Past work optimization related to MDC has focussed on the two coder case, with optimization directed at minimizing the average distortion subject to the failure of one coder, [15]-[16]. By contrast our goal is to optimize in the failure free case. Specifically, we select the LTI filters F_i, H_i, and allocate bits among the Q_i, subject to the bit rate constraints specified by the problem, to minimize the average output distortion variance. The optimization occurs under an orthonormality condition, specifically that the arrgangements to the left and right of the quantizers are *all pass*.

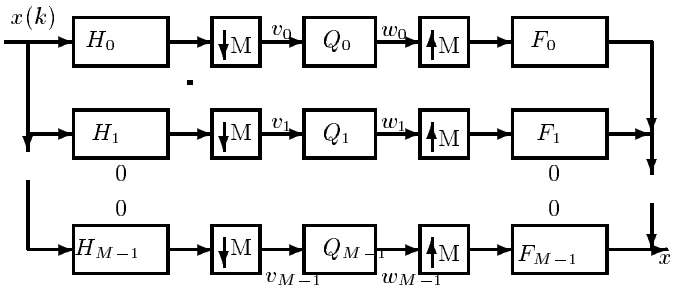

Figure 2. A Maximally Decimated Uniform Filter Bank

1.3. Subband Coding of Cyclostationary Signals

We consider optimum orthonormal subband coding of zero mean wide sense cyclostationary (WSCS) signals. A signal, $x(k)$ is WSCS with period N if for all k, l:

$$\mathcal{E}[x(k)x^*(l)] = \mathcal{E}[x(k+N)x^*(l+N)],$$

where $\mathcal{E}[\cdot]$ denotes the expectation operator.A wide variety of man made signals encountered in communication, telemetry, radar and sonar systems, as well as several generated by nature [6], are WSCS. Examples of manmade signals exhibiting cyclostationarity include signals found in amplitude, phase and frequency modulation systems, periodic keying of amplitude, phase and frequency in digital modulation systems, and periodic scanning in television, facsimile and some radar systems, [6]. Further, [7] demonstrates that WSCS models provide more accurate descriptions of speech signals than do traditional WSS models.

We assume that the filter bank is orthonormal. That is, for all square summable inputs $x(k)$, the combined energy of the M subband signals $v_i(k)$ equals the energy in $x(k)$, and in the absence of the quantizers the filter bank output $\hat{x}(k)$ matches $x(k)$ for all $x(k)$. It is easy to show that under these conditions the subband signals are themselves WSCS with period N. We adopt a *Periodically Dynamic Bit Allocation* (PDBA) scheme where we choose each $b_i(k)$ to be N-periodic, that is

$$b_i(k+N) = b_i(k). \tag{1..1}$$

Our goal is to select $b_i(k)$ and the filters $H_i(k,z)$ and $F_i(k,z)$ so that the *average* variance of $\hat{x}(k) - x(k)$ is minimum, subject to orthonormality and the constraint that the average bit rate at each time instant is constant.

1.4. Outline

In Section 2. we expose the commonality of the underlying optimzation problems. Section 3. reviews the theory of majorization and explains its applicability to the solutions we seek. Section 4. describes the optima. Section 5. is the Conclusion.

2. FORMULATION

Underlying each of the three problems there are two essential tasks. *Optimum Bit Allocation (OBA)* that given a selection of the filters, distributes the bits among the various subchannels subject to the bit rate constarints. *Filter Selection* which involves selecting the filters in an optimal way. In this section we will focus on developing the objective functions and demonstrating that they reduce to the same form under OBA.

2.1. DMT

Generally, to preserve orthogonality $G = [G_{ij}]_{i,j=1}^{M}$ is unitary i.e.

$$GG^H = I. \tag{2..2}$$

One can show, [5], under mild assumptions on $C(z)$, that given any G as in (2..2), $H_i(z)$ can be found to render the Perfect Reconstruction (PR), condition:

$$\hat{x}_i(n) = x_i(n), \quad \forall i \in \{0, \cdots, M-1\}.$$

Let the input power in the j-th subband of the k-th user be $\sigma^2_{x_{j,k}}$. Due to PR, this is also the output signal power $\sigma^2_{\hat{x}_{j,k}}$ in the j-th subband of the k-th user. Let the output noise power in this subband be $\sigma^2_{e_{j,k}}$, and $b_{j,k}$ be the number of bits allocated in this subchannel. Due to different QoS requirements, we may have different bit rate constraints for the users. The average number of bits for the k-th user is $b_k = \frac{1}{L}\sum_{j=0}^{L-1} b_{j,k}$. However we need to account for the reduction in bit rate due to the zero padding. The average bit budget for the k-th user is then $t_k = \frac{L}{N} b_k = \frac{1}{N}\sum_{j=0}^{L-1} b_{j,k}$.

With a high bit rate assumption made on the modulation system, we have, [5], for the k-th user

$$\sigma^2_{x_{j,k}} = c_k 2^{2b_{j,k}} \sigma^2_{e_{j,k}}$$

where the constant c_k depends on the SER η_k. We seek to minimize the average transmission power given by

$$f = \frac{1}{M}\sum_{k=1}^{r}\sum_{j=0}^{L-1} \sigma^2_{x_{j,k}} \tag{2..3}$$

$$= \frac{1}{M}\sum_{k=1}^{r}\sum_{j=0}^{L-1} c_k 2^{2b_{j,k}} \sigma^2_{e_{j,k}} \tag{2..4}$$

subject to the bit rate budgets

$$t_k = \frac{1}{N}\sum_{j=0}^{L-1} b_{j,k}, \quad k = 1, \ldots, r, \tag{2..5}$$

and the PR requirement. Now apply the AM-GM inequality that states that the arithmetic mean is always greater than the geometric mean, with equality iff the numbers whose means they represent are identical. Thus,

$$f = \frac{1}{M}\sum_{k=1}^{r}\sum_{j=0}^{L-1} c_k 2^{2b_{j,k}}\sigma^2_{e_{j,k}} \tag{2..6}$$

$$\geq \frac{L}{M}\sum_{k=1}^{r} c_k\Big(\prod_{j=0}^{L-1} 2^{2b_{j,k}}\sigma^2_{e_{j,k}}\Big)^{1/L} \tag{2..7}$$

$$= \frac{c}{r}\sum_{k=1}^{r} c_k\big(2^{2Nt_k}\prod_{j=0}^{L-1}\sigma^2_{e_{j,k}}\big)^{1/L} \tag{2..8}$$

with equality holding iff for all i, k:

$$c_k\big(2^{2Nt_k}\prod_{j=0}^{L-1}\sigma^2_{e_{j,k}}\big)^{1/L} = c_i\big(2^{2Nt_i}\prod_{j=0}^{L-1}\sigma^2_{e_{j,i}}\big)^{1/L}. \tag{2..9}$$

This is the *optimum bit allocation strategy.* The optimal transceiver design is to find *unitary matrix* G so as to minimize

$$J = \sum_{k=1}^{r}(\alpha_k\prod_{j=0}^{L-1} a_{j,k})^{1/L} \tag{2..10}$$

where

$$\alpha_k = c_k 2^{2Nt_k} \quad a_{j,k} = \sigma^2_{e_{j,k}}. \tag{2..11}$$

One can show that the quantities $\sigma^2_{e_{j,k}}$ are the diagonal elements of R_e given by

$$R_e = G_0^T R_{\tilde{e}} G_0, \tag{2..12}$$

where $R_{\tilde{e}}$ is a known matrix obtained from the statistics of $v(n)$.

2.2. MDC

In this case the bit budget constraint is:

$$\sum_{i=0}^{L-1} b_{jL+i} = B_j \quad \forall j \in \{0, \cdots, r-1\}. \tag{2..13}$$

One must select the LTI filters F_i, H_i to be such that in the absence of quantizers $\hat{x}(k) = x(k)$, i.e. the filter bank is PR. In addition one imposes the requirement that $E(z)$, the $M \times M$, M-fold lifted equivalent of the arrangement to the left of the quantizers is *all pass.* Then the goal is to select all pass $E(z)$ and allocate bits among the subbands, subject to (2..13), and PR, so that the average quantizer induced mean-square distortion in $\hat{x}(k)$ is minimized. Under high bit rates the quantizer noise model is [11],

$$w_i(k) = v_i(k) + q_i(k)$$

where $q_i(k)$ is zero mean, white, independent from $v_i(k)$ and has variance

$$\sigma^2_{q_i} = c2^{-2b_i}\sigma^2_{v_i}. \tag{2..14}$$

The average output distortion is then given by:

$$\frac{1}{Lr}\sum_{k=0}^{r-1}\sum_{j=0}^{L-1}\sigma^2_{q_{jL+k}} \tag{2..15}$$

Because of (2..14) under optimum bit allocation one can show that the optimization problem reduces to finding an all pass $M \times M$, $E(z)$, so that (2..10) is minimized with $\alpha_k = 1$ and $a_{j,k}$ the variance of v_{jL+i}. Notice in this case one must find the all pass *operator* $E(z)$ and that the variance of v_{jL+i} are the diagonal elements of the matrix

$$\frac{1}{2\pi}\int_0^{2\pi} S_{\bar{\mathbf{v}}}(\omega)d\omega \tag{2..16}$$

and that

$$S_{\bar{\mathbf{v}}}(\omega) = E(e^{-j\omega})S_{\bar{x}}(\omega)\left[E(e^{-j\omega})\right]^{\dagger} \tag{2..17}$$

where $S_{\bar{x}}(\omega)$ is the known Power Spectral Density (PSD) matrix of the vector

$$[x(k), x(k-1), \cdots, x(k-Lr+1]^T.$$

Of course the all pass constraint reduces to

$$E(e^{-j\omega})\left[E(e^{-j\omega})\right]^{\dagger} = I. \tag{2..18}$$

2.3. WSCS

Suppose, now $x(k)$ in fig. 2 is has N-periodic second order statistics. Then the goal is to select N-periodic H_i and F_i, and bit allocation to minimize the distortion in $\hat{x}(k)$, subject to PR, and the condition that, $E(z)$ the $NM \times NM$, NM-fold lifted version of the arrangement to the left of the quantizers is *all pass.* In this case we select the b_i to be N-periodic and subject to the Periodically Dynamic Bit Allocation: with $b_i(k+N) = b_i(k)$ i.e.

$$b = \frac{1}{M}\sum_{i=0}^{M-1} b_i(k).$$

Clearly, the subband signals $v_i(k)$ are themselves WSCS with period N, that is

$$\sigma^2_{v_i}(k) = \sigma^2_{v_i}(k+N).$$

We will assume that the quantizers are modeled by additive zero mean noise sources, independent of the $v_i(k)$, with variances of the form

$$\sigma^2_{q_i}(k) = c2^{-2b_i(k)}\sigma^2_{v_i}(k). \tag{2..19}$$

Note that under (1..1), $\sigma^2_{q_i}(k)$ are N-periodic. Then the distortion $\hat{q}(k) = \hat{x}(k) - x(k)$ is *WSCS with period* MN, [17]. We propose to minimize the *average* variance of $\hat{q}(k)$,

$$\frac{1}{MN}\sum_{k=0}^{MN-1}\sigma^2_{\hat{q}}(k) = \frac{1}{MN}\sum_{k=0}^{N-1}\sum_{l=0}^{M-1}\sigma^2_{q_i}(k) \tag{2..20}$$

Under optimum bit allocation one can show that one must now find all pass $E(z)$ so that the following is minimized:

$$J_{SBC} = \sum_{j=0}^{N-1} \left(\prod_{i=0}^{M-1} \sigma_{v_i}^2(j) \right)^{1/M} . \qquad (2..21)$$

Note the similarity to (2..10). Again $\sigma_{v_i}^2(j)$ arte the diagonal elements of a matrix as in (2..16), with (2..17) and (2..18) in force. Now however, $S_{\tilde{x}}(\omega)$ and $S_{\tilde{\mathbf{V}}}(\omega)$ are respectively, the PSD's of

$$\begin{aligned} \tilde{x}(k) &= [x_0(Nk), \ldots, x_0(NK-N+1), \\ &\quad \ldots, x_{M-1}(Nk), \ldots, x_{M-1}(Nk-N+1)], \end{aligned}$$

$$\begin{aligned} \tilde{\mathbf{V}}(k) &= [v_0(Nk), \ldots, v_0(NK-N+1), \\ &\quad \ldots, v_{M-1}(Nk), \ldots, v_{M-1}(Nk-N+1)]. \end{aligned}$$

3. MAJORIZATION

We define majorization and Schur concavity [8].

Definition 3..1 *Consider two sequences $x = \{x_i\}_{i=1}^n$ and $y = \{y_i\}_{i=1}^n$ with $x_i \geq x_{i+1}$ and $y_i \geq y_{i+1}$. Then we say that y majorizes x, denoted as $x \prec y$, if the following holds with equality at $k = n$*

$$\sum_{i=1}^{k} x_i \leq \sum_{i=1}^{k} y_i, \quad 1 \leq k \leq n.$$

Definition 3..2 *A real valued function $\phi(z) = \phi(z_1, \ldots, z_n)$ defined on a set $\mathcal{A} \subset R^n$ is said to be Schur concave on $\mathcal{A}$ if*

$$x \prec y \quad on\, \mathcal{A} \quad \Rightarrow \quad \phi(x) \geq \phi(y).$$

We will now state a theorem that results in a test for strict Schur concavity. We denote

$$\phi_{(k)}(z) = \frac{\partial \phi(z)}{\partial z_k} \quad and \quad \phi_{(i,j)}(z) = \frac{\partial^2 \phi(z)}{\partial z_i \partial z_j}.$$

Theorem 3..1 *Let $\phi(z)$ be a scalar real valued function defined and continuous on $\mathcal{D}$, and twice differentiable on the interior of $\mathcal{D}$. Then $\phi(z)$ is strictly Schur concave on $\mathcal{D}$ iff (i) ϕ is symmetric in its arguments, (ii) $\phi_{(k)}(z)$ is increasing in k, and (iii) $\phi_{(k)}(z) = \phi_{(k+1)}(z) \Rightarrow \phi_{(k,k)}(z) - \phi_{(k,k+1)}(z) - \phi_{(k+1,k)}(z) + \phi_{(k+1,k+1)}(z) < 0$.*

Theorem 3..2 *If H is an $n \times n$ hermitian matrix with diagonal elements $h_1, \ldots, h_n$ and eigenvalues $\lambda_1, \ldots, \lambda_n$, then $h \prec \lambda$ on R^n.*

Now turn to (2..10), the common objective function for all three problems. Suppose, given $\{a_{j,k}\}$ one were to seek the rearrangement of these to achieve the minimum value possible. Then it follows from [18] that the optimum arrangement must obey the following property:

$$a_{m,k_1} \geq a_{n,k_2} \Rightarrow \alpha_{k_1} \prod_{j \neq m}^{L-1} a_{j,k_1} \leq \alpha_{k_2} \prod_{j \neq n}^{L-1} a_{j,k_2} \qquad (3..22)$$

and

$$\alpha_m \geq \alpha_n \Rightarrow \prod_{j=0}^{L-1} a_{j,m} \leq \prod_{j=0}^{L-1} a_{j,n}. \qquad (3..23)$$

Call J under such an *optimum arrangement* J^*. Then one can show from Theorem 3..1 that:

Theorem 3..3 *The real valued scalar function J as defined in (2..10) under the optimality conditions (3..22-3..23) is strictly Schur concave.*

4. THE SOLUTION

All three problems have remarkably similar structure. Using the theory of majorization, and in particular Theorems 3..2 and 3..3, one can show the following.

- For DMT, the optimizing G is to within a permutation matrix the Karunen-Loeve Transform matrix of the autocorrelation matrix of the M-fold lifted version of $v_i(n)$.
- For Multiple Description Coding the solution is as follows. Suppose $S_{\tilde{\mathbf{V}}}(\omega)$ is the Power Spectral Density (PSD) matrix of the vector of $v_i(n)$ in fig. 2. Suppose $\Lambda(\omega)$ is the diagonal matrix of the eigenvalues of $S_{\tilde{\mathbf{V}}}(\omega)$, $\lambda_i(\omega)$, with $\lambda_i(\omega) \geq \lambda_{i+1}(\omega)$. Define $\Omega(\omega)$ to be the matrix that is unitary at all ω and in addition forces
  $$\Omega(\omega) S_{\tilde{\mathbf{V}}}(\omega) \Omega^H(\omega) = \Lambda(\omega).$$
  Then for a constant permutation matrix, P, $E(e^{j\omega}) = P\Omega(\omega)$.
- The solution for the WSCS problem is trivially similar.

Here the frequency invariant permutation matrix is used to achieve the optimum arrangement exemplified in (3..22-3..23).

5. CONCLUSION

We have shown that three problems in signal processing and communications, with differing motivations and genesis have similar solutions. All three benefit from the powerful and elegant theory of Majorization. Given that both MDC and WSCS problems relate to subband coding similarity in their solutions is not a surprise. That they are also equivalent to the optimal DMT problem can be attributed to the fact that the optimum DMT can be interpreted as a dual problem to subband coding.

REFERENCES

[1] J.S. Chow, J.C. Tu, J.M. Cioffi, "A discrete multitone transceiver system for HDSL applications", *IEEE Journal on Selected Areas in Communications*, pp 895-908, Aug 1991.

[2] S. Dasgupta, C. Schwarz and B.D.O. Anderson, "Optimal subband coding of cyclostationary signals", *IEEE International Conference on Acoustics, Speech, and Signal Processing*, pp 1489-1492, Mar 1999.

[3] L.M.C. Hoo, J. Tellado, J.M. Cioffi, "Discrete dual QoS loading algorithms for multicarrier systems ", *IEEE International Conference on Communications*, pp 796-800, 1999.

[4] B.S. Krongold, K. Ramchandran, D.L. Jones, "Computationally efficient optimal power allocation algorithms for multicarrier communication systems", *IEEE Transactions on Communications*, pp 23-27, Jan 2000.

[5] Y. P. Lin, S.M. Phoong, "Perfect discrete multitone modulation with optimal transceivers", *IEEE Transactions on Signal Processing*, pp 1702 -1711, June 2000.

[6] W. A. Gardner "Exploitation of spectral redundancy in cyclostationary signals", *IEEE Signal Processing Magazine*, pp 14-37, April 1991.

[7] Y. Grenier, "Time dependent ARMA modelling of nonstationary signals", *IEEE Transactions on Accoustics, Speech, and Signal Processing*, pp 899-911, 1983.

[8] A. W. Marshall and I. Olkin, *Inequalities: Theory of Majorization and its applications*, Academic Press, 1979.

[9] A. Scaglione, S. Barbarossa, G.B. Giannakis, "Filterbank transceivers optimizing information rate in block transmissions over dispersive channels", *IEEE Transactions on Information Theory*, pp 1019-1032, Apr 1999.

[10] T. Starr, J.M. Cioffi, P. Silverman, *Understanding Digital Subscriber Line Technology*, Prentice Hall, 1999.

[11] P.P. Vaidyanathan, *Multirate Systems and Filter Banks*, Prentice Hall, 1992.

[12] Asymmetric Digital Subscriber Line (ADSL) Metallic Interface, ANSI T1E1.4/94-007R8, 1994.

[13] K. Pahlvan, A. Zahedi and P. Krishnamurthy, "Wideband local access: Wireless LAN and wireless ATM", *IEEE Communications Magazine*, pp 35-40, November 1997.

[14] L. J. Cimini, J. C. I. Chuang, and N. Sollenberger, "Advanced cellular internet service (ACIS)", *IEEE Communications Magazine*, pp 35-40, October 1998.

[15] X. Yang and K. Ramachandran, "Optimal subband filters for multidescription coding", *IEEE Transactions on Information Theory*, 2001.

[16] P.L. Dragotti, S.D. Servetto and M. Vetterli, "Analysis of optimal filter banks for multidescription quantization", *Proc. IEEE ICIP* , March 2000. 2000.

[17] V. P. Sathe and P. P. Vaidyanathan, "Effects of Multirate Systems on the Statistical Properties of Random Signals", *IEEE Transactions on Signal Processing* , pp 1766-1777, Aug 1995.

[18] G. M. Hardy, J. E. Littlewood and G. Polya, *Inequalities*, Cambridge University Press, 1934.

OPTIMUM COMPACTION FILTERS FOR SUBBAND CODING OF WIDESENSE CYCLOSTATIONARY SIGNALS

Ashish Pandharipande and Soura Dasgupta

Electrical and Computer Engineering Department, The University of Iowa, Iowa City, IA-52242, USA.
Email: pashish@engineering.uiowa.edu and dasgupta@eng.uiowa.edu

ABSTRACT

In this paper, we develop an optimum compaction filter based design of filter banks for the subband coding of widesense cyclostationary (WSCS) signals. The design of the optimal orthonormal filter bank is specified in terms of optimal compaction filters. Each filter is designed by just the apriori knowledge of the cyclic autocorrelation of the input WSCS signal. This design theory is developed by first providing further insight to the optimal compaction filter design in the case of wide-sense stationary (WSS) signals.

1. INTRODUCTION

The energy compaction concept plays an important role in subband coding theory, and energy compaction filters find applications in the design of orthonormal subband coders. Optimality of filter banks is in the sense of maximizing coding gain, which is a measure of the distortion due to subband quantization. The optimal orthonormal subband coding of WSS and WSCS signals has been treated in [10], [11] and [1], [6] respectively. It has been shown [8], [11] that the optimal orthonormal filter bank in the WSS case can be constructed by designing the analysis filters one at a time by choosing them to be optimal compaction filters for appropriate power spectral densities (psds) derived from the input signal psd. Compaction filters thus are of interest due to their connection with optimal subband coding and principal component filter banks. Compaction filters have been treated in some detail for the WSS case in [8], [9], [11]. The compaction filter was formulated as an eigen problem in [8] and given a principal component approach. In [9], compaction filters were derived by an energy analysis. Properties of compaction filters have been further studied in [11].

In this paper, we develop the compaction filter concept in the context of WSCS signals. Cyclostationarity is exhibited by some parameters for most manmade signals encountered in communication, telemetry, radar, and sonar systems, [2]. Considering these underlying periodicities and modeling the random signals as cyclostationary can lead to improvements in performance of signal processors.

A signal $x(k)$ is WSCS with period M if for all k, l:

$$\mathcal{E}[x(k)x^*(l)] = \mathcal{E}[x(k+M)x^*(l+M)],$$

where $\mathcal{E}[\cdot]$ denotes the expectation operator. The subband coder considered is an N-channel uniform maximally decimated filter bank depicted in fig. 1. We will consider a 2-channel ($N = 2$) subband coder in this paper to illustrate the ideas. Here $x(k)$ is WSCS with period M and at time k, Q_i is a $b_i(k)$-bit quantizer. When $x(k)$ is Wide Sense Stationary (WSS) one selects the analysis filters $H_i(k, z)$ and the synthesis filters $F_i(k, z)$ to be linear time invariant (LTI). Since $x(k)$ here is WSCS with period M, we assume that these filters are *Linear Periodically Time Varying (LPTV) with period* M. A linear filter with impulse response $h(k, l)$ is called M-periodic, if for all k, l:

$$h(k, l) = h(k + M, l + M). \tag{1.1}$$

The time index k in $H_i(k, z)$ and $F_i(k, z)$ recognizes their lack of time invariance.

Given the autocorrelation of the WSCS signal $x(k)$, the psd matrix of the M-blocked version of $x(k)$, which is WSS, can be found and will be assumed to be known. We are thus interested in designing the filters $H_i(k, z)$, $F_i(k, z)$ by an energy compaction approach. We shall suitably extend the idea of an optimum compaction filter for WSCS signals in this paper. We show that the optimal orthonormal filter bank for a WSCS input can be designed by choosing each analysis filter to be an optimum compaction filter for an appropriately "peeled-off" signal, with the peeled-off signal derived from the input signal. We first provide useful insight to the compaction filter design for WSS signals. This analysis is then paralleled to the case when the input to the filter bank is WSCS.

In Section 2, we recapitulate the optimum compaction filter design for WSS signals. The results essentially provide a different interpretation to the compaction process described in [11]. Section 3 then introduces the notion of an

This work was supported by US Army contract, DAAAD19-00-1-0534, and NSF grants ECS-9970105 and CCR-9973133

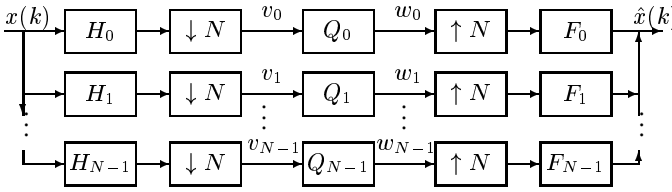

Fig. 1. An N-channel filter bank as subband coder

optimum compaction filter as applicable to WSCS inputs, and then describes the energy compaction approach to subband coder design when the input signals are WSCS. Section 4 sums the contributions of this paper.

Notation: For compactness, we use $[x(0:1:N-1)]$ to denote the vector

$$[x(0), x(1), \ldots, x(N-1)],$$

and $[x(0:-1:N-1)]$ to denote the vector

$$[x(0), x(-1), \ldots, x(-N+1)].$$

We use $[X(z)]^\dagger$ to denote the transposed conjugate of the matrix $[X(z^{-1})]$.

2. OPTIMUM COMPACTION FILTERS FOR WSS SIGNALS

Consider fig. 2. The filter $H(z)$ is said to be an *optimum compaction filter* for the zero-mean WSS input signal $x(k)$ if it maximizes the output variance σ_v^2 subject to the constraint that $|H(\omega)|^2$ is Nyquist-N, that is,

$$\sum_{k=0}^{N-1} |H(\omega - \frac{2\pi k}{N})|^2 = N, \quad \forall \omega.$$

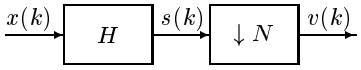

Fig. 2. Illustration for compaction filter

We now state a result which essentially describes the optimum compaction filter design process for WSS signals.

Theorem 2.1 *Consider fig. 1 with WSS $x(k)$. Given that $H_0(\omega)$ is an optimum compaction filter of the signal $x(k)$. Then the analysis filter $H_1(\omega)$ is an optimum compaction filter of $x^{(1)}(k) = x(k) - \frac{H_0(\omega)}{\sqrt{N}} x(k), \ldots,$ and $H_{N-1}(\omega)$ is an optimum compaction filter of $x^{(N-1)}(k) = x^{(N-2)}(k) - \frac{H_{N-2}(\omega)}{\sqrt{N}} x^{(N-2)}(k)$.*

Observe that Theorem 2.1 is a different interpretation to the design methodology discussed in [11].

3. OPTIMUM COMPACTION FILTERS FOR WSCS SIGNALS

Define for $i = 0, 1$,

$$x_i(k) = x(2k-i), \quad s_i(k) = s(2k-i),$$

and denote the M blocked versions of $x_i(k), s_i(k), i = 0, 1$ as

$$\tilde{x}_i(k) = [x(2(Nk - (0:1:N-1)) - i)]^T,$$
$$\tilde{s}_i(k) = [s(2(Nk - (0:1:N-1)) - i)]^T.$$

Call

$$\tilde{x}(k) = [\tilde{x}_0^T(k), \tilde{x}_1^T(k)]^T,$$
$$\tilde{s}(k) = [\tilde{s}_0^T(k), \tilde{s}_1^T(k)]^T.$$

Every LPTV system with period M can be interpreted as a multiple-input/multiple-output system LTI system with M inputs and M outputs. Let $\tilde{h}_{mn}(k,l)$ be the $M \times M$ impulse response matrix relating $\tilde{x}_n(k)$ and $\tilde{s}_m(k)$. Obviously this is an LTI system, and we can define

$$\tilde{H}_{mn}(z) = \sum_k \tilde{h}_{mn}(k) z^{-k}.$$

Note that $\tilde{H}_{00}(z)$ and $\tilde{H}_{01}(z)$ respectively represent the LTI systems relating the blocked even and odd samples of the input of the M-periodic system $H(k,z)$ to the *blocked even samples* of the output of $H(k,z)$.

Define the $2M \times 1$ vector

$$\tilde{v}(k) = [v_0(Nk-(0:1:N-1)), v_1(Nk-(N-1:-1:0)]^T.$$

Even when the analysis and synthesis filters are LPTV, the polyphase representation shown in fig. 3 still holds, [12]. The analysis and synthesis sides in fig. 1 are respectively replaced by the $2M \times 2M$ LTI operators $\tilde{E}(z)$, $\tilde{R}(z)$. Note that the operator $\tilde{E}(z)$ relates the $2M \times 1$ vectors $\tilde{x}(k)$ and $\tilde{v}(k)$.

Perfect reconstructability reduces to the requirement that $\tilde{R}(z) = \tilde{E}^{-1}(z)$, and orthonormality to the requirement that for all ω

$$[E(\omega)]^\dagger E(\omega) = [R(\omega)]^\dagger R(\omega) = I.$$

Since $S_{\tilde{x}}(\omega)$, the psd matrix of $\tilde{x}(k)$, is positive definite Hermitian symmetric, it can be expressed as

$$S_{\tilde{x}}(\omega) = \tilde{U}(\omega)\tilde{\Lambda}(\omega)\left[\tilde{U}(\omega)\right]^\dagger \tag{3.2}$$

with $\tilde{U}(\omega)$ unitary at all ω, and

$$\tilde{\Lambda}(\omega) = \text{diag}\,\{\tilde{\lambda}_0(\omega), \cdots . \tilde{\lambda}_{2N-1}(\omega)\} \tag{3.3}$$

obeying at all ω

$$\tilde{\lambda}_i(\omega) \geq \tilde{\lambda}_{i+1}(\omega) > 0. \tag{3.4}$$

Further, $S_{\tilde{v}}(\omega)$, the psd matrix of $\tilde{v}(k)$, obeys

$$S_{\tilde{v}}(\omega) = \tilde{E}(\omega) S_{\tilde{x}}(\omega) \left[\tilde{E}(\omega)\right]^{\dagger}. \tag{3.5}$$

The *canonical solution* to the subband coding problem under dynamic bit allocation and static bit allocation treated in [1], [6] respectively is given by

$$\tilde{E}(\omega) = \left[\tilde{U}(\omega)\right]^{\dagger}. \tag{3.6}$$

In this case $S_{\tilde{v}}(\omega) = \tilde{\Lambda}(\omega)$. The $H_i(k,z)$ and $F_i(k,z)$ can be obtained by unblocking $\tilde{E}(z)$ and $\tilde{E}^{-1}(z)$.

The main points of this Section are to define an optimum compaction process for WSCS signals that leads to the design of the subband coder. To do so we first define the M-periodic optimum compaction of an M-periodic WSCS process. The definition of optimum compaction of a WSS signal given earlier involves a filter $H(z)$ for which $H(z)H^*(z^{-1})$ is Nyquist-2. For an LPTV system H define the *adjoint filter* H^a whose impulse response $h^a(k,l)$ is related to the impulse response $h(k,l)$ of H by

$$h^a(k,l) = h^*(l,k). \tag{3.7}$$

Observe that the adjoint of an LTI systems with transfer $H(z)$ has transfer function $H^*(z^{-1})$. Thus the analog of a system with transfer function $H(z)H^*(z^{-1})$ in the Linear Time Varying (LTV) case, is the LTV system HH^a.

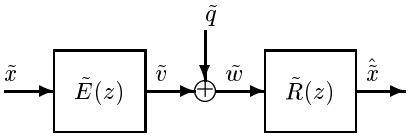

Fig. 3. Blocked polyphase representation

We now give the appropriate definition of *LTV Nyquist-2* filters. When $H(k,z)$ is M-periodic then HH^a is Nyquist-2 iff for all ω,

$$\left[\tilde{H}_{00}(\omega), \tilde{H}_{01}(\omega)\right] \begin{bmatrix} \left[\tilde{H}_{00}(\omega)\right]^{\dagger} \\ \left[\tilde{H}_{01}(\omega)\right]^{\dagger} \end{bmatrix} = I. \tag{3.8}$$

We now define the optimum compaction process for WSCS signals.

Definition 3.1 *Consider fig. 2, with $x(k)$ WSCS with period M, H LPTV with period M, and $N = 2$. Then H is an optimum compaction filter for $x(k)$ if subject to HH^a being Nyquist-2, and for some index set $\{k_0, k_1, \cdots, k_{M-1}\} = \{0, \cdots, M-1\}$, it simultaneously maximizes the partial variance sums*

$$\sum_{i=0}^{l} \sigma_v^2(k_i), \tag{3.9}$$

for all $0 \le l \le M-1$.

Observe that this definition is targetted to accomodate the fact that $v(k)$ is WSCS with period M. Consequently M variance values must be considered. In the sequel, we will call an optimum compaction filter *canonical* if in (3.9),

$$k_i = i.$$

Note that even the canonical optimum compaction filter is nonunique. This is consistent with the fact that LTI optimum compaction filters for WSS processes are also nonunique, [11].

We now state the main results of this Section.

Theorem 3.1 *Consider fig. 1 with $N = 2$, $H_i(k,z)$ M-periodic, and $x(k)$ WSCS with period M. Then the $H_0(k,z)$ provided by the canonical solution (3.6) is an M-periodic canonical optimum compaction filter of $x(k)$.*

Denote by $S_{\underline{x}}(\omega)$ the $M \times M$ psd matrix of the $M \times 1$ WSS vector $\underline{x}(k)$ obtained by blocking $x(k)$. We can write

$$S_{\underline{x}}(\omega) = V(\omega)\underline{\Lambda}(\omega)[V(\omega)]^{\dagger}$$

with $V(\omega)$ unitary for all ω. Denote

$$\hat{V}(\omega) = \begin{bmatrix} V(\frac{\omega}{2}) & 0 \\ 0 & V(\frac{\omega - 2\pi}{2}) \end{bmatrix}. \tag{3.10}$$

Theorem 3.2 *Given $H_0(k,z)$ is an optimum compaction filter of the WSCS signal $x(k)$. Then the filter $H_1(k,z)$ is an optimum compaction filter of the signal obtained by unblocking the $2M \times 1$ vector $\tilde{x}^{(1)}(k) = \left[\hat{V}(\omega) - \frac{\mathbf{H}_0(\omega)}{\sqrt{2}}\right] \tilde{x}(k)$, where $\mathbf{H}_0(\omega)$, a $2M \times 2M$ matrix, is the $2M$ blocked version of $H_0(k,z)$.*

Theorem 3.1 together with 3.2 defines the optimum compaction filter design for WSCS signals.

4. CONCLUSIONS

In this paper, we presented the optimum compaction filter design for the subband coding of WSCS signals. We first gave a different interpretation to the compaction process in the case of subband coding of WSS signals. The design procedure was then extended to WSCS signals by considering a 2-channel subband coder. We showed that the analysis filters of the orthonormal filter bank can be designed sequentially by an optimal compaction process, with the optimum compaction filters designed with the apriori knowledge of just the second order statistics of the input WSCS signal.

5. REFERENCES

[1] S. Dasgupta, C. Schwarz, B.D.O. Anderson, "Optimum subband coding of cyclostationary signals", *IEEE International Conference on Acoustics, Speech and Signal Processing - Proceedings*, pp 1489-1492, Mar 15-Mar 19 1999.

[2] W. A. Gardner, "Exploitation of spectral redundancy in cyclostationary signals", *IEEE Signal Processing*, pp 14-36, Apr 1991.

[3] R.A. Horn, C.R. Johnson, *Matrix Analysis*, Cambridge University Press, 1999.

[4] P. Moulin, K.M. Mihcak, "Theory and design of signal-adapted FIR paraunitary filter banks", *IEEE Transactions on Signal Processing*, pp 920-929, Apr 1998.

[5] S. Ohno, H. Sakai, "Optimization of filter banks using cyclostationary spectral analysis", *IEEE Transactions on Signal Processing*, pp 2718 -2725, Nov 1996.

[6] A. Pandharipande, S. Dasgupta, "Subband coding of cyclostationary signals with static bit allocation", *IEEE Signal Processing Letters*, pp 284 -286, Nov 1999.

[7] V. Sathe, P.P. Vaidyanathan, "Effects of multirate systems on the statistical properties of random signals", *IEEE Transactions on Signal Processing*, pp 131-146, Jan 1993.

[8] M.K. Tsatsanis, G.B. Giannakis, "Principal component filter banks for optimal multiresolution analysis", *IEEE Transactions on Signal Processing*, pp 1766-1776, Aug 1995.

[9] M. Unser, "On the optimality of ideal filters for pyramid and wavelet signal approximation", *IEEE Transactions on Signal Processing*, pp 3591-3596, Dec 1993.

[10] P.P. Vaidyanathan, "Properties of optimal compaction filters in subband coding", *IEEE Digital Signal Processing Workshop*, pp 89-92, Sep 1-4 1996.

[11] P.P. Vaidyanathan, "Theory of optimal orthonormal subband coders", *IEEE Transactions on Signal Processing*, pp 1528-1543, Jun 1998.

[12] P.P. Vaidyanathan, S.K. Mitra, "Polyphase networks, block digital filtering, LPTV systems, and alias-free QMF banks: a unified approach based on pseudocirculants", *IEEE Transactions on Acoustics, Speech, and Signal Processing*, pp 381-391, Mar 1988.

OPTIMAL TRANSCEIVERS FOR DMT BASED MULTIUSER COMMUNICATION

Ashish Pandharipande and Soura Dasgupta

Electrical and Computer Engineering, The University of Iowa, Iowa City, IA-52242, USA.
Email: pashish@engineering.uiowa.edu and dasgupta@eng.uiowa.edu

ABSTRACT

This paper considers discrete multitone modulation (DMT) for multiuser communications where different users are supported by the same system. These users may have differing quality of service (QoS) requirements, as quantified by their respective bit rate and symbol error rate specifications. Our goal is to minimize the transmitted power given the QoS specifications for the different users, subject to the knowledge of colored interference at the receiver input. In particular we find an optimum bit loading scheme that distributes the bit rate transmitted across the various subchannels belonging to the different users, and subject to this bit allocation, determine an optimum transceiver.

1. INTRODUCTION

The discrete multitone modulation (DMT) channel coding scheme has established itself as an effective high rate data communication technique in both wired and wireless environments and is used for example in ADSL and HDSL, [1]. We consider DMT in a multiuser environment. Thus the DMT system studied here supports multiple users, with varying quality of service (QoS) requirements, quantified by their respective bit rate and symbol error rate (SER) specifications.

Specifically, consider the DMT system as in fig. 1 which depicts an M-subchannel filterbank model of a DMT system. We consider an overinterpolated ($N > M$) filterbank as the transceiver. We assume that the channel $C(z)$ is FIR of lenth κ (preequalization is assumed to have been done), and $v(n)$ is additive colored noise with known spectrum. Thus for example $v(n)$ could represent co-channel interference. Note, [8] provides models for cochannel interference in a variety of settings. To mitigate intersymbol interference (ISI), a form of redundancy is incorporated by choosing $N = M + \kappa$. The transmitting filters, $F_k(z)$, and the receiving filters, $H_k(z)$, are constrained to length N, and act as modulating and demodulating transforms respectively. In a DFT based DMT implementation [1], the IDFT and DFT are used as the modulating and demodulating transforms respectively.

In this paper, as in [5] we will consider more general transformations leading to a *generalized DMT* system. To capture a multiuser environment, we assume that there are L-users each having been assigned M/L subchannels. Further the k-th user requires a bit rate of t_k, and an SER of no more than η_k. Our goal is to select F_i and H_i, and distribute the bit rates among the various sub-channels to achieve the above specifications with the *minimum possible transmitted power*. The problem addressed here thus directly generalizes that in [5], which also addresses the same power minimization issue, but assuming a single user subject to only one bit rate and SER constraint. The multiuser setting renders the optimization problem highly nontrivial in comparison to the single user case. Further we show as much as 8 dB and 12 dB savings in transmit power in our simulations with general DMT systems over DFT based DMT systems with optimal bit allocation and no bit allocation respectively.

Related literature includes [4] which develops fast loading algorithms using table lookups and a fast Lagrange bisection method for a single user setting. [7] considers a single user optimization of the transceiver mutual information. [3], considers the optimum bit loading problem when two users are present.

Section 2, defines the generalized DMT system and formulates a precise mathematical problem. Sections 3 and 4 respectively consider the bit rate allocation and filterselection problems. Section 5 gives simulations.

2. DMT BASED MULTIUSER SYSTEM MODEL

In this Section we give some preliminaries. Specifically, in Section 2.1, we recount the details of the generalized DMT system provided in [5]. Section 2.2 provides a precise optimization problem.

2.1. Polyphase representation of the DMT system

Consider the filterbank based DMT model in fig. 1. $v(n)$ is a zero mean wide sense stationary additive noise. As

This work was supported by US Army contract, DAAAD19-00-1-0534, and NSF grants ECS-9970105 and CCR-9973133

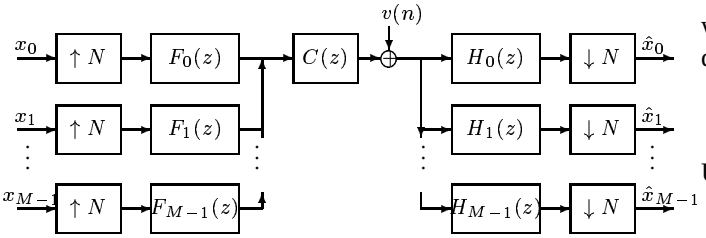

Fig. 1. Filter bank based DMT model.

the filters $F_k(z)$ and $H_k(z)$ have lengths $\leq N$, we may write the following polyphase decompositions: $F_k(z) = \sum_{i=0}^{N-1} z^{-i} G_{i,k}$, and $H_k(z) = \sum_{i=0}^{N-1} z^{i} S_{k,i}$, with constant $G_{i,j}$ and $S_{i,j}$. Define the $N \times M$ matrix G with ij-th element $G_{i,j}$ and the $M \times N$ matrix S with elements $S_{i,j}$. Call the constant matrices G and S the transmitting and receiving matrix repectively. Then with $\mathbf{x}$ and $\hat{\mathbf{x}}$ the vector of the signals x_i and $\hat{x}_i$, repectively, $\tilde{\mathbf{v}}$, the blocked version of $v(n)$, one has the equivalent system in fig. 2. Here the pseudocirculant matrix $\mathbf{C}(z)$ [9], is formed by the coefficients of the FIR channel $C(z) = c_0 + c_1 z^{-1} + \ldots + c_\kappa z^{-\kappa}$. It obeys:

$$\mathbf{C}(z) = \left[\begin{array}{cc} \mathbf{C_0} & \mathbf{C_1}(z) \end{array} \right] \tag{2.1}$$

where $\mathbf{C_0}$ is constant, $N \times M$, and $\mathbf{C_1}(z)$ is $N \times \kappa$. Note the knowledge of the autocorrelation of v, yields the autocorrelation matrix of $\tilde{\mathbf{v}}$.

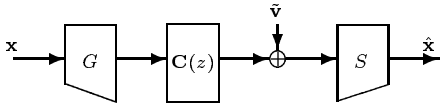

Fig. 2. Polyphase representation of the DMT system.

For DMT systems using zero padding, the transmitting and receiving matrices are respectively given by

$$G = \left[\begin{array}{c} W^\dagger \\ 0 \end{array} \right], \quad S = \Gamma^{-1} \left[\begin{array}{cc} W & W_0 \end{array} \right] \tag{2.2}$$

where W is the $M \times M$ unitary DFT matrix with $[W]_{l,m} = \frac{1}{\sqrt{M}} e^{-\frac{j2\pi lm}{M}}$, $l, m = 0, \ldots, M-1$, W_0 is the $M \times \kappa$ submatrix of W having the first κ columns of W, and Γ is the $M \times M$ diagonal matrix with elements that are the M-point DFTs of the channel impulse response, [1]. We consider more general DMT systems that can lead to reduction in sidelobes and better noise rejection properties of the filters. The transmitting matrix of such a general DMT is given by

$$G = \left[\begin{array}{c} G_0 \\ 0 \end{array} \right] \tag{2.3}$$

where G_0 is an arbitrary $M \times M$ unitary matrix. The condition for perfect reconstruction (PR) is given as

$$S\mathbf{C}(z)G = I \tag{2.4}$$

Using (2.1) and (2.3), the PR condition reduces to

$$S\mathbf{C_0}G_0 = I \tag{2.5}$$

Using singular value decomposition, $\mathbf{C_0}$ can be written as

$$\mathbf{C_0} = \underbrace{\left[\begin{array}{cc} U_0 & U_1 \end{array} \right]}_{U} \left[\begin{array}{c} \Lambda \\ 0 \end{array} \right] V^T = U_0 \Lambda V^T \tag{2.6}$$

where U and V are respectively $N \times N$ and $M \times M$ unitary matrices whose columns are the eigenvectors of $\mathbf{C_0}\mathbf{C_0}^T$ and $\mathbf{C_0}^T\mathbf{C_0}$. Λ is the $M \times M$ diagonal matrix with diagonal elements that are the singular values of $\mathbf{C_0}$.

Using (2.6), one clear choice for S satisfying (2.5) is

$$S = G_0^T V \Lambda^{-1} U_0^T \tag{2.7}$$

2.2. Problem definition

The optimum bit loading problem is to find the best bit rate allocation scheme to minimize the transmit power, under different bit rate and SER budgets of the users. The optimal transceiver is then designed to minimize the power subject to optimum bit loading.

Assume there are r users, with each user being allocated L subbands (in fig. 1, $M = rL$ and $N = M + \kappa$). Let the input power in the j-th subband of the k-th user be $\sigma^2_{x_{j,k}}$. Due to PR, this is also the output signal power $\sigma^2_{\hat{x}_{j,k}}$ in the j-th subband of the k-th user. Let the output noise power in this subband be $\sigma^2_{e_{j,k}}$, and $b_{j,k}$ be the number of bits allocated in this subchannel. Due to different QoS requirements, we may have different bit rate constraints for the users. The average number of bits for the k-th user is $b_k = \frac{1}{L}\sum_{j=0}^{L-1} b_{j,k}$. However we need to account for the reduction in bit rate due to the zero padding. The average bit budget for the k-th user is then $t_k = \frac{L}{N} b_k = \frac{1}{N}\sum_{j=0}^{L-1} b_{j,k}$.

With a high bit rate assumption made on the modulation system, we have, [5], for the k-th user

$$\sigma^2_{x_{j,k}} = c_k 2^{2b_{j,k}} \sigma^2_{e_{j,k}}$$

where the constant c_k depends on the SER η_k. We seek to minimize the average transmission power given by

$$f = \frac{1}{M} \sum_{k=1}^{r} \sum_{j=0}^{L-1} \sigma^2_{x_{j,k}} \tag{2.8}$$

$$= \frac{1}{M} \sum_{k=1}^{r} \sum_{j=0}^{L-1} c_k 2^{2b_{j,k}} \sigma^2_{e_{j,k}} \tag{2.9}$$

subject to the bit rate budgets

$$t_k = \frac{1}{N}\sum_{j=0}^{L-1} b_{j,k}, \quad k = 1, \ldots, r, \tag{2.10}$$

and the PR requirement (2.7).

3. OPTIMUM BIT ALLOCATION

The problem of minimizing (2.9) under the set of constraints (2.10) is a constrained optimization problem. Using the AM-GM[1] inequality and (2.10),

$$f = \frac{1}{M}\sum_{k=1}^{r}\sum_{j=0}^{L-1} c_k 2^{2b_{j,k}}\sigma^2_{e_{j,k}} \tag{3.11}$$

$$\geq \frac{L}{M}\sum_{k=1}^{r} c_k\Big(\prod_{j=0}^{L-1} 2^{2b_{j,k}}\sigma^2_{e_{j,k}}\Big)^{1/L} \tag{3.12}$$

$$= \frac{c}{r}\sum_{k=1}^{r} c_k\Big(2^{2Nt_k}\prod_{j=0}^{L-1}\sigma^2_{e_{j,k}}\Big)^{1/L} \tag{3.13}$$

with equality holding iff for all j, k:

$$b_{j,k} = \frac{N}{L}t_k + \frac{1}{2}log_2\Big(\prod_{j=0}^{L-1}\sigma^2_{e_{j,k}}\Big)^{1/L} - \frac{1}{2}log_2(\sigma^2_{e_{j,k}}). \tag{3.14}$$

This is the *optimum bit allocation strategy*. The optimal transceiver design is to find matrices S, G so as to minimize

$$J = \sum_{k=1}^{r}(\alpha_k\prod_{j=0}^{L-1} a_{j,k})^{1/L} \tag{3.15}$$

where

$$\alpha_k = c_k 2^{2Nt_k} \quad a_{j,k} = \sigma^2_{e_{j,k}}. \tag{3.16}$$

Observe, if one chooses $L = 2$, and $\alpha_k = \alpha$ for all k, then (3.15) reduces to the optimization function considered in [2], for the subband coding of cyclostationary signals.

Optimal arrangement: Observe, [2, 6], that given a set of positive numbers $\{\delta_k\}_{k=1}^{2l}$, $\delta_k \geq \delta_{k+1}$ the minimum among all possible $\sum\delta_{k_i}\delta_{k_j}$ is $\sum_{k=1}^{l}\delta_k\delta_{2l-k+1}$. Thus among the various permutations of $a_{j,k}$, any that minimizes (3.15) must have the following property:

$$a_{m,k_1} \geq a_{n,k_2} \Rightarrow \alpha_{k_1}\prod_{j\neq m}^{L-1} a_{j,k_1} \leq \alpha_{k_2}\prod_{j\neq n}^{L-1} a_{j,k_2} \tag{3.17}$$

and

$$\alpha_m \geq \alpha_n \Rightarrow \prod_{j=0}^{L-1} a_{j,m} \leq \prod_{j=0}^{L-1} a_{j,n}. \tag{3.18}$$

[1] The arithmetic mean (AM) of a set of positive numbers is greater than or equal to their geometric mean (GM), with equality iff all the numbers are equal.

4. OPTIMUM TRANSCEIVER DESIGN

In this Section we address the problem of filter selection to minimize (3.15). This reduces to selecting a unitary matrix G_0. Given that the matrices in (2.6) are known, (2.7) fixes S. Observe that the situation in fig. 3 prevails, and $R_{\tilde{e}}$, the autocorrelation of $\tilde{\mathbf{e}}$, is known. Further the autocorrelation matrix of $\mathbf{e}$ is given by

$$R_e = G_0^T R_{\tilde{e}} G_0, \tag{4.19}$$

and that $a_{j,k}$ in (3.15), are simply the diagonal elements of R_e.

We need a few results from the theory of majorization that will be used in solving the optimization problem at hand. We will first introduce the notion of majorization and Schur concavity [6].

Definition 4.1 *Consider two sequences $x = \{x_i\}_{i=1}^n$ and $y = \{y_i\}_{i=1}^n$ with $x_i \geq x_{i+1}$ and $y_i \geq y_{i+1}$. Then we say that y majorizes x, denoted as $x \prec y$, if the following holds with equality at $k = n$*

$$\sum_{i=1}^{k} x_i \leq \sum_{i=1}^{k} y_i, \quad 1 \leq k \leq n.$$

Definition 4.2 *A real valued function $\phi(z) = \phi(z_1, \ldots, z_n)$ defined on a set $\mathcal{A} \subset R^n$ is said to be Schur concave on $\mathcal{A}$ if*

$$x \prec y \quad on\ \mathcal{A} \quad \Rightarrow \quad \phi(x) \geq \phi(y).$$

ϕ is strictly Schur concave on $\mathcal{A}$ if strict inequality $\phi(x) > \phi(y)$ holds when x is not a permutation of y.

We will now state a theorem that results in a test for strict Schur concavity. We denote

$$\phi_{(k)}(z) = \frac{\partial\phi(z)}{\partial z_k} \quad and \quad \phi_{(i,j)}(z) = \frac{\partial^2\phi(z)}{\partial z_i \partial z_j}.$$

Theorem 4.1 *Let $\phi(z)$ be a scalar real valued function defined and continuous on $\mathcal{D}$, and twice differentiable on the interior of $\mathcal{D}$. Then $\phi(z)$ is strictly Schur concave on $\mathcal{D}$ iff*

(i) ϕ is symmetric in its arguments,

(ii) $\phi_{(k)}(z)$ is increasing in k, and

(iii) $\phi_{(k)}(z) = \phi_{(k+1)}(z) \Rightarrow \phi_{(k,k)}(z) - \phi_{(k,k+1)}(z) - \phi_{(k+1,k)}(z) + \phi_{(k+1,k+1)}(z) < 0$.

Theorem 4.2 *If H is an $n \times n$ hermitian matrix with diagonal elements $h_1, \ldots, h_n$ and eigenvalues $\lambda_1, \ldots, \lambda_n$, then $h \prec \lambda$ on R^n.*

To connect the results from majorization theory developed to our optimization problem, we state the following lemma.

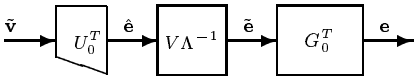

Fig. 3. Receiver block diagram.

Theorem 4.3 *The real valued scalar function J as defined in (3.15) under the optimality conditions (3.17-3.18) is strictly Schur concave.*

In particular as the search of G_0 is restricted to unitary matrices, if one chooses G_0 to be Ω a matrix of orthonormal eigenvectors of $R_{\tilde{e}}$, then R_e is a diagonal matrix containing the eigenvalues of $R_{\tilde{e}}$. Note that diagonal elements of R_e are $\sigma^2_{e_{j,k}}$. Thus from theorem 4.2, this choice of G_0 yields a sequence of $\sigma^2_{e_{j,k}}$ that majorizes all other achievable sequences. Consequently if arranged optimally, Theorem 4.3 holds, that such a sequence will minimize (3.15). It remains simply to arrange the eigenvalues of $R_{\tilde{e}}$ among the $\sigma^2_{e_{j,k}}$, through exhaustive search if need be, so that an arrangement that minimizes (3.15) is obtained. Thus for a suitable permuation matrix, P, the optimizing G_0 is

$$G_0 = P\Omega. \tag{4.20}$$

5. SIMULATION RESULTS

In this section, we compare the trasmitting power of the DFT based DMT under no bit allocation and optimum bit allocation with our optimum transceiver. We assume the channel to be $C(z) = 1 + 0.5z^{-1}$, and a noise source $v(n)$ whose power spectral density is shown in fig. 4. The plot shows that there is an 8 dB saving in transmit power with our design over the DFT based DMT under optimum bit allocation, and a 12 dB improvement over the conventional DMT with no optimum bit allocation. We however note that there may exist noise environments where the DFT based DMT performs as well as our optimal design.

6. CONCLUSIONS

In this paper, we have presented an optimum bit allocation strategy and transceiver design for minimizing the transmit power when different users have varied QoS requirements. Simulations confirmthe efficacy of our results.

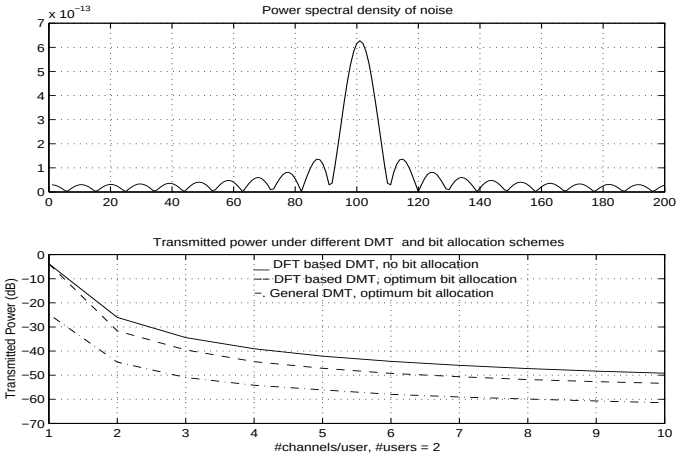

Fig. 4.

[2] S. Dasgupta, C. Schwarz and B.D.O. Anderson, "Optimal subband coding of cyclostationary signals", *IEEE International Conference on Acoustics, Speech, and Signal Processing*, pp 1489-1492, Mar 1999.

[3] L.M.C. Hoo, J. Tellado, J.M. Cioffi, "Discrete dual QoS loading algorithms for multicarrier systems ", *IEEE International Conference on Communications*, pp 796-800, 1999.

[4] B.S. Krongold, K. Ramchandran, D.L. Jones, "Computationally efficientoptimal power allocation algorithms for multicarrier communication systems", *IEEE Transactions on Communications*, pp 23-27, Jan 2000.

[5] Y. P. Lin, S.M. Phoong, "Perfect discrete multitone modulation with optimal transceivers", *IEEE Transactions on Signal Processing*, pp 1702 -1711, June 2000.

[6] A. W. Marshall and I. Olkin, *Inequalities: Theory of Majorization and its applications*, Academic Press, 1979.

[7] A. Scaglione, S. Barbarossa, G.B. Giannakis, "Filter - bank transceivers optimizing information rate in block transmissions over dispersive channels", *IEEE Transactions on Information Theory*, pp 1019-1032, Apr 1999.

[8] T. Starr, J.M. Cioffi ,P. Silverman, *Understanding Digital Subscriber Line Technology*, Prentice Hall, 1999.

[9] P.P. Vaidyanathan, *Multirate Systems and Filter Banks*, Prentice Hall, 1992.

7. REFERENCES

[1] J.S. Chow, J.C. Tu, J.M. Cioffi, "A discrete multitone transceiver system for HDSL applications", *IEEE Journal on Selected Areas in Communications*, pp 895-908, Aug 1991.

OPTIMUM DMT BASED TRANSCEIVERS FOR MULTIUSER COMMUNICATIONS

Ashish Pandharipande and Soura Dasgupta*

Abstract

This paper considers discrete multitone (DMT) modulation for multiuser communications when multiple users are supported by the same system, and a zero padding redundancy is employed at the transmitter output. These users may have differing quality of service (QoS) requirements, as quantified by bit rate and symbol error rate specifications. Our goal is to minimize the transmitted power given the QoS specifications, subject to the knowledge of the second order statistics of the colored interference at the receiver input. In particular we find an optimum bit loading scheme that distributes the bit rate transmitted across the various subchannels belonging to each user, and subject to this bit allocation, determine the optimum transceiver. A major conclusion of this paper is to demonstrate that even though the optimum bit rate allocation differs from the single user case, the optimum transceiver is the same, to within a permutation of the transmit and receive filters, for both the single and the multiuser cases.

*Department of Electrical and Computer Engineering, The University of Iowa, Iowa City, IA-52242, USA. Email: pashish@engineering.uiowa.edu and dasgupta@eng.uiowa.edu. This work was supported by US Army contract, DAAAD19-00-1-0534, and NSF grants ECS-9970105 and CCR-9973133.

1 Introduction

The discrete multitone (DMT), modulation channel coding scheme, also known as Orthogonal Frequency Division Multiplexed (OFDM) system, has established itself as an effective high rate data communication technique in both wired and wireless environments. It is used for example in high speed ADSL and HDSL modems, [3], [16] and has been proposed as the modulation scheme of choice in the Mill Bahama and Magic Wand wireless ATM systems, [4] as well as in the IEEE 802.11a wireless standard. We consider DMT in a multiuser environment, specifically when a single DMT system simultaneously supports multiple quality of service (QoS) provisioned flows. The various flows may represent different multimedia services such as data, speech, and video, each endowed with different QoS requirements quantified in this paper by bit rates and symbol error rates (SER). Our goal is to characterize optimal DMT systems, employing zero padding redundancy that achieve these multiple QoS specifications, with the minimum transmission power.

We are motivated by the knowledge that future broadband networks will be expected to provide a wide range of multimedia services. Thus, even wireless networks must support video conferencing, voice, and data, with different end-to-end QoS requirements at data rates that can be several orders (e.g. 4G in IMT2000) higher than today's second-generation (2G) systems [1][2]. Thus the same OFDM channel in such future systems will be called upon to deliver data flows with multiple QoS specifications. Since power conservation is important, data transfer must occur at the smallest level of permissible power.

Figure 1 depicts the broad contours of DMT communication systems. The basic idea in this multicarrier technique is to partition the dispersive transmission channel into a large number of parallel independent subchannels by applying an orthogonal block transform. Specifically the incoming data stream is converted into M-parallel data streams each operating, at a rate that is M-times smaller than the original symbol rate, and each having a distinct carrier. An M-point block orthogonal transformation of these streams of data is followed by a parallel to serial conversion, prior

to transmission through the communication channel. Typically for an FIR channel of length κ, extra redundancy of length κ is added at the channel input to infuse resistance to channel induced ISI. Consequently, the effective rate reduction in each subchannel is by a factor N, where $N = M + \kappa$. The equalizer in fig. 1 is used to keep the effective channel length, κ, small. The fact that each data stream operates at a slower rate reduces the dispersive channel effects it experiences. At the channel output one performs in succession the operations of redundancy removal, parallel to serial conversion, and the application of an inverse block transform. In traditional OFDM, the input transform is an Inverse Discrete Fourier Transform (IDFT) operation, and the output transformation is a block DFT operation. The redundancy at the channel input in the standard OFDM is a cyclic prefix. Recently several authors have proposed more general orthogonal block transforms, and the injection of zero padding redundancy, [8], [11], [7], [15] leading to the so called *Generalized DMT systems*. It is such a zero-padding generalized DMT system that is the subject of this paper.

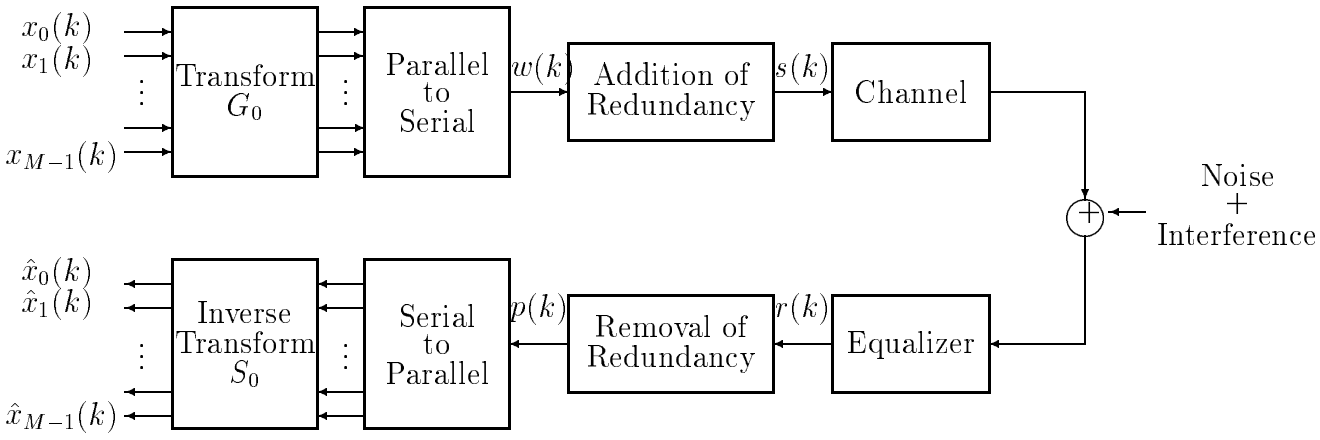

Figure 1: The DMT system.

The overall system can be captured by the discrete time baseband model described in fig. 2. The transmitting filters, $F_k(z)$, and the receiving filters, $H_k(z)$, model the transformation, and redundancy injection and removal operations, and have length N each. In conventional OFDM, the coefficients of $F_k(z)$ and $H_k(z)$, are respectively,

related to M-point Inverse DFT (IDFT) and DFT coefficients. In this figure the channel equalizer combination is assumed to have an equivalent discrete time FIR transfer function $C(z)$ of order κ. The signal $v(k)$ models the effect of the noise and interference experienced at the *equalizer output*.

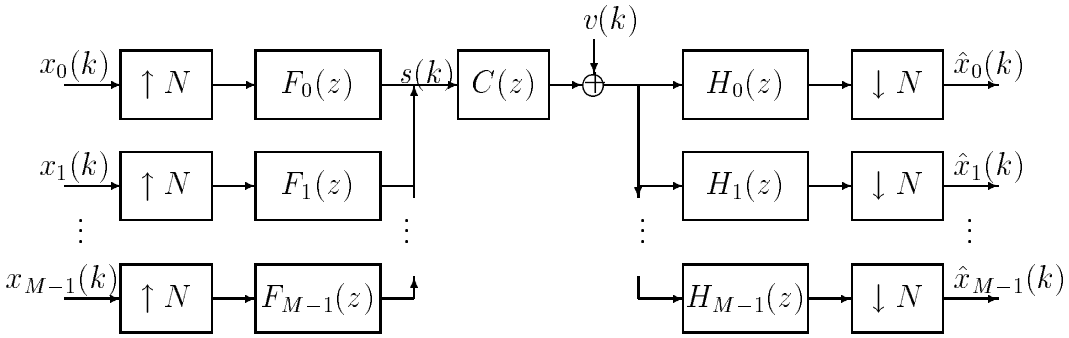

Figure 2: Filter bank based DMT model.

Several authors have studied the optimum trasceiver design in the single user case [19], [11], [10], [22], [13]. While [11], [10] and [22] are concerned with optimizing the transmitted power, [19] focusses on the maximization of the mutual information between the trasmitted and received signals. We explain the underlying concept of the optimization procedure by taking the example of [11], as it most directly influences the development of this paper. Specifically, [11], assumes no equalizer, zero padding redundancy, known channel, and noise $v(n)$ of known power spectral density (psd) modelling co-channel interference. This is partially motivated by the fact that in HDSL applications, the dominant interference is generated by near end cross talk (NEXT), [3]. Assuming a single user framework, subject to a specified target SER, average bit rate, [11] seeks to optimize against the transceiver structure, i.e. the transmit and receive filters, and the number of bits/symbol assigned to each subchannel, to minimize the transmitted power. This is done under the assumption of perfect reconstruction (PR), i.e. that the transceiver output equals the transceiver input in the noise free case, an orthogonality condition on the transmitter, and the use of zero-padding redundancy. These ideas are extended in [12] to more general settings.

The approach of [11] can be best characterized as water-pouring. Suppose a given set of subchannels see deeper channel nulls or experience higher levels of cochannel interference. Then the bit loading scheme must assign fewer bits/symbols to these subchannels. To avoid too many of such "low performing" subchannels, the subchannel selection process must try to *squeeze out problematic frequency bands with more adverse conditions* as best as one can, specifically by forcing channel nulls or interference spectral peaks, to occupy as few subchannels as possible. In essence, [11], [12] develop formalisms that capture these tasks.

In this paper, we extend the notions developed in [11], to a multiuser environment. Specifically we assume that there are n-users with each assigned M/n subchannels. Further the k-th user requires a bit rate of b_k, and an SER of no more than η_k. Our goal is to select filters $F_k(z)$ and $H_k(z)$, and distribute the bit rates among the various sub-channels, to achieve the above specifications with the minimum possible transmitted power. As in [11] we assume that a zero-padding redundancy is employed and that the transmitter satisfies an orthogonality condition.

Past treatment of optimum resource allocation in a multiuser setting, is restricted mostly to bit loading algorithms. Loading algorithms using efficient table lookups and a fast Lagrange bisection search method for a single user setting are developed in [10]. [6] considers a water-filling approach to the bit loading problem when two users are present. Other related papers are [24], [26], [27], each of which provide algorithms for bit and power allocation under a multiuser setting. None considers filter optimization.

Section 2 ties the DMT model of fig. 1 to the filter bank model of fig. 2 It also presents a polyphase representation of the DMT system that facilitates the optimization task central to this paper. Section 3 converts the power minimization problem to a precise optimization problem. Sections 4 and 5 consider bit loading and filter selection respectively. Section 6 provides numerical examples. Section 7 is the conclusion.

Notation: In the sequel, the superscripts $(.)^T, (.)^H$ will stand for the transpose, and Hermitian transpose respectively. I_M will denote the $M \times M$ identity matrix.

2 DMT based multiuser system model

In this Section we consider the generalized DMT structure of [11], and tie it to the filter bank structure of fig. 2, and a polyphase representation.

2.1 Generalized DMT with zero padding redundancy

Consider a block of M samples of $w(k)$ in fig.1, i.e.

$$[w(Mk), w(Mk-1), \ldots, w(Mk-M+1)]^T .$$

Then the redundancy injection process converts this to an N-block signal by appending each M-block by additional κ zeros to obtain the N-block below, prior to transmission.

$$[w(Mk), w(Mk-1), \ldots, w(Mk-M+1), 0, \ldots, 0] ,$$

Thus, with

$$\mathcal{I}_{\mathcal{ZP}} = \left[\begin{array}{c} I_M \\ 0_{\kappa \times M} \end{array} \right] , \tag{2.1}$$

$$\left[\begin{array}{cccc} s(Nk) & s(Nk-1) & \cdots & s(Nk-N+1) \end{array} \right]^T = \mathcal{I}_{\mathcal{ZP}} \left[\begin{array}{cccc} w(Mk) & w(Mk-1) & \cdots & w(Mk-M+1) \end{array} \right]^T \tag{2.2}$$

The redundancy removal operation is a general linear operation. Specifically with S_1 a suitable $M \times N$ matrix,

$$\left[\begin{array}{cccc} p(Nk) & p(Nk-1) & \cdots & p(Nk-N+1) \end{array} \right]^T = S_1 \left[\begin{array}{cccc} r(Mk) & r(Mk-1) & \cdots & r(Mk-M+1) \end{array} \right]^T . \tag{2.3}$$

Define in fig. 1, G_0 and S_0 as the $M \times M$ transmitter and receiver transform matrices respectively. In the sequel, as in [11], we assume G_0 is unitary, i.e.,

$$G_0^H G_0 = I. \tag{2.4}$$

Define

$$\underline{x}(k) = \left[\begin{array}{cccc} x_0(k), & x_1(k), & \ldots, & x_{M-1}(k) \end{array} \right]^T , \tag{2.5}$$

and

$$\underline{\hat{x}}(k) = \left[\begin{array}{cccc} \hat{x}_0(k), & \hat{x}_1(k), & \ldots, & \hat{x}_{M-1}(k) \end{array} \right]^T. \tag{2.6}$$

Define also the N-fold blocked version of the channel-equalizer combination $C(z) = c_0 + c_1 z^{-1} + \ldots + c_\kappa z^{-\kappa}$ to be

$$\mathbf{C}(z) = \left[\begin{array}{cccc} c_0 & z^{-1}c_{N-1} & \ldots & z^{-1}c_1 \\ c_1 & c_0 & & z^{-1}c_2 \\ \vdots & & \ddots & \vdots \\ c_{N-1} & c_{N-2} & \ldots & c_0 \end{array} \right], \tag{2.7}$$

with $c_i = 0$, for all $\kappa < i < N$. The above matrix can be written as:

$$\mathbf{C}(z) = \left[\begin{array}{cc} \mathbf{C_L} & \mathbf{C_R}(z) \end{array} \right] \tag{2.8}$$

where $\mathbf{C_L}$ is an $N \times M$, constant matrix, and $\mathbf{C_R}(z)$ is $N \times \kappa$.

With $v(k)$ the noise and interference effect at the output of $C(z)$, define

$$\tilde{v}(k) = \left[\begin{array}{cccc} v(Nk), & v(Nk-1), & , \ldots, & v(Nk-N+1) \end{array} \right]^T \tag{2.9}$$

a the N-fold blocked version of $v(k)$. Then one has

$$\underline{\hat{x}}(k) = S_0 S_1 \mathbf{C_L} G_0 \hat{x}(k) + S_0 S_1 \tilde{v}(k). \tag{2.10}$$

2.2 Polyphase representation and perfect reconstruction

All three structures discussed can be viewed as being represented by the scheme in fig. 3, where the $N \times M$ matrix G and $M \times N$ matrix S are given by

$$S = S_0 S_1, \quad G = \mathcal{I}_{\mathcal{ZP}} G_0. \tag{2.11}$$

Since the output of G and the input to S in fig. 3 are respectively, the N-fold blocked versions of the channel input and the equalizer output (see fig. 1), one has, [21], the familiar transmultiplexer structure of fig. 2, where with

$$F_k(z) = \sum_{i=0}^{N-1} z^{-i} G_{i,k}, \quad H_k(z) = \sum_{i=0}^{N-1} z^{i} S_{k,i}, \tag{2.12}$$

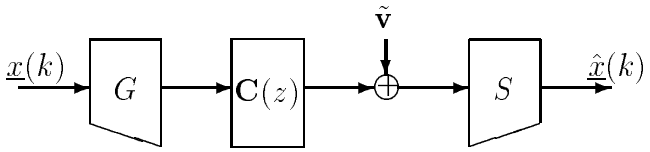

Figure 3: Polyphase representation of the DMT system.

$$G = [G_{i,k}]_{i=0,k=0}^{N-1,M-1}, \quad S = [S_{k,i}]_{k=0,i=0}^{M-1,N-1}. \tag{2.13}$$

Observe, $F_k(z)$ are each of degree $M-1$, and $H_k(z)$ have degree $N-1$.

We impose the perfect reconstruction (PR) condition:

$$S\mathbf{C}(z)G = I, \tag{2.14}$$

i.e., in the absence of noise/interference

$$\underline{\hat{x}}(k) = \underline{x}(k), \text{ for all } k.$$

In other words, the DMT system has no Inter Symbol Interference (ISI).

To obtain a more useful characterization of PR, consider the singular value decomposition of $\mathbf{C_L}$ defined in (2.8):

$$\mathbf{C_L} = U \begin{bmatrix} \Lambda \\ 0 \end{bmatrix} V^H = U_0 \Lambda V^H \tag{2.15}$$

where U and V are respectively $N \times N$ and $M \times M$ unitary matrices whose columns are the eigenvectors of $\mathbf{C_L}\mathbf{C_L}^H$ and $\mathbf{C_L}^H\mathbf{C_L}$. Λ is the $M \times M$ real, positive definite diagonal matrix with diagonal elements that are the singular values of $\mathbf{C_L}$. Then, because of (2.10), given G_0, the class of all S enforcing PR is completely characterized by

$$S = S_0 S_1 = G_0^H V \Lambda^{-1} \begin{bmatrix} I_M & A \end{bmatrix} U^H, \tag{2.16}$$

where A is any arbitrary $M \times \kappa$ matrix. In the sequel it will be useful to pratition U as

$$U = \begin{bmatrix} U_0 & U_1 \end{bmatrix}, \tag{2.17}$$

where U_0 is $N \times M$ and U_0 is $N \times \kappa$.

Filter selection for power minimization subject to optimum bit rate allocation will be performed by optimizing against $M \times M$ unitary G_0 and the arbitrary matrix A. Once G_0 is found (2.11) provides G, just as G_0 and A together with the knowledge of $\mathbf{C_L}$, provides S through (2.16). The filters F_k, H_k can then be found using (2.12) and (2.13).

3 Power Minimization: Formulation

We now give a precise mathematical formulation of the multiuser power minimization problem defined broadly in the Introduction. To recount, n users are assigned L subchannels each; the precise channel assignments will emerge from the optimization process. The k-th user must meet a maximum SER of η_k, and must maintain a bit rate b_k. Thus, assuming that $b_{j,k}$ is the bit rate sustained in the j-th subchannel of the k-th user, one must have for all $1 \leq k \leq n$,

$$b_k = \frac{1}{N} \sum_{j=0}^{L-1} b_{j,k}. \tag{3.18}$$

The goal is to assign bit rates among the various subchannels and select the filters $F_k(z)$ and $H_k(z)$ so that the target SER is met with the minimum collective transmitter power, subject to PR, constraint (3.18), and the orthonormality conditions particular to the scheme.

We do not require each user to employ the same modulation scheme. Thus the problem considered here generalizes [11] in several important respects: (A) It has to contend with n separate bit rate budgets (3.18) as opposed to a single budget in [11]. (B) Separate modulation schemes are permitted for different users. (C) Different users may have different SER requirements.

To achieve a given SER, most modulation schemes, with b-bit symbol constellations, b large, require an output SNR of $d2^b$ with $d > 0$ determined by the SER and the modulation scheme. Thus for example, for a b-bit square QAM the SER is given by

$$\eta = 4\left(1 - \frac{1}{\sqrt{2^b}}\right) Q\left(\sqrt{\frac{3\mathrm{SNR}}{(2^b-1)}}\right) \approx 4Q\left(\sqrt{\frac{3\mathrm{SNR}}{2^b}}\right), \quad \text{when } 2^b \gg 1. \tag{3.19}$$

where

$$Q(a) = \int_a^\infty \frac{1}{\sqrt{2\pi}} e^{-x^2/2} dx.$$

Thus for large b, SNR$= d2^b$ with $d = \frac{1}{3}[Q^{-1}(\frac{\eta}{4})]^2 > 0$. Consequently, since under the PR condition the output signal power equals the input signal power, in the j-th channel of the k-th user

$$\sigma^2_{x_{j,k}} = d_k 2^{b_{j,k}} \sigma^2_{e_{j,k}}, \tag{3.20}$$

where $\sigma^2_{e_{j,k}}$ is the output noise variance in this subchannel and d_k is a constant determined by the SER and modulation scheme used for the k-th user. Because G_0 is unitary, in the DMT system with zero padding redundancy, the total transmitted power equals

$$\sum_{k=1}^{n} \sum_{j=0}^{L-1} \sigma^2_{x_{j,k}} = \sum_{k=1}^{n} \sum_{j=0}^{L-1} d_k 2^{b_{j,k}} \sigma^2_{e_{j,k}} \tag{3.21}$$

Now observe that $\sigma^2_{e_{j,k}}$ are the diagonal elements of the output noise autocorrelation matrix R_e. We note that

$$R_e = G_0^H R G_0 \tag{3.22}$$

where because of (2.16)

$$R = V \Lambda^{-1} \begin{bmatrix} I_M & A \end{bmatrix} \begin{bmatrix} U_0^H \\ U_1^H \end{bmatrix} R_{\tilde{v}} \begin{bmatrix} U_0 & U_1 \end{bmatrix} \begin{bmatrix} I_M \\ A^H \end{bmatrix} \Lambda^{-1} V^H. \tag{3.23}$$

Here $R_{\tilde{v}}$ is the known autocorrelation matrix of $\tilde{v}(k)$ and the knowledge of the channel equalizer combination provides Λ, U_i and V from the SVD of $\mathbf{C_L}$.

We then have the following formal statement of the problem to be solved

Problem 3.1 *Given $d_k, b_k, M \times M$ positive definite, Hermitian symmetric, $R_{\tilde{v}}$, find $b_{i,k}$, $M \times \kappa$, A and $M \times M$ unitary matrix G_0 such that with $\sigma^2_{e_{i,k}}$ the diagonal elements of R_e as in (3.22) and (3.23), (3.21) is minimized under (2.4) and (3.18).*

We will adopt a three step approach to solving this problem.

- *Step I:* Subject to a given choice of $\sigma^2_{e_{j,k}}$, G_0 and A, find the optimum bit rate allocations $b_{j,k}$.

- *Step II:* Given A find the optimizing G_0.
- *Step III:* Find the optimizing A.

Such a separation becomes possible due to the following considerations. Observe that $\sigma^2_{e_{j,k}}$ are simply the diagonal elements of R_e. Consequently they only depend on G_0 and A and are independent of the selected $b_{j,k}$. Further, given any choice of $\sigma^2_{e_{j,k}}$, the optimum bit rate allocations $b_{j,k}$ produced by Step I, transforms (3.21) to an expression that is in fact *independent of* $b_{j,k}$ and dependent only on $\sigma^2_{e_{j,k}}$, in turn determined by G_0 and A, and b_k and d_k supplied by the problem specification. Thus Step I can be conceptually separated from the selection of G_0 and A.

Similarly, regardless of the choice of A, G_0 yielded by Step II reduces (3.21) to an expression that is entirely determined by the eigenvalues of the matrix R in (3.23). These eigenvalues are of course independent of G_0 and determined exclusively by A. Thus Step III need only find the A that renders these eigenvalues to be the most favorable. Thus indeed the separation above is justified.

4 Optimum bit rate allocation

The two components to the optimization problems considered in Section 3 are optimum bit rate allocation, i.e. selection of the $b_{j,k}$, and filter selection. In this Section we ask: Given certain $\sigma^2_{e_{j,k}}$, how does one allocate bit rates $b_{j,k}$ to minimmize (3.21)? The problem of minimizing (3.21) under the set of constraints (3.18) is a constrained optimization problem. Using the AM-GM inequality, which states that the arithmetic mean (AM) of a set of positive numbers is greater than or equal to their geometric mean (GM) with equality iff all the numbers are equal, and (3.18),

$$\sum_{k=1}^{n}\sum_{j=0}^{L-1} d_k 2^{b_{j,k}}\sigma^2_{e_{j,k}} \geq L\sum_{k=1}^{n} d_k\Big(\prod_{j=0}^{L-1} 2^{b_{j,k}}\sigma^2_{e_{j,k}}\Big)^{1/L} \tag{4.24}$$

$$= L\sum_{k=1}^{n} d_k\Big(2^{Nb_k}\prod_{j=0}^{L-1} \sigma^2_{e_{j,k}}\Big)^{1/L} \tag{4.25}$$

with equality holding iff for all i, j, k:

$$2^{b_{j,k}}\sigma^2_{e_{j,k}} = 2^{b_{i,k}}\sigma^2_{e_{i,k}}.$$

This in turn requires that for all j,k:

$$b_{j,k} = \frac{N}{L} b_k + \frac{1}{2}\log_2(\prod_{j=0}^{L-1} \sigma_{e_{j,k}}^2)^{1/L} - \frac{1}{2}\log_2(\sigma_{e_{j,k}}^2). \tag{4.26}$$

This is the *optimum bit allocation strategy*. Note that as in [11] this bit allocation strategy does not impose the obvious requirement that the $b_{j,k}$ be positive integers. Nonetheless by suitable rounding off it represents a good approximation of the attainable minimum.

The optimal transceiver design is to find matrices A and G_0 so as to minimize

$$J = \sum_{k=1}^{n} (\alpha_k \prod_{j=0}^{L-1} a_{j,k})^{1/L} \tag{4.27}$$

where

$$\alpha_k = d_k^L 2^{Nb_k} > 0, \quad a_{j,k} = \sigma_{e_{j,k}}^2 > 0. \tag{4.28}$$

Observe that this cost function depends only on b_k, d_k and $\sigma_{e_{j,k}}^2$, and not on the the particular selection of $b_{j,k}$, reinforcing the point made at the conclusion of the previous section.

We note that the setting in [11] considers minimization of the cost function

$$\prod_{j,k} a_{j,k}. \tag{4.29}$$

The altered nature of the cost function underlying the multiuser case of this paper, makes the extension to this setting nontrivial.

Given a set of $a_{j,k}$, α_k in (4.27) it behooves us to ask the following question: Which ordering of $a_{j,k}$, α_k leads to the smallest value of J? To answer, we provide the following extension of a result by Hardy and Polya, [14].

Lemma 4.1 *Given a set of positive numbers $\{\delta_k\}_{k=1}^{2l}$, with $\delta_k \geq \delta_{k+1}$. Consider $\sum_{k=1}^{l} \delta_{k_1}\delta_{k_2}$, with $\delta_{k_1}, \delta_{k_2}$ distinct for all k. Then this quantity attains its minimum value iff whenever for some $i \in \{1,2\}$, $\delta_{k_i} \geq \delta_{l_i}$ then $\delta_{k_j} \leq \delta_{l_j}$, $\quad i \neq j$.*

Proof: Sufficiency is in [14]. Suppose without loss of generality that $\delta_{11} > \delta_{21}$ and $\delta_{12} > \delta_{22}$. Then

$$\delta_{11}\delta_{12}+\delta_{21}\delta_{22}-(\delta_{11}\delta_{22}+\delta_{21}\delta_{12}) = \delta_{11}(\delta_{12}-\delta_{22})-\delta_{21}(\delta_{12}-\delta_{22}) = (\delta_{11}-\delta_{21})(\delta_{12}-\delta_{22}) > 0. \tag{4.30}$$

Hence the result. ∎

Thus the largest δ_i must be paired with the smallest δ_j, the second largest with the second smallest, etc. Thus, given α_k, $k \in \{1, 2, \ldots, L\}$, among the various permutations of $\{a_{j,k}\}$, any permutation that minimizes (4.27) must have the following property:

$$a_{m,k_1} \geq a_{n,k_2} \Rightarrow \alpha_{k_1} \prod_{j=1, j\neq m}^{L-1} a_{j,k_1} \leq \alpha_{k_2} \prod_{j=1, j\neq n}^{L-1} a_{j,k_2} \tag{4.31}$$

and

$$\alpha_m \geq \alpha_n \Rightarrow \prod_{j=0}^{L-1} a_{j,m} \leq \prod_{j=0}^{L-1} a_{j,n}. \tag{4.32}$$

5 Optimum transceiver design

In this Section we address the problem of filter selection to minimize (4.27). Specifically we must find an $M \times M$ unitary G_0 and an $M \times \kappa$ A to minimize (4.27) under (4.31,4.32) and (3.22, 3.23), where $a_{j,k}$ are the diagonal elements of R_e.

Much of the development in this section exploits elements from the theory of Majorization, [14]. Section 5.1 provides a quick primer. Section 5.2 considers the selection of G_0 given and R in (3.23), i.e. given A. Section 5.3 characterizes the optimum A. Section 5.4 consolidates these results.

5.1 Majorization and Schur Concavity

We first introduce the notion of majorization, [14].

Definition 5.1 *Consider two sequences $x = \{x_i\}_{i=1}^l$ and $y = \{y_i\}_{i=1}^l$ with $x_i \geq x_{i+1}$ and $y_i \geq y_{i+1}$. Then we say that y majorizes x, denoted as $x \prec y$, if the following holds with equality at $k = l$*

$$\sum_{i=1}^{k} x_i \leq \sum_{i=1}^{k} y_i, \quad 1 \leq k \leq l.$$

We say that y weakly super majorizes x, i.e. $x \prec^W y$ if

$$\sum_{i=j}^{l} x_i \geq \sum_{i=j}^{l} y_i, \quad 1 \leq j \leq l.$$

If y majorizes x, then any permutation of y also majorizes any permutation of x. The following facts are self evident.

Fact 1 *If $x \prec y$ then $x \prec^W y$.*

Fact 2 *If $x \prec^W y$ and $y \prec^W q$ then $x \prec^W q$.*

Fact 3 *Suppose $a = \{a_i\}_{i=1}^l$, $a_i \geq 0$, the $(x + a) \prec^W x$.*

We also have the following Fact from [14].

Fact 4 *Consider any $M \times M$ Hermitian matrix R with eigenvalues $\lambda_1 \geq \lambda_2 \geq \ldots \geq \lambda_M$, and an $M \times M$ matrix R_e, which obeys (3.22) for an $M \times M$ matrix G_0. Then the diagonal elements $R_{e,i,i}$ of R_e obey*

$$\{R_{e,i,i}\}_{i=1}^M \prec \{\lambda_1, \ldots, \lambda_M\}. \tag{5.33}$$

We also note the following important result from [14].

Lemma 5.1 *Consider two $M \times M$ Hermitian matrices Q_1 and Q_2. Suppose the eigenvalues of Q_1, Q_2 and $Q_1 + Q_2$ are respectively $\lambda_i(Q_1)$, $\lambda_i(Q_2)$, and $\lambda_i(Q_1 + Q_2)$, $\lambda_i(\cdot) \geq \lambda_{i+1}(\cdot)$. Then*

$$\{\lambda_i(Q_1 + Q_2)\}_{i=1}^M \prec \{\lambda_i(Q_1) + \lambda_i(Q_2)\}_{i=1}^M.$$

We now consider the notion of Schur concavity, [14].

Definition 5.2 *A real valued function $\phi(z) = \phi(z_1, \ldots, z_n)$ defined on a set $\mathcal{A} \subset R^n$ is said to be Schur concave on $\mathcal{A}$ if*

$$x \prec y \quad \text{on } \mathcal{A} \quad \Rightarrow \quad \phi(x) \geq \phi(y).$$

ϕ is strictly Schur concave on $\mathcal{A}$ if strict inequality $\phi(x) > \phi(y)$ holds when x is not a permutation of y.

We will now state a theorem that results in a test for strict Schur concavity. We denote

$$\phi_{(k)}(z) = \frac{\partial \phi(z)}{\partial z_k} \quad \text{and} \quad \phi_{(i,j)}(z) = \frac{\partial^2 \phi(z)}{\partial z_i \partial z_j}.$$

Theorem 5.1 *Let $\phi(z)$ be a scalar real valued function defined and continuous on $\mathcal{D} = \{(z_1, \ldots, z_n) : z_1 \geq \ldots \geq z_n\}$, and twice differentiable on the interior of $\mathcal{D}$. Then $\phi(z)$ is strictly Schur concave on $\mathcal{D}$ if*

(i) $\phi_{(k)}(z)$ is increasing in k,

and

(ii) $\phi_{(k)}(z) = \phi_{(k+1)}(z) \Rightarrow \phi_{(k,k)}(z) - \phi_{(k,k+1)}(z) - \phi_{(k+1,k)}(z) + \phi_{(k+1,k+1)}(z) < 0$.

Finally we have the following other important fact from [14].

Fact 5 *Suppose $\phi(z)$ satisfies the conditions of Theorem 5.1. Then $\phi(x) > \phi(y)$ whenever $x \prec^W y$.*

5.2 Selecting G_0

Observe that by fixing A one automatically fixes R in (3.23). In this section we solve the following modified problem addressing step II of the three step procedure referred to in the foregoing.

Modified Problem: Given an $M \times M$ positive definite, Hermitian symmetric, R, find an $M \times M$ unitary G_0 to minimize (4.27) under (4.31,4.32) and (3.22), where $a_{j,k}$ are the diagonal elements of R_e.

To this end we have the following pivotal theorem.

Theorem 5.2 *The real valued scalar function J with $a_{j,k}$ as its arguments as defined in (4.27), and $\alpha_k, a_{j,k}$ positive, is strictly Schur concave under the optimal arrangement conditions (4.31-4.32).*

Proof: We note that

$$\frac{\partial J}{\partial a_{j,k}} = \frac{1}{L} \frac{\left(\alpha_k \prod_{i=0}^{L-1} a_{i,k}\right)^{1/L}}{a_{j,k}}.$$

Thus if $a_{j,k} \geq a_{l,k}$,

$$\frac{\partial J}{\partial a_{j,k}} \leq \frac{\partial J}{\partial a_{l,k}}.$$

Now suppose for some $p \neq m$, $0 \leq i, l \leq L-1$, $a_{i,p} \geq a_{l,m}$. Then from (4.31),

$$\alpha_p \prod_{j=1, j\neq i}^{L-1} a_{j,p} \leq \alpha_m \prod_{j=1, j\neq l}^{L-1} a_{j,m}$$

Consequently

$$\begin{aligned} \frac{\partial J}{\partial a_{i,p}} &= \frac{1}{L} \frac{\left(\alpha_p \prod_{j=1, j\neq i}^{L-1} a_{j,p}\right)^{1/L}}{(a_{i,p})^{1-1/L}} \\ &\leq \frac{1}{L} \frac{\left(\alpha_m \prod_{j=1, j\neq l}^{L-1} a_{j,m}\right)^{1/L}}{(a_{l,m})^{(1-1/L)}} \\ &= \frac{\partial J}{\partial a_{l,m}} \end{aligned}$$

Thus condition (i) of Theorem 5.1 is met.

Now observe

$$\frac{\partial^2 J}{\partial a_{i,p}^2} = -(\frac{L-1}{L^2}) \frac{\left(\alpha_k \prod_{j=1, j\neq i}^{L-1} a_{j,k}\right)^{1/L}}{(a_{i,k})^{(2-1/L)}} < 0.$$

Also with $j \neq i$,

$$\frac{\partial^2 J}{\partial a_{i,k} \partial a_{j,k}} = (\frac{1}{L^2}) \frac{\left(\alpha_k \prod_{l=0}^{L-1} a_{l,k}\right)^{1/L}}{a_{j,k} a_{i,k}} > 0.$$

Finally with $p \neq m$,

$$\frac{\partial^2 J}{\partial a_{j,p} \partial a_{i,m}} = 0.$$

Thus (ii) of Theorem 5.1 always holds. Hence the result. ∎

We now use this result to solve this modified problem.

Theorem 5.3 *Suppose the positive definite Hermitian $M \times M$ matrix R has eigenvalues $\lambda_1 \geq \lambda_2 \geq \ldots \geq \lambda_M$, with corresponding eigenvectors $\psi_1, \psi_2, \ldots, \psi_M$. Then the G_0 that solves the modified problem above is as below with P a suitable permutation matrix.*

$$G_0 = P \begin{bmatrix} \psi_1^H \\ \psi_2^H \\ \vdots \\ \psi_M^H \end{bmatrix} \tag{5.34}$$

Further the $a_{j,k}$ that result are simply these λ_i.

Proof: From Fact 4 and Theorem 5.1, the optimizing A must have diagonal elements $\lambda_1, \lambda_2, \ldots, \lambda_M$. Thus the rows of G_0 must be the Hermitian transpose of the corresponding eigenvectors. The permutation matrix P simply arranges these eigenvalues in a way to ensure that an optimum arrangement that minimizes (4.27), with $a_{j,k} = \lambda_i$, is attained. ∎

In both cases, the optimizing matrix R_e is diagonal, i.e. under optimality the noise components in the various subchannel outputs are mutually uncorrelated. The optimizing G_0 consists of the eigenvectors of R, and the subchannel output noise variances are the eigenvalues of R_{v_1} and R respectively. These eigenvalues must be rearranged between the subchannels to ensure that J in (4.27) is minimum. This will in effect specify the permutation matrix P, which, however, may not be unique.

Most importantly, reinforcing the arguments made in the justification of the three step breakdown of the overall power minimization problem, the cost function (4.27) reduces under the optimum selection of G_0 to one in which the $a_{j,k}$ are the eigenvalues of R optimally arranged. Consequently the selection of A must be guided by the need to assign these eigenvalues in an optimal way.

5.3 Selecting A

Since the optimizing G_0 results in the cost function having a value obtained by replacing $a_{j,k}$ by suitably arranged eigenvalues of R in (3.23), Fact 5 and Theorem 5.2, show that the optimmizing A must be such that the set of resulting eigenvalues of R must weakly super majorize all possible sets of attainable eigenvalues. As V is unitary in (3.22), the eigenvalues of R are the same as those of

$$\begin{aligned}
\Omega(A) &= \Lambda^{-1} \begin{bmatrix} I_M & A \end{bmatrix} \begin{bmatrix} U_0^H \\ U_1^H \end{bmatrix} R_{\tilde{v}} \begin{bmatrix} U_0 & U_1 \end{bmatrix} \begin{bmatrix} I_M \\ A^H \end{bmatrix} \Lambda^{-1} \\
&= \Lambda^{-1} \begin{bmatrix} I_M & A \end{bmatrix} \begin{bmatrix} U_0^H R_{\tilde{v}} U_0 & U_0^H R_{\tilde{v}} U_1 \\ U_1^H R_{\tilde{v}} U_0 & U_1^H R_{\tilde{v}} U_1 \end{bmatrix} \begin{bmatrix} I_M \\ A^H \end{bmatrix} \Lambda^{-1} \\
&= \Lambda^{-1} \left[U_0^H R_{\tilde{v}} U_0 + U_0^H R_{\tilde{v}} U_1 A^H + A U_1^H R_{\tilde{v}} U_0 + A U_1^H R_{\tilde{v}} U_1 A^H \right] \Lambda^{-1} \quad (5.35)
\end{aligned}$$

Now observe that as $R_{\tilde{v}}$ is positive definite, and $U = \left[\begin{array}{cc} U_0 & U_1 \end{array} \right]$ is unitary,

$$\left[\begin{array}{c} U_0^H \\ U_1^H \end{array} \right] R_{\tilde{v}} \left[\begin{array}{cc} U_0 & U_1 \end{array} \right] = \left[\begin{array}{cc} U_0^H R_{\tilde{v}} U_0 & U_0^H R_{\tilde{v}} U_1 \\ U_1^H R_{\tilde{v}} U_0 & U_1^H R_{\tilde{v}} U_1 \end{array} \right] \tag{5.36}$$

is positive definite. Thus, the matrices, $U_1^H R_{\tilde{v}} U_1$, $U_0^H R_{\tilde{v}} U_0$ and

$$U_0^H R_{\tilde{v}} U_0 - U_0^H R_{\tilde{v}} U_1 \left(U_1^H R_{\tilde{v}} U_1 \right)^{-1} U_1^H R_{\tilde{v}} U_0$$

must each be positive definite and nonsingular. Direct verification shows that because of (5.35),

$$\begin{aligned} \Omega(A) &= \Lambda^{-1} \Big\{ U_0^H R_{\tilde{v}} U_0 - U_0^H R_{\tilde{v}} U_1 \left(U_1^H R_{\tilde{v}} U_1 \right)^{-1} U_1^H R_{\tilde{v}} U_0 \\ &+ \left[U_0^H R_{\tilde{v}} U_1 \left(U_1^H R_{\tilde{v}} U_1 \right)^{-1} + A \right] U_1^H R_{\tilde{v}} U_1 \left[A^H + \left(U_1^H R_{\tilde{v}} U_1 \right)^{-1} U_1^H R_{\tilde{v}} U_0 \right] \Big\} \Lambda^{-1}. \end{aligned}$$

Define

$$Q_1 = \Lambda^{-1} \left[U_0^H R_{\tilde{v}} U_0 - U_0^H R_{\tilde{v}} U_1 \left(U_1^H R_{\tilde{v}} U_1 \right)^{-1} U_1^H R_{\tilde{v}} U_0 \right] \Lambda^{-1} \tag{5.37}$$

and

$$Q_2 = \Lambda^{-1} \left[U_0^H R_{\tilde{v}} U_1 \left(U_1^H R_{\tilde{v}} U_1 \right)^{-1} + A \right] U_1^H R_{\tilde{v}} U_1 \left[A^H + \left(U_1^H R_{\tilde{v}} U_1 \right)^{-1} U_1^H R_{\tilde{v}} U_0 \right] \Lambda^{-1}. \tag{5.38}$$

Clearly Q_1 is positive definite and Q_2 is positive semidefinite. Only Q_2 depends on A. Defining $\lambda_i(\Omega(A))$ as the eigenvalues of $\Omega(A)$, from Lemma 5.1, and Fact 1,

$$\begin{aligned} \{\lambda_i(\Omega(A))\}_{i=1}^M &\prec \{\lambda_i(Q_1) + \lambda_i(Q_2)\}_{i=1}^M \\ \Rightarrow \{\lambda_i(\Omega(A))\}_{i=1}^M &\prec^W \{\lambda_i(Q_1) + \lambda_i(Q_2)\}_{i=1}^M. \end{aligned}$$

Since $\lambda_i(Q_2) \geq 0$, from Fact 3

$$\{\lambda_i(Q_1) + \lambda_i(Q_2)\}_{i=1}^M \prec^W \{\lambda_i(Q_1)\}_{i=1}^M. \tag{5.39}$$

Thus, from Fact 2

$$\{\lambda_i(\Omega(A))\}_{i=1}^M \prec^W \{\lambda_i(Q_1)\}_{i=1}^M. \tag{5.40}$$

Thus the optimizing A is one which forces $Q_2 = 0$, i.e.

$$A = -U_0^H R_{\tilde{v}} U_1 \left(U_1^H R_{\tilde{v}} U_1 \right)^{-1}. \tag{5.41}$$

This is independent of G_0 and the optimum bit rate allocations $b_{i,j}$. Instead it is determined exclusively by $R_{\tilde{v}}$, provided by the second order statistics of $v(k)$, and U_i provided by the SVD of the blocked channel equalizer combination $\mathbf{C}(z)$. The resulting value of R is

$$R = V \Lambda^{-1} \left[U_0^H R_{\tilde{v}} U_0 - U_0^H R_{\tilde{v}} U_1 \left(U_1^H R_{\tilde{v}} U_1 \right)^{-1} U_1^H R_{\tilde{v}} U_0 \right] \Lambda^{-1} V^H. \tag{5.42}$$

5.4 Consolidation

To summarize, the optimizing A is obtained directly using (5.41) with the channel characteristics supplying U_i and the second order statistics of $v(k)$ supplying $R_{\tilde{v}}$. This gives R from (5.42). G_0 is the provided by the egenvectors of R permuted so that with $a_{j,k}$ the eigenvalues of R, an optimum arrangement of (4.27) is attained. This gives the requisite $\sigma^2_{e_{j,k}}$ and (4.26) gives the optimum bit allocations $b_{j,k}$.

It is interesting to note that the solution of A is identical to that given in [11] for the single user case. Modulo the permutation required to enforce the optimum rearrangement requirement, the optimizing G_0 is also the same as for the single user case. The only practical effect of the permutations is to rearrange the rows of G_0 and the columns of S, i.e. rearranging $F_i(z)$ and $H_i(z)$. Thus, even though the optimum bit rate allocations differ in the single and multiuser settings, the transceiver itself is identical.

6 Numerical Examples

We now present two numerical examples illustrating the theory developed in the previous sections. Our goal is to compare the required transmission power in three schemes: (i) DFT based DMT under no optimum bit allocation. (ii) DFT based DMT with optimum bit allocation. (iii) Zero padding Generalized DMT.

In all cases the channel/equalizer combination has the transfer function $C(z) = 1 + 0.25z^{-1}$.

We consider first a two user case, with the same SER requirement and modulation scheme for each user. The target bit rate of one user is 5/3 of the other. Figure 4, compares transmit powers of the three schemes listed above (normalized by the same constant for each user) as the number of channels per user (L) is varied. It also depicts the power spectral density (psd) of the noise at the equalizer output.

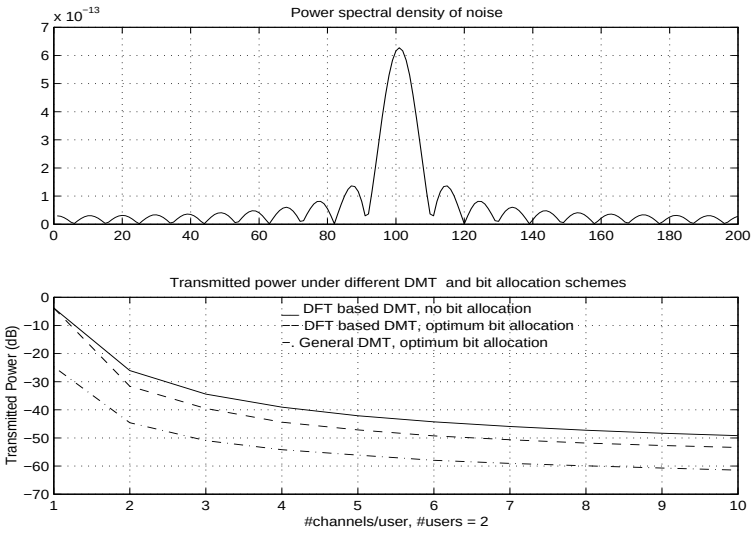

Figure 4: Noise psd and relative transmitted power levels for schemes (i)-(iii) in the two user case.

We note that the Generalized DMT provides roughly 8 dB savings in transmitted power over scheme (ii), and about 14 db over scheme (i).

These experiments are repeated for a three user case, with the same SER requirement and modulation scheme for each user. The target bit rate ratios are 2:3:5. Plots in figure 5, compare the transmit powers with the curves for the four schemes appearing in the same order. Generalized DMT provides roughly 10 dB savings in transmit power over (ii), and about 15 db over (i).

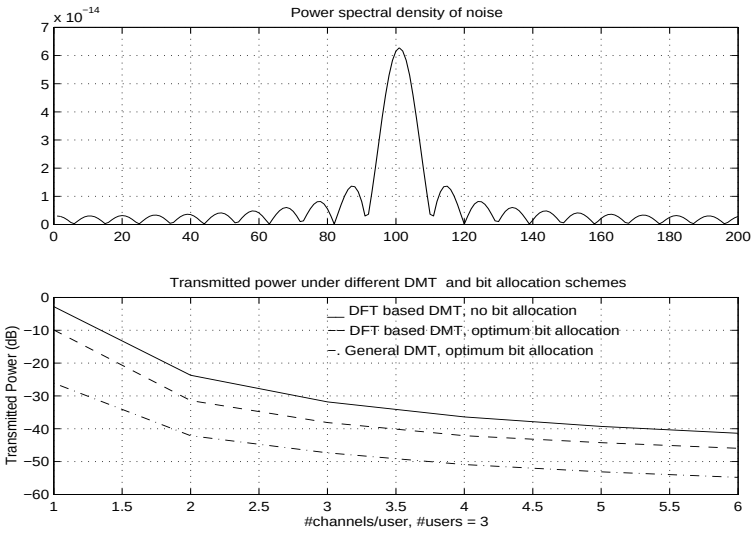

Figure 5: Noise psd and relative transmitted power levels for schemes (i)-(iii) in the three user case.

7 Conclusions

In this paper, we have presented an optimum bit rate allocation strategy and transceiver design for minimizing the transmitted power when different users have different QoS requirements. The underlying assumption is that while each user is assigned the same number of subchannels, the SER and bit rate requirements may vary from user to user, as may the modulation scheme. A Generalized DMT structure with zero padding redundancy is considered. Simulations demonstrate vastly improved performance over traditional DFT based DMT structures. It is shown that while the optimum bit rate allocation strategy differes from the single user case, the optimum transceiver design is identical in both the single and multiuser cases. Our theory assumes that each user is assigned the same number of subchannels. A logical extension is to consider the setting where users may be assigned different number of subchannels in accordance with their respective priorities.

References

[1] National Science Foundation, "Tetherless T3 and Beyond - an NSF Workshop Interim Report", Denver, CO. November 19, 1998.

[2] ITU-R Recomendation M.1035, "Framework for the radio interface(s) and radio sub-system functionality for International Mobile Telecommunications-2000 (IMT-2000)," 1998.

[3] J.S. Chow, J.C. Tu, J.M. Cioffi, "A discrete multitone transceiver system for HDSL applications", *IEEE Journal on Selected Areas in Communications*, pp 895-908, Aug 1991.

[4] K. Pahlvan, A. Zahedi and P. Krishnamurthy, "Wideband local access: Wireless LAN and wireless ATM", *IEEE Communications Magazine*, pp 35-40, November 1997.

[5] S. Dasgupta, C. Schwarz, B.D.O. Anderson, "Optimal subband coding of cyclostationary signals", *IEEE International Conference on Acoustics, Speech, and Signal Processing*, pp 1489-1492, Mar 1999.

[6] L.M.C. Hoo, J. Tellado, J.M. Cioffi, "Discrete dual QoS loading algorithms for multicarrier systems", *IEEE International Conference on Communications*, pp 796-800, 1999.

[7] X.-G. Xia, "New precoding for intersymbol interference cancellation using nonmaximally decimated Multirate Filterbanks with ideal FIR equalizers", *IEEE Trans. Signal Processing*, 45:2431-2441, Oct. 1997.

[8] A. Scaglione, G. B. Giannakis, and S. Barbarossa, "Redundant Filterbank Precoders and Equalizers", *IEEE Transactions on Signal Processing*, SP-47:1988-2022, July 1999.

[9] R.A. Horn, C.R. Johnson, *Matrix Analysis*, Cambridge University Press, 1999.

[10] B.S. Krongold, K. Ramchandran, D.L. Jones, "Computationally efficient optimal power allocation algorithms for multicarrier communication systems", *IEEE Transactions on Communications*, pp 23-27, Jan 2000.

[11] Y.P. Lin, S.M. Phoong, "Perfect discrete multitone modulation with optimal transceivers", *IEEE Transactions on Signal Processing*, pp 1702 -1711, June 2000.

[12] Y.P. Lin, S.M. Phoong, Optimal ISI-free DMT transceivers for distorted channels with colored noise *IEEE Transactions on Signal Processing*, pp 2702 -2712, November 2001.

[13] Y.P. Lin, P.P. Vaidyanathan, S. Akkarakaran, S.M. Phoong, "On the duality of optimal DMT systems and biorthogonal subband coders", *IEEE International Conference on Acoustics, Speech, and Signal Processing*, pp 2505-2508, Mar 2000.

[14] A.W. Marshall, I. Olkin, *Inequalities: Theory of Majorization and its applications*, Academic Press, 1979.

[15] B. Muquet, M. de Courville, P. Dunamel, G. Giannakis, "OFDM with trailing zeros versus OFDM with cyclic prefix: links, comparisons and application to the HiperLAN/2 system", *IEEE International Conference on Communications*, pp 1049-1053, 2000.

[16] Network to Customer Installation Interfaces - Asymmetric Digital Subscriber Line (ADSL) Metallic Interface, ANSI Standard, T1.413-1998, Nov 1998.

[17] A. Peled, A. Ruiz, "Frequency domain data transmission using reduced computational complexity algorithms", *IEEE International Conference on Acoustics, Speech and Signal Processing*, pp 964-967, Apr 9-11 1980.

[18] J.G. Proakis, *Digital Communications*, McGraw-Hill, Third Edition, 1995.

[19] A. Scaglione, S. Barbarossa, G.B. Giannakis, "Filterbank transceivers optimizing information rate in block transmissions over dispersive channels", *IEEE Transactions on Information Theory*, pp 1019-1032, Apr 1999.

[20] T. Starr, J.M. Cioffi, P. Silverman, *Understanding Digital Subscriber Line Technology*, Prentice Hall, 1999.

[21] P.P. Vaidyanathan, *Multirate Systems and Filter Banks*, Prentice Hall, 1992.

[22] P.P. Vaidyanathan, "Filter Banks in Digital Communications", *IEEE Circuits and Systems Magazine*, pp 4-25, Mar 2001.

[23] R. Van Nee, R. Prasad, *OFDM for Wireless Multimedia Communications*, Artech House, 1998.

[24] C.Y. Wong, R.S. Cheng, K.B. Lataief, R.D. Murch, "Multiuser OFDM with adaptive subcarrier, bit, and power allocation", *IEEE Journal on Selected Areas in Communications*, pp 1747-1758, Oct 1999.

[25] H. Zheng, K.J.R. Liu, "Multimedia services over digital subscriber lines", *IEEE Signal Processing Magazine*, pp 44-60, July 2000.

[26] H. Zheng, K.J.R. Liu, "Power minimization for delivering integrated multimedia services over digital subscriber line", *IEEE Journal on Selected Areas in Communications*, pp 841-849, June 2000.

[27] H. Zheng, K.J.R. Liu, "Robust image and video transmission over spectrally shaped channels using multicarrier modulation", *IEEE Transcations on Multimedia*, pp 88-103, Mar 2000.

On Biorthogonal Nonuniform Filter Banks and Tree Structures

Ashish Pandharipande, Soura Dasgupta

January 11, 2002

Abstract

This paper concerns biorthogonal nonuniform filter banks. It is shown that a tree structured filter bank is biorthogonal iff it is equivalent to a tree structured filter bank whose matching constituent levels on the analysis and synthesis sides are themselves biorthogonal pairs. We then show that a stronger statement can be made about dyadic filter banks in general: That a dyadic filter bank is biorthogonal iff both the analysis and synthesis banks can be decomposed into dyadic trees. We further show that these decompositions are stability and FIR preserving. These results, derived for filter banks having filters with rational transfer functions, thus extend some of the earlier comparable results for orthonormal filter banks.

Index Terms: Biorthogonal, nonuniform, dyadic, filter banks, tree structures.

Author Information

Manuscript received _____

Affiliation of Authors: Department of Electrical and Computer Engineering, The University of Iowa, Iowa City, IA-52242, USA.

Email: pashish@engineering.uiowa.edu and dasgupta@eng.uiowa.edu.

Contact Author: Soura Dasgupta.

Work supported by NSF Grants ECS-9970105 and CCR-9973133, and ARO Grant DAAD 19-00-1-0534.

List of Figures

1 Introduction

This paper considers certain structural issues associated with biorthogonal maximally decimated nonuniform filter banks, with emphasis on studying their relationship to tree structured filter banks. The class of filter banks under consideration is depicted in fig. 1, with $H_i(z)$ and $F_i(z)$ rational. Maximal decimation refers to the condition that

$$\sum_{i=0}^{K} \frac{1}{n_i} = 1. \tag{1.1}$$

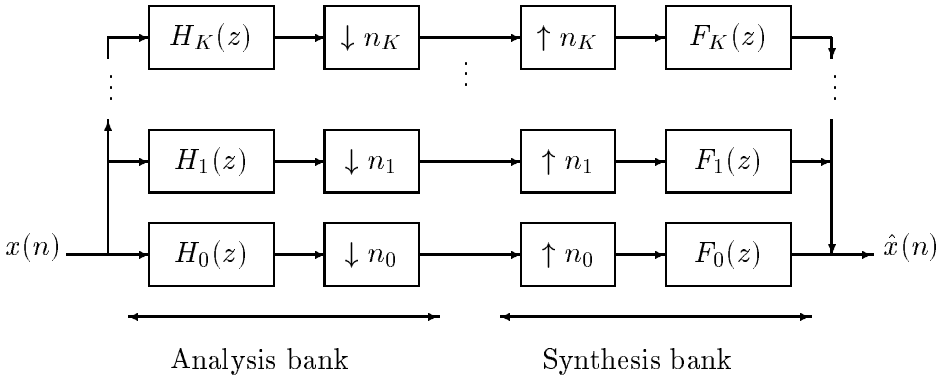

Figure 1: A nonuniform filter bank.

The arrangement to the left of the filter bank consisting of the n_i-fold decimators and the analysis filters $H_i(z)$ is the analysis bank, and that to the right with the n_i-fold interpolators with $F_i(z)$ as the synthesis filters is the synthesis bank. This filter bank has the *perfect reconstruction* (PR) property if its output always equals its input, $\hat{x}(n) = x(n)$. It is known, [6], that the analysis and synthesis filters of a maximally decimated filter bank with the PR property form a biorthogonal system. We will henceforth use the terms biorthogonality and PR interchangeably.

Of particular interest are *dyadic* filter banks as depicted in fig. 2, a special case of nonuniform filter banks wherein $K = M - 1$, $n_i = 2^{i+1}$ for $0 \leq i \leq M-2$ and $n_{M-1} = 2^{M-1}$. The relations between wavelets and such multirate filter banks have been known for some time: [19], [11], [4], [20] connect filter banks to wavelet bases. In particular the dyadic filter bank generates Discrete Time Wavelet Transform (DTWT) bases, [15], while the more general structure of fig. 1 generates wavelet packet bases, [11]. Also important are dyadic tree structured filter banks (TSFBs). Fig. 3 and 4 respectively depict an $(L+1)$-level dyadic tree structured analysis bank (TSAB) and the corresponding tree structured synthesis bank

(TSSB). These typically capture DTWT bases, [15].

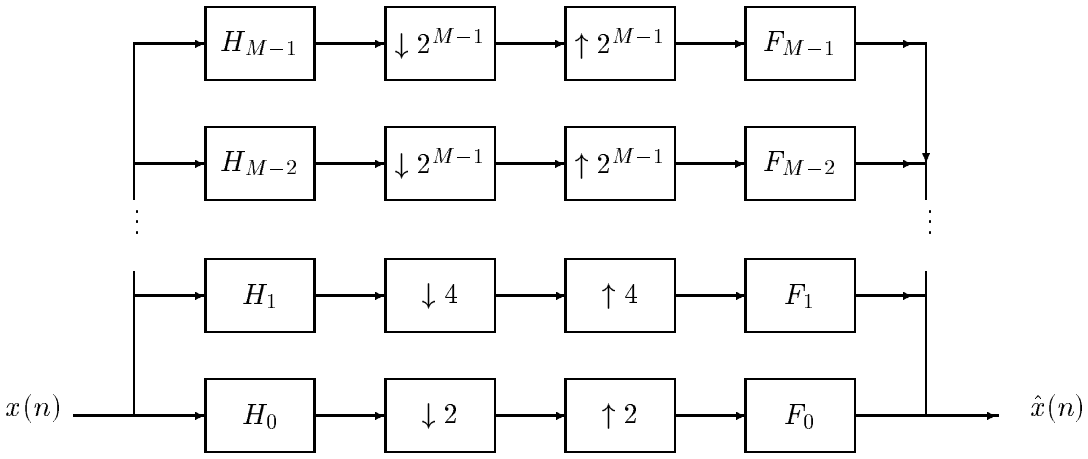

Figure 2: An M-channel dyadic filter bank.

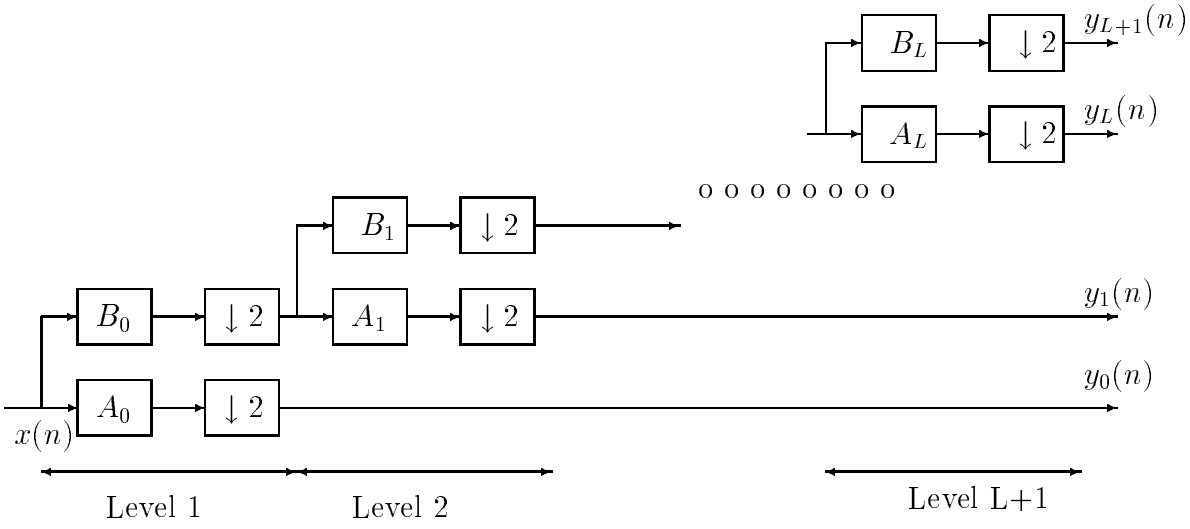

Figure 3: An $(L+1)$-level dyadic tree structured analysis bank.

The study of biorthogonal filter banks and tree structures is also motivated by their applications in image coding and compression. Most transforms used in signal processing are orthonormal, having the energy preservation property. Orthonormality is however not compatible with phase linearity in the case of FIR (finite impulse response) filter banks [4], [19]. Biorthogonality on the other hand allows additional freedom to have arbitrary length linear phase filters. Consequently, in the last few years, biorthogonal transforms in general, and biorthogonal wavelet transforms arising from tree structures

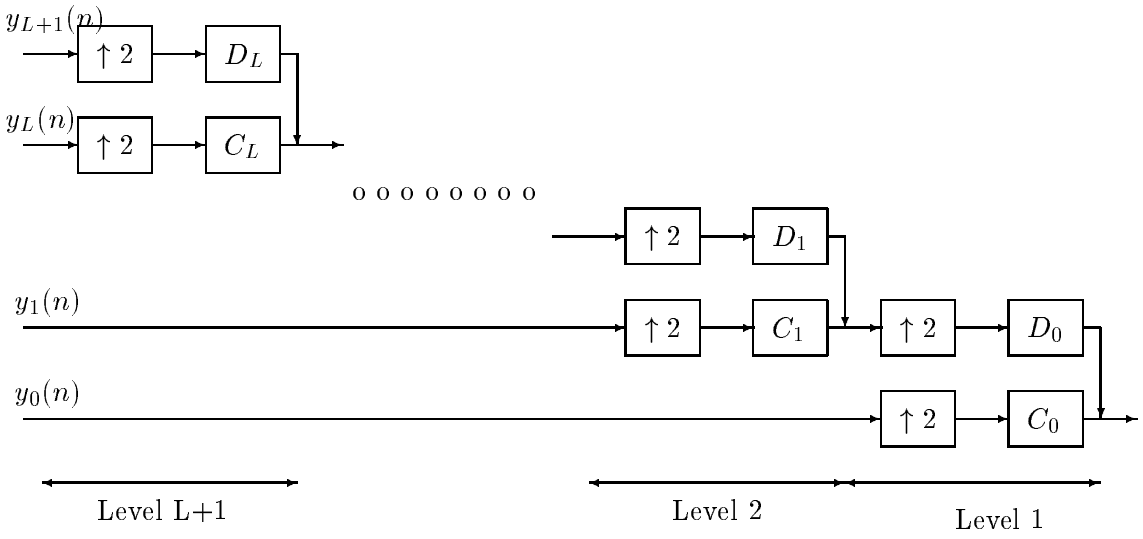

Figure 4: An $(L+1)$-level dyadic tree structured synthesis bank.

in particular, are gaining increasing currency in image coding applications, where phase linearity is desirable. Biorthogonal wavelets have also been used in the design of wavelet filters with binary coefficients [4], [12]. Other applications can be found in the areas of image compression [5], [13], fingerprint compression [10], and image coding [3], [9]. Given the importance of biorthogonal wavelets and filter banks in these wide-ranging applications, it becomes natural to investigate connections between filter banks and tree structures under the biorthogonality constraint.

The results presented in this paper extend two results by Soman and Vaidyanathan, [11]. Specifically, [11] shows that (i) every orthonormal dyadic filter bank is equivalent to a tree structured filter bank; (ii) while this is not true for more general nonuniform filter banks, a general tree structured filter bank is orthonormal iff its each constituent level is orthonormal.

These results are extended in this work to the biorthogonal case. We show first that a tree structured filter bank is biorthogonal iff it is equivalent to a tree structured filter bank whose matching consituent levels on the analysis and synthesis sides are themselves biorthogonal pairs. We then show that a stronger statement can be made about dyadic filter banks in general: *That a dyadic filter bank as in fig. 2 is biorthogonal iff both the analysis bank and the synthesis bank can be decomposed into dyadic trees as in fig. 3 and 4 with each pair of matching levels on the analysis and synthesis sides forming biorthogonal pairs.* It is instructive to note that even if the analysis bank in fig. 2, taken as an operator, is left invertible, there may not exist a synthesis bank of the form in fig. 2 such that the overall filter bank

is biorthogonal. Effectively our result shows that only in such a case is a tree structured decomposition impossible. We note that using different proof techniques, recently Akkarakaran, [21], has independently derived certain results on nonuniform filter banks that can be specialized to the results given here.

In Section 2, some preliminary definitions are given. Basic results on extended polyphase matrices and their invertibility are developed in Section 3. Results related to the decomposibility of biorthogonal nonuniform filter banks to tree structured filter banks are explored in Sections 4 and 5. Section 4 considers general biorthogonal tree structured filter banks, and Section 5 specializes to the dyadic case. Section 6 then discusses certain stability and FIR issues related to these decompositions. Section 7 presents conclusions.

2 Preliminaries

The general nonuniform filter bank structure of fig. 1 is closely connected to wavelet packet bases. Specifically, with $f_i(n)$ and $h_i(n)$, the impulse responses of the synthesis and analysis filters respectively, one has that

$$\hat{x}(n) = \sum_{k=0}^{K} \sum_{m} y_k(m) f_k(n - n_k m) \tag{2.2}$$

and

$$y_k(n) = \sum_{m} h_k(m) x(n_k n - m) \tag{2.3}$$

The functions $f_k(n-n_k m)$ constitute wavelet packet bases, while $y_k(n)$ are the corresponding coefficients. We will call the FB in fig. 1 *biorthogonal*, if for all $x(n)$,

$$\hat{x}(n) = x(n) \quad \forall n \tag{2.4}$$

It can be readily shown from a variation of arguments in [6], [15], that this is equivalent to the requirement that, with $\delta(.)$ the Kronecker delta,

$$\sum_{n} f_k(n - n_k i) h_m(-n + n_m l) = \delta(m - k)\delta(l - i) \tag{2.5}$$

This contrasts with the *orthonormality* property that requires

$$\sum_{n} f_k(n - n_k i) f_m^{\star}(n - n_m l) = \delta(m - k)\delta(l - i) \tag{2.6}$$

and

$$h_k(n) = f_k^{\star}(-n) \tag{2.7}$$

The results presented in the paper are derived using polyphase representations. We now present the idea of extended polyphase matrices. Assuming that the filters $H_k(z)$ and $F_k(z)$ have rational transfer functions, in the sequel, we will call $E_{kl}(z)$ and $R_{lk}(z)$ the l-th n_k-fold type-I and type-II polyphase components of $H_k(z)$ and $F_k(z)$ respectively, if one has

$$H_k(z) = \sum_{l=0}^{n_k-1} z^{-l} E_{kl}(z^{n_k}), \tag{2.8}$$

$$F_k(z) = \sum_{l=0}^{n_k-1} z^{l} R_{lk}(z^{n_k}). \tag{2.9}$$

To obtain a matrix polyphase representation of fig. 1, one must use an additional device from [16]: The idea is to redraw the nonuniform filter bank in fig. 1 as an equivalent uniform maximally decimated system. Define N to be the least common multiple (l.c.m.) of the n_i. Then observe that fig. 5-(a) is equivalent to the p_k-channel filter bank in fig. 5-(b) with

$$p_k = \frac{N}{n_k}. \tag{2.10}$$

Now define the $p_k \times N$ matrix $E_k(z)$ whose ij-th element is the j-th N-fold type-I polyphase component of $z^{-in_k} H_k(z)$. Similarly define the $N \times p_k$ matrix $R_k(z)$ whose ji-th element is the j-th N-fold type-II polyphase component of $z^{in_k} F_k(z)$. Henceforth we will call $E_k(z)$ and $R_k(z)$ the N-fold extended polyphase representation of $H_k(z)$ and $F_k(z)$ respectively. It is readily seen that in fact fig. 5-(b) is equivalent to fig. 5-(c). Further $v_{ki}(n)$, the output of the downsamplers in fig. 5-(b), are simply certain samples of $y_k(n)$, i.e. $v_{ki}(n) = y_k(p_k n + i)$. Then the $N \times N$ matrices

$$E(z) = \begin{bmatrix} E_K^T(z) & \dots & E_0^T(z) \end{bmatrix}^T \tag{2.11}$$

and

$$R(z) = \begin{bmatrix} R_K(z) & \dots & R_0(z) \end{bmatrix} \tag{2.12}$$

are the N-fold extended polyphase representations of the analysis and synthesis banks of fig. 1 respectively. Further for any $i_1, i_2, \dots, i_l$, a subset of $\{0, 1, \dots, K\}$, $\begin{bmatrix} E_{i_1}^T(z) & E_{i_2}^T(z) & \dots & E_{i_l}^T(z) \end{bmatrix}^T$ will be the N-fold extended type-I polyphase representation of $\begin{bmatrix} H_{i_1}(z) & H_{i_2}(z) & \dots & H_{i_l}(z) \end{bmatrix}^T$. Under these conditions, the overall filter bank in fig. 1 has the equivalent representation in fig. 7.

Thus, for the 3-channel filter bank of fig. 6, one has the equivalent representation of fig. 7, with

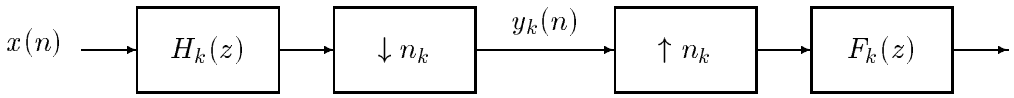

(a)

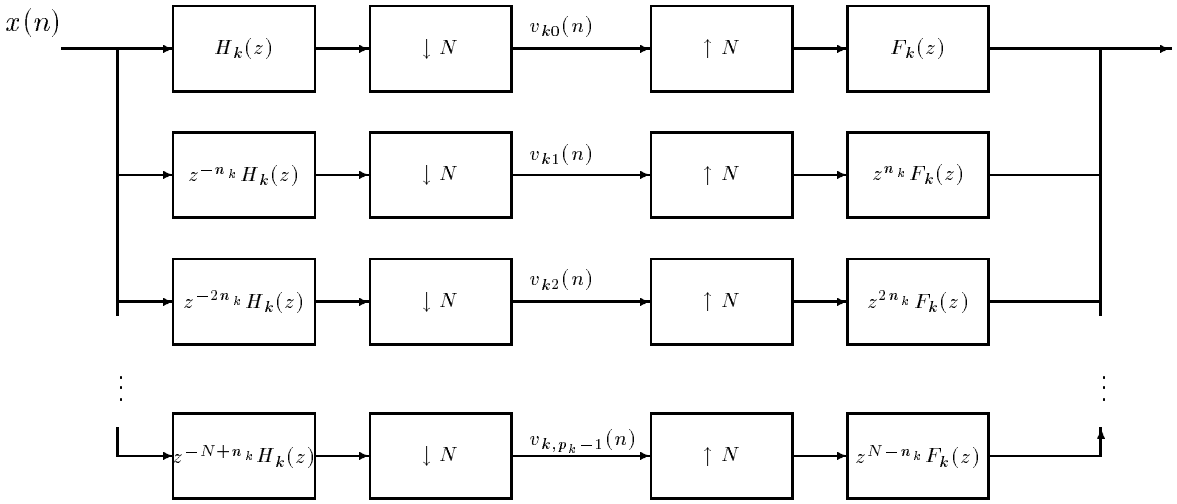

(b)

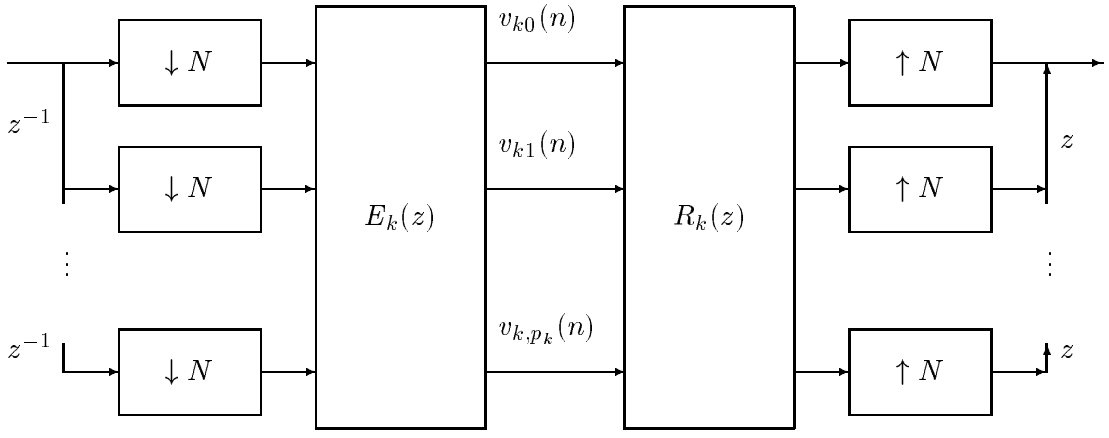

(c)

Figure 5: Extended polyphase representation of H_k, F_k.

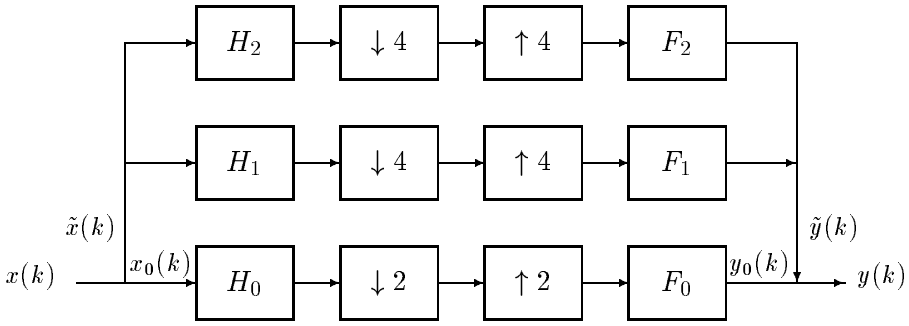

Figure 6: A 3-channel dyadic filter bank.

$N = 4$.

Here, with $E_{kl}(z)$, the 4-fold type-I polyphase components, one has $E(z)$ given by

$$E(z) = \begin{bmatrix} E_{20}(z) & E_{21}(z) & E_{22}(z) & E_{23}(z) \\ E_{10}(z) & E_{11}(z) & E_{12}(z) & E_{13}(z) \\ E_{00}(z) & E_{01}(z) & E_{02}(z) & E_{03}(z) \\ z^{-1}E_{02}(z) & z^{-1}E_{03}(z) & E_{00}(z) & E_{01}(z) \end{bmatrix}. \tag{2.13}$$

Likewise with $R_{lk}(z)$, the 4-fold type-II components of $F_k(z)$, one has

$$R(z) = \begin{bmatrix} R_{02}(z) & R_{01}(z) & R_{00}(z) & zR_{20}(z) \\ R_{12}(z) & R_{11}(z) & R_{10}(z) & zR_{30}(z) \\ R_{22}(z) & R_{21}(z) & R_{20}(z) & R_{00}(z) \\ R_{32}(z) & R_{31}(z) & R_{30}(z) & R_{10}(z) \end{bmatrix}. \tag{2.14}$$

Note the structural constraints on $R(z)$ and $E(z)$. We will call the analysis (respectively, synthesis) bank left (respectively, right) invertible if there is a $1 \times (K+1)$ (respectively, $(K+1) \times 1$) operator $\mathcal{L}$ such that the arrangement in fig. 8-(a) (respectively, fig. 8-(b)) is identity. Here onwards we will drop the qualifiers left and right, that is, the invertibility of an analysis bank will automatically refer to its left invertibility, and that of a synthesis bank to its right invertibility.

Also, observe that invertibility of the analysis bank necessitates the nonsingularity of $E(z)$ (that is, $\det(E(z))$ is not the zero function): To see this, suppose in fig. 8-(a), the arrangement represents an identity operator. Observe that the input to $E(z)$, see fig. 7, is the blocked vector $\begin{bmatrix} x(nN), x(nN-1), \ldots, x(nN-N+1) \end{bmatrix}^T$. Then since this vector can be constructed by a linear operation from $x(n)$, and the outputs of $E(z)$ are simply certain rearranged outputs of samples of the

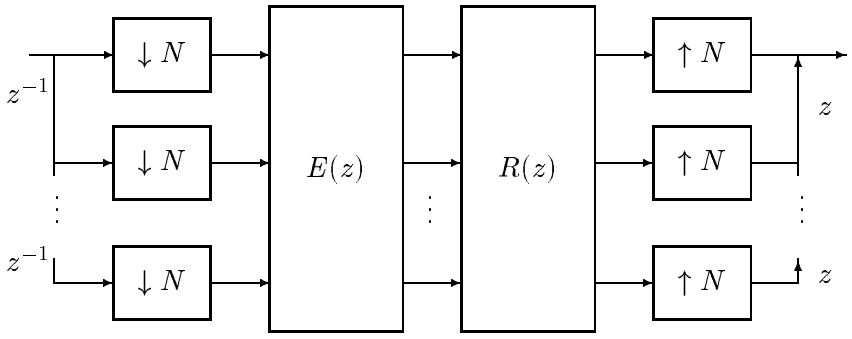

Figure 7: Polyphase representation of filter bank in fig. 1.

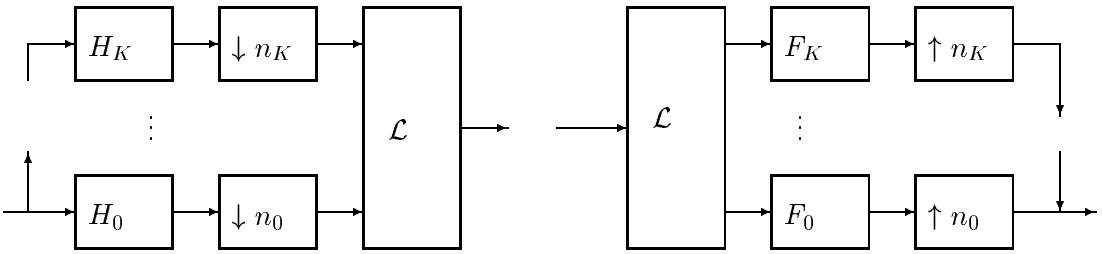

Figure 8: Illustration of invertibility.

analysis bank in fig. 1, there is an $N \times N$ operator $\hat{\mathcal{L}}$ such that $\hat{\mathcal{L}}E(z) = I$. Since $E(z)$ is a square matrix, it must be nonsingular. A similar reasoning proves that the invertibility of a synthesis bank requires the nonsingularity of $R(z)$. Further, it follows that the filter bank in fig. 1 is biorthogonal iff $R(z)E(z) = I$.

Notice that, *even if $E(z)$ is invertible, $E^{-1}(z)$ may not have the structure that the polyphase matrix of the synthesis bank must have.* Thus for example, consider an analysis bank with polyphase matrix

$$E(z) = \begin{bmatrix} 1+2z^{-1} & 1 & 0 & 0 \\ 1 & 0 & 1+z^{-1} & 2 \\ 1 & 1 & z^{-1} & 2 \\ z^{-2} & 2z^{-1} & 1 & 1 \end{bmatrix}.$$

The inverse is then

$$E^{-1}(z) = \frac{1}{2z^2+5z+4}\begin{bmatrix} 3z+z^2 & -z+2z^2 & z-z^2 & -2z^2 \\ -2+z^2 & 2-3z-2z^2 & -2+z+z^2 & 4z+2z^2 \\ -2+z^2 & 6+2z & -6+4z+z^2 & 4z+2z^2 \\ z^{-1}+1-2z-z^2 & -3z^{-1}-2+2z & 3z^{-1}+5+2z+z^2 & -2-3z \end{bmatrix}.$$

Observe that $E^{-1}(z)$ fails to obey the structure in (2.14). Thus even if $E(z)$ is invertible, there may not be a synthesis bank as in fig. 1 that renders the filter bank in fig. 1 biorthogonal. Henceforth should the analysis bank (respectively, synthesis bank) in fig. 1 be such that there exists a synthesis bank (respectively, analysis bank) of the form in fig. 1 for which the filter bank is biorthogonal, then we will call the analysis bank (respectively, synthesis bank) *conformally invertible.*

3 Some results on extended polyphase matrices

We now present some preliminary results on polyphase matrices, to be used in later sections. Although these results are stated for analysis banks, they trivially extend to synthesis banks as well.

We will say that a matrix $P(z)$ has linearly dependent rows if there exists a rational vector $q(z) \neq 0$ such that

$$q^T(z)P(z) = 0.$$

Lemma 3.1 *Consider fig. 9(a) and 9(b) with $L = lcm(n_1, n_2, \ldots, n_M)$ $p_i = L/n_i$, and all filters rational. The L-fold extended polyphase matrix of the AB in fig. 9(a) has linearly dependent rows iff the system in fig. 9(b) is identically zero for some transfer functions $\theta_i(z)$ not all zero.*

Proof: Using the p_i-fold Type-I representation, $\theta_i(z) = \sum_{j=0}^{p_i-1} z^{-j}\hat{\theta}_{i,j}(z^{p_i})$ and making use of the Noble identities, fig. 9(b) can be redrawn as shown in fig. 9(c). Also the polyphase matrix of the arrangement to the left of the $\hat{\theta}_{i,j}(z)$ in fig. 9(c) is simply the L-fold extended polyphase matrix $E(z)$ of the AB in fig. 9(a). Redrawing the nonuniform AB as a uniform AB in polyphase form as explained in the earlier section, $E(z)$ has linearly dependent rows iff $\begin{bmatrix} \hat{\theta}_{1,0}(z) & \ldots & \hat{\theta}_{M,n_M-1}(z) \end{bmatrix} E(z) = 0$, with not all $\hat{\theta}_i(z) = 0$.

■

Lemma 3.2 *Consider fig. 9(a) and 10(a), with $L = lcm(n_1, n_2, \ldots, n_M)$ and all filters rational. If the L-fold extended polyphase matrix of the AB in fig. 9(a) has linearly dependent rows, so does the NKL-fold extended polyphase matrix of the AB in fig. 10(a).*

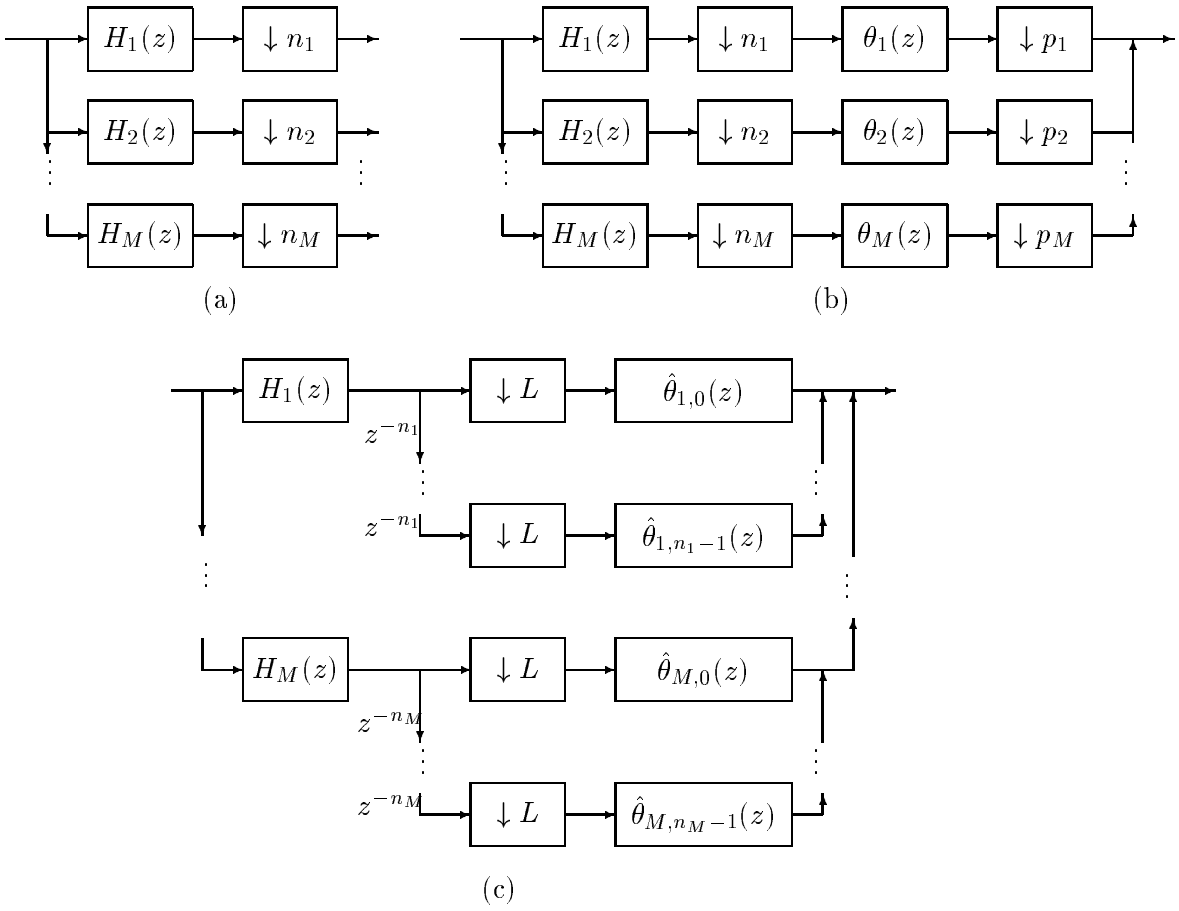

Figure 9: Setup and illustration for lemma 3.1.

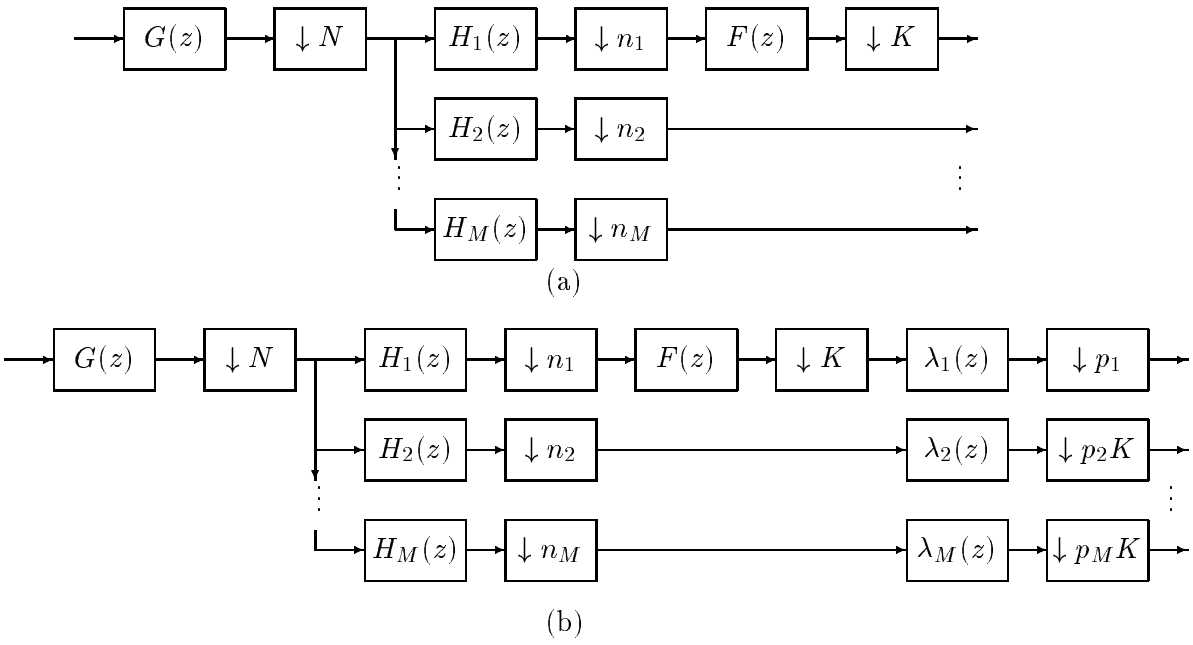

Figure 10: Setup and illustration for lemma 3.2.

Proof: By lemma 3.1, there exist $\theta_i(z)$, not all zero, such that the system in fig. 9(b) is identically zero. We need to show that there exist $\lambda_i(z)$, not all identically zero, such that the system in fig. 10b is identically zero. Consider a system wherein the system in fig. 9(b) is preceded by the system consisting of $G(z)$ and the decimator N, and the output of fig. 9(b) is appended by a decimator K. This new system is also identically zero. Now choosing $\lambda_1(z) = 1$ and $\lambda_i(z) = \theta_i(z)$ for $i > 1$ makes this new system identical to fig. 10b provided $\theta_1(z) = F(z)$. Indeed the $\theta_i(z)$ can be so scaled that $\theta_1(z) = F(z)$ provided that $F(z), \theta_i(z) \neq 0$, completing the proof. The case $F(z) = 0$ is trivial, and for the case $\theta_1(z) = 0$ we only have to make the choice $\lambda_1(z) = 0$ instead of $\lambda_1(z) = 1$. ∎

4 Biorthogonal Tree Structured Filter Banks

The Introduction had given the example of a dyadic tree structured filter bank. In this section we deal with more general tree structured filter banks, and discuss conditions under which such a filter bank is biorthogonal. Some notation for general tree structured filter banks will be introduced first.

A general TSAB is depicted in fig. 11(a). Through the repeated use of Noble identities, any such filter bank is equivalent to the analysis bank in fig. 1. For example, the analysis bank in fig. 11(a) is

equivalent to that in fig. 11(b).

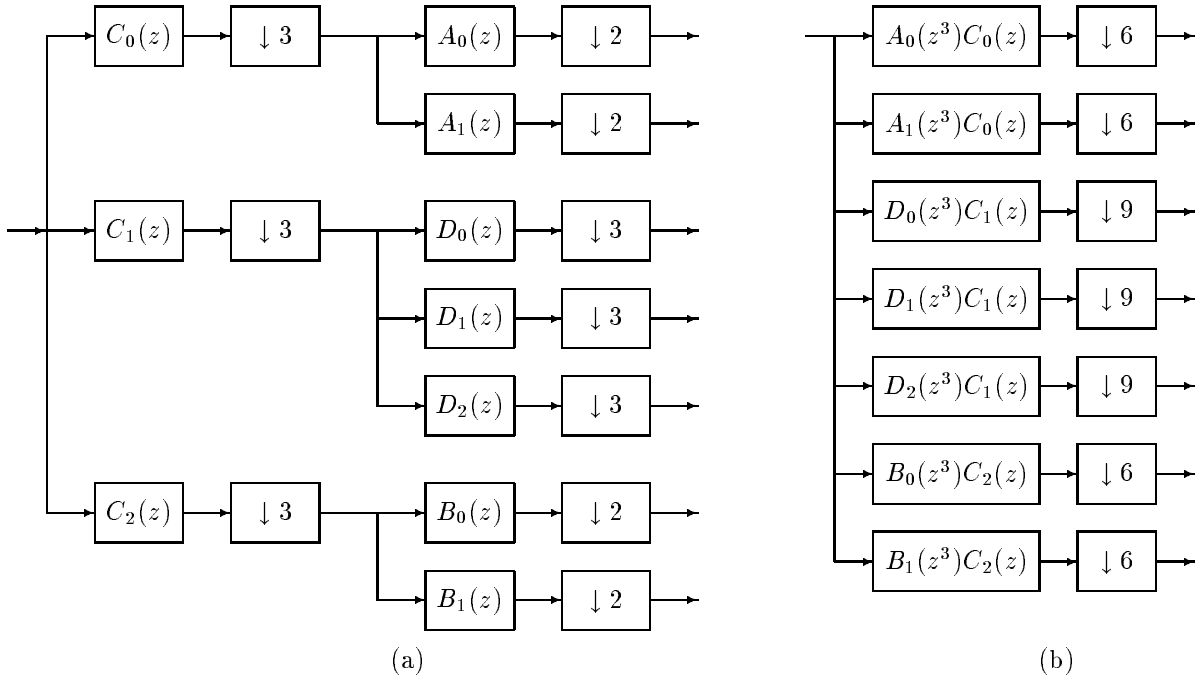

Figure 11: An example tree (analysis side).

Whereas in a dyadic tree, only one of the two branches on a given level divides further, this is not in general the case with arbitrary trees. Further, in a general tree, two different levels may have different number of branches. In the dyadic case, each level has precisely two branches.

In a general TSAB, filters that have the same input will be said to belong to the same level. Thus, in fig. 11(a), the filter sets $\{A_0, A_1\}$, $\{D_0, D_1, D_2\}$, $\{B_0, B_1\}$, and $\{C_0, C_1, C_2\}$ each contribute a separate level. We will call a level an *output level*, if its outputs do not branch out further. For example, $\{A_0, A_1\}$, $\{D_0, D_1, D_2\}$, $\{B_0, B_1\}$ are all at output levels. We will say a TSSB matches a TSAB if it is topologically a mirror image of the TSAB. For example, the TSSB in fig. 12 matches that in fig. 11(a). Of course the filters appearing in a matching TSSB may differ from their counterparts in the TSAB in question.

Further we will designate the levels constituting $\{P_0, P_1\}$, $\{Q_0, Q_1\}$, $\{S_0, S_1, S_2\}$, $\{T_0, T_1, T_2\}$ as respectively the matching levels of $\{A_0, A_1\}$, $\{B_0, B_1\}$, $\{C_0, C_1, C_2\}$, $\{D_0, D_1, D_2\}$. We will call the tree structured filter bank *critically sampled* if its equivalent in fig. 1 is also *critically sampled*.

Throughout, the following assumption applies:

Assumption 4.1 *Each level in the TSAB is a critically sampled uniform analysis bank with all filters*

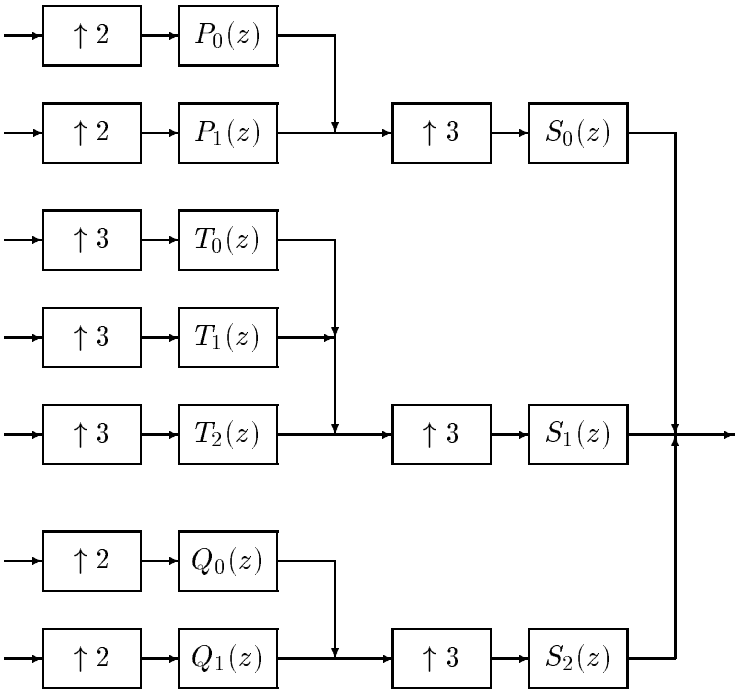

Figure 12: Matching tree structured synthesis bank.

rational.

In a dyadic tree, each level is a 2-channel critically sampled uniform filter bank. Observe Assumption 4.1 guarantees that the TSAB is critically sampled.

Throughout this section the results presented are for TSABs. Proof of extensions to the TSSBs, being trivially similar, are omitted. We now state and prove the main result of this section.

Theorem 4.1 *A TSAB satisfying Assumption 4.1 is invertible iff each of its constituent levels is invertible. Under this condition the TSAB has an inverse that is a matching TSSB, with each matching level the inverse of its counterpart in the TSAB.*

Proof: The if part is trivial. The only if part is proved by contradiction. If any of the levels is not invertible, its polyphase matrix has linearly dependent rows. Hence by lemma 3.2 the extended polyphase matrix of the TSAB also has linearly dependent rows, a contradiction. ■

Thus if a TSAB is invertible, then not only is it conformally invertible, but in fact its left inverse is a matching TSSB. This thus generalizes the comparable result in [11] derived for orthonormal trees.

The question remains: Suppose a conformally invertible, nonuniform analysis bank has a set of decimation ratios that are compatible with a tree structure. Is it then necessarily decomposable into

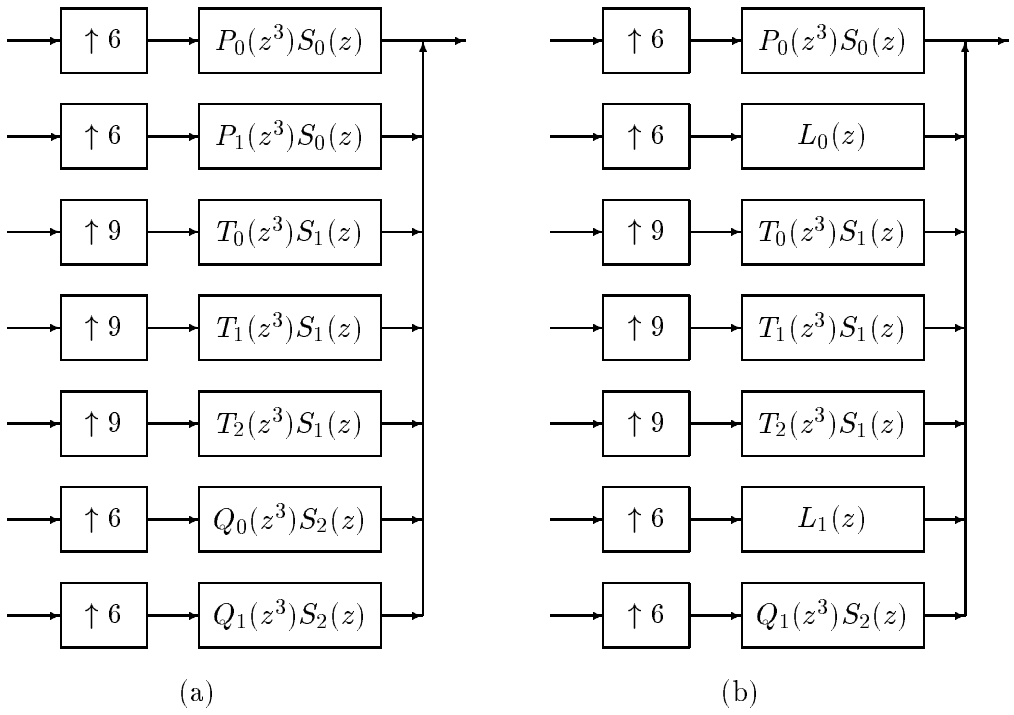

Figure 13: Synthesis bank which cannot be decomposed into a tree structure.

a TSAB? The answer in general is no. To see this, consider the example, [11], of a TSSB shown in fig. 12. This can be redrawn using noble identities as in fig. 13(a). Suppose this synthesis side is conformally invertible. Now consider the synthesis bank in fig. 13(b), with $L_0(z) = (P_1(z^3)S_0(z) + Q_0(z^3)S_2(z))/\sqrt{2}, L_1(z) = (P_1(z^3)S_0(z) - Q_0(z^3)S_2(z))/\sqrt{2}$. Clearly fig. 13(a) and fig. 13(b) have the same MISO (multiple input single output) relationship. However, it is not possible to decompose fig. 13(b) into a tree structure. The reason is as follows. For this synthesis bank to be represented as a tree, $L_0(z)$ (and $L_1(z)$) must be expressible in the form $P_1'(z^3)S_0(z)$ or $Q_0'(z^3)S_2(z)$ (see fig. 12 and fig. 13(a)). Neither is possible unless $S_0(z) = S_2(z)$. However, since the synthesis bank at each level of the tree in fig. 12 is invertible, $S_0(z) \neq S_2(z)$. Hence this synthesis bank cannot be decomposed into a tree structure. In the next section we show that for dyadic nonuniform analysis banks, this result does hold.

5 Dyadic filter banks and tree structures

The previous section showed that every invertible TSAB admits an inverse that is a matching TSSB. We now turn to the special case of dyadic filter banks where a stronger result is possible.

Recall that a general dyadic tree structured filter bank is equivalent to a dyadic nonuniform filter bank of the form in fig. 2. In this section we show that a dyadic nonuniform analysis bank (respectively, synthesis bank) of the form in fig. 2 is conformally invertible iff it admits a tree structured decomposition. In view of the results of the previous section this therefore also shows that every conformally invertible dyadic analysis bank has a tree structured inverse.

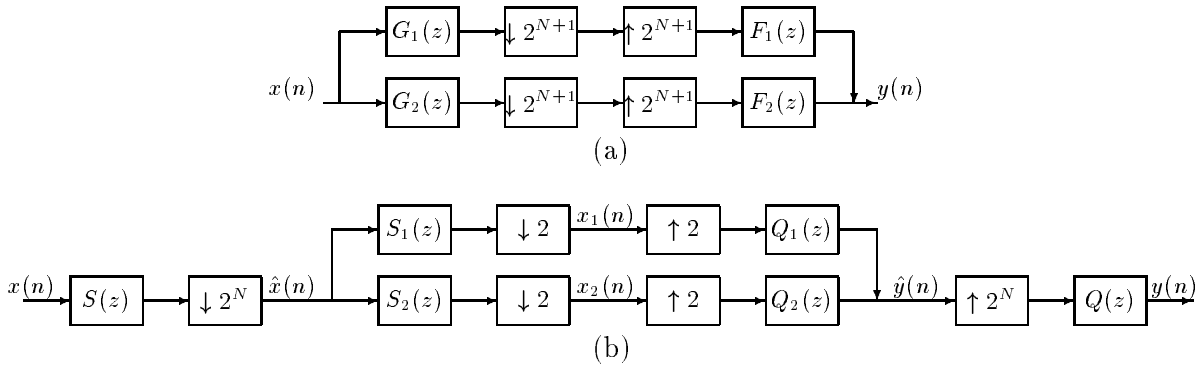

Figure 14: Tree decomposition of a dyadic filter bank obeying (5.15) and (5.16).

Consider now two channels of a dyadic nonuniform filter bank depicted in fig. 14, with $G_i(z)$, $F_i(z)$ all rational. Then from the noble identities it is evident that this nonuniform filter bank is decomposable as in fig. 14(b) if and only if

$$G_i(z) = S(z)S_i(z^{2^N}) \tag{5.15}$$

and

$$F_i(z) = Q(z)Q_i(z^{2^N}). \tag{5.16}$$

This in turn requires that

$$\frac{G_1(z)}{G_2(z)} = \frac{S_1(z^{2^N})}{S_2(z^{2^N})} \tag{5.17}$$

and

$$\frac{F_1(z)}{F_2(z)} = \frac{Q_1(z^{2^N})}{Q_2(z^{2^N})}. \tag{5.18}$$

Put differently, the decomposability of fig. 14(a) into fig. 14(b) is equivalent to the requirement that for all $0 \leq k \leq 2^N - 1$,

$$\frac{G_1(z)}{G_2(z)} = \frac{G_1(\beta_k z)}{G_2(\beta_k z)} \quad \text{and} \quad \frac{F_1(z)}{F_2(z)} = \frac{F_1(\beta_k z)}{F_2(\beta_k z)} \tag{5.19}$$

where $\beta_k = e^{\frac{-j2\pi k}{2^N}}$.

Lemma 5.1 describes a setting in which this is necessary.

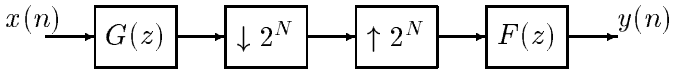

Figure 15: An equivalent structure to fig. 14(a).

Lemma 5.1 *Consider the structure in fig. 14(a) with $G_i(z)$, $F_i(z)$ all non-zero. Suppose for some $G(z)$, $F(z)$, fig. 14(a) is equivalent to fig. 15. Then (5.19) holds.*

Proof: Define $W_L^p = e^{\frac{-j2\pi p}{L}}$,

$$\mathcal{G}_e(z) = \begin{bmatrix} G_1(z) & G_1(zW_{2^{N+1}}^2) & \dots & G_1(zW_{2^{N+1}}^{2^{N+1}-2}) \\ G_2(z) & G_2(zW_{2^{N+1}}^2) & \dots & G_2(zW_{2^{N+1}}^{2^{N+1}-2}) \end{bmatrix} \tag{5.20}$$

$$\mathcal{G}_o(z) = \begin{bmatrix} G_1(zW_{2^{N+1}}) & G_1(zW_{2^{N+1}}^3) & \dots & G_1(zW_{2^{N+1}}^{2^{N+1}-1}) \\ G_2(zW_{2^{N+1}}) & G_2(zW_{2^{N+1}}^3) & \dots & G_2(zW_{2^{N+1}}^{2^{N+1}-1}) \end{bmatrix} \tag{5.21}$$

$$X_e(z) = \begin{bmatrix} X(z) & X(zW_{2^{N+1}}^2) & \dots & X(zW_{2^{N+1}}^{2^{N+1}-2}) \end{bmatrix}^T \tag{5.22}$$

$$X_o(z) = \begin{bmatrix} X(zW_{2^{N+1}}) & X(zW_{2^{N+1}}^3) & \dots & X(zW_{2^{N+1}}^{2^{N+1}-1}) \end{bmatrix}^T \tag{5.23}$$

and

$$\mathcal{G}(z) = \begin{bmatrix} G(z) & G(zW_{2^N}) & G(zW_{2^N}^2) & \dots & G(zW_{2^N}^{2^N-1}) \end{bmatrix} \tag{5.24}$$

Note

$$W_{2^{N+1}}^{2k} = W_{2^N}^k. \tag{5.25}$$

Thus, in fig. 14(a)

$$Y(z) = \frac{1}{2^{N+1}} \begin{bmatrix} F_1(z) & F_2(z) \end{bmatrix} \{\mathcal{G}_e(z)X_e(z) + \mathcal{G}_o(z)X_o(z)\}. \tag{5.26}$$

Because of (5.25), in fig. 15

$$Y(z) = \frac{1}{2^N} F(z)\mathcal{G}_e(z)X_e(z). \tag{5.27}$$

Thus for all combinations of $X_e(z)$, $X_o(z)$, the right hand sides of (5.26) and (5.27) are equal. Consequently for all z,

$$\begin{bmatrix} F_1(z) & F_2(z) \end{bmatrix} \mathcal{G}_o(z) = 0. \tag{5.28}$$

Thus, from (5.21), for all $0 \le k \le 2^N - 1$,

$$\frac{F_1(z)}{F_2(z)} = -\frac{G_2(zW_{2^{N+1}}^{2k+1})}{G_1(zW_{2^{N+1}}^{2k+1})}. \tag{5.29}$$

Note that $W_{2^{N+1}}^{2k+1} = e^{-\frac{j2\pi k}{2^N}} e^{-\frac{j2\pi}{2^{N+1}}} = W_{2^N}^k W_{2^{N+1}}$. Thus, for all $0 \le k \le 2^N - 1$,

$$\frac{F_1(z)}{F_2(z)} = -\frac{G_2(\alpha z \beta_k)}{G_1(\alpha z \beta_k)} \tag{5.30}$$

where $\alpha = W_{2^{N+1}}$. Consequently, choosing $\hat{z} = \alpha z$, for all $1 \le k \le 2^N - 1$

$$\frac{G_1(\hat{z})}{G_2(\hat{z})} = \frac{G_2(\hat{z}\beta_k)}{G_1(\hat{z}\beta_k)} \tag{5.31}$$

that is, the first equality in (5.19) holds.

Further, since for every $0 \le k, l \le 2^N - 1$, there exists $0 \le m \le 2^N - 1$, for which $\beta_k \beta_l = \beta_m$, the second equality in (5.19) also holds. ∎

The next lemma shows that, in fact, in the decomposition in fig. 14(b), the $\hat{x}(n)$ to $\hat{y}(n)$ relation can be chosen to be biorthogonal.

Lemma 5.2 *Consider the structure in fig. 14(b) with all filters non-zero rationals. Suppose the system from $x(n)$ to $y(n)$ is non-zero and is equivalent to the structure in fig. 15. Then one can select the filters in such a way that*

(i) the $\hat{x}(n)$ to $\hat{y}(n)$ relation is the identity system, and
(ii) the $x(n)$ to $\begin{bmatrix} x_1(n) & x_2(n) \end{bmatrix}^T$, and $\begin{bmatrix} x_1(n) & x_2(n) \end{bmatrix}^T$ to $y(n)$ relationship is preserved.

Proof: We first argue that the uniform filter bank relating $\hat{x}(n)$ to $\hat{y}(n)$ in fig. 14(b) is alias free. From [15], this is guaranteed if

$$\begin{aligned} & Q_1(z)S_1(-z) + Q_2(z)S_2(-z) = 0 \\ \Leftrightarrow\ & \frac{Q_1(z)}{S_2(-z)}\left[\frac{S_1(-z)}{S_2(-z)} + \frac{Q_2(z)}{Q_1(z)}\right] = 0. \end{aligned} \tag{5.32}$$

From (5.17), (5.18)

$$\frac{S_1(z)}{S_2(z)} = \frac{G_1(z^{\frac{1}{2^N}})}{G_2(z^{\frac{1}{2^N}})} \quad , \quad \frac{Q_1(z)}{Q_2(z)} = \frac{F_1(z^{\frac{1}{2^N}})}{F_2(z^{\frac{1}{2^N}})}.$$

Thus (5.32) is equivalent to

$$\frac{G_1(z^{\frac{1}{2^N}} e^{-\frac{j\pi}{2^N}})}{G_2(z^{\frac{1}{2^N}} e^{-\frac{j\pi}{2^N}})} + \frac{F_2(z^{\frac{1}{2^N}})}{F_1(z^{\frac{1}{2^N}})} = 0.$$

This clearly holds from (5.30) with $k = 0$, and from the fact that $\alpha = e^{-\frac{j\pi}{2^N}}$.

Thus, the $\hat{x}(n)$ to $\hat{y}(n)$ relationship is LTI with transfer function $T(z)$. Clearly $T(z) \neq 0$, as otherwise the $x(n)$ to $y(n)$ relation will be zero. Then replacing $Q_i(z)$ by $T^{-1}(z)Q_i(z)$ and $Q(z)$ by $T(z^{2^N})Q(z)$ yields the result. ∎

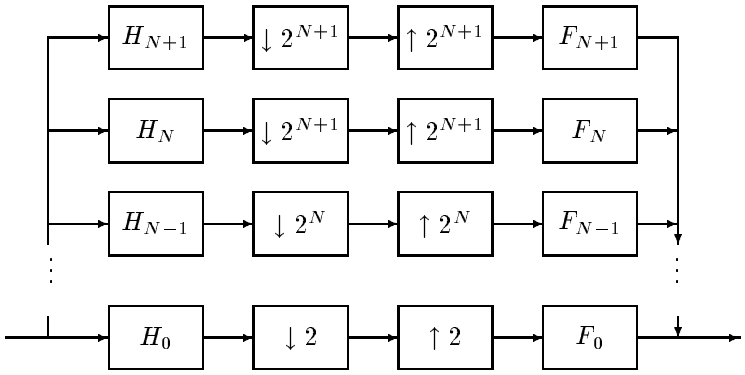

Figure 16: An $(N+2)$-channel filter bank.

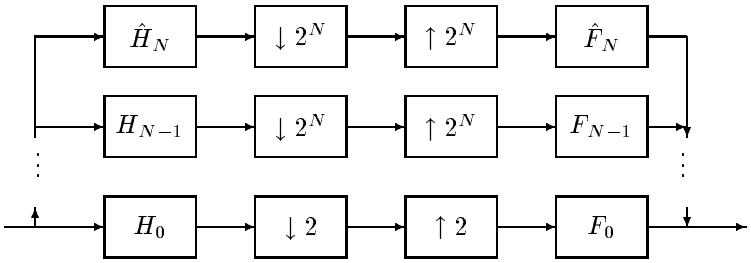

Figure 17: Modified dyadic filter bank.

The next Lemma (see [2] for details) relates the 2^N-fold extended polyphase matrices of a filter bank to its 2^{N+1}-fold extended polyphase matrices.

Lemma 5.3 *Consider the last N channels of the dyadic filter bank in fig. 16 with all filters rational. Let $E(z)$ (respectively, $R(z)$) be the 2^N-fold extended type-I (respectively, type-II) polyphase matrices of the AB (respectively, SB), and $\overline{E}(z)$ (respectively, $\overline{R}(z)$) their extended 2^{N+1}-fold counterparts. Suppose*

$$E(z) = E_0(z^2) + z^{-1}E_1(z^2) \quad \textit{and} \quad R(z) = R_0(z^2) + zR_1(z^2).$$

Then

$$\overline{E}(z) = \begin{bmatrix} E_0(z) & E_1(z) \\ z^{-1}E_1(z) & E_0(z) \end{bmatrix} \quad \textit{and} \quad \overline{R}(z) = \begin{bmatrix} R_0(z) & zR_1(z) \\ R_1(z) & R_0(z) \end{bmatrix}. \tag{5.33}$$

We need one more preparatory lemma.

Lemma 5.4 *Consider the dyadic filter bank in fig. 16, with all filters rational and $N \geq 1$. Suppose this filter bank is biorthogonal. Then there exist rational $\hat{H}_N(z)$ and $\hat{F}_N(z)$ such that the filter bank in fig. 17 is biorthogonal.*

Proof: Call $\hat{E}(z)$ (respectively, $\hat{R}(z)$), the 2^{N+1}-fold extended type-I (respectively, type-II) polyphase matrix of the analysis bank (respectively, synthesis bank) in fig. 16. Further call $\overline{E}(z)$ (respectively, $\overline{R}(z)$), the 2^{N+1}-fold extended type-I (respectively, type-II) polyphase matrix of the analysis bank (respectively, synthesis bank) obtained by removing the upper two channels in fig. 16, and $E(z)$ (respectively, $R(z)$) the 2^N-fold extended polyphase matrix of this N-channel AB (respectively, SB). Then

$$\hat{R}(z)\hat{E}(z) = I \quad \Leftrightarrow \quad \hat{E}(z)\hat{R}(z) = I.$$

Since for some $\tilde{E}(z)$, $\tilde{R}(z)$,

$$\hat{E}(z) = \begin{bmatrix} \tilde{E}(z) \\ \overline{E}(z) \end{bmatrix} \quad , \quad \hat{R}(z) = \begin{bmatrix} \tilde{R}(z) & \overline{R}(z) \end{bmatrix}$$

one has

$$\overline{E}(z)\overline{R}(z) = I.$$

With $E_i(z)$, $R_i(z)$ as in lemma 5.3, by lemma 5.3

$$\begin{bmatrix} E_0(z) & E_1(z) \\ z^{-1}E_1(z) & E_0(z) \end{bmatrix} \begin{bmatrix} R_0(z) & zR_1(z) \\ R_1(z) & R_0(z) \end{bmatrix} = I.$$

Thus

$$\begin{aligned} E_0(z)R_0(z) + E_1(z)R_1(z) &= I, \\ zE_0(z)R_1(z) + E_1(z)R_0(z) &= 0. \end{aligned}$$

Thus

$$\begin{aligned} E(z)R(z) &= \left[E_0(z^2) + z^{-1}E_1(z^2)\right]\left[R_0(z^2) + zR_1(z^2)\right] \\ &= E_0(z^2)R_0(z^2) + E_1(z^2)R_1(z^2) + z^{-1}E_1(z^2)R_0(z^2) + zE_0(z^2)R_1(z^2) \\ &= I. \end{aligned}$$

Note $E(z)$ is $(2^N - 1) \times 2^N$ and $R(z)$ is $2^N \times (2^N - 1)$. Clearly there exist rational 2^N-vectors $p_1(z)$, $p_2(z)$ such that

$$\begin{bmatrix} p_1^T(z) \\ E(z) \end{bmatrix} \begin{bmatrix} p_2(z) & R(z) \end{bmatrix} = I.$$

Hence the result. ∎

The result goes beyond the results of Section 4 in the following respect. It shows that if an $N+1$-channel dyadic analysis bank is conformally invertible, then one can augment its channels indexed from 0 to $N-1$ in a manner depicted in fig. 17 in a way that the resulting N-channel dyadic analysis bank is not only conformally invertible, but that its inverse's channels indexed from 0 to $N-1$ coincide with the corresponding channels of the inverse of the $N+1$-channel dyadic analysis bank.

We can now prove the main result of this section.

Theorem 5.1 *Consider the dyadic nonuniform filter bank in fig. 2 with $M > 2$ and all filters rational. Suppose the filter bank is biorthogonal. Then the analysis bank and the synthesis bank are equivalent to a TSAB and a TSSB respectively.*

Proof: Suppose the result holds for some $N = M - 1 \geq 2$. Consider the filter bank in fig. 16 and assume it is biorthogonal. Then from Lemma 5.4, there exists a filter bank of the form in fig. 17 that is biorthogonal and has all filters rational. Consequently channels $N+1$ and $N+2$ in fig. 16 are together equivalent to the top channel in fig. 17. Thus from Lemmas 5.2 and 5.3 the top two channels in fig. 16 are equivalent to a structure as in fig. 14(b) with the 2-channel uniform filter bank relating $\hat{x}(n)$ to $\hat{y}(n)$, biorthogonal. Thus the filter bank in fig. 17 with $S(z) = \hat{H}_N(z)$ and $Q(z) = \hat{F}_N(z)$ is biorthogonal. Then a simple inductive argument proves the result. ∎

Taken together with the results of the previous section, we have the following result for dyadic analysis banks.

Theorem 5.2 *A critically sampled dyadic analysis bank with rational filters, is conformally invertible, iff both the following conditions hold:*

(i) The analysis bank can be decomposed into a dyadic TSAB.

(ii) The two channel filter banks appearing at every level of this dyadic tree are themselves invertible.

Further, the inverse is also decomposable into a dyadic TSSB. The levels of the TSSB can be chosen so that they form biorthogonal pairs with their matching levels in the TSAB.

Note also that this provides a simple test for conformal invertibility: check if the analysis bank or synthesis bank is decomposable into a dyadic tree structure with invertibility of each level. Decomposability of course requires testing if for all $i \geq 1$, the ratios $H_i(z)/H_{i+1}(z)$ are rational functions in z^{2^i}, and is simple to verify.

Indeed turn to the example at the end of Section 2, of a dyadic analysis bank that though left invertible, was not conformally so. In that case $H_1(z) = 1+z^{-2}+2z^{-3}+z^{-6}$ and $H_2(z) = 1+z^{-1}+2z^{-4}$. Clearly, one cannot express $H_1(z)/H_2(z)$ as $G(z^2)$, with $G(z)$ rational. Hence this analysis bank is not decomposable into a tree structure.

On the other hand consider the example below.

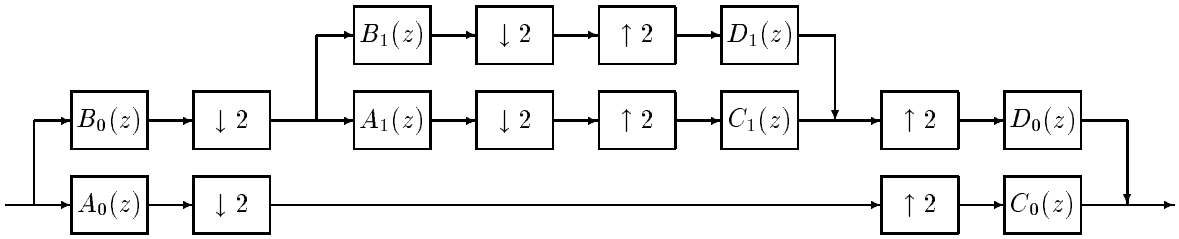

Figure 18: A two level tree structured filter bank.

Example 5.1 *Consider the set of analysis filters* $H_0(z) = (z^6 - z^4 - z^2 - z + 1 + z^{-1})/(z^{12} - 2z^8 + 1), H_1(z) = (z^6+z^4-z-z^{-1})/(z^{16}-z^8-2z^4-1), H_2(z) = (-z^8+z^6+z^3+z^2-z-z^{-3})/(z^{16}-z^8-2z^4-1)$. *The corresponding polyphase analysis matrix is then*

$$E(z) = \begin{bmatrix} -\frac{z+1}{z^4-2z-z^2-1} & \frac{z(z+1)}{z^4-2z-z^2-1} & \frac{z}{z^4-2z-z^2-1} & -\frac{z^2}{z^4-2z-z^2-1} \\ -\frac{z}{z^4-2z-z^2-1} & \frac{z^2}{z^4-2z-z^2-1} & -\frac{1}{z^4-2z-z^2-1} & \frac{z}{z^4-2z-z^2-1} \\ -\frac{1}{-1+z^2-z} & \frac{1}{z^3-2z^2+1} & \frac{z}{-1+z^2-z} & -\frac{z}{z^3-2z^2+1} \\ \frac{1}{-1+z^2-z} & -\frac{1}{z^3-2z^2+1} & -\frac{1}{-1+z^2-z} & \frac{1}{z^3-2z^2+1} \end{bmatrix}.$$

The inverse $E^{-1}(z)$ *exists and is given by*

$$E^{-1}(z) = \begin{bmatrix} 1 & z & z & z^2 \\ z-1 & z(z-1) & 1 & z \\ -z & z+1 & z & z \\ -z(z-1) & (z+1)(z-1) & 1 & 1 \end{bmatrix}.$$

The ratio $H_2(z)/H_1(z) = (-z^6 + z^4 + 1)/(z^4 + z^2) = B_1(z^2)/A_1(z^2)$ *is an even rational function in* z. *Compare the analysis sides of fig. 6 and fig. 18. The set of filters on the analysis side of the tree structure in fig. 18 are then given by* $A_0(z) = (z^6 - z^4 - z^2 - z + 1 + z^{-1})/(z^{12} - 2z^8 + 1), B_0(z) = (z^2-z^{-3})/(z^{16}-z^8-2z^4-1), A_1(z) = z^2+z$, *and* $B_1(z) = -z^3+z^2+1$. *From the expression of* $E^{-1}(z)$, *we obtain the synthesis filters* $F_0(z) = z^6+z^4+z^3+z, F_1(z) = z^{11}+z^9+z^6-z^5+z^4-z^3+z^2, F_2(z) =$

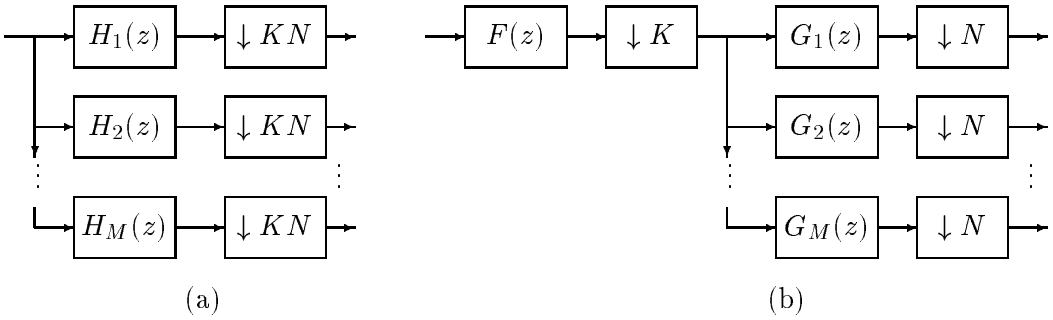

Figure 19: Illustration of Lemma 6.1.

$-z^{11} + z^7 - z^6 + z^5 - z + 1$. *The ratio* $F_2(z)/F_1(z) = (-z^6+1)/(z^6+z^4+z^2) = D_1(z^2)/C_1(z^2)$. *Comparing the synthesis sides of fig. 6 and fig. 18, the set of synthesis filters of the tree structure in fig. 18 are then given by* $C_0(z) = z^6 + z^4 + z^3 + z, D_0(z) = z^5 - z + 1, C_1(z) = z^3 + z^2 + z, D_1(z) = z^3 - 1$. *Thus we have an equivalent tree structured filter bank to the given dyadic biorthogonal filter bank.*

6 Stable and FIR decompositions

We now turn to the following questions. Suppose an analysis or synthesis bank comprises stable (respectively, FIR) filters, and is decomposable to a tree structure. Then can the tree structure be chosen so as to comprise exclusively of stable (respectively, FIR) filters? Lemma 6.1 below provides an affirmative answer.

Lemma 6.1 *Suppose the structure in figure 19(a) is equivalent to that in figure 19(b), with all filter transfer functions rational.* $F(z)$ *is scalar,* $H(z) = \left[\begin{array}{cccc} H_1(z), & H_2(z), & \ldots, & H_M(z) \end{array} \right]^T$ *and* $G(z) = \left[\begin{array}{cccc} G_1(z), & G_2(z), & \ldots, & G_M(z) \end{array} \right]^T$ *are* $M \times 1$. *Suppose the filters in figure 19(a) are stable (respectively, FIR). Then all filters in figure 19(b) can also be selected to be stable (respectively, FIR).*

Proof: We will prove the result for the stable case. The FIR case is similar. The equivalence ensures that

$$H(z) = F(z)G(z^K).$$

Suppose $F(z)$ is unstable. Write it as

$$F(z) = \frac{\hat{F}(z)}{z - \beta}$$

with β an unstable pole. Thus as $H(z)$ is stable, $z - \beta$ must be a common factor of each $G_i(z^K)$. Since

these are rational in z^K,

$$G(z^K) = \hat{G}(z^K)(z^K - \beta^K).$$

Consequently, with $\beta(z)$ the polynomial $(z^K - \beta^K)/(z - \beta)$,

$$H(z) = \left[\hat{F}(z)\beta(z)\right]\left[\hat{G}(z^K)\right].$$

Thus by replacing $F(z)$ by $\hat{F}(z)\beta(z)$ and $\hat{G}(z)$, in fig. 19, one retains the equivalence while removing the unstable pole β from $F(z)$, and without adding new poles to $G(z)$. Continuing this procedure it follows that $F(z)$ can be chosen to be stable.

Now suppose $G(z)$ is unstable, and at least one $G_i(z)$ has the unstable pole η. Then one can write, in a possibly nonminimal way:

$$G(z^K) = \frac{\tilde{G}(z^K)}{z^K - \eta},$$

where some elements of $\tilde{G}(z^K)$ may have the zero η. It follows that as $F(z)$ has no unstable poles, for some rational stable $\tilde{F}(z)$,

$$F(z) = \tilde{F}(z)(z^K - \eta).$$

Thus, one can write

$$H(z) = \left[\tilde{F}(z)\right]\left[\tilde{G}(z^K)\right].$$

Thus by replacing $F(z)$ by $\tilde{F}(z)$ and $\tilde{G}(z)$, in fig. 19, one retains the equivalence while removing the unstable pole η from $G(z)$, and without adding new poles to $F(z)$. Continuing this procedure it follows that $G(z)$ can be chosen to be stable.

■

A similar result applying to synthesis structures can also be used. Using this Lemma one can prove the following strenghtened version of Theorems 4.1 and 5.1. Note first that an analysis or synthesis bank has a stable inverse if its extended polyphase matrix is minimum phase, that is, its determinant is minimum phase. Similarly an FIR analysis or synthesis bank is FIR invertible if its extended polyphase matrix is unimodular, that is, has constant determinant.

Theorem 6.1 *Suppose a stable (respectively, FIR) nonuniform analysis bank/synthesis bank with rational filters is decomposable into a tree structure satisfying Assumption 4.1. Then this TSAB/TSSB can be chosen to have all elements stable (respectively, FIR). Further suppose the extended polyphase representation of the TSAB/TSSB is invertible and minimum phase (respectively, unimodular). Then the inverse is a stable (respectively, FIR) TSSB/TSAB.*

Proof: The first part of the theorem follows from repeated application of Lemma 6.1. To prove the second part invoke Theorem 4.1. Suppose the analysis bank is invertible and minimum phase (respectively, unimodular). Then it has a stable (respectively, FIR) inverse, which by Theorem 4.1 can be decomposed into a tree structure prescribed by the theorem. By the first part of this theorem, that tree structure must be stable (respectively, FIR). The result with respect to stably (respectively, FIR) invertible TSSB follows similarly. ■

7 Conclusions

Two principal results have been presented relating biorthogonal nonuniform filter banks with tree structures: (i) That every TSAB is invertible iff its inverse can be decomposed into a matching TSSB, with each matching level of the resulting tree structured filter bank, being itself a biorthogonal uniform filter bank. (ii) That a dyadic analysis bank is conformally invertible iff it can be decomposed into a TSAB with the 2-channel uniform filter banks on each level, themselves invertible. The second result thus also provides an easy test for conformal invertibility of dyadic filter banks. All these decompositions preserve stability. If a stable (respectively, FIR) analysis bank or synthesis bank is decomposable into a TSAB or synthesis bank, then this equivalent tree structure can be chosen to have all constituent filters stable (respectively, FIR).

These results were derived under the assumption that all filters have rational transfer functions. Barring the results of Section 6, this assumption is in fact unnecessary, and has been invoked primarily to use the Noble identitities. Thus, the notion of extended polyphase representation and the results of Sections 3 and 4 can be derived independently of the rationality assumption. The two key devices used in Section 5, are (5.19) and Lemma 5.1. The latter does not assume rationality, and the former can be proved independently of rationality by using techniques similar to the proof of Lemma 5.1.

References

[1] A. Akansu and R. Haddad, *Multiresolution Signal Decomposition - Transforms, Subbands, and Wavelets*, Academic Press, Inc., 1992.

[2] S. Akkarakaran and P.P. Vaidyanathan,"New Results and Open Problems on Nonuniform Filterbanks", in *Proceedings of ICASSP*, pp 1501-1504, Mar. 15-19, 1999.

[3] M. Antonini, M. Barlaud, P. Mathieu and I. Daubechies, "Image Coding Using Wavelet transform", *IEEE Transactions on Image Processing*, pp 205-220, Apr. 1992.

[4] A. Cohen, I. Daubechies and J.-C. Feauveau "Biorthonormal Bases of Compactly Supported Wavelets", *Comm. on Pure and App. Math.*, pp 485-560, Jun. 1992.

[5] F. M. de Saint-Martin, P. Siohan and A. Cohen, "Application of Multiwavelet Filterbanks to Image Processing", *IEEE Transactions on Image Processing*, pp 205-220, Feb. 1999.

[6] I. Djokovic and P.P. Vaidyanathan, "Results on biorthogonal filter banks", *Applied and computational harmonic analysis*, vol. 1, pp 329-343, 1994.

[7] P.Q. Hoang and P.P. Vaidyanathan, "Non-Uniform Multirate Filter Banks: Theory and Design", *Proceedings of ISCAS* , pp 371-374, 1989.

[8] A. Kirac and P.P. Vaidyanathan, "On existence of FIR principal component filter banks", *IEEE International Conference on Acoustics, Speech and Signal Processing - Proceedings*, pp 1329-1332, v 3 May 12-15, 1998.

[9] G. F. Ribeiro and G. V. Mendonca, "Image Coding using Biorthonormal Wavelet Transform", *Midwest Symposium on Circuits and Systems 2*, Aug. 13-16, 1995.

[10] B.G. Sherlock and D.M. Monro,"Optimized Wavelets for Fingerprint Compression", *ICASSP, IEEE International Conference on Acoustics, Speech and Signal Processing - Proceedings*, pp 1447-1450, May 7-10, 1996.

[11] A. K. Soman and P.P. Vaidyanathan, "On Orthonormal Wavelets and Paraunitary Filter Banks", *IEEE Transactions on Signal Processing*, pp 1170-1183, Mar. 1993.

[12] G. Strang and T. Nguyen, *Wavelets and Filter Banks*, Wellesly-Cambridge Press, 1996.

[13] V. Strela, P. N. Heller, G. Strang, P. Topiwala and C. Heil, "Biorthonormal Filterbanks and Energy Preservation Property in Image Compression", *IEEE Transactions on Image Processing*, pp 548-563, Apr. 1999.

[14] M.K. Tsatsanis, G.B. Giannakis, "Principal component filter banks for optimal multiresolution analysis", *IEEE Transactions on Signal Processing*, pp 1766-1776, Aug. 1995.

[15] P.P. Vaidyanathan, *Multirate Systems and Filter Banks*, Prentice Hall, 1992.

[16] P.P. Vaidyanathan, "Orthonormal and Biorthonormal Filter Banks as Convolvers, and Convolutional Coding Gain", *IEEE Transactions on Signal Processing*, pp 2110-2130, Jun. 1993.

[17] P.P. Vaidyanathan, "Theory of optimal orthonormal subband coders", *IEEE Transactions on Signal Processing*, pp 1528-1543, Jun. 1998.

[18] P.P. Vaidyanathan and A. Kirac, "Results on Optimal Biorthonormal Filter Banks", *IEEE Transactions on Signal Processing*, pp 932-947, Aug. 1998.

[19] M. Vetterli and C. Herley, "Wavelets and Filter Banks: Theory and Design", *IEEE Transactions on Signal Processing*, pp 2207-2232, Sep. 1992.

[20] M.H. Yaou and W.T. Chang, "M-ary Wavelet Transform and Formulation for Perfect Reconstruction in M-band Filter Bank", *IEEE Transactions on Signal Processing*, pp 3508-3512, Dec. 1994.

[21] S. Akkarakaran, *Filter Bank Optimization with Applications in Noise Suppression and Communications*, Ph. D. dissertation, Chapter 6, California Institute of Technology, 2001.

A Novel Channel Identification Method for Wireless Communication Systems

Honghui Xu[1], Soura Dasgupta[1], and Zhi Ding[2]

[1]Electrical & Computer Engineering Department

The University of Iowa

Iowa City, IA-52242, USA.

[2]Department of Electrical & Computer Engineering

University of California

Davis, CA 95616, USA.

Emails: hoxu, dasgupta@engineering.uiowa.edu, zding@ece.ucdavis.edu

Keywords: Identification, Equalization, Feedback, Wireless, Training

[1]Work supported in part by NSF grants ECS-9970105 and CCR-9973133.

[2]Work supported in part by NSF grant CCR-9996206

Abstract

We present a novel dual channel identification approach for mobile wireless communication systems. Unlike traditional channel estimation methods that rely on training symbols, we propose a bent-pipe feedback mechanism which requires the mobile station (MS) to send portions of its received signal back to the Base Station (BS) for wireless channel identification. Using a filter-bank decomposition concept, we introduce an effective algorithm that can identify both the forward and the reverse channels based only on this feedback information. This new method permits transfer of computational burden from the MS to the resource rich BS and leads to significant savings in bandwidth consuming training signals.

I. Introduction

We propose a new approach to the estimation and compensation of forward link channels in mobile wireless communication systems that centers on a novel *bent pipe feedback* mechanism. In principle, this feedback mechanism enables Base Stations (BS) to simultaneously estimate both the Forward Link Channel (FLC) from the BS to a Mobile (MS) and the Reverse Link Channel (RLC) from the MS to the BS, without any training signals or resorting to blind estimation techniques. While practical realities temper these theoretical expectations, as we will demonstrate in this paper, our techniques bring with them certain significant advantages.

Our paper is motivated by the strong surge in mobile wireless communication systems. The rapidly expanding arena of wireless services including mobile computing and broadband multimedia would require much higher wireless capacity and higher data rates than is currently needed, over the often unreliable wireless medium. Indeed, unlike their wireline counterparts, wireless communication links are highly susceptible to channel variations, particularly in mobile environments. Three specific advantages motivate our approach.

(A) Adaptive Coding

The high variability of wireless links poses a serious challenge to assuring quality of service (QoS) to various traffic flows under harsh and dynamically distortive channel conditions. To address QoS needs, future wireless communication systems must respond to potentially rapid channel changes in an effective and timely manner. Currently, FLC estimation and equalization responsibilities are assigned almost entirely to the MS [1], [2], [3]. At the same time, to improve adaptivity to channel conditions, several researchers have proposed a number of schemes that require at least a partial awareness of the FLC at the BS. Thus, Paulraj et. al., [6] demonstrate substantially improved performance through the use of adaptive

space time coding that assumes that the BS has partial knowledge of the FLC. Goeckel et. al. [10] propose other forms of adaptive coding again relying on similar information. Bit loading in OFDM systems similarly assumes a channel aware BS, [8], as indeed does the power minimization scheme of [9]. Similarly precoding techniques [11] can be significantly improved should the BS have partial knowledge of the FLC. Our bent pipe feedback technique naturally apprises the BS of the prevailing FLC conditions that are needed by these schemes.

(B) **Shared FLC compensation**

As noted earlier, the tasks of FLC compensation and estimation are often assigned to the MS. It is recognized that most future wireless cellular services will be characterized by an FLC that supports higher data rates than does the RLC. For a given channel, higher data rate induces longer delay spread and more severe ISI. In other words the discrete time baseband model is of a higher order, and its equalization and compensation more onerous. At the same time it is the BS that houses greater computational reserves, even though it is assigned the less burdensome task of estimating and compensating the RLC. It is thus desirable to shift at least a part of the FLC compensation and estimation burden to the more resource rich BS. The feedback mechanism we propose permits a better utilization of this resource disparity, by transferring much of the FLC estimation and compensation tasks to network nodes with greater resources.

More specifically, our method in principle permits the BS to estimate and pre-compensate the wireless channel. In practice, because of roundtrip delays and channel variations that occur within the resolution of such delays, the BS will only partially compensate the dynamic channel, and the MS must take part in combatting the residual ISI. Nonetheless, this partially compensated channel will induce reduced levels of ISI, whose removal would consequently impose far less computational burden on the MS.

(C) **Reduced Training**

Channel estimation at the MS is typically assisted by the frequent transmission of training data. As the FLC supports higher data rates, and is consequently described by a higher order discrete time model, it requires longer training sequences, transmitted more frequently. This is obviously at the expense of the all too precious forward link bandwidth. In GSM for

example roughly one sixth of the transmission time is devoted to training signals.

As noted in (B), due to roundtrip delays our scheme permits the the BS to only partially compensate the FLC, and the MS must combat the residual ISI with the assistance of some training. Nonetheless, this partially compensated channel suffers from reduced levels of ISI. As we demonstrate through simulations in a later section, the number of training symbols needed for the estimation and compensation of the partially compensated FLC is significantly lower, with consequent savings in the bandwidth allocated to FLC training. This advantage is buttressed by the fact that *no training* is needed on the RLC, and that instead the time slot normally used for RLC training can be used for the feedback data. ■

It should be noted that 2G CDMA systems and emerging 3G systems do employ some simple feedback. Such feedback, however, is often limited to an estimated power loss parameter that enables the BS to compensate multipath distortion via power-control. Although power-control or higher SNR can improve MS performance, particularly against flat fading channels, channel distortion as a result of multipath fading cannot be efficiently compensated by mere increase of transmission power. Other proposals for channel information feedback are in [4]-[6], which involve feeding back channel parameter estimates to the BS at appropriate instants of time. These proposals continue the practice of assigning the sole responsibility of channel estimation to the resource challenged MS, and do not reduce the training burden on the FLC.

Unlike the conventional feedback of channel estimates in [4], [5], our new approach only requires that the MS feed back to the BS a portion of the received signal, over the time slot conventionally reserved for RLC training, in epochs where either it normally transmits or in epochs where it detects a performance degradation. Clearly, this permits the BS to estimate the Roundtrip Channel (RTC).

However, the key novelty of our approach lies in the following discovery: By feeding back only a portion, rather than the entire received signal, one empowers the BS to identify both the FLC and the RLC from the roundtrip feedback signal alone. This novel channel feedback does not require high speed reverse links and can naturally accommodate asymmetric data link structures. Furthermore, no additional training signals are necessary for estimating the RLC at the BS. As will be explained further, this scheme requires no greater overhead than

those associated with [4]-[6], while *at the same time* having the fundamental advantage of shifting substantial processing burden from the MS to BS, and reduced levels of training data.

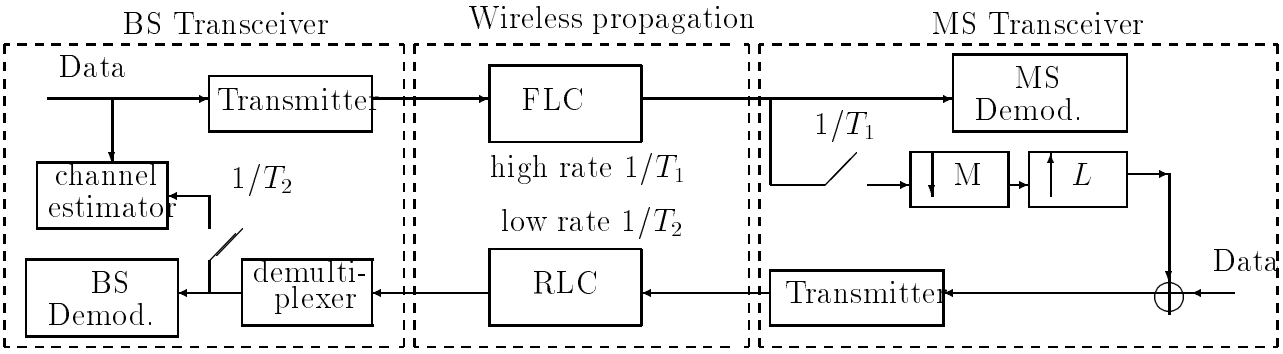

Fig. 1. A wireless communication system with signal feed back.

Our paper is structured as follows. First, the basic principle of roundtrip feedback is presented in Section II. Its implementation issues are addressed and practical caveats analyzed. Conditions under which RLC and FLC can be obtained from the RTC are in Section III. An algorithm to estimate the roundtrip dynamics is formulated in Section IV. Section V provides the unravelling algorithm. Simulations are in Section VI.

II. Bentpipe Feedback

The feedback scheme we use is depicted in Fig. 1. Specifically in this figure the FLC and RLC respectively, operate at the rates $1/T_1$ and $1/T_2$, with $T_1 < T_2$ and $T_1/T_2 = L/M$ for integers L and M that need not be coprime. The sampled data at the FLC output is converted to the RLC rate by the decimator/interpolator combination depicted in the figure. This is interlaced in the stead of normal RLC training data, with the data that the MS needs to transmit through the RLC in its normal course of operation, and fed back to the MS.

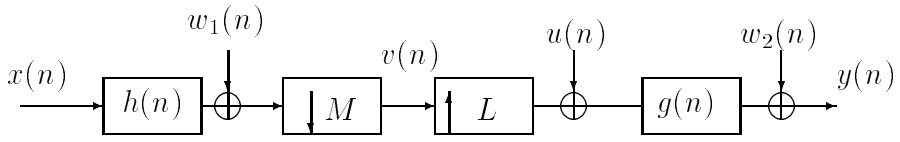

Fig. 2. The equivalent digital expression of the system (noise and interference considered)

Fig. 1 can be transformed into Fig. 2, where $x(n)$ is the digital data sequence transmitted

by BS at time nT_1 at the rate $1/T_1$, $y(n)$ is the data sequence received by BS at time nT_2 after sampling at the rate $1/T_2$, and $h(n)$ and $g(n)$ are the FIR impulse response of the FLC and RLC respectively. Further, $w_1(n)$ and $w_2(n)$ are the noise sequences at the FLC and RLC outputs, and $u(n)$ models the interference caused by the normal RLC data due to imperfect synchronization. Throughout we make the following standing assumption.

Assumption 1: The signals $x(n)$, $u(n)$, $w_1(n)$, $w_2(n)$ are zero mean, white and mutually uncorrelated.

It is clear that given that the BS is aware of the data it has transmitted, under assumption 1 it can estimate the RTC. *Using ideas from [12], we show that under mild assumptions on the FLC and RLC, the BS can in fact directly unravel the FLC and RLC from the RTC, without any training in either FLC or RLC.* This ability to separate RLC and FLC from RTC estimate can be seen as a consequence of the rate changing mechanism that separates the two channels. Rate changers are time varying systems, and consequently, even when $w_1(n) = w_2(n) = u(n) = 0$, the LTI operators $h(n)$ and $g(n)$ cannot be arbitrarily interchanged.

We now pose and answer two questions surrounding the practicality of this approach. In doing so at appropriate places we discuss the data and computational overheads associated with this scheme relative to those of the feedback schemes mentioned in [4]-[6].

(i) **What about roundtrip delay?** Over reasonable distances the roundtrip delay is in tens of microseconds. Thus, for example, over a roundtrip distance of 5 km, this delay is about 16.67 μs. Over such time spans, the environment as seen by the mobile unit undergoes little change. This is underscored by the fact that in GSM each data frame has a duration of 557 μs, and training occurs only once per data frame. Thus the channel variation within the resolution of this delay occurs mainly because of Doppler effect. Still, even with Doppler effect on high speed mobiles, the channel characteristics are unlikely to change drastically within such a short time interval. As a case in point, a vehicle traveling at 100km/hr suffers a maximum Doppler shift of 50 Hz at cellular band. The channel variation thus endured will not be enough to prevent the transmitter from substantially compensating the FLC. Thus the residual ISI that must be equalized at the receiver will be significantly milder leading to the need for much shorter training sequences on the FLC. Given that no training is needed

on the RLC, and that feedback data occupies the RLC training slot used in conventional communication, this implies substantial savings in the bandwidth devoted to the overall training. Simulations presented later support this contention. Since the BS has greater computational reserves, this would also effect a beneficial transfer of computational burden to such a resource rich BS.

We should also note that the feedback schemes suggested in [4]-[6] would suffer the same latency effects manifested by the roundtrip delay. Thus while the addition of the other advantages of our scheme are conspicuously absent in the approaches of [4]-[6] the effectiveness of adaptive coding noted in the introduction should be comparable in both instances.

(ii) **What about battery life?** Overly frequent feedback transmissions may deplete power resources at the receiver. In epochs where the receiver also transmits, the training data currently sent can be substituted by the feedback data, as RLC training is no longer needed. During silent uplink episodes, feedback can be restricted to epochs where the receiver detects a high level of packet loss due to obsolete channel estimates, in much the same way as existing proposals for channel estimate feedback require. Thus, the associated overhead is again comparable to that in [4]-[6].

Taking a more long range view, whereas battery technology continuously improves, with ever lengthening battery life, bandwidth resources will remain scarce. Given the bandwidth savings reduced training brings about, one can expect bent pipe feedback to gain an increasing advantage in this trade-off. ■

III. Conditions for estimating RLC/FLC from RTC

Borrowing ideas from [12] we show that it is possible in principle to unravel the FLC and RLC dynamics from the RTC. We consider the case without noise and user interference at first. The case with noise and interference will be treated later.

Consider the polyphase representation of the FLC and RLC transfer functions $H(z)$ and $G(z)$ [13], given below.

$$H(z) = \sum_{i=0}^{M-1} H_i(z^M) z^{-i} \tag{1}$$

$$G(z) = \sum_{i=0}^{L-1} G_i(z^L) z^{-(L-1-i)}. \tag{2}$$

In the sequel $H_i(z)$ and $G_i(z)$ will be called the polyphase components of $H(z)$ and $G(z)$, respectively. Then with

$$x_i(n) = x(nM - i) \text{ and } y_i(n) = y(nL + L - 1 - i), \tag{3}$$

we can redraw Fig. 2 as Fig. 3.

Thus, in principle the knowledge of $x(i)$ and $y(i)$ estimates the rank one matrix transfer function

$$F(z) = \begin{bmatrix} G_0(z) \\ G_1(z) \\ \vdots \\ G_{L-1}(z) \end{bmatrix} \begin{bmatrix} H_0(z) & H_1(z) & \cdots & H_{M-1}(z) \end{bmatrix}. \tag{4}$$

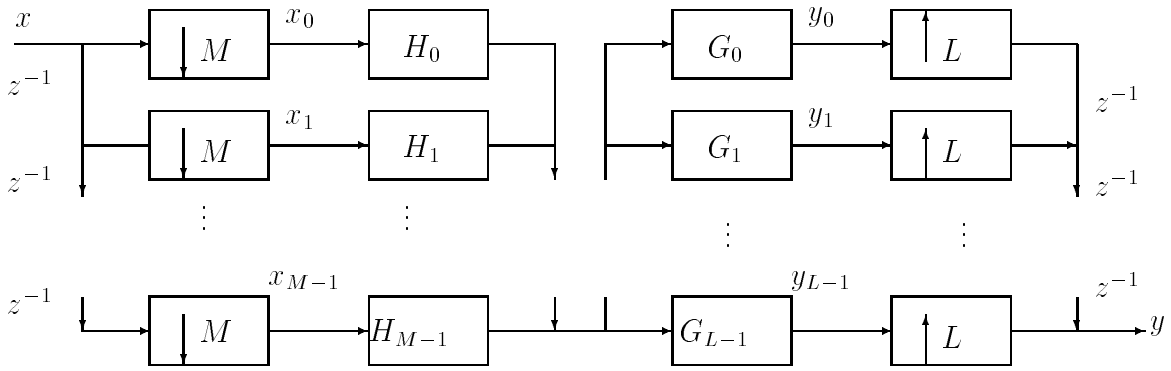

Fig. 3. The polyphase representation of the system.

Now we will need one of the following two assumptions (both need not be satisfied).

Assumption 2: The greatest common divisor (gcd) of the set of polynomials $H_i(z)$ is a pure delay z^{-d} (d integer). Further their maximum order is known.

Assumption 3: The gcd of set of the set of polynomials $G_i(z)$ is a pure delay z^{-d} (d integer). Further their maximum order is known.

Assumption 2 for example is quite common in fractionally spaced blind equalization, [15], [16]. Further pure delay common factors in $H_i(z)$ and $G_i(z)$ result from delays in $H(z)$ and $G(z)$, respectively, though the converse need not be true. In particular only delays of M (respectively L) or larger result in the $H_i(z)$ (respectively $G_i(z)$) having a pure delay as a common factor. Then we have the following Theorem.

Theorem 1: Suppose one or both of the two assumptions 2 or 3 hold. Then the matrix in (4) gives $H(z)$ and $G(z)$ to within a common nonzero scaling factor and a delay as long as $H(z)G(z) \neq 0$.

Proof: Suppose assumption 2 holds. Observe, that one has available $G_0(z)H_i(z)$, $i \in \{0, \cdots, M-1\}$. Then the gcd of $G_0(z)H_i(z)$, $i \in \{0, \cdots, M-1\}$ is $\alpha z^{-d} G_0(z)$ for some scalar α and integer d. Thus by dividing by this gcd one obtains the $H_i(z)$ to within a scalar and delay, and hence also the $G_i(z)$. The relation to assumption 3 can be similarly deduced.

■

Should however, the $H_i(z)$ and $G_i(z)$ have respective common factors $1-\alpha z^{-1}$ and $1-\beta z^{-1}$, $\alpha \neq \beta$, then these can be exchanged between the $G_i(z)$ and $H_i(z)$ in (4) without changing the input output relationship exemplified by (4). Consequently the $G_i(z)$ and $H_i(z)$ cannot be separately extracted. This of course does not show how the $H(z)$, $G(z)$ can be determined to within a scaling factor. The sequel provides such algorithms. Note, [12] does not have these algorithms.

IV. Estimating the roundtrip dynamics

In this section, we describe how the roundtrip dynamics can be estimated at the BS using the feedback information. To this end, in Section IV-A we provide a z-domain description of the relation between $x(n)$ and $y(n)$. Section IV-B explains how this description leads to an estimation algorithm.

A. An input output relationship

Consider now Fig. 2 with $u(k)$ the interference caused by the normal RLC data due to imprecise synchronization. Adopt the standard notation of representing the z-transform of signals represented by small letters such as $a(n)$, by capital letters, e.g. $A(z)$.

Define,

$$w_{2k}(n) \stackrel{\text{def}}{=} w_2(nL+L-k-1), 0 \leq k \leq L-1 \text{ and } u_k(n) \stackrel{\text{def}}{=} u(nL-k), 0 \leq k \leq L-1.$$

Then, [13]

$$Y(z) = \sum_{k=0}^{L-1} z^{-(L-1-k)} Y_k(z^L) \text{ and } X(z) = \sum_{k=0}^{M-1} z^{-k} X_k(z^M).$$

Likewise,

$$W_2(z) = \sum_{k=0}^{L-1} z^{-(L-1-k)} W_{2k}(z^L) \text{ and } U(z) = \sum_{k=0}^{L-1} z^{-k} U_k(z^L).$$

Thus we can rewrite

$$\begin{aligned} \sum_{k=0}^{L-1} z^{-(L-1-k)} Y_k(z^L) &= \sum_{k=0}^{L-1} z^{-(L-1-k)} G_k(z^L) V(z^L) + \sum_{k=0}^{L-1} z^{-(L-1-k)} W_{2k}(z^L) \\ &+ \sum_{k=0}^{L-1} \sum_{j=0}^{L-1} z^{-(L-1-(k-j))} G_k(z^L) U_j(z^L) \end{aligned} \tag{5}$$

Equating coefficients on both sides of (5) one obtains:

$$\begin{pmatrix} Y_0(z) \\ \vdots \\ Y_{L-1}(z) \end{pmatrix} = \begin{pmatrix} G_0(z) \\ \vdots \\ G_{L-1}(z) \end{pmatrix} V(z) + \widehat{G}(z) \begin{pmatrix} U_0(z) \\ \vdots \\ U_{L-1}(z) \end{pmatrix} + \begin{pmatrix} W_{20}(z) \\ \vdots \\ W_{2(L-1)}(z) \end{pmatrix} \tag{6}$$

where

$$\widehat{G}(z) = \begin{pmatrix} G_0(z) & G_1(z) & \cdots & G_{L-1}(z) \\ G_1(z) & G_2(z) & \cdots & z^{-1}G_0(z) \\ \vdots & & & \vdots \\ G_{L-1}(z) & z^{-1}G_0(z) & \cdots & z^{-1}G_{L-2}(z) \end{pmatrix} \tag{7}$$

Observe,

$$V(z) = \sum_{j=0}^{M-1} X_j(z) H_j(z) + W_{10}(z) \tag{8}$$

where

$$w_{10}(n) = w_1(Mn). \tag{9}$$

Thus one has

$$\begin{pmatrix} Y_0(z) \\ \vdots \\ Y_{L-1}(z) \end{pmatrix} = F(z) \begin{pmatrix} X_0(z) \\ \vdots \\ X_{M-1}(z) \end{pmatrix} + \widehat{G}(z) \begin{pmatrix} U_0(z) \\ \vdots \\ U_{L-1}(z) \end{pmatrix} + \begin{pmatrix} W_{20}(z) \\ \vdots \\ W_{2(L-1)}(z) \end{pmatrix} \tag{10}$$

where $F(z)$ is given by (4).

B. Estimation of RTC

Roundtrip dynamics estimation involves the estimation of $F(z)$ from (10). The key thing to note about the estimation of $F(z)$ is that under Assumption 1, $x(k)$ is uncorrelated with $w_{10}(n)$, $v_i(n)$ and $w_{2i}(n)$. Thus one can express (10) as

$$\begin{pmatrix} Y_0(z) \\ \vdots \\ Y_{L-1}(z) \end{pmatrix} = F(z) \begin{pmatrix} X_0(z) \\ \vdots \\ X_{M-1}(z) \end{pmatrix} + \Gamma(z) \tag{11}$$

where $\gamma(n)$ is uncorrelated with $x(n)$.

Suppose the order of $H(z)$ is l_H and the order of $G(z)$ is l_G. In (1), $H_i(z) = \sum_n h_i(n) z^{-n}$, where

$$h_i(n) = h(Mn+i) \quad 0 \le i \le M-1, 0 \le (Mn+i) \le l_H \tag{12}$$

Similarly, in (2), $G_i(z) = \sum_n g_i(n) z^{-n}$, where

$$g_i(n) = g(Ln+L-1-i) \quad 0 \le i \le L-1, 0 \le (Ln+L-1-i) \le l_G \tag{13}$$

By padding zeros, let the length of the sequence of coefficients of $H_i(z)$ be l_h+1 and that of $G_i(z)$ be l_g+1, where l_h and l_g are the maximum orders of polynomial set $H_i(z)$ and polynomial set $G_i(z)$ respectiveley. They are related to l_H and l_G as follows:

$$l_h + 1 = \lceil (l_H+1)/M \rceil$$
$$l_g + 1 = \lceil (l_G+1)/L \rceil$$

where $\lceil x \rceil$ stands for the smallest integer that is greater than or equal to x.

Let $l_f = l_g + l_h$ and define

$$F_{ij}(z) = G_i(z) H_j(z) = \sum_{k=0}^{l_f} f_{ij}(k) z^{-k} \tag{14}$$

For some integer N to be specified in a later section, the Toeplitz filtering matrix of $F_{ij}(z)$ is defined as

$$\mathcal{T}_N(F_{ij}) = \begin{pmatrix} f_{ij}(0) & \cdots & f_{ij}(l_f) & & 0 \\ & \ddots & \ddots & \ddots & \\ 0 & & f_{ij}(0) & \cdots & f_{ij}(l_f) \end{pmatrix} \tag{15}$$

$\mathcal{T}_N(F_{ij})$ is an $N \times (l_f + N)$ matrix.

Denote

$$\mathcal{X}_i(k) = [x_i(k), \cdots, x_i(k - l_f - N + 1)]^T, 0 \leq i \leq M - 1 \tag{16}$$

$$\mathcal{X}(k) = [\mathcal{X}_0^T(k), \cdots, \mathcal{X}_{M-1}^T(k)]^T \tag{17}$$

$$\mathcal{Y}_i(k) = [y_i(k), \cdots, y_i(k - N + 1)]^T \tag{18}$$

By aligning M matrices $\mathcal{T}_N(F_{ij})$, we get the block Toeplitz matrix

$$\mathcal{F}_i(N) = [\mathcal{T}_N(F_{i0}), \cdots, \mathcal{T}_N(F_{i(M-1)})] \tag{19}$$

Hence, equation (10) can be expressed as

$$\mathcal{Y}_i(k) = \mathcal{F}_i(N)\mathcal{X}(k) + \eta(k) \quad 0 \leq i \leq L, \tag{20}$$

where $\eta(k)$ is uncorrelated with $\mathcal{X}(k)$. The inverse of $R_{\mathcal{X}\mathcal{X}} = E(\mathcal{X}\mathcal{X}^T)$ exists because of assumption 1. Then we have

$$\mathcal{F}_i(N) = R_{\mathcal{Y}_i\mathcal{X}} R_{\mathcal{X}\mathcal{X}}^{-1} \tag{21}$$

where $R_{\mathcal{Y}_i\mathcal{X}} = E(\mathcal{Y}_i\mathcal{X}^T)$ and $E(\cdot)$ denotes the expectation operation. Observe, the estimation of $\mathcal{F}_i(N)$ for each i in $\{0, 1, \cdots L - 1\}$ provides $F(z)$ accomplishing the estimation of the roundtrip dynamics.

V. Unraveling FLC and RLC from the estimated RTC

We now demonstrate how the estimate of $\mathcal{F}_i(N)$ obtained in the previous section can be used to separate the FLC and RLC dynamics. For simplicity sections V-A and V-B provide unraveling algorithms under assumptions 3 and 2 respectively, with the added assumption that the cognizant polyphase components do not even share delays. Recall that this does not necessarily imply the absence of delays in the pertinent channels but rather that delays are smaller than M or L depending on whether the channel in question is the FLC or RLC. Methods of accomodating common delay factors among the polyphase components are in section V-C.

A. Algorithm when the $G_i(z)$ are coprime and do not share a delay

Similar to the definition of $\mathcal{T}_N(F_{ij})$ in equation (15), we can define $\mathcal{T}_N(H_i)$ and $\mathcal{T}_N(G_i)$ as the Toeplitz filtering matrix associated with $H_i(z)$ and $G_i(z)$ respectively. $\mathcal{T}_N(H_i)$ has a dimension $N \times (l_h + N)$ and $\mathcal{T}_N(G_i)$'s dimension is $N \times (l_g + N)$. Define the $LN \times (N + l_g)$ block Toeplitz matrix,

$$\mathcal{G} = \begin{bmatrix} \mathcal{T}_N(G_0) \\ \mathcal{T}_N(G_1) \\ \vdots \\ \mathcal{T}_N(G_{L-1}) \end{bmatrix} \tag{22}$$

We note first the following well known fact, [16]:

Fact 1: If the $G_i(z)$ have no common factors, not even delays, then for a sufficiently large N specified in [16], $\mathcal{G}$ has full column rank. Further, the left null space of $\mathcal{G}$ provides $G_i(z)$ to within a scaling constant.

In the sequel choose N to be the smallest integer for which $\mathcal{G}$ has full column rank. Now define the $(l_g + N) \times M(l_h + N)$ matrix

$$\mathcal{H} = \begin{bmatrix} \mathcal{T}_{l_g+N}(H_0) & \mathcal{T}_{l_g+N}(H_1) & \cdots & \mathcal{T}_{l_g+N}(H_{M-1}) \end{bmatrix}. \tag{23}$$

Note that the following relation holds

$$\mathcal{T}_N(F_{ij}) = \mathcal{T}_N(H_j)\mathcal{T}_{l_h+N}(G_i) = \mathcal{T}_N(G_i)\mathcal{T}_{l_g+N}(H_j) \tag{24}$$

Consequently, one obtains:

$$\mathcal{F} = \mathcal{G}\mathcal{H} \tag{25}$$

Define

$$\mathcal{F} = [\mathcal{F}_0(N)^T, \cdots, \mathcal{F}_{L-1}(N)^T]^T \tag{26}$$

and recall that section IV provides $\mathcal{F}$.

It is evident that $\mathcal{H}$ is full row rank. Therefore, the column vectors of $\mathcal{F}$ spans the same subspace defined by the column vectors of $\mathcal{G}$, referred to in the sequel as the signal subspace. More importantly the left null space of $\mathcal{F}$ is identical to the left null space of $\mathcal{G}$. Fact 1 then sets up the direct estimation of $G(z)$ from the left null space of the estimate of $\mathcal{F}$ provided in the previous section.

Allowing for estimation errors because of finite data records, call $\hat{\mathcal{F}}$ the estimate of $\mathcal{F}$ provided by the algorithm in the previous section. Denote the error matrix as $\mathcal{N}$, i.e.

$$\hat{\mathcal{F}} = \mathcal{G}\mathcal{H} + \mathcal{N}.$$

Hence we have the following result after performing a singular value decomposition (SVD) of $\hat{\mathcal{F}}$:

$$\hat{\mathcal{F}} = \mathcal{G}\mathcal{H} + \mathcal{N} = (V_s \; V_n) \begin{pmatrix} \Sigma_s & 0 \\ 0 & \Sigma_n \end{pmatrix} \begin{pmatrix} W_s^H \\ W_n^H \end{pmatrix} \tag{27}$$

where $(\cdot)^H$ stands for the Hermitian transpose, the column vectors in V_s span the signal subspace, and the column vectors in V_n span the left null space of $\mathcal{F}$ and hence of $\mathcal{G}$. The dimension of V_s and V_n are $LN \times (l_g + N)$ and $LN \times (LN - l_g - N)$.

If there is no estimation error, the i-th column p_i of V_n satisfies

$$p_i^H \mathcal{G} = 0 \tag{28}$$

where $p_i = [p_i(0), \cdots, p_i(LN-1)]^T$. In practice, when estimation errors exist, (28) can be solved in the least square sense, i.e. by minimizing the following quadratic form

$$q(\mathbf{g}) = \sum_{i=0}^{LN-l_g-N-1} |p_i^H \mathcal{G}|^2, \tag{29}$$

where

$$\mathbf{g} = [g_0(0), \cdots, g_0(l_g), \cdots, g_{L-1}(0), \cdots, g_{L-1}(l_g)]. \tag{30}$$

In order to solve for $\mathbf{g}$ in equation (29), we follow the method in [16]. Similar to the definition of $\mathcal{T}_N(F_{ij})$, we define the filtering matrix $\mathcal{T}_{l_g+1}(P_{ij})$ associated with $P_{ij}(z)$, $0 \le i \le LN - l_g - N - 1, 0 \le j \le L-1$, where

$$P_{ij}(z) = \sum_{k=0}^{N-1} p_i(jN+k) z^{-k} \tag{31}$$

The dimension of $\mathcal{T}_{l_g+1}(P_{ij})$ is $(l_g+1) \times (l_g+N)$. Define

$$\mathcal{P}_i = [\mathcal{T}_{l_g+1}(P_{i0})^T, \cdots, \mathcal{T}_{l_g+1}(P_{i(L-1)})^T]^T \tag{32}$$

Then equation (29) can be transformed into

$$q(\mathbf{g}) = \mathbf{g} P \mathbf{g}^H, \; where \; P = \sum_{i=1}^{LN-l_g-N-1} \mathcal{P}_i \mathcal{P}_i^H \tag{33}$$

The solution of $\mathbf{g}$ is the smallest eigenvalue of matrix P. Note that $\mathbf{g}$ consists of all the coefficients of $G(z)$. Thus the RLC is identified up to a multiplicative constant. From the estimated $G(z)$, we can construct $\mathcal{G}$ as in (22). From

$$\mathcal{H} = \mathcal{G}^{\dagger}\hat{\mathcal{F}} \tag{34}$$

where $(\cdot)^{\dagger}$ indicates pseudoinverse, we can also identify the FLC up to a multiplicative constant.

B. Algorithm when the $H_i(z)$ are coprime and do not share a delay

The foregoing algorithm deals with the case when assumption 3 is satisfied together with the stronger condition that the polyphase components $G_i(z)$ do not share any delays. In this case, we identify $G(z)$ first, and then identify $H(z)$ from the estimated $G(z)$. Now suppose that assumption 2 is satisfied together with the condition that the polyphase components $H_i(z)$ do not share any delays.

Define for some integer $\tilde{N}$

$$\tilde{\mathcal{H}} = \begin{bmatrix} \mathcal{T}_{\tilde{N}}(H_0) \\ \mathcal{T}_{\tilde{N}}(H_1) \\ \vdots \\ \mathcal{T}_{\tilde{N}}(H_{M-1}) \end{bmatrix}. \tag{35}$$

Under assumption 2 and the lack of common delay factors among the $H_i(z)$ there exists an $\tilde{N}$ for which $\tilde{\mathcal{H}}$ has full column rank. Choose

$$\tilde{\mathcal{F}}_i(\tilde{N}) = [\mathcal{T}_{\tilde{N}}(F_{0i}), \cdots, \mathcal{T}_{\tilde{N}}(F_{(L-1)i})]$$

$$\tilde{\mathcal{F}} = [\mathcal{F}_0(\tilde{N})^T, \cdots, \mathcal{F}_{M-1}(\tilde{N})^T]^T$$

and

$$\tilde{\mathcal{G}} = \begin{bmatrix} \mathcal{T}_{l_h+\tilde{N}}(G_0) & \mathcal{T}_{l_h+\tilde{N}}(G_1) & \cdots & \mathcal{T}_{l_h+\tilde{N}}(G_{L-1}) \end{bmatrix}.$$

Then (24) leads to:

$$\tilde{\mathcal{F}} = \tilde{\mathcal{H}}\tilde{\mathcal{G}},$$

and an algorithm very similar to that in Section V-A accomplishes the desired unraveling.

C. Treating common delay factors

We now consider the situation where the pertinent polyphase components may have common delay factors. We will explain the underlying ideas with Assumption 3 in force. Similar ideas apply to the case where Assumption 2 holds.

Suppose that $G_i(z) = z^{-l}\bar{G}_i(z)$ where the $\bar{G}_i(z)$ have no common factors, i.e. z^{-l} is the gcd of the $G_i(z)$. Suppose $H_i(z) = z^{-n_i}\bar{H}_i(z)$. Then because of the upper triangular Toeplitz nature of $\mathcal{T}_N(G_i)$ and $\mathcal{T}_N(H_i)$, and because of (24), $\mathcal{T}_N(F_{ij})$ has $l + n_j$ columns that are zero vectors. These zero columns also appear in $\mathcal{F}$. The matrix $\bar{\mathcal{F}}$ obtained by removing these zero columns can be expressed as

$$\bar{\mathcal{F}} = \bar{\mathcal{G}}\bar{\mathcal{H}}$$

where $\bar{\mathcal{G}}$ in particular is

$$\bar{\mathcal{G}} = \begin{bmatrix} \mathcal{T}_N(\bar{G}_0) \\ \mathcal{T}_N(\bar{G}_1) \\ \vdots \\ \mathcal{T}_N(\bar{G}_{L-1}) \end{bmatrix} \tag{36}$$

and as the $\bar{G}_i(z)$ have no common factors has full rank and has identical null space as $\bar{\mathcal{F}}$. Consequently the algorithm in section V-A working with $\bar{\mathcal{F}}$ rather than $\mathcal{F}$ suffices to estimate $G(z)$ and $H(z)$ to within a scalar and delay ambiguity.

VI. Simulations

We present two simulation examples, the first to illustrate the basic performance of the algorithm, and the second to illustrate the reduction of training levels needed on the FLC when the channel parameters change with time. Before presenting these simulations we make precise our notions of SNR and SIR (caused by the interference effect of poorly synchronized RLC data.)

Denote noise, interference and signal at the output of RLC as $w(n)$, $u_o(n)$ and $z(n)$ respectively. We can see $y(n) = z(n) + w(n) + u_o(n)$. SNR and SIR are defined as

$$SNR = \frac{E(z^2(n))}{E(w^2(n))} \tag{37}$$

$$SIR = \frac{E(z^2(n))}{E(u_o^2(n))} \tag{38}$$

If the variance of $x(n)$,$w_1(n)$,$w_2(n)$ and $u(n)$ are σ_x^2,$\sigma_{w_1}^2$, $\sigma_{w_2}^2$ and σ_u^2 respectively, and if the signals are wide sense stationary (WSS), by a derivation given in the appendix, we have

$$SNR = \frac{\sigma_x^2 \sum_{i=0}^{L-1} \sum_{j=0}^{M-1} \sum_{k=0}^{l_f} f_{ij}^2(k)}{\sigma_{w_1}^2 \sum_{k=0}^{l_G} g^2(k) + L\sigma_{w_2}^2} \tag{39}$$

$$SIR = \frac{\sigma_x^2 \sum_{i=0}^{L-1} \sum_{j=0}^{M-1} \sum_{k=0}^{l_f} f_{ij}^2(k)}{L\sigma_u^2 \sum_{k=0}^{l_G} g^2(k)} \tag{40}$$

where $f_{ij}(k)$ is defined in (14) and l_G is the order of RLC.

Simulation example I: The FLC and RLC are generated from two delayed raised-cosine pulse $C(t, \alpha)$, where α is the roll-off factor. $C(t)$ is limited in $8T$ for FLC and in $6T$ for RLC, where T is the symbol interval.

$$FLC = 0.1C(t, 0.25) + 0.8C(t - T/2, 0.25) \tag{41}$$

$$RLC = 0.5C(t, 0.10) - 0.7C(t - T/3, 0.10) \tag{42}$$

Their corresponding discrete time channel coefficients are

$$FLC = [0.0129, -0.0326, 0.0693, -0.1485, 0.6019, 0.5019, -0.1485, 0.0693, -0.0326] \tag{43}$$

$$RLC = [0.0521, -0.0786, 0.1423, -0.0783, -0.2882, 0.1128, -0.0677] \tag{44}$$

We use down sampling factor $M = 3$ and upsampling factor $L = 2$. Hence $l_h = 3$ and $l_g = 4$. Noise signal $w_1(n)$ and $w_2(n)$ are zero mean and have the same variance. The input signal is i.i.d BPSK. We focus on estimating and compensating the FLC in the interference free case.

To quantify the quality of channel estimation, we define the normalized root-mean-square error(NRMSE) as

$$NRMSE = \frac{1}{\| h \|_2} \sqrt{\frac{1}{M_t} \sum_{i=1}^{M_t} \| \hat{h}_{(i)} - h \|_2^2} \tag{45}$$

where M_t is the number of Monte Carlo runs; h is the real channel and $\hat{h}_{(i)}$ is the estimate in the i-th run. Fig. 5 shows NRMSE versus total SNR, where total SNR is defined in (39).

After FLC and RLC are estimated, a pre-equalizer is built for the FLC and a post-equalizer for the RLC. The length of the zero-forcing equalizer is three times the corresponding real channel length. The equalizer SNR is SNR at the output of the equalized system. That is,

for FLC SNR is that at the output of the channel, but for RLC SNR is that at the output of the post-equalizer. BER versus equalizer SNR is displayed in Fig.6.

To evaluate the effect of iterference due to uplink data, Fig.7 shows the BER versus SIR at fixed SNR.

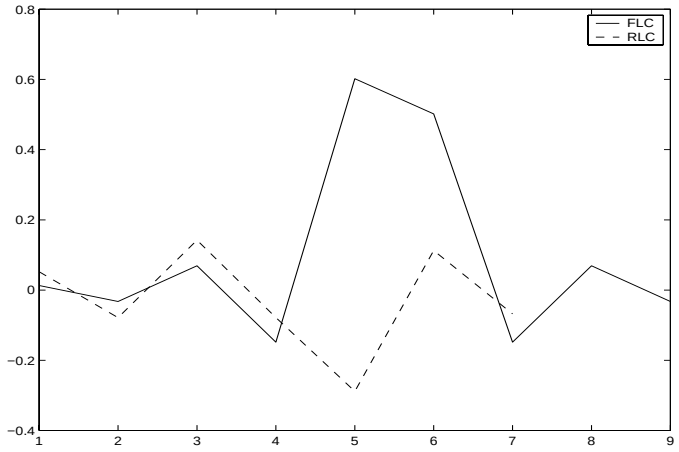

Fig. 4. The channel impulse responses of FLC and RLC.

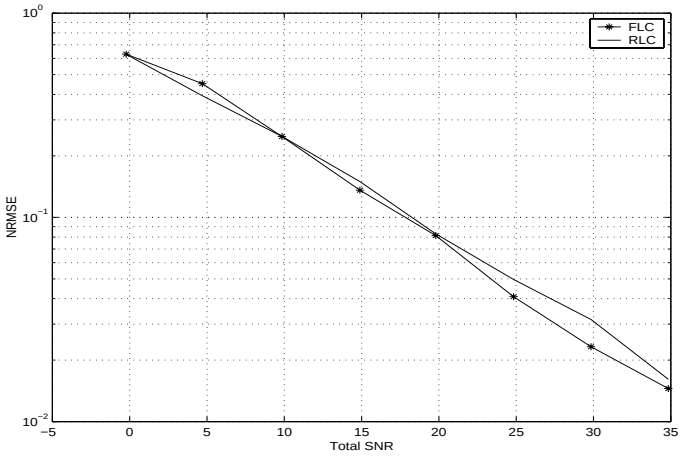

Fig. 5. NRMSE versus total SNR without interference. 100 Monte Carlo runs. 500 symbols for each run.

Simulation example II: Reduced training for a time varying channel:

We use COST-207 Typical Urban(TU) [7] model with 100 echo paths, BPSK data and maximum Doppler frequency 55Hz. We assume the channels to be quasistatic, i.e. time-invariant in one frame and time-variant from frame to frame. Each frame lasts 400μsecond (cf 557 μsecond for GSM) and the roundtrip delay is 16.67μsecond. The receive filters for FLC and RLC are raised cosine functions with roll-off factors 0.2 and 0.1 respectively. The

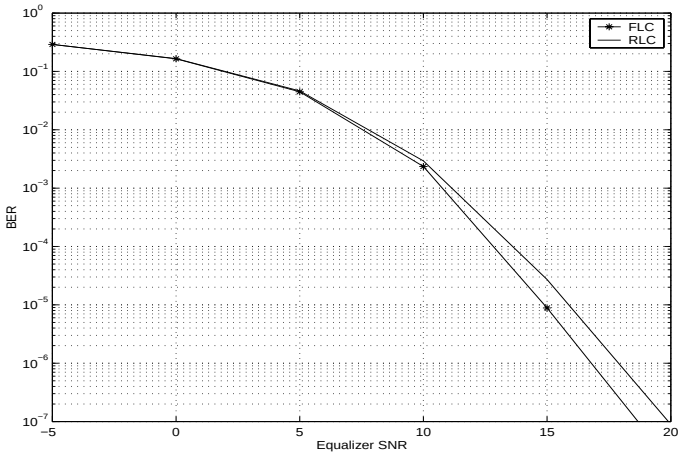

Fig. 6. BER versus equalizer SNR without interference. Channels are estimated at 20dB with 500 symbols in each run. 100 Monte Carlo runs.

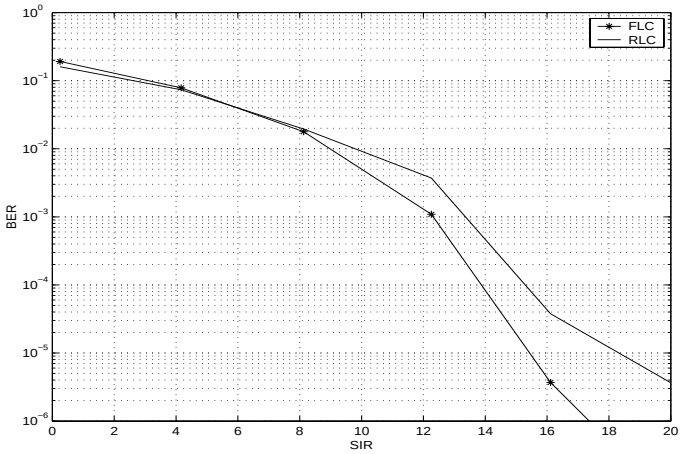

Fig. 7. BER versus SIR with 20dB total SNR and 25dB equalizer SNR. 500 symbols in each run. 100 Monte Carlo runs.

FLC sustains a data rate of 1 Mbps, and the RLC supports 0.667 Mbps.

Two situations are compared:

(a) Training aided equalization of FLC at the MS and of the RLC at the BS, with no feedback.

(b) No training on the RLC, but instead sending feedback data of the same length as the RLC training data in (a). A precompensator, obtained using the scheme of this paper is used on the FLC and is augmented by a post-equalizer estimated at the receiver using reduced training.

Both methods use the same input signal power and noise power. Figure 8 shows n_b/n_t

versus input SNR for both methods to achieve the same BER. Here n_t is the length of the FLC training sequence used in (a) and n_b the length of training used for partially compensated channel estimation in (b), so that the same FLC BER is obtained in both cases.

As is evident from the simulation that at 18db SNR *oyr algorithm requires only 32% training length on the FLC than the conventional training based FLC compensation.* Translated to a GSM setting instead of devoting 1/6th of transmission time for training only 1/19th is needed to achieve the same performance in this time varying setting.

Given that the feedback data on the RLC replaces and has the same length as the training data in (a), this represents substantial savings in bandwidth.

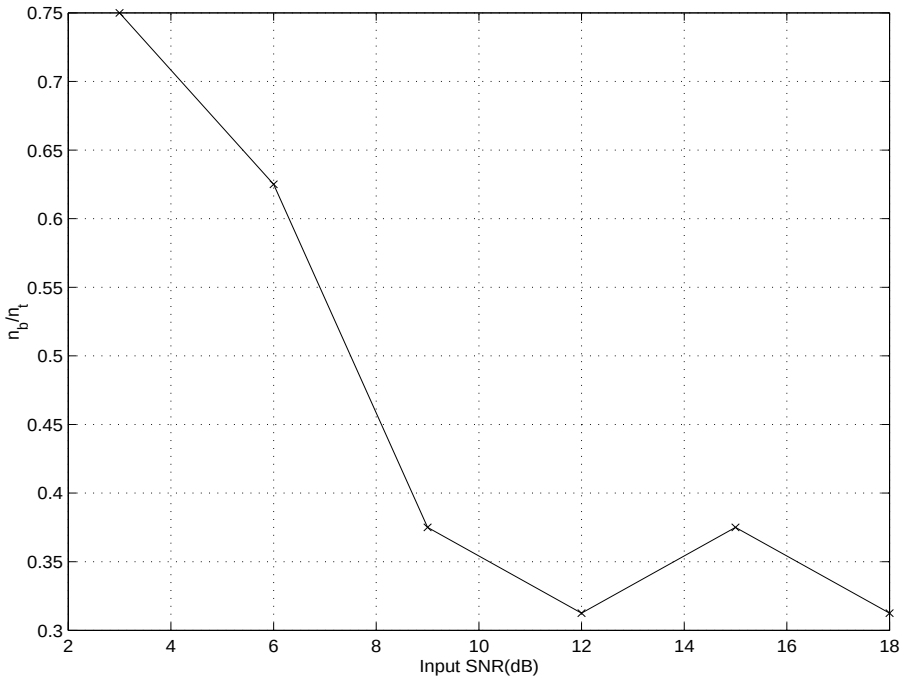

Fig. 8. n_b/n_t versus SNR at the same BER.

VII. Conclusion

We have proposed a new feedback scheme that permits FLC and RLC channel estimation from the BS, in principle without the use of training signals or blind estimation methods. In practice it leads to significant savings in the bandwidth consumed by training signals, and the transfer of some of the computational burden currently shouldered by the MS, to the more resource rich BS. The feasibility of these ideas have been demonstrated through both

theory and simulations. The possibility of unraveling FLC and RLC from the information of RTC is a core novelty of the paper.

Appendix

Similar to equation (3), we define

$$z_i(n) = z(nL + L - 1 - i), 0 \leq i \leq L - 1 \tag{46}$$

So $E(z^2(n)) = \sum_{i=0}^{L-1} E(z_i^2(n))/L$. And we know $z_i(n) = \sum_{j=0}^{M-1} \sum_{k=0}^{l_f} f_{ij}(k) x_j(n-k)$

$$E(z_i^2(n)) = E[\sum_{j=0}^{M-1} \sum_{k=0}^{l_f} f_{ij}(k) x_j(n-k) \sum_{p=0}^{M-1} \sum_{q=0}^{l_f} f_{ip}(q) x_p(n-q)] \tag{47}$$

From assumption 1, we know $E(x_j(n-k)x_p(n-q)) = \delta(p-j)\delta(k-q)\sigma_x^2$,where δ is Kronecker's delta. Then,

$$E(z_i^2(n)) = \sigma_x^2 \sum_{j=0}^{M-1} \sum_{k=0}^{l_f} f_{ij}^2(k) \tag{48}$$

$$E(z^2(n)) = \sigma_x^2 \sum_{i=0}^{L-1} \sum_{j=0}^{M-1} \sum_{k=0}^{l_f} f_{ij}^2(k)/L \tag{49}$$

From equation(10) and (8), we can see $w_{10}(n)$ will pass through $G_i(z)$ for all $0 \leq i \leq L-1$. Note that the variance of $w_1(n)$ is equal to $w_{10}(n)$, and $w_1(n)$ and $w_2(n)$ are uncorrelated and zero mean. Similar to the derivation of $E(z_i^2(n))$, we have

$$E(w^2(n)) = \sigma_{w_1}^2 \sum_{i=0}^{L-1} \sum_{k=0}^{l_g} g_i^2(k)/L + \sigma_{w_2}^2 \tag{50}$$

And we know $\sum_{i=0}^{L-1} \sum_{k=0}^{l_g} g_i^2(k) = \sum_{k=0}^{l_G} g^2(k)$. From (49) and (50), we get the expression for SNR in (39). It's easily seen that the interference component at the output of RLC is the signal by passing $u(n)$ through channel $G(z)$. So we have

$$E(u_o^2(n)) = \sigma_u^2 \sum_{i=0}^{l_G} g^2(i) \tag{51}$$

References

[1] T. Krauss and M. D. Zoltowski, "Multiuser Second-Order Statistics Based Blind Channel Identification for Using a Linear Parameterization of the Channel Matrix," IEEE Trans. on Signal Processing, vol. 48, no. 9, September 2000, pp. 2473-2486.

[2] Y. Zhang, K. Yang, and M. Amin, "Adaptive array processing for multipath fading mitigation," IEEE Transactions on Antennas and Propagation, vol.49, no.4, pp.505-516, April 2001.

[3] S. Kayhan and M. Amin, "The application of spatial evolutionary spectrum to direction finding and blind source separation," IEEE Transactions on Signal Processing, April 2000.

[4] J.H. Winters, "Switched diversity with feedback for DPSK mobile radio stations", *IEEE Transactions on Vehicular Technology*, pp 134-150, 1983.

[5] G. Raleigh and J. Cioffi, "Spatio-Temporal Coding for Wireless Communications", *IEEE Transactions on Communications*, COM-46(3): 357-366, March 1996.

[6] R. W. Heath, Jr. and A. Paulraj, "A Simple Scheme for Transmit Diversity using Partial Channel Feedback," *Proc. of 32nd Asilomar Conf. on Signals, Systems and Computers*, pp.1073-8, Pacific Grove, CA, 1998.

[7] P.Hoeher,"A statistical discrete-time model for the WSSUS multipath channel", *IEEE Trans. on Vehicular Technology*, VT-41(4):461-468,April 1992.

[8] L.M.C. Hoo, J. Tellado, J.M. Cioffi, "Discrete dual QoS loading algorithms for multicarrier systems", *IEEE International Conference on Communications*, pp 796-800, 1999.

[9] J. Zhang, A. Sayeed and B. Van Veen, "Optimal transceiver design for selective wireless broadcast with channel sttae estimation", in *Proceedings of ICASSP*, May 2002, Orlando, Fla.

[10] D. L. Goeckel, "Adaptive Coding for Fading Channels using Outdated Channel Estimates", *IEEE Transactions on Communications*, Vol. 47, pp. 844-855, June 1999.

[11] X.-G. Xia, "New precoding for intersymbol interference cancellation using nonmaximally decimated Multirate Filterbanks with ideal FIR equalizers", *IEEE Trans. Signal Processing*, 45:2431-2441, Oct. 1997.

[12] G. Williamson, S. Dasgupta and M. Fu, "Adaptive Multirate, Multistage Filters", *Proc. of ICASSP*, 1996.

[13] P. P. Vaidyanathan, *Multirate Systems and Filter Banks*, Prentice Hall, 1992.

[14] A. J. Goldsmith and P. P. Varaiya, "Capacity of fading channels with channel side information", *IEEE Trans. on Information Theory*, 43(6):1986-1993, November 1997.

[15] L. Tong, G. Xu and T. Kailath, "Blind identification and equalization based on second-order statistics: A time-domain approach", *IEEE Trans. Information Theory,* vol. 40 no. 2, pp. 340-350, March 1994.

[16] E. Moulines, P. Duhamel, J.-F. Cardoso and S. Mayrargue, "Subspace methods for the blind identification of multichannel FIR filters", *IEEE Trans. Signal Processing,* vol. 43 no. 2, pp. 516-525, Feb. 1995.

Channel and flow adaptive multiuser DMT

Soura Dasgupta, Ashish Pandharipande

Department of Electrical and Computer Engineering, The University of Iowa, Iowa City, IA, USA.
Email: {dasgupta, pashish}@engineering.uiowa.edu

ABSTRACT

This paper considers the design of biorthogonal DMT multicarrier transceiver systems supporting multiple services. The supported user services may have differing quality of service (QoS) requirements, quantified in this paper by bit rate and symbol error rate specifications. Our goal is to minimize the transmitted power given the QoS specifications for the different users, subject to the knowledge of colored interference at the receiver input of the DMT system. In particular we find an optimum bit loading scheme that distributes the bit rate transmitted across the various subchannels belonging to the different users, and subject to this bit allocation, determine an optimum transceiver. This work differs from our prior work [6] where orthonormal transceivers were considered.

1. Introduction

Future broadband communication systems will be expected to deliver multiple services, such as voice, data, video, with multiple-stream support. Because delivery of these streams will be under differing requirements such as information rate and error performance, allocation of critical resources like power would have a significant impact on the overall performance of the communication system. Discrete Multitone (DMT) transmission involves a channel coding technique to achieve reliable, high data rate communications in such systems. It is a current standard in various wireline applications like ADSL, VDSL, [10], and in the form of Orthogonal frequency division multiplexing (OFDM) has been proposed for fixed wireless standards like IEEE 802.11a, [12]. This paper considers transceiver optimization for such multicarrier transmission systems operating in a multiuser environment.

More specifically, we assume that a single DMT system supports r users, each having its own QoS specification quantified by its bit rate and symbol error rate (SER). The k-th user requires a bit rate of t_k, and an SER of no more than η_k. An equal number of subchannels are assigned to each user. As proposed in several recent papers, [7], [6], [9], we consider general DMT transceivers which are more general than the traditional DFT based systems in that the input and output transforms are general block transforms. We consider biorthogonal systems employing zero padding redundancy with the redundancy removal at the receiver being a general linear operation. Our goal is to select the input and output block transforms G_0, S_0 (see fig. 1), the linear operation reflecting redundancy removal, the number of bits/symbol assigned to each subchannel, and the subchannels assigned to each user to achieve the QoS specifications, under a zero intersymbol interference (ISI) condition with the minimum possible transmitted power. We assume that the channel and equalizer are known and so is the interference autocorrelation.

We thus generalize our earlier result reported in [6], where the same optimization problem was considered with an *orthonormal transceiver* under the assumption that each user is assigned the same number of subchannels. We shall see in the following sections how the extension to [6], considered here nontrivially modifies the optimization problem.

Figure 1 depicts the DMT communications system under consideration. An incoming data stream is converted into M parallel data streams of lower rate. An M-point block transformation G_0, of these streams of data is followed by a parallel-to-serial conversion, prior to transmission through the communication channel. An equalizer is employed to shorten the dispersive effects of the transmission channel. The *equalized* channel $C(z)$ is assumed to be FIR of length κ. For an FIR equalized channel of length κ, extra redundancy of length κ in the form of zero padding is added at the channel input to infuse resistance to channel induced ISI. At the channel output, one performs in succession the operations of redundancy removal, serial-to-parallel conversion, and the application of an inverse block transform, S_0.

Past treatment of optimum resource allocation, [1], [2], [3], has been restricted mostly to bit loading and power allocation algorithms. Some authors have studied the optimum transceiver design in the single user case, [7], [9]. While [7] was concerned with optimizing the transmitted power, [9] focussed on the maximization of the mutual informa-

Supported by ARO grant DAAD19-00-1-0534 and NSF grants ECS-9970105 and CCR-9973133.

tion between the transmitted and received signals. In [5] the authors consider the problem considered here for the single user case of $r = 1$, and with orthonormality condition enforced. In [7] the single user case is considered with orthogonality removed. Reference [7] shows that in the single user case biorthogonality leads to no improvement in the transmitted power. Likewise a major conclusion of this paper is to show that even in the multiuser environment with potentially asymmetric subchannel allocations, optimal performance is acheived by orthonormal transformations.

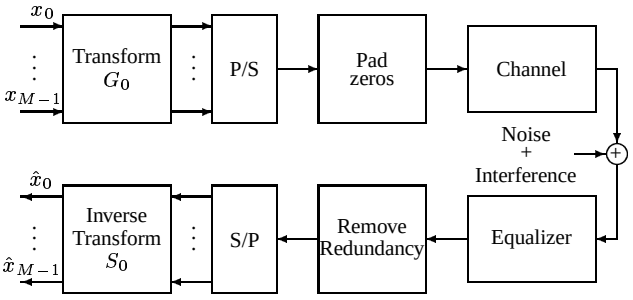

Fig. 1. DMT communication system.

2. Formulation

In this Section we give some preliminaries. Specifically, in Section 2.1, we recount the details of the generalized DMT system, along the lines of [7]. Section 2.2 provides a precise description of the optimization problem.

2.1. Preliminaries

Barring [7], most papers assume that G_0 is unitary, i.e.

$$G_0^H G_0 = I. \tag{2.1}$$

In the *biorthogonal case* considered here we *relax (2.1)* and simply assume that G_0 and S_0 can be *arbitrary nonsingular* $M \times M$ *matrices*. Denote the blocks of M input and output symbols respectively by $\mathbf{x}(n) = [x_0(n), \cdots, x_{M-1}(n)]^T$, and $\hat{\mathbf{x}}(n) = [\hat{x}_0(n), \cdots, \hat{x}_{M-1}(n)]^T$. With $v(n)$, the noise and interference effect at the output of the equalizer, denote $\mathbf{v}(n) = [v(Nn), v(Nn+1), \cdots, v(Nn+N-1)]^T$, as the N-fold blocked version of $v(n)$, with $N = M + \kappa$. Then one can show, [5] that with $\mathbf{C_L}$ an $N \times M$ constant matrix characterized by the κ order FIR equalized channel, and S_1, an $M \times N$ matrix, representing the linear redundancy removal operation, the blocked input-output relation of the system is given by

$$\hat{\mathbf{x}}(n) = S_0 S_1 \mathbf{C_L} G_0 \mathbf{x}(n) + S_0 S_1 \mathbf{v}(n). \tag{2.2}$$

We impose the perfect reconstruction (PR) condition, i.e., in the absence of noise/interference, $\hat{\mathbf{x}}(n) = \mathbf{x}(n)$ for all n. In other words,

$$S_0 S_1 \mathbf{C_L} G_0 = I, \tag{2.3}$$

and the DMT system has no ISI. To obtain a more useful characterization of PR, consider the singular value decomposition of $\mathbf{C_L}$

$$\mathbf{C_L} = U_c \begin{bmatrix} \Lambda_c \\ 0 \end{bmatrix} V_c^H = U_0 \Lambda_c V_c^H \tag{2.4}$$

where U_c and V_c are respectively $N \times N$ and $M \times M$ unitary matrices and Λ_c is a $M \times M$ real, positive definite diagonal matrix. Then, because of (2.3), given G_0, the class of all $S_0 S_1$ enforcing PR is completely characterized by

$$S_0 = G_0^{-1}. \tag{2.5}$$

and

$$S_1 = V_c \Lambda_c^{-1} \begin{bmatrix} I_M & A \end{bmatrix} U_c^H, \tag{2.6}$$

where A is any arbitrary $M \times \kappa$ matrix. In the sequel it will be useful to partition U_c as $U_c = [U_0 \quad U_1]$, where U_0 is $N \times M$ and U_1 is $N \times \kappa$.

Note, as V_c, U_c and Λ_c are supplied by the channel, the only quantities that need to be found to determine the transceiver completely are G_0 and A.

2.2. Problem formulation

As mentioned earlier the M subchannels are distributed among the r users with each of the users being allocated $L = M/r$ subchannels. Thus consider disjoint subsets $\mathcal{I}_k \subset \{0, \ldots, M-1\}$ with $|\mathcal{I}_k| = L > 1$, and $\mathcal{I}_k \cap \mathcal{I}_j = \emptyset, k \neq j$. Subchannel assignment to the k-th user constitutes determining $\mathcal{I}_k$. We assume that the j-th subchannel of the k-th user is assigned $b_{j,k}$ bits per symbol. To meet the bit rate specification for the k-th user one requires that

$$\frac{1}{N} \sum_{j \in \mathcal{I}_k} b_{j,k} = t_k. \tag{2.7}$$

Let the input power in the j-th subchannel of the k-th user be $\sigma^2_{x_{j,k}}$. Assume that $\sigma^2_{e_{j,k}}$ is the noise power in this subchannel. Under high SNR most modulation schemes, [8], require that to achieve a given SER the required SNR is proportional to $2^{b_{j,k}}$. More precisely,

$$\sigma^2_{x_{j,k}} = d_k 2^{b_{j,k}} \sigma^2_{e_{j,k}}, \tag{2.8}$$

where the constant d_k depends on the desired SER, η_k, for the k-th user. For example, for QAM, $d_k = \frac{1}{3}[Q^{-1}(\frac{\eta_k}{4})]^2$.

Under this framework, the transmitted power for the biorthogonal DMT system is given by

$$P_B = \sum_{k=1}^{r} \sum_{j \in \mathcal{I}_k} \sigma^2_{x_{j,k}} [G_0^H G_0]_{jj} \quad (2.9)$$

$$= \sum_{k=1}^{r} \sum_{j \in \mathcal{I}_k} d_k 2^{b_{j,k}} \sigma^2_{e_{j,k}} [G_0^H G_0]_{jj}. \quad (2.10)$$

Define R_v denoting the *known* autocorrelation matrix of the noise vector $\mathbf{v}(n)$, and

$$R_e = S_0 R_w S_0^H \quad \text{and} \quad R_w = S_1 R_v S_1^H. \quad (2.11)$$

Then $\sigma^2_{e_{j,k}}$ are the diagonal elements of R_e, the autocorrelation matrix of the receiver output noise vector $\mathbf{e}(n)$. Thus, because of (2.5), (2.10) can be rewritten as

$$P_B(S_0) = \sum_{k=1}^{r} \sum_{j \in \mathcal{I}_k} d_k 2^{b_{j,k}} [S_0^{-H} S_0^{-1}]_{jj} [S_0 R_w S_0^H]_{jj}. \quad (2.12)$$

Thus the optimization problem becomes: Given R_v, L, η_k, t_k, minimize (2.12) subject to (2.7) by selecting $b_{j,k}$ (bit loading), selection of $\mathcal{I}_k$ (subchannel assignment), S_0 (transformation selection) and because of (2.6), A (redundancy removal selection).

We show that there is a conceptual separation between the three selections, i.e. the optimizing A is determined exclusively by R_v, provided by the knowledge of the interference and equalizer characteristics; S_0 is determined entirely by A and the channel characteristics; $\mathcal{I}_k$ are determined entirely by R_e, in turn provided by S_1 and S_0, and the bit allocations are determined once the above quantities are found. Further as noted in the introduction, we will show that without loss of generality, the optimizing S_0, G_0 are unitary.

3. Optimum selections

In this section we consider the selection of the various variables.

3.1. Optimum Bit Loading

From the Arithmetic Mean-Geometric Mean (AM-GM) inequality that states that the Arithmetic Mean, exceeds the Geometric mean, with equality if all samples are equal, we have that *for a given choice of $\mathcal{I}_k$ and S_0, under (2.7),*

$$P_B \geq P_{BOPT} = \sum_{k=1}^{r} d_k \left[2^{N t_k} \prod_{j \in \mathcal{I}_k} [S_0^{-H} S_0^{-1}]_{jj} [S_0 R_w S_0^H]_{jj} \right]^{1/L}$$

with equality iff for all k and i, j

$$2^{b_{j,k}} [S_0^{-H} S_0^{-1}]_{jj} [S_0 R_w S_0^H]_{jj} = 2^{b_{i,k}} [S_0^{-H} S_0^{-1}]_{ii} [S_0 R_w S_0^H]_{ii}. \quad (3.13)$$

This is in turn equivalent to the optimum bit loading rule:

$$b_{j,k} = \frac{N t_k}{L} - \log_2 \left[\frac{\sigma^2_{e_{j,k}} [G_0^H G_0]_{jj}}{(\prod_{j \in \mathcal{I}_k} \sigma^2_{e_{j,k}} [G_0^H G_0]_{jj})^{1/L}} \right]. \quad (3.14)$$

Note that P_{BOPT} is much more complicated than its specializations, $r = 1$, studied in [5]. Thus, under optimum bit loading the remaining variables must be selected to minimize P_{BOPT}. *Observe, that while the choice of these other variables impacts the selection of $b_{j,k}$, P_{BOPT} itself is independent of $b_{j,k}$. This underscores the fact that the remaining variables can be selected regardless of the precise values of $b_{j,k}$ obtained through (3.14).*

3.2. Selection of S_0, $\mathcal{I}_k$ and A

Assume for the moment that A and hence S_1 has been selected and that the resulting positive definite Hermitian R_w has the SVD:

$$R_w = U \Lambda^2 U^H \quad (3.15)$$

with $\Lambda = \{\lambda_0, \cdots, \lambda_{M-1}\}$ real, diagonal and U unitary. The goal is to select S_0 and $\mathcal{I}_k$ to minimize P_{BOPT}.

For convenience we first work with the minimization of

$$J(S_0) = \sum_{i=0}^{M-1} \alpha_i [S_0 R_w S_0^H]_{ii} [S_0^{-H} S_0^{-1}]_{ii} \quad (3.16)$$

given positive α_i. Note $J(S_0)$ has the form of P_B.

It is noteworthy that in [5], the $S_0 = PU^H$, with P a permutation matrix miminimizes P_{B-OPT}. If S_0 is restricted to be unitary, then [11] shows that this choice of S_0 also minimizes (3.16). Consider, however, the example where $\alpha_i = 1$, $M = 2$ and $R_w = \text{diag}\{9, 1\}$. Then observe that $J(I) = 10$ but with

$$C = \frac{1}{\sqrt{2}} \begin{bmatrix} 1 & 1 \\ 1 & -1 \end{bmatrix} \begin{bmatrix} 1/\sqrt{3} & 0 \\ 0 & 1 \end{bmatrix}$$

$J(C) = 8$. Thus in general $S_0 = U^H$ does not minimize (3.16). However, we will show in the sequel that it *does minimize P_{BOPT}*.

The following result shows that the search space of S_0 can be restricted to a particular form.

Lemma 3.1 *For some unitary V, (3.16) is minimized by*

$$S_0 = V \Lambda^{-1/2} U^H \quad (3.17)$$

and (3.16) becomes

$$J(S_0) = \sum_{i=0}^{M-1} \alpha_i \left[V \Lambda V^H \right]_{ii}^2 \quad (3.18)$$

Denote $\beta_k = d_k 2^{Nt_k/L}$ and $\mu_j = \left[V\Lambda V^H\right]_{jj}$. Then under optimum bit loading it suffices to restrict the search of S_0 to (3.17) and to seek to minimize under unitary V:

$$P_B^\star = \sum_{k=1}^{r} \beta_k \prod_{j\in\mathcal{I}_k^\star} \mu_k^{2/L} \tag{3.19}$$

with $\mathcal{I}_k^\star$ defining the optimal arrangement of the sequence of μ_k.

Before proceeding, we need a few results from the theory of majorization, [4].

Definition 3.1 *Consider two sequences $x = \{x_i\}_{i=1}^n$ and $y = \{y_i\}_{i=1}^n$ with $x_i \geq x_{i+1}$ and $y_i \geq y_{i+1}$. Then we say that y majorizes x, denoted as $x \prec y$, if*

$$\sum_{i=1}^{k} x_i \leq \sum_{i=1}^{k} y_i$$

holds for $1 \leq k \leq n$, with equality at $k = n$. We say that y weakly supermajorizes x, denoted $x \prec^W y$, if $\sum_{i=j}^n x_i \geq \sum_{i=j}^n y_i, 1 \leq j \leq n$.

Fact 1 *If H is an $n \times n$ Hermitian matrix with diagonal elements $h = \{h_i\}_{i=1}^n$ and eigenvalues $\lambda = \{\lambda_i\}_{i=1}^n$, then $h \prec \lambda$.*

Definition 3.2 *A real valued function $\phi(z) = \phi(z_1, \ldots, z_n)$ defined on a set $\mathcal{A} \subset R^n$ is said to be Schur concave on $\mathcal{A}$ if*

$$x \prec y \text{ on } \mathcal{A} \Rightarrow \phi(x) \geq \phi(y).$$

ϕ is strictly Schur concave on $\mathcal{A}$ if strict inequality $\phi(x) > \phi(y)$ holds when x is not a permutation of y. Further if $x \prec^W y$ then also $\phi(x) > \phi(y)$.

We will now state a theorem that results in a test for strict Schur concavity. We denote $\phi_{(k)}(z) = \frac{\partial\phi(z)}{\partial z_k}$.

Lemma 3.2 *Let $\phi(z)$ be a scalar real valued function defined and continuous on $\mathcal{D} = \{(z_1, \ldots, z_n) : z_1 \geq \ldots \geq z_n\}$, and twice differentiable on the interior of $\mathcal{D}$. Then $\phi(z)$ is Schur concave on $\mathcal{D}$ if $\phi_{(k)}(z)$ is increasing in k.*

The following Lemma provides an important property of $\mathcal{I}_k^\star$ the *optimum arrangement of the subchannels*.

Lemma 3.3 *Consider for $L \geq 2$ and $\alpha, \beta, a_i, b_j > 0$,*

$$f = (\alpha \prod_{k=0}^{L-1} a_k)^{2/L} + (\beta \prod_{l=0}^{L-1} b_l)^{2/L}$$

with $a_i \geq a_{i+1}$ and $b_i \geq b_{i+1}$. Suppose for some i, j

$$a_i > b_j \text{ and } \frac{\partial f}{\partial a_i} > \frac{\partial f}{\partial b_j}. \tag{3.20}$$

Then

$$g = (\alpha \prod_{k=0,k\neq i}^{L-1} a_k.b_j)^{2/L} + (\beta \prod_{l=0,l\neq j}^{L-1} b_l.a_i)^{2/L} < f.$$

Further $\partial f/\partial a_i \leq \partial f/\partial a_{i+1}$ and $\partial f/\partial b_i \leq \partial f/\partial b_{i+1}$.

Thus from Lemma 3.3, any optimum arrangement for (3.19) requires that for all

$$\mu_k > \mu_l \quad \Rightarrow \quad \frac{\partial P_B^\star}{\partial \mu_k} < \frac{\partial P_B^\star}{\partial \mu_l}.$$

Under this condition, $P_B^\star$ is Schur concave. Thus from Fact 1, as

$$\{\left[V\Lambda V^H\right]_{ii}\}_{i=0}^{M-1} \prec \{\lambda_0, \ldots, \lambda_{M-1}\},$$

the choice of V as a permutation matrix that enforces an optimum arrangement of subchannels, minimizes (3.19). Thus to within a permutation matrix P, under optimum bit allocation, one can choose as an optimizing $S_0 = P\Lambda^{-1/2}U^H$. Now note that for any diagonal nonsingular matrix Ω,

$$J(S_0) = J(\Omega S_0),$$

and that for some diagonal matrix $\tilde{\Lambda}$,

$$S_0 = P\Lambda^{-1/2}U^H = \tilde{\Lambda}^{-1/2}PU^H.$$

Thus as in [5], the minimizing $S_0 = PU^H$ with P enforcing the optimum arrangement. Under these conditions

$$[S_0^{-H}S_0^{-1}]_{jj}[S_0 R_w S_0^H]_{jj}$$

and indeed $\sigma^2_{e_{j,k}}$ are the eigenvalues of R_w.

Thus, regardless of A the best S_0 is a Karhunen-Loeve Transform of R_w, and the $\sigma^2_{e_{j,k}}$ equal the eigenvalues of R_w. From the comment on supermajorization made at the end of Definition 3.2, it follows that the optimizing A must be such that the set of resulting eigenvalues of R_w weakly supermajorize all possible sets of attainable eigenvalues. The optimizing A can then be shown to be given by, [6],

$$A = -U_0^H R_v U_1 \left(U_1^H R_v U_1\right)^{-1}. \tag{3.21}$$

4. Simulation results

In this section, we compare the transmitting power of the DFT based DMT under no bit allocation and optimum bit allocation with an optimum unitary transceiver. We assume the equalized channel to be $C(z) = 1 + 0.5z^{-1}$, and a noise source $v(n)$ whose power spectral density is shown in fig. 2. We assume the DMT system supports three user services, where each user is allocated an equal number of subchannels and with the same SER requirement and modulation scheme for each user. The plot in fig. 2 compares

the transmit power levels as the number of subchannels allotted to the users is varied. The plot shows that there is a 10 dB saving in transmit power with our design over the DFT based DMT under optimum bit allocation, and a 14 dB improvement over the conventional DMT with no optimum bit allocation.

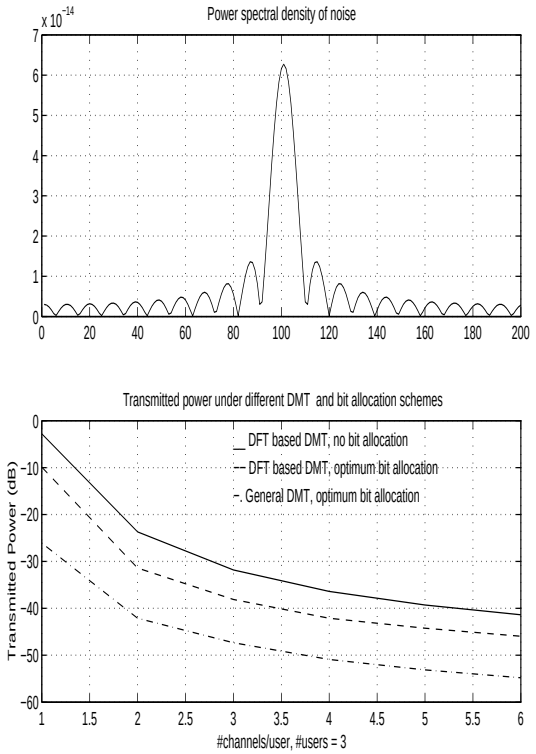

Fig. 2. Comparison of transmit power levels.

5. Conclusions

In this paper, an optimum bit allocation strategy and design of a general biorthogonal DMT multicarrier transceiver system employing zero padding redundancy were presented, for minimizing the transmit power when different users with varied QoS requirements are supported and are assigned potentially different number of subchannels. We showed that no gains in transmit power can be obtained by considering biorthogonal transceivers over orthogonal transceivers. These results also show that the optimum transceiver depends *only on the channel and interference conditions and not on the QoS requirements*. Indeed to within a permutation of subchannels, the optimum transceiver obtained here is identical to that obtained in [5]. Equally should the channel/interference remain invariant after the initial connection is established, then only bit loading and subchannel selection need be updated in response to changing traffic needs.

6. References

[1] L.M.C. Hoo, J. Tellado and J.M. Cioffi, "Discrete dual QoS loading algorithms for multicarrier systems ", *IEEE International Conference on Communications*, pp 796-800, 1999.

[2] D. Kivanc and H. Liu, "Subcarrier allocation and power control for OFDMA", *IEEE Journal on Selected Areas in Communications*, To appear.

[3] B. S. Krongold, K. Ramchandran and D. L. Jones, "Computationally Efficient Optimal Power Allocation Algorithms for Multicarrier Communication Systems", *IEEE Transactions on Communications*, pp 23-27, Jan 2000.

[4] A. W. Marshall and I. Olkin, *Inequalities: Theory of Majorization and its applications*, Academic Press, 1979.

[5] Y.-P. Lin and S.-M. Phoong, "Perfect discrete multitone modulation with optimal transceivers", *IEEE Transactions on Signal Processing*, pp 1702 -1711, June 2000.

[6] A. Pandharipande and S. Dasgupta, "Optimal transceivers for DMT based multiuser communication", *IEEE International Conference on Acoustics, Speech, and Signal Processing*, pp 2369 -2372, 2001. Also *IEEE Transactions on Communications*, accepted subject to modifications.

[7] Y.-P. Lin and S.-M. Phoong, "Optimal ISI-free DMT transceivers for distorted channels with colored noise", *IEEE Transactions on Signal Processing*, pp 2702 -2712, Nov 2001.

[8] J.G. Proakis, *Digital Communications*, McGraw-Hill, Third Edition, 1995.

[9] A. Scaglione, S. Barbarossa and G.B. Giannakis, "Filterbank transceivers optimizing information rate in block transmissions over dispersive channels", *IEEE Transactions on Information Theory*, pp 1019-1032, Apr 1999.

[10] T. Starr, J.M. Cioffi and P. Silverman, *Understanding Digital Subscriber Line Technology*, Prentice Hall, 1998.

[11] S. Akkarakaran and P.P. Vaidyanathan, "Filterbank optimization with convex objectives and the optimality of principal component forms", *IEEE Transactions on Signal Processing*, pp 100-114, January 2001.

[12] R. Van Nee and R. Prasad, *OFDM for Wireless Multimedia Communications*, Artech House, 2000.

OPTIMUM BIORTHOGONAL DMT SYSTEMS FOR MULTI-SERVICE COMMUNICATION

Soura Dasgupta and Ashish Pandharipande

Department of Electrical and Computer Engineering, The University of Iowa, Iowa City, USA.
Email: {dasgupta, pashish}@engineering.uiowa.edu

ABSTRACT

This paper considers the design of biorthogonal DMT multicarrier transceiver systems supporting multiple services. The supported user services may have differing quality of service (QoS) requirements, quantified in this paper by bit rate and symbol error rate specifications. To reflect their service priorities, different users on the system can be potentially assigned different number of subchannels. Our goal is to minimize the transmitted power given the QoS specifications for the different users, subject to the knowledge of colored interference at the receiver input of the DMT system. In particular we find an optimum bit loading scheme that distributes the bit rate transmitted across the various subchannels belonging to the different users, and subject to this bit allocation, determine an optimum transceiver.

1. INTRODUCTION

Future broadband communication systems will be expected to deliver multiple services, such as voice, data, video, with multiple-stream support. Because delivery of these streams will be under differing requirements such as information rate and error performance, allocation of critical resources like power would have a significant impact on the overall capacity of the communication system. Discrete multitone (DMT) is a channel coding technique to achieve reliable, high data rate communications in such systems. It is a current standard in various wireline applications like ADSL, VDSL, [9], and in the form of Orthogonal frequency division multiplexing (OFDM) has been proposed for fixed wireless standards like WLAN's, [11]. This paper considers transceiver optimization for such multicarrier transmission systems operating in a multiuser environment.

More specifically, we assume that a single DMT system supports r users, each having its own QoS specification quantified by its bit rate and symbol error rate (SER). The k-th user is assumed to have been assigned n_k subchannels, and requires a bit rate of t_k, and an SER of no more than η_k. The number of subchannels assigned to each user is fixed *a priori* according to some priorities determined by the user service. As proposed in several recent papers, [4], [6], [8], [10], we consider general DMT transceivers which are more general than the traditional DFT based systems in that the input and output transforms are general block transforms. We consider biorthogonal systems employing zero padding redundancy with the redundancy removal at the receiver being a general linear operation. Our goal is to select transforms G_0, S_0 (see fig. 1), and the linear operation reflecting redundancy removal, and assign bits/symbol to each subchannel, to achieve the QoS specifications, under a zero intersymbol interference (ISI) condition with the minimum possible transmitted power. We assume that the channel and equalizer are known and so is the interference autocorrelation.

Supported in part by US Army contract, DAAAD19-00-1-0534, and NSF grants ECS-9970105 and CCR-9973133.

We thus generalize our earlier result reported in [6], where the same optimization problem was considered with an *orthonormal transceiver* under the assumption that each user is assigned the *same number of subchannels.* We shall see in the following sections how the extension to [6] considered here modifies the optimization problem. Further, the asymmetric subchannel assignment considered here is by contrast more realistic as service priorities may cause certain users to receive greater number of subchannels than others. For example, one may assign more subchannels to video services than to audio services.

Figure 1 depicts the broad contours of a DMT communications system. An incoming data stream is converted into M-parallel data streams of lower rate. An M-point block transformation of these streams of data is followed by a parallel-to-serial conversion, prior to transmission through the communication channel. An equalizer is employed to shorten the dispersive effects of the transmission channel. The *equalized* channel $C(z)$ is assumed to be FIR of length κ. For an FIR equalized channel of length κ, extra redundancy of length κ in the form of zero padding is added at the channel input to infuse resistance to channel induced ISI. At the channel output, one performs in succession the operations of redundancy removal, serial-to-parallel conversion, and the application of an inverse block transform.

Past treatment of optimum resource allocation, [1], [2], [3], has been restricted mostly to bit loading and power allocation algorithms. Some authors have studied the optimum transceiver design in the single user case, [4], [8], [10]. While [4] was concerned with optimizing the transmitted power, [8] focussed on the maximization of the mutual information between the transmitted and received signals. Essentially, [4] considers the same optimization as presented here but under the assumption that only a single user is supported by the system, i.e. $r = 1$. In comparison with [4], the multiuser environment considered in this paper renders the optimization problem highly non-trivial as shall be seen.

In Section 2, we give a description of the DMT system and the optimization problem under consideration. Section 3 presents our results on optimum transceiver selection and the optimum bit rate allocation strategy that needs to be adopted. Section 4 presents some simulation results showing improvements in transmitted power levels obtained with our optimum design. Section 5 concludes.

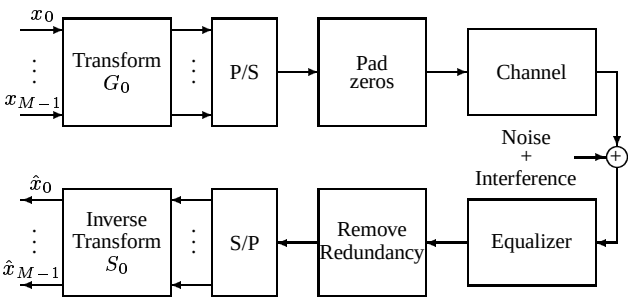

Fig. 1. DMT communication system.

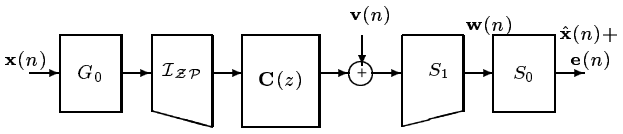

Fig. 2. Block representation of DMT communications system.

2. MULTIUSER DMT SYSTEM MODEL

2.1. Preliminaries

Define in fig. 1, G_0 and S_0 as the nonsingular $M \times M$ transmitter and receiver transform matrices respectively. We assume a biorthogonal system, i.e.

$$S_0 = G_0^{-1}. \tag{2.1}$$

Thus, the input block transformation is a general nonsingular transformation, and the output transformation is its inverse. Denote the collection of M input and output symbols respectively by $\mathbf{x}(n) = [x_0(n), \cdots, x_{M-1}(n)]^T$, and $\hat{\mathbf{x}}(n) = [\hat{x}_0(n), \cdots, \hat{x}_{M-1}(n)]^T$. With $v(n)$, the noise and interference effect at the output of the equalizer, denote $\mathbf{v}(n) = [v(Nn), v(Nn+1), \cdots, v(Nn+N-1)]^T$, as the N-fold blocked version of $v(n)$, with $N = M + \kappa$. Then the system in fig. 1 has the equivalent description of fig. 2. Here $\mathbf{C}(z)$ is the N-fold blocked version of the channel-equalizer combination $C(z) = c_0 + c_1 z^{-1} + \ldots + c_\kappa z^{-\kappa}$. One can show that

$$\mathbf{C}(z) = \left[\begin{array}{cc} \mathbf{C_L} & \mathbf{C_R}(z) \end{array} \right] \tag{2.2}$$

where $\mathbf{C_L}$ is an $N \times M$ constant matrix, and $\mathbf{C_R}(z)$ is an $N \times \kappa$ matrix.

The addition of zero padding redundancy to an M-block vector is equivalent to premultiplication by

$$\mathcal{I}_{\mathcal{ZP}} = \left[\begin{array}{c} I_M \\ 0_{\kappa \times M} \end{array} \right]. \tag{2.3}$$

Denote by S_1, a suitable $M \times N$ matrix, representing the linear redundancy removal operation. Then the input-output relation of the system in fig. 2 is given by

$$\begin{aligned} \hat{\mathbf{x}}(n) &= S_0 S_1 \mathbf{C}(z) \mathcal{I}_{\mathcal{ZP}} G_0 \mathbf{x}(n) + S_0 S_1 \mathbf{v}(n) && (2.4) \\ &= S_0 S_1 \mathbf{C_L} G_0 \mathbf{x}(n) + S_0 S_1 \mathbf{v}(n). && (2.5) \end{aligned}$$

We impose the perfect reconstruction (PR) condition, i.e., in the absence of noise/interference, $\hat{\mathbf{x}}(n) = \mathbf{x}(n)$ for all n. In other words,

$$S_0 S_1 \mathbf{C_L} G_0 = I, \tag{2.6}$$

and the DMT system has no ISI. To obtain a more useful characterization of PR, consider the singular value decomposition of $\mathbf{C_L}$ defined in (2.2):

$$\mathbf{C_L} = U_c \left[\begin{array}{c} \Lambda_c \\ 0 \end{array} \right] V_c^H = U_0 \Lambda_c V_c^H \tag{2.7}$$

where U_c and V_c are respectively $N \times N$ and $M \times M$ unitary matrices whose columns are the eigenvectors of $\mathbf{C_L}\mathbf{C_L}^H$ and $\mathbf{C_L}^H\mathbf{C_L}$. Λ_c is the $M \times M$ real, positive definite diagonal matrix with diagonal elements that are the singular values of $\mathbf{C_L}$. Then, because of (2.6), given G_0, the class of all $S_0 S_1$ enforcing PR is completely characterized by (2.1) and

$$S_1 = V_c \Lambda_c^{-1} \left[\begin{array}{cc} I_M & A \end{array} \right] U_c^H, \tag{2.8}$$

where A is any arbitrary $M \times \kappa$ matrix. In the sequel it will be useful to partition U_c as $U_c = [U_0 \quad U_1]$, where U_0 is $N \times M$ and U_1 is $N \times \kappa$.

Note, as V_c, U_c and Λ_c are supplied by the channel, the only quantities that need to be found to determine the transceiver completely are G_0 and A.

2.2. Problem formulation

As mentioned earlier the M subchannels are distributed among the r users with the k-th user allocated n_k subchannels. Thus consider disjoint subsets $\mathcal{I}_k \subset \{0, \ldots, M-1\}$ with $|\mathcal{I}_k| = n_k$, and $\mathcal{I}_k \cap \mathcal{I}_j = \emptyset, k \neq j$. Subchannel assignment ro the k-th user constitutes determining $\mathcal{I}_k$. We assume that the j-th subchannel of the k-th user is assigned $b_{j,k}$ bits per symbol. To meet the bit rate specification for the k-th user one requires that

$$\frac{1}{N} \sum_{j \in \mathcal{I}_k} b_{j,k} = t_k. \tag{2.9}$$

Let the input power in the j-th subchannel of the k-th user be $\sigma^2_{x_{j,k}}$. Assume that $\sigma^2_{e_{j,k}}$ is the noise power in this subchannel. Under high SNR most modulation schemes, [7], require that to achieve a given SER the required SNR is proportional to $2^{b_{j,k}}$. More precisely,

$$\sigma^2_{x_{j,k}} = d_k 2^{b_{j,k}} \sigma^2_{e_{j,k}}, \tag{2.10}$$

where the constant d_k depends on the desired SER for the k-th user, η_k. For example, for QAM, $d_k = \frac{1}{3}[Q^{-1}(\frac{\eta_k}{4})]^2$. Under this framework, the transmitted power for the biorthogonal DMT system is given by

$$\begin{aligned} P_B &= \sum_{k=1}^{r} \sum_{j \in \mathcal{I}_k} \sigma^2_{x_{j,k}} [G_0^H G_0]_{jj} && (2.11) \\ &= \sum_{k=1}^{r} \sum_{j \in \mathcal{I}_k} d_k 2^{b_{j,k}} \sigma^2_{e_{j,k}} [G_0^H G_0]_{jj}. && (2.12) \end{aligned}$$

The minimization of the transmission power involves optimal selection of $b_{j,k}$ (bit loading), selection of $\mathcal{I}_k$ (subchannel assignment), G_0 (transformation selection) and A (redundancy removal selection).

3. OPTIMUM SELECTIONS

With R_e, R_w and R_v denoting the autocorrelation matrices of the noise vectors $\mathbf{e}(n), \mathbf{w}(n)$ and $\mathbf{v}(n)$ respectively,

$$R_e = S_0 R_w S_0^H \quad \text{and} \quad R_w = S_1 R_v S_1^H. \tag{3.13}$$

Note that $\sigma^2_{e_{j,k}}$ in (2.12) are the diagonal elements of R_e. Thus (2.12) can be rewritten as

$$P_B(S_0) = \sum_{k=1}^{r} \sum_{j \in \mathcal{I}_k} d_k 2^{b_{j,k}} [S_0^{-H} S_0^{-1}]_{jj} [S_0 R_w S_0^H]_{jj}. \tag{3.14}$$

First consider the problem of determining optimum G_0, or equivalently chossing S_0. Observe that the problem of choosing S_0, under (2.1), minimizing (3.14) has the following form:

Problem 3.1 *With $M \times M$ positive definite Hermitian R_w and $M \times M$ nonsingular S_0, $\alpha_i > 0$, determine S_0 to minimize*

$$J(S_0) = \sum_{i=0}^{M-1} \alpha_i [S_0 R_w S_0^H]_{ii} [S_0^{-H} S_0^{-1}]_{ii} \tag{3.15}$$

Now note that for any diagonal nonsingular matrix Ω, $J(S_0) = J(\Omega S_0)$. This means that in finding a minimizing S_0 to (3.15), one can restrict the search to an S_0 for which the diagonal elements of $S_0^{-H} S_0^{-1}$ are $1/\alpha_i$. The following Lemma considers the *equivalent constrained optimization* of Problem 3.1.

Lemma 3.1 *With $M \times M$ positive definite Hermitian matrix R_w, $M \times M$ nonsingular S_0, consider the minimization of*

$$\sum_{i=0}^{M-1} [S_0 R_w S_0^H]_{ii} \tag{3.16}$$

such that for all $i \in \{0, \ldots, M-1\}$ and some $\alpha_i > 0$,

$$[S_0^{-H} S_0^{-1}]_{ii} = 1/\alpha_i. \tag{3.17}$$

Then the minimizing S_0 obeys for some real, positive definite, diagonal Γ,

$$(S_0 R_w S_0^H)(S_0 S_0^H) = \Gamma. \tag{3.18}$$

In fact one minimizing S_0 for (3.15) obeys

$$(S_0 R_w S_0^H)(S_0 S_0^H) = I.$$

The following result shows a particular S_0 minimizing (3.15).

Lemma 3.2 *Let the SVD of positive definite Hermitian R_w be*

$$R_w = U \Lambda^2 U^H \tag{3.19}$$

with Λ real, diagonal and U unitary. Then for some unitary V, (3.15) is minimized by

$$S_0 = V \Lambda^{-1/2} U^H \tag{3.20}$$

and (3.15) becomes

$$J(S_0) = \sum_{i=0}^{M-1} \alpha_i \left[V \Lambda V^H \right]_{ii}^2 \tag{3.21}$$

Before proceeding, we need a few results from the theory of majorization, [5].

Definition 3.1 *Consider two sequences $x = \{x_i\}_{i=1}^n$ and $y = \{y_i\}_{i=1}^n$ with $x_i \geq x_{i+1}$ and $y_i \geq y_{i+1}$. Then we say that y majorizes x, denoted as $x \prec y$, if $\sum_{i=1}^k x_i \leq \sum_{i=1}^k y_i$ holds for $1 \leq k \leq n$, with equality at $k = n$. We say that y weakly supermajorizes x, denoted $x \prec^W y$, if $\sum_{i=j}^n x_i \geq \sum_{i=j}^n y_i, 1 \leq j \leq n$.*

Fact 1 *If H is an $n \times n$ Hermitian matrix with diagonal elements $h = \{h_i\}_{i=1}^n$ and eigenvalues $\lambda = \{\lambda_i\}_{i=1}^n$, then $h \prec \lambda$.*

Definition 3.2 *A real valued function $\phi(z) = \phi(z_1, \ldots, z_n)$ defined on a set $\mathcal{A} \subset R^n$ is said to be Schur concave on $\mathcal{A}$ if $x \prec y$ on $\mathcal{A} \Rightarrow \phi(x) \geq \phi(y)$. ϕ is strictly Schur concave on $\mathcal{A}$ if strict inequality $\phi(x) > \phi(y)$ holds when x is not a permutation of y. Further if $x \prec^W y$ then also $\phi(x) > \phi(y)$.*

We will now state a theorem that results in a test for strict Schur concavity. We denote $\phi_{(k)}(z) = \frac{\partial \phi(z)}{\partial z_k}$.

Lemma 3.3 *Let $\phi(z)$ be a scalar real valued function defined and continuous on $\mathcal{D} = \{(z_1, \ldots, z_n) : z_1 \geq \ldots \geq z_n\}$, and twice differentiable on the interior of $\mathcal{D}$. Then $\phi(z)$ is Schur concave on $\mathcal{D}$ if $\phi_{(k)}(z)$ is increasing in k.*

We now return to the minimization of (3.14) with R_w having the form (3.19). Because of Lemma 3.2, with $S_0 = V \Lambda^{-1/2} U^H$, for any choice of $\mathcal{I}_k$ and $b_{j,k}$, and subject to V being unitary

$$\begin{aligned} P_B &\geq \min_{VV^H = I} \sum_{k=1}^{r} d_k \sum_{j \in \mathcal{I}_k} 2^{b_{j,k}} \left(\left[V \Lambda V^H \right]_{jj} \right)^2 \\ &\geq \min_{VV^H = I} \sum_{k=1}^{r} d_k 2^{Nt_k/n_k} \prod_{j \in \mathcal{I}_k} \left(\left[V \Lambda V^H \right]_{jj} \right)^{2/n_k} \end{aligned}$$

Denote $\beta_k = d_k 2^{Nt_k/n_k}$ and $a_j = \left[V \Lambda V^H \right]_{jj}$. Then

$$P_B \geq P_B^\star = \min_{VV^H = I} \sum_{k=1}^{r} \beta_k \prod_{j \in \mathcal{I}_k^\star} a_k^2 \tag{3.22}$$

with $\mathcal{I}_k^\star$ defining the optimal arrangement of the sequence of a_k. The following Lemma characterizes such *optimum arrangements.*

Lemma 3.4 *Consider for integers $p, q \geq 2$,*

$$f = (\alpha \prod_{k=0}^{p-1} a_k)^{2/p} + (\beta \prod_{l=0}^{q-1} b_l)^{2/q}$$

with $\alpha, \beta, a_i, b_j > 0$. Suppose for some i, j

$$a_i > b_j \text{ and } \frac{\partial f}{\partial a_i} > \frac{\partial f}{\partial b_j}. \tag{3.23}$$

Then $g = (\alpha \prod_{k=0, k \neq i}^{p-1} a_k . b_j)^{1/p} + (\beta \prod_{l=0, l \neq j}^{q-1} b_l . a_i)^{1/q} < f$.

Hence if there exist pairs a_i, b_j such that (3.23) holds, violating the Schur concavity condition in Lemma 3.3, the value of f can be reduced by interchanging a_i, b_j. From Lemma 3.4, an optimum arrangement for (3.22) requires that for all $a_k > a_l$, $\frac{\partial P_B^\star}{\partial a_k} < \frac{\partial P_B^\star}{\partial a_l}$. Under this condition, $P_B^\star$ is Schur concave. Thus from Fact 1, as $\{\left[V\Lambda V^H\right]_{ii}\}_{i=0}^{M-1} \prec \{\lambda_0, \ldots, \lambda_{M-1}\}$, the choice $V = I$ minimizes (3.22). Thus the optimizing $S_0 = \Lambda^{-1/2}U^H$, under optimum bit allocation.

The optimum bit loading is obtained by using the fact that the arithmetic-mean of the n_k numbers $\{2^{b_{j,k}}\sigma^2_{e_{j,k}}[G_0^H G_0]_{jj}\}_{j\in\mathcal{I}_k}$ in (2.12) is greater than their geometric mean, with equality iff

$$b_{j,k} = \frac{Nt_k}{n_k} - \log_2\left[\frac{\sigma^2_{e_{j,k}}[G_0^H G_0]_{jj}}{(\prod_{j\in\mathcal{I}_k}\sigma^2_{e_{j,k}}[G_0^H G_0]_{jj})^{1/n_k}}\right].$$

Thus under the above *optimum bit allocation*, and because of (3.13) and Fact 1, the optimum G_0 (from (2.1)) is a matrix of eigenvectors of R_w, and $[G_0^H G_0]_{jj}[G_0^{-1}R_w G_0^{-H}]_{jj}$ are the eigenvalues of R_w. Thus even under the relaxed conditions on G_0, the best power is achieved with orthogonal G_0. Further, the optimizing A must be such that the set of resulting eigenvalues of R_w weakly supermajorize all possible sets of attainable eigenvalues. The optimizing A can then be shown to be given by, [6],

$$A = -U_0^H R_v U_1 \left(U_1^H R_v U_1\right)^{-1}. \tag{3.24}$$

4. SIMULATION RESULTS

In this section, we compare the transmitting power of the DFT based DMT under no bit allocation and optimum bit allocation with an optimum unitary transceiver. We assume the equalized channel to be $C(z) = 1 + 0.5z^{-1}$, and a noise source $v(n)$ whose power spectral density is shown in fig. 3. We assume the DMT system supports two user services. The (i, j) on the x-axis of the plot indicates that user 1 and 2 were respectively allocated i, j number of channels. The plot shows that there is a 10 dB saving in transmit power with our design over the DFT based DMT under optimum bit allocation, and a 14 dB improvement over the conventional DMT with no optimum bit allocation.

5. CONCLUSIONS

In this paper, an optimum bit allocation strategy and design of a general biorthogonal DMT multicarrier transceiver system employing zero padding redundancy were presented, for minimizing the transmit power when different users with varied QoS requirements are supported and are assigned potentially different number of subchannels. We showed that no gains in transmit power can be obtained by considering biorthogonal transceivers - the optimum power is achieved through an orthogonal transceiver. Simulations demonstrated potential improvements in performance over DFT based DMT systems.

6. REFERENCES

[1] L.M.C. Hoo, J. Tellado and J.M. Cioffi, "Discrete dual QoS loading algorithms for multicarrier systems ", *IEEE International Conference on Communications*, pp 796-800, 1999.

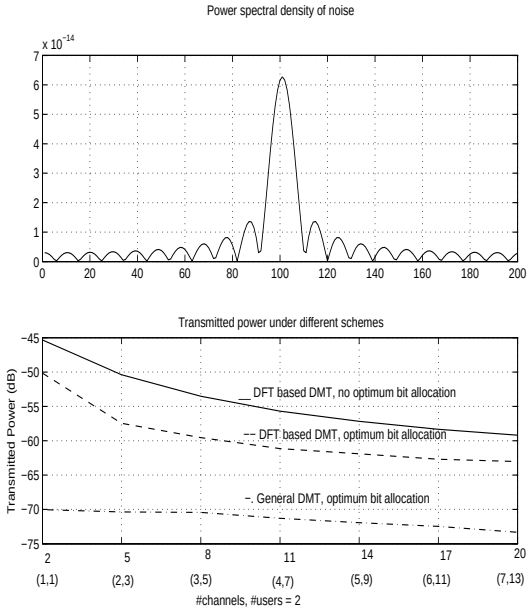

Fig. 3. Comparison of transmit power levels.

[2] D. Kivanc and H. Liu, "Subcarrier allocation and power control for OFDMA", *IEEE Journal on Selected Areas in Communications*, To appear.

[3] B. S. Krongold, K. Ramchandran and D. L. Jones, "Computationally Efficient Optimal Power Allocation Algorithms for Multicarrier Communication Systems", *IEEE Transactions on Communications*, pp 23-27, Jan 2000.

[4] Y.-P. Lin and S.-M. Phoong, "Optimal ISI-free DMT transceivers for distorted channels with colored noise", *IEEE Transactions on Signal Processing*, pp 2702 -2712, Nov 2001.

[5] A. W. Marshall and I. Olkin, *Inequalities: Theory of Majorization and its applications*, Academic Press, 1979.

[6] A. Pandharipande and S. Dasgupta, "Optimal transceivers for DMT based multiuser communication", *IEEE International Conference on Acoustics, Speech, and Signal Processing*, pp 2369 -2372, 2001. Also submitted to *IEEE Transactions on Communications.*

[7] J.G. Proakis, *Digital Communications*, McGraw-Hill, Third Edition, 1995.

[8] A. Scaglione, S. Barbarossa and G.B. Giannakis, "Filterbank transceivers optimizing information rate in block transmissions over dispersive channels", *IEEE Transactions on Information Theory*, pp 1019-1032, Apr 1999.

[9] T. Starr, J.M. Cioffi and P. Silverman, *Understanding Digital Subscriber Line Technology*, Prentice Hall, 1998.

[10] P.P. Vaidyanathan, Y.-P. Lin, S. Akkarakaran and S.-M. Phoong, "Discrete multitone modulation with principal component filter banks", *IEEE Transactions on Circuits and Systems I: Fundamental Theory and Applications*, pp 1397 - 1412, Oct 2002.

[11] R. Van Nee and R. Prasad, *OFDM for Wireless Multimedia Communications*, Artech House, 2000.

OPTIMUM CHANNEL- AND MULTIFLOW-ADAPTIVE BIORTHOGONAL DMT SYSTEMS

Ashish Pandharipande*and Soura Dasgupta†

Abstract

This paper considers the design of biorthogonal DMT multicarrier transceiver systems supporting multiple services. The supported user services may have differing quality of service (QoS) requirements, quantified in this paper by bit rate and symbol error rate specifications. To reflect their service priorities, different users on the system can be potentially assigned different number of subchannels. Our goal is to minimize the transmitted power given the QoS specifications for the different users, subject to the knowledge of colored interference at the receiver input of the DMT system. In particular we find an optimum bit loading scheme that distributes the bit rate transmitted across the various subchannels belonging to the different users, and subject to this bit allocation, determine an optimum transceiver.

Keywords: Multiuser, DMT system, biorthogonal, optimum transceiver design, bit loading.

*Was with the Department of Electrical and Computer Engineering, the University of Iowa, Iowa City, IA-52242, USA when this work was completed. He is now with the Department of Electrical and Computer Engineering, University of Florida, Gainesville, FL 32611-6130, USA. Email: ashish@dsp.ufl.edu

†Department of Electrical and Computer Engineering, The University of Iowa, Iowa City, IA-52242, USA. Email: dasgupta@engineering.uiowa.edu. This work was supported by US Army contract, DAAAD19-00-1-0534, and NSF grants ECS-9970105, ECS-0225432 and CCR-9973133.

1 Introduction

Discrete multi-tone (DMT) modulation has proved to be an effective solution to the problem of reliable and efficient data transmission over frequency selective communication channels. It is a curent standard in various wireline applications like ADSL, VDSL, [2], and in the form of Orthogonal frequency division multiplexing (OFDM) has been proposed for fixed wireless standards like IEEE 802.11a. With growing and changing user needs, such communication systems are expected to deliver multiple services, such as voice, data and video, with multiple stream support. Because delivery of these streams can be under different requirements on parameters like error performance, appropriate allocation of bandwidth and rates among the various services becomes an important problem. The subject of this paper is to consider transceiver optimization of *general biorthogonal* DMT systems operating in such a multi-user environment.

We consider multiple flows supported on a general biorthogonal DMT system. Fig. 1 depicts the general DMT communication system under consideration. This system is more general as compared to the conventional DMT systems in that the transmitter and receiver transforms are characterized by square matrices G_0 and S_0, and the redundancy removal at the receiver is a general linear transformation S_1. In contrast, conventional DMT systems employ an Inverse discrete Fourier transform (IDFT) and DFT at the transmitter and receiver ends respectively, and the redundancy removal is done by simply discarding certain symbols. Also, we consider zero padding as the form of redundancy injection, as proposed in several recent papers, [7], [10], [13]. We assume that this DMT system supports r service flows. Each flow may have its own quality of service (QoS) requirement quantified in this paper by its bit rate and symbol error rate (SER). Further, depending on their respective service priorities, each flow is assumed to have been *a priori* allotted a certain number of subchannels. Thus for instance, large bandwidth consuming video flows may receive more subchannels than voice or data flows. We thus assume that the k-th flow is assigned n_k subchannels, requires a bit rate of t_k and an SER of no more than η_k. We desire to minimize

the total transmitted power given these service-flow QoS specifications so that inter symbol interference (ISI) free transmission occurs. The goal is to select the input and output block transforms G_0 and S_0, the linear redundancy matrix S_1, the number of bits/symbol assigned to each subchannel, and the subchannel assignment to each service flow, in order to achieve the QoS specifications under a zero ISI condition with minimum transmitted power. We assume knowledge of the equalized channel and the second-order statistics of the noise at the receiver input.

We thus extend in this paper our results reported in [11], where the same optimization was considered with an *orthonormal* transceiver under the assumption that each flow is assigned the *same number of subchannels*. The unequal subchannel assignment considered in this work is more realistic as service priorities may cause certain flows to be assigned greater number of subchannels than others. We shall find that relaxing the orthonormality condition, that is considering a biorthogonal system, and having unequal subchannel assignment renders the underlying optimization methodology to be non-trivially different from the considerations in [11].

Related treatments in literature are [3], [5], [6], [7], [8], [13], [16], [17]. A great amount of work has been done in dealing with the problem of bit loading and power allocation. References [3], [17] provide algorithms for the bit loading problem while [5], [6] treat the power allocation problem for the multi-user and single user cases respectively. The problem of minimizing the overall transmit power with multiple users on an OFDM system was considered in [17], where the minimization was done by adaptively assigning subcarriers to the various users along with adjusting the number of bits and user power levels. The problem of transceiver optimization has received attention only recently, with works [7], [8], [13] dealing with optimum designs when a single user is supported on the DMT system. While [13] treated the problem of maximization of mutual information between transmitted and received signals, works [7] and [8] considered the problem of minimizing transmit power. In particular, [7] considered the design of an optimum orthonormal DMT system that achieves minimum transmit power under certain specified error probability and rate requirement. This work was extended in [8] with the orthonormality constraint relaxed. In both

[7], [8] however it was assumed that a single user is supported on the DMT system.

The problem we consider in this paper differs from the treatments [7], [8], [17] in the following ways. As in these works, we consider the problem of minimizing transmit power. However in contrast to [17], which restricts its treatment to the problem of resource allocation to conventional fixed DFT based systems, we consider the problem of optimum transceiver design of a general biorthogonal system as well. Further the multiuser environment in our paper makes our treatment substantively different from the single user case considered in [7], [8].

Our approach in this paper follows closely up on the formalisms developed in [8]. The bit loading solution of [8] can be considered as a water-pouring approach. Suppose a set of subchannels experience a high level of attenuation. Then the optimum bit loading scheme assigns fewer bits/symbol on these subchannels. Further to avoid too many of such low performing subchannels, the subchannel selection process (optimum transform selection) has to squeeze out those frequency bands with adverse conditions as best as possible, specifically by forcing channel nulls or noise/interference peaks to occupy as few subchannels as possible. These notions are developed for the multiuser case in our paper. A major conclusion of our work will be to show that, as in the single user case of [8], *even in the multiuser case with asymmetric subchannel assignments, optimal performance is achieved through orthonormal transforms.* Specifically, we show that the optimum receiver transform is one which diagonalizes the autocorrelation matrix of a certain noise vector at the receiver input, and the optimum transmit transform is then the inverse of this optimum receiver transform matrix.

The remainder of the paper is organized as follows. In Section 2, the general biorthogonal DMT system is described, and the characterization of such a system is developed along the lines of [8]. The precise optimization problem of minimizing transmit power is formulated in Section 3. The optimal selections of the optimization variables are described in Section 4. Section 5 provides some simulations and Section 6 concludes. The Appendix provides some useful results from the theory of majorization employed to solve the optimization problem at hand.

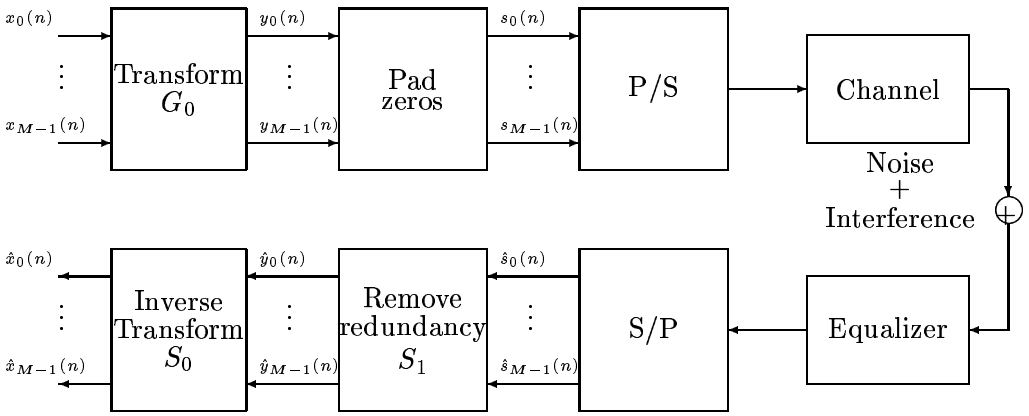

Figure 1: DMT communication system.

The following notation will be followed in the subsequent Sections. Discrete time signals will be denoted by $x(n), y(n)$ etc., with n being the time index. An $M \times M$ diagonal square matrix with diagonal elements $d_1, \ldots, d_M$ is written as $\text{diag}\{d_1, \ldots, d_M\}$. $[A]_{ij}$ denotes the element in the i-th row, j-th coloumn of matrix A. A^T, A^H respectively denote the transpose and transpose-conjugate of matrix A. An $M \times M$ identity matrix will be denoted by I_M, with the subscript usually dropped when the dimensions are clear from context.

2 General DMT system

In this Section, we describe the general biorthogonal DMT system supporting the various user flows. Consider the biorthogonal general DMT system shown in fig. 1. In a biorthogonal DMT system, the transmit and receive matrices G_0 and S_0 are *arbitrary nonsingular* $M \times M$ matrices, in contrast to orthonormal systems, [7], where G_0, S_0 are unitary, i.e. $G_0^H G_0 = I = S_0^H S_0$. In conventional DMT systems, G_0 is an IDFT and S_0 is the DFT matrix. We assume that the data streams $x_0(n), x_1(n), \ldots, x_{M-1}(n)$ result from the r service flows. The $M \times M$ block transformation G_0 is applied to the M-symbol data stream $[x_0(n), x_1(n), \ldots, x_{M-1}(n)]^T$, and redundancy in the form of padded zeros is introduced followed by parallel-to-serial conversion, prior to transmis-

sion. Thus consider the M symbol vector $\mathbf{y}(n) = [y_0(n), y_1(n), \ldots, y_{M-1}(n)]^T$. Each such block is converted in to an N-block, with $N = M + \kappa$, by simply appending κ zeros to it, obtaining the block

$$\begin{aligned} \mathbf{s}(n) &= [s_0(n), s_1(n), \ldots, s_{N-1}(n)]^T \\ &= [y_0(n), y_1(n), \ldots, y_{M-1}(n), 0, \ldots, 0]^T. \end{aligned}$$

Thus with

$$\mathcal{I}_{\mathcal{ZP}} = \begin{bmatrix} I_M \\ 0_{\kappa \times M} \end{bmatrix}, \tag{2.1}$$

we have

$$\mathbf{s}(n) = \mathcal{I}_{\mathcal{ZP}} \mathbf{y}(n).$$

Most practical transmission channels are characterized by dispersion that spreads over a very large number of samples. A time domain equalizer is employed to limit these dispersive effects and contain most of its energy in a few samples. Thus the combination of the transmission channel and equalizer, given by the equalized-channel $C(z)$, is assumed to be FIR of length κ. For such a κ length FIR equalized-channel, addition of zero padding redundancy of length κ infuses resistance to channel induced ISI. Denote the multiple-input multiple-output system relating $\hat{\mathbf{s}}(n) = [\hat{s}_0(n), \hat{s}_1(n), \ldots, \hat{s}_{N-1}(n)]^T$ to $\mathbf{s}(n)$ by the $N \times N$ channel matrix $\mathbf{C}(z)$. This matrix is obtained from the coefficients of the equalized-channel $C(z) = c_0 + c_1 z^{-1} + \ldots + c_\kappa z^{-\kappa}$, and is given by

$$\mathbf{C}(z) = \begin{bmatrix} c_0 & z^{-1}c_{N-1} & z^{-1}c_{N-2} & \cdots & z^{-1}c_1 \\ c_1 & c_0 & z^{-1}c_{N-1} & \cdots & z^{-1}c_2 \\ \vdots & \vdots & \vdots & \vdots & \vdots \\ c_{N-1} & c_{N-2} & \cdots & c_1 & c_0 \end{bmatrix} \tag{2.2}$$

with $c_i = 0$, for $i > \kappa$. At the equalized-channel output, the redundancy is removed using an $M \times N$ linear transform matrix S_1. The M-block output samples $\hat{x}_0(n), \hat{x}_1(n), \ldots, \hat{x}_{M-1}(n)$ are then obtained by the application of the $M \times M$ transformation S_0.

Denote the blocks of M input and output symbols by $\mathbf{x}(n) = [x_0(n), \cdots, x_{M-1}(n)]^T$ and $\hat{\mathbf{x}}(n) = [\hat{x}_0(n), \cdots, \hat{x}_{M-1}(n)]^T$ respectively. With $v(n)$, the noise and interference

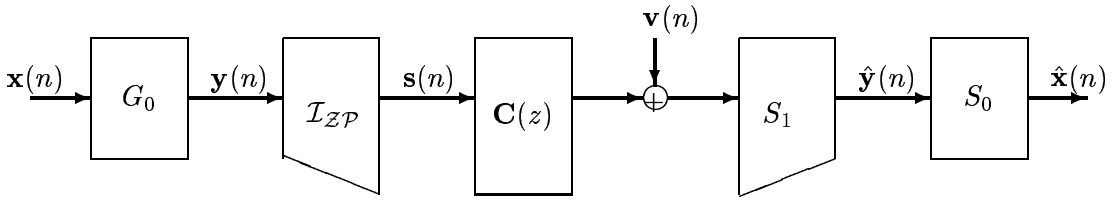

Figure 2: Block model of DMT system.

effect at the output of the equalizer, denote $\mathbf{v}(n) = [v(Nn), v(Nn+1), \cdots, v(Nn+N-1)]^T$, as the N-fold blocked version of $v(n)$. We thus can redraw fig. 1 in the equivalent form shown in fig. 2. It is easy to see that $\mathbf{C}(z)\mathcal{I}_{\mathcal{ZP}} = \mathbf{C_L}$, an $N \times M$ constant matrix. The output symbol vector $\hat{\mathbf{x}}(n)$ is then given by

$$\hat{\mathbf{x}}(n) = S_0 S_1 \mathbf{C_L} G_0 \mathbf{x}(n) + S_0 S_1 \mathbf{v}(n). \tag{2.3}$$

We impose the perfect reconstruction (PR) condition, i.e., in the absence of noise/interference, $\hat{\mathbf{x}}(n) = \mathbf{x}(n)$ for all n. In other words,

$$S_0 S_1 \mathbf{C_L} G_0 = I, \tag{2.4}$$

and the DMT system has no ISI. To obtain a more useful characterization of PR, consider the singular value decomposition of $\mathbf{C_L}$

$$\mathbf{C_L} = U_c \begin{bmatrix} \Lambda_c \\ 0 \end{bmatrix} V_c^H = U_0 \Lambda_c V_c^H \tag{2.5}$$

where U_c and V_c are respectively $N \times N$ and $M \times M$ unitary matrices, Λ_c is a $M \times M$ real, positive definite diagonal matrix, and U_c is partitioned as $U_c = [U_0 \quad U_1]$, where U_0 is $N \times M$ and U_1 is $N \times \kappa$. Then, because of (2.4), given G_0, the class of all $S_0 S_1$ enforcing PR is completely characterized by

$$S_0 = G_0^{-1}. \tag{2.6}$$

and

$$S_1 = V_c \Lambda_c^{-1} \begin{bmatrix} I_M & A \end{bmatrix} U_c^H, \tag{2.7}$$

where A is any arbitrary $M \times \kappa$ matrix. Note that as V_c, U_c and Λ_c are supplied by the channel, the only quantities that need to be found to determine the transceiver completely are G_0 and A.

3 Problem formulation

As mentioned earlier the M subchannels are distributed among the r users with the k-th user allocated n_k subchannels. Assume that the n_k indices of the subchannels assigned to the k-th user are contained in the set $\mathcal{I}_k$. Thus consider disjoint subsets $\mathcal{I}_k \subset \{0, \ldots, M-1\}$ with $|\mathcal{I}_k| = n_k > 1$, and $\mathcal{I}_k \cap \mathcal{I}_j = \emptyset, k \neq j$. Subchannel assignment to the k-th user then constitutes determining $\mathcal{I}_k$. We assume that the j-th subchannel of the k-th user is assigned $b_{j,k}$ bits per symbol. To meet the bit rate specification for the k-th user one requires that, for each $1 \leq k \leq r$,

$$\sum_{j \in \mathcal{I}_k} b_{j,k} = t_k. \tag{3.8}$$

We assume that each service flow employs a different modulation scheme and has to meet a certain SER. Most b-bit symbol constellation schemes require an output signal-to-noise ratio (SNR) of $d2^{\zeta b}$, b large, in order to achieve a given SER, say η. Here $d > 0$ is determined by SER η and the employed modulation scheme and constant $\zeta > 0$ depends on the particular modulation scheme used. For example, for a b-bit square QAM, the SER is given by

$$\eta = 4\left(1 - \frac{1}{\sqrt{2^b}}\right) Q\left(\sqrt{\frac{3\text{SNR}}{(2^b-1)}}\right) \approx 4Q\left(\sqrt{\frac{3\text{SNR}}{2^b}}\right), \quad \text{when } 2^b \gg 1, \tag{3.9}$$

where

$$Q(a) = \int_a^\infty \frac{1}{\sqrt{2\pi}} e^{-x^2/2} dx.$$

Thus for large b, SNR$= d2^{\zeta b}$ with $\zeta = 1$, $d = \frac{1}{3}[Q^{-1}(\frac{\eta}{4})]^2 > 0$. In the case of PAM, $\zeta = 2$, $d = \frac{1}{3}[Q^{-1}(\frac{\eta}{2})]^2 > 0$.

Let the input power in the j-th subchannel of the k-th user be $\sigma^2_{x_{j,k}}$, and $\sigma^2_{e_{j,k}}$ be the output noise variance in this subchannel. Since under perfect reconstruction, the

input power equals the output power in that subchannel, the relation between the input signal power and the output noise power are related by

$$\sigma_{x_{j,k}}^2 = d_k 2^{\zeta_k b_{j,k}} \sigma_{e_{j,k}}^2, \tag{3.10}$$

where the constant d_k is determined by the modulation scheme used and the desired SER, η_k, for the k-th user, and ζ_k depends on the modulation scheme employed by the k-th user. Here we have assumed that each of the subchannels of a particular user has the same error rate. The error rates can however vary across different users.

The total transmitted power of the DMT system can be written as

$$P_B = \sum_{i=0}^{N-1} \sigma_{s_i}^2$$

where $\sigma_{s_i}^2$ is the variance of the stream $s_i(n)$ in fig. 1. Rewritting in terms of G_0 and $\sigma_{x_{j,k}}^2$, we have

$$P_B = \sum_{k=1}^{r} \sum_{j \in \mathcal{I}_k} \sigma_{x_{j,k}}^2 [G_0^H G_0]_{jj} \tag{3.11}$$

Denote R_v to be the *known* autocorrelation matrix of the noise vector $\mathbf{v}(n)$, and $\mathbf{e}(n)$, $\mathbf{w}(n)$ be the noise vectors at the output of S_0, S_1 respectively in fig. 2, with respective autocorrelation matrices R_e, R_w. We then have the relations

$$R_e = S_0 R_w S_0^H \quad \text{and} \quad R_w = S_1 R_v S_1^H. \tag{3.12}$$

Note that $\sigma_{e_{j,k}}^2$ are the diagonal elements of R_e. Thus, because of (2.6), (3.10) and (3.12), expression (3.11) can be rewritten as

$$P_B = \sum_{k=1}^{r} \sum_{j \in \mathcal{I}_k} d_k 2^{\zeta_k b_{j,k}} [S_0^{-H} S_0^{-1}]_{jj} [S_0 R_w S_0^H]_{jj}. \tag{3.13}$$

Thus the precise optimization problem can be stated as follows.

Problem 3.1 *Given positive n_k, η_k, t_k, $M \times M$ positive definite Hermitian R_v, minimize (3.13) by selecting $b_{j,k}$ (bit loading) subject to (3.8), selecting $\mathcal{I}_k$ (subchannel assignment), $M \times M$ nonsingular S_0 (transformation selection) and $M \times \kappa$ matrix A (redundancy removal selection, under (2.7)).*

We shall adopt a multi-step strategy to solve the above optimization problem. First, for a given choice of S_0, A and $\mathcal{I}_k$, we shall minimize P_B by determining the optimum $b_{j,k}$ under the rate constraint (3.8). This, as will be shown in Section 4.1, will result in a lower bound for P_B, denoted P_{BOPT}, under optimal selection of $b_{j,k}$. The expression for P_{BOPT} will itself be shown to be independent of $b_{j,k}$ and the strategy will then be minimize P_{BOPT} through selection of the remaining optimization variables. In the next step, assuming fixed A, which in turn fixes R_w, we shall minimize P_{BOPT} by the selection of S_0 and $\mathcal{I}_k$. It will be shown in Section 4.2 that regardless of the choice of A, P_{BOPT} reduces to an expression that is determined by the eigenvalues of R_w. These eigenvalues are determined exclusively by A and are independent of the choice of S_0. The final step in our optimization solution process will hence be to find an A that renders these eigenvalues to be most favorable.

4 Optimum selections

In this section we consider the optimum selection of the various variables. First consider the problem of bit loading.

4.1 Optimum Bit Loading

As discussed in the earlier Section, we separate the optimization problem into different parts. First we ask: For a given choice of transceiver, i.e. given S_0, S_1, and a certain choice of $\mathcal{I}_k$, what is the optimum allocation of $b_{j,k}$ so that (3.13) is minimized under the constraint (3.8). This is a constrained optimization problem and can be solved using the Lagrangian multiplier method. In fact, using the Arithmetic Mean-Geometric Mean (AM-GM) inequality which states that the Arithmetic Mean of a set of positive numbers is greater or equal to its Geometric Mean, with equality if and only if all numbers are equal, we have that *for a given choice of* $\mathcal{I}_k$ *and* S_0, S_1, *under (3.8),*

$$P_B \geq P_{BOPT} = \sum_{k=1}^{r} d_k \left[n_k 2^{\zeta_k t_k} \prod_{j \in \mathcal{I}_k} [S_0^{-H} S_0^{-1}]_{jj} [S_0 R_w S_0^H]_{jj} \right]^{1/n_k} \tag{4.14}$$

with equality iff for all k and i, j

$$2^{\zeta_k b_{j,k}}[S_0^{-H}S_0^{-1}]_{jj}[S_0 R_w S_0^H]_{jj} = 2^{\zeta_k b_{i,k}}[S_0^{-H}S_0^{-1}]_{ii}[S_0 R_w S_0^H]_{ii}. \tag{4.15}$$

This is in turn equivalent to the *optimum bit loading rule*:

$$b_{j,k} = \frac{t_k}{n_k} - \frac{1}{\zeta_k}\log_2\left[\frac{[S_0^{-H}S_0^{-1}]_{jj}[S_0 R_w S_0^H]_{jj}}{(\prod_{j\in\mathcal{I}_k}[S_0^{-H}S_0^{-1}]_{jj}[S_0 R_w S_0^H]_{jj})^{1/n_k}}\right]. \tag{4.16}$$

The remaining variables $S_0, A, \mathcal{I}_k$ must now be selected to minimize P_{BOPT}. *Note, that while the choice of these other variables impacts the selection of $b_{j,k}$, P_{BOPT} itself is independent of $b_{j,k}$. This underscores the fact that the remaining variables can be selected regardless of the precise values of $b_{j,k}$ obtained through (4.16).*

Note that P_{BOPT} is much more complicated than its specializations, $r = 1$, studied in [7] and, $n_k = L$ for all k along with $S_0^H S_0 = I$, studied in [11].

4.2 Selection of S_0, $\mathcal{I}_k$ and A

In this Section, we address the problem of designing the optimum transceiver and optimal subchannel assignment. Specifically, we have to find the optimum $S_0, \mathcal{I}_k$ and A minimizing P_{BOPT} in (4.14).

Assume for the moment that A and hence S_1 has been selected. Note that this then fixes the autocorrelation matrix R_w in (3.12). For convenience we first consider the minimization of P_B in (3.13). Our goal will now be to determine the search space for S_0, i.e. determine the class of S_0 minimizing $P_B(S_0)$, for a given matrix A. Consider then the following optimization problem.

Problem 4.1 *With $M \times M$ positive definite Hermitian R and $M \times M$ nonsingular S, $\alpha_i > 0$, determine S to minimize*

$$J(S) = \sum_{i=1}^{M} \alpha_i (e_i^T S R S^H e_i)(e_i^T S^{-H} S^{-1} e_i) \tag{4.17}$$

where e_i is the $M \times 1$ column vector with all elements zero except for the i-th element which is unity.

Observe that (3.13) has this form. Let the positive definite Hermitian R have the SVD:

$$R = U\Lambda^2 U^H \tag{4.18}$$

with Λ real, diagonal and U unitary. It is noteworthy that in all the papers [1], [7], [8], the choice $S = \tilde{P}U^H$, with $\tilde{P}$ a permutation matrix minimizes P_{BOPT}. If S is restricted to be unitary, then [1] shows that this choice of S also minimizes (4.17). Consider, however, the example where $\alpha_i = 1$, $M = 2$ and $R_w = \text{ diag } \{9, 1\}$. Then observe that $J(I) = 10$ but with

$$B = \frac{1}{\sqrt{2}} \begin{bmatrix} 1 & 1 \\ 1 & -1 \end{bmatrix} \begin{bmatrix} 1/\sqrt{3} & 0 \\ 0 & 1 \end{bmatrix}$$

$J(B) = 8 < J(I)$. Thus in general $S = U^H$ does not minimize (4.17). However, we will show in the following results that it *does minimize* P_{BOPT}.

The following Lemma shows that J is invariant under any diagonal scaling of S.

Lemma 4.1 *With $J(S)$ as above,*

$$J(S) = J(\Omega S)$$

for any diagonal nonsingular Ω.

Proof: Proved by direct verification. ∎

This in particular means that one can restrict attention to S such that the diagonal elements of $S^{-H}S^{-1}$ are $1/\alpha_i$. Lemma 4.2 shows an important property of this equivalent constrained optimization problem.

Lemma 4.2 *With $M \times M$ positive definite Hermitian matrix R, $M \times M$ nonsingular S, consider the minimization of*

$$\sum_{i=1}^{M} e_i^T S R S^H e_i \tag{4.19}$$

such that for all $i \in \{1, \ldots, M\}$ and some $\alpha_i > 0$,

$$e_i^T S^{-H} S^{-1} e_i = 1/\alpha_i. \tag{4.20}$$

Then the minimizing S obeys for some real diagonal Γ,

$$(SRS^H)(SS^H) = \Gamma. \tag{4.21}$$

Proof: Denote $[S]_{kl} = s_{kl}$, and let $s_{kl}^{(R)}$ and $s_{kl}^{(I)}$ be the real and imaginary parts of s_{kl} respectively. Note that

$$\begin{aligned}
\frac{\partial S}{\partial s_{kl}^{(R)}} &= e_k e_l^T, & \frac{\partial S}{\partial s_{kl}^{(I)}} &= j e_k e_l^T, \\
\frac{\partial S^H}{\partial s_{kl}^{(R)}} &= e_l e_k^T, & \frac{\partial S^H}{\partial s_{kl}^{(I)}} &= -j e_l e_k^T, \\
\frac{\partial S^{-1}}{\partial s_{kl}^{(R)}} &= -S^{-1} e_k e_l^T S^{-1}, & \frac{\partial S^{-1}}{\partial s_{kl}^{(I)}} &= -j S^{-1} e_k e_l^T S^{-1}, \\
\frac{\partial S^{-H}}{\partial s_{kl}^{(R)}} &= -S^{-H} e_l e_k^T S^{-H}, & \frac{\partial S^{-H}}{\partial s_{kl}^{(I)}} &= j S^{-H} e_l e_k^T S^{-H}.
\end{aligned}$$

Using real Lagrange multipliers γ_i, one obtains the cost function

$$\Phi = \sum_{i=1}^{M} e_i^T S R S^H e_i + \sum_{i=1}^{M} \gamma_i \left(e_i^T S^{-H} S^{-1} e_i - 1/\alpha_i \right).$$

The minimizing S must obey, for all k, l

$$\frac{\partial \Phi}{\partial s_{kl}^{(R)}} = \frac{\partial \Phi}{\partial s_{kl}^{(I)}} = 0. \tag{4.22}$$

Now

$$\begin{aligned}
\frac{\partial \Phi}{\partial s_{kl}^{(R)}} &= \sum_{i=1}^{M} \left[e_i^T e_k e_l^T R S^H e_i + e_i^T S R e_l e_k^T e_i \right] \\
&\quad - \sum_{i=1}^{M} \gamma_i \left[e_i^T S^{-H} e_l e_k^T S^{-H} S^{-1} e_i + e_i^T S^{-H} S^{-1} e_k e_l^T S^{-1} e_i \right] \\
&= e_l^T R S^H e_k + e_k^T S R e_l \\
&\quad - e_k^T S^{-H} S^{-1} (\sum_{i=1}^{M} \gamma_i e_i e_i^T) S^{-H} e_l - e_l^T S^{-1} (\sum_{i=1}^{M} \gamma_i e_i e_i^T) S^{-H} S^{-1} e_k.
\end{aligned}$$

Then with $\Gamma = \mathrm{diag}\{\gamma_1, \ldots, \gamma_M\}$,

$$\frac{\partial \Phi}{\partial s_{kl}^{(R)}} = e_l^T \left[R S^H - S^{-1} \Gamma S^{-H} S^{-1} \right] e_k + e_k^T \left[S R - S^{-H} S^{-1} \Gamma S^{-H} \right] e_l. \tag{4.23}$$

Similarly

$$-j \frac{\partial J}{\partial s_{kl}^{(I)}} = e_l^T \left[R S^H - S^{-1} \Gamma S^{-H} S^{-1} \right] e_k - e_k^T \left[S R - S^{-H} S^{-1} \Gamma S^{-H} \right] e_l. \tag{4.24}$$

From (4.22), (4.23), (4.24), one has for all k, l,

$$e_l^T \left[RS^H - S^{-1}\Gamma S^{-H} S^{-1} \right] e_k = 0. \tag{4.25}$$

Thus

$$\begin{aligned} RS^H &= S^{-1}\Gamma S^{-H} S^{-1} && (4.26) \\ \Leftrightarrow SRS^H SS^H &= \Gamma. && (4.27) \end{aligned}$$

Hence the result. ∎

Matrix S minimizing (4.19) under (4.20) thus has to satisfy (4.21). Condition (4.21) can be rewritten using the following Lemma.

Lemma 4.3 *Under the hypothesis of Lemma 4.2, with* $\Gamma = diag\{\gamma_1, \ldots, \gamma_M\}$,

$$\gamma_i > 0, \quad i = 1, \ldots, M. \tag{4.28}$$

and

$$SRS^H = \Gamma^{1/2} S^{-H} S^{-1} \Gamma^{1/2}. \tag{4.29}$$

Proof: Denote

$$\tilde{A} = SRS^H \quad \text{and} \quad \tilde{B} = (SS^H)^{-1},$$

and observe that $\tilde{A}$ and $\tilde{B}$ are Hermitian positive definite. Then under (4.21),

$$\tilde{A} = \Gamma \tilde{B}.$$

Further since $\tilde{A}$ and $\tilde{B}$ are both positive definite, for all i, $e_i^T \tilde{B} e_i > 0$, and

$$0 < e_i^T \Gamma \tilde{B} e_i = \gamma_i e_i^T \tilde{B} e_i,$$

implying $\gamma_i > 0$. Hence $\Gamma^{1/2}$ is a diagonal real positive definite matrix. Also as $\tilde{A} = \tilde{A}^H, \tilde{B} = \tilde{B}^H$, and Γ is diagonal,

$$\Gamma \tilde{B} = \tilde{B} \Gamma. \tag{4.30}$$

Further because of (4.30), for each i, j,

$$\gamma_i b_{ij} = b_{ij} \gamma_j$$

holding if and only if either

$$\gamma_i = \gamma_j \tag{4.31}$$

or

$$b_{ij} = 0. \tag{4.32}$$

Now if (4.31) holds then

$$[\Gamma \tilde{B}]_{ij} = \gamma_i b_{ij} = \gamma_i^{1/2} b_{ij} \gamma_j^{1/2}$$

The above clearly holds even under (4.32). Thus

$$\Gamma \tilde{B} = \Gamma^{1/2} \tilde{B} \Gamma^{1/2}$$

and (4.29) holds.

■

We now have the following Lemma, which shows that at least one S minimizing (4.17) has in fact a simpler expression.

Lemma 4.4 *At least one minimizing S for (4.17) obeys*

$$SRS^H = S^{-H} S^{-1}. \tag{4.33}$$

Proof: Because of Lemma 4.1, if $\hat{S}$ minimizes (4.17) then so does $S = \Gamma^{-1/4} \hat{S}$, with Γ as in Lemma 4.3.

From Lemmas 4.2 and 4.3, there exists a positive definite diagonal Γ such that $\hat{S}$ obeys

$$\hat{S} R \hat{S}^H = \Gamma^{1/2} \hat{S}^{-H} \hat{S}^{-1} \Gamma^{1/2}.$$

Then $S = \Gamma^{-1/4} \hat{S}$ also minimizes (4.17), as

$$\begin{aligned} SRS^H &= \Gamma^{-1/4} \hat{S} R \hat{S}^H \Gamma^{-1/4} \\ &= \Gamma^{1/4} \hat{S}^{-H} \hat{S}^{-1} \Gamma^{1/4} \\ &= S^{-H} S^{-1}. \end{aligned}$$

■

We now show that the search space of S_0 minimizing (4.17) can be restricted to a particular form. Consider then the following result.

Lemma 4.5 *Let the SVD of positive definite Hermitian R be*

$$R = U\Lambda^2 U^H \tag{4.34}$$

with Λ real, diagonal and U unitary. Then for some unitary V, (4.17) is minimized by

$$S = V\Lambda^{-1/2}U^H \tag{4.35}$$

and (4.17) becomes

$$J(S) = \sum_{i=1}^{M} \alpha_i \left[V\Lambda V^H\right]_{ii}^2 \tag{4.36}$$

Proof: From Lemma 4.4, S obeys (4.33). Let S have the SVD

$$S = \hat{V}\tilde{\Gamma}\tilde{V}^H \tag{4.37}$$

with $\tilde{\Gamma}$ positive definite real diagonal, $\hat{V}, \tilde{V}$ unitary. Then (4.33) holds if and only if

$$\begin{aligned} \hat{V}\tilde{\Gamma}\tilde{V}^H U\Lambda^2 U^H \tilde{V}\tilde{\Gamma}\hat{V}^H &= \hat{V}\tilde{\Gamma}^{-2}\hat{V}^H \\ \Leftrightarrow (\tilde{V}^H U)\Lambda^2(U^H\tilde{V}) &= \tilde{\Gamma}^{-4} \end{aligned} \tag{4.38}$$

Since $\tilde{U} = \tilde{V}^H U$ is unitary, for some permutation matrix P,

$$\begin{aligned} \tilde{\Gamma}^{-4} &= P\Lambda^2 P^T \\ \Leftrightarrow \tilde{\Gamma} &= P\Lambda^{-1/2}P^T \end{aligned} \tag{4.39}$$

Thus

$$SRS^H = \hat{V}\tilde{\Gamma}^{-2}\hat{V}^H = \hat{V}P\Lambda P^T\hat{V}^H = S^{-H}S^{-1}.$$

Thus with $V = \hat{V}P$, (4.36) holds. Further it is easily checked that S in (4.35) achieves (4.36). ∎

We now return to the minimization of (3.13) with $R = R_w$ having the form (4.34). Because of Lemma 4.5, with $S_0 = V\Lambda^{-1/2}U^H$, for any choice of $\mathcal{I}_k$ and $b_{j,k}$, and subject to V being unitary

$$P_B \geq \min_{VV^H=I} \sum_{k=1}^{r} d_k \sum_{j\in\mathcal{I}_k} 2^{\zeta_k b_{j,k}} \left(\left[V\Lambda V^H\right]_{jj}\right)^2 \tag{4.40}$$

$$\geq \min_{VV^H=I} \sum_{k=1}^{r} d_k n_k 2^{\zeta_k t_k/n_k} \prod_{j\in\mathcal{I}_k} (\left[V\Lambda V^H\right]_{jj})^{2/n_k} \tag{4.41}$$

$$= \min_{VV^H=I} \sum_{k=1}^{r} \beta_k \prod_{j\in\mathcal{I}_k} a_j^{2/n_k} \tag{4.42}$$

with

$$\beta_k = d_k n_k 2^{\zeta_k t_k/n_k},$$

and

$$a_j = \left[V\Lambda V^H\right]_{jj}. \tag{4.43}$$

For given β_k and a_k consider the quantity in (4.42). For such a given choice, one must determine the arrangement of a_k that minimizes this quantity. Such an arrangement is called an *optimum arrangement*. The following Lemma characterizes an important property of such arrangements.

Lemma 4.6 *Consider for integers $p, q \geq 2$,*

$$f = (\alpha \prod_{k=0}^{p-1} a_k)^{2/p} + (\beta \prod_{l=0}^{q-1} b_l)^{2/q}$$

with $\alpha, \beta, a_k, b_l > 0$. Suppose for some i, j

$$a_i > b_j \text{ and } \frac{\partial f}{\partial a_i} > \frac{\partial f}{\partial b_j}. \tag{4.44}$$

Then

$$g = (\alpha \prod_{k=0,k\neq i}^{p-1} a_k.b_j)^{2/p} + (\beta \prod_{k=0,k\neq j}^{q-1} b_k.a_i)^{2/q} < f. \tag{4.45}$$

Further if the a_i, b_i obey the ordering $a_i \geq a_{i+1}, b_i \geq b_{i+1}$, then $\partial f/\partial a_i \leq \partial f/\partial a_{i+1}$ and $\partial f/\partial b_i \leq \partial f/\partial b_{i+1}$.

Proof: The derivative condition in (4.44) holds iff

$$\frac{2}{p}\frac{(\alpha \prod_{k=0,k\neq i}^{p-1} a_k)^{2/p}}{a_i^{1-2/p}} > \frac{2}{q}\frac{(\beta \prod_{k=0,k\neq j}^{q-1} b_k)^{2/q}}{b_j^{1-2/q}}$$

which is equivalent to

$$(\alpha \prod_{k=0,k\neq i}^{p-1} a_k)^{2/p} > \frac{p}{q}\frac{a_i^{1-2/p}}{b_j^{1-2/q}}(\beta \prod_{k=0,k\neq j}^{q-1} b_k)^{2/q}.$$

Consider

$$\begin{aligned} f-g &= (\alpha \prod_{k=0,k\neq i}^{p-1} a_k)^{2/p}\left[a_i^{2/p}-b_j^{2/p}\right]+(\beta \prod_{k=0,k\neq j}^{q-1} b_k)^{2/q}\left[b_j^{2/q}-a_i^{2/q}\right] \\ &> \frac{p}{q}\frac{a_i^{1-2/p}}{b_j^{1-2/q}}(\beta \prod_{k=0,k\neq j}^{q-1} b_k)^{2/q}\left[a_i^{2/p}-b_j^{2/p}\right]+(\beta \prod_{k=0,k\neq j}^{q-1} b_k)^{2/q}\left[b_j^{2/q}-a_i^{2/q}\right] \\ &= (\beta \prod_{k=0}^{q-1} b_k)^{2/q}\left[\frac{p}{q}.(\frac{a_i}{b_j})-\frac{p}{q}.(\frac{a_i}{b_j})^{1-2/p}+1-(\frac{a_i}{b_j})^{2/q}\right]. \end{aligned}$$

Denote

$$h(\lambda)=\frac{p}{q}.\lambda-\frac{p}{q}.\lambda^{1-2/p}+1-\lambda^{2/q}.$$

Since $a_i > b_j$, to prove (4.45), it suffices to show that

$$h(\lambda)=\frac{p}{q}\lambda-\frac{p}{q}\lambda^{1-2/p}+1-\lambda^{2/q}>0, \qquad \forall \lambda>1.$$

Indeed note that

$$h(1)=0,$$

and as $p, q \geq 2$,

$$\begin{aligned} h'(\lambda) &= \frac{p}{q}-\frac{p}{q}(1-\frac{2}{p}).\lambda^{-2/p}-\frac{2}{q}.\lambda^{2/q-1} \\ &> \frac{p}{q}-\frac{p}{q}(1-\frac{2}{p})-\frac{2}{q} \quad \forall \quad \lambda>1 \\ &= 0. \end{aligned}$$

Further

$$\partial f/\partial a_i=\frac{2}{p}\frac{(\alpha \prod_{k=0}^{p-1} a_k)^{2/p}}{a_i}$$

and since $a_i \geq a_{i+1}$, it follows that $\partial f/\partial a_i \leq \partial f/\partial a_{i+1}$. Similarly one can show that under $b_i \geq b_{i+1}$, one has $\partial f/\partial b_i \leq \partial f/\partial b_{i+1}$.

Hence the result. ∎

We thus have

$$P_B \geq \min_{VV^H=I} \sum_{k=1}^{r} \beta_k \prod_{j\in\mathcal{I}_k^\star} a_k^2 = P_B^\star \tag{4.46}$$

with $\mathcal{I}_k^\star$ defining the optimal arrangement of the sequence of a_k. From Lemma 4.6 such an optimum arrangement requires that for all $a_k > a_l$,

$$\frac{\partial P_B^\star}{\partial a_k} < \frac{\partial P_B^\star}{\partial a_l}.$$

Then using Theorem 6.1 and under the above condition, $P_B^\star$ is Schur concave. Thus from Fact 4, as $\{\left[V\Lambda V^H\right]_{ii}\}_{i=1}^M \prec \{\lambda_1,\ldots,\lambda_M\}$, the choice $V=I$ minimizes (4.46), i.e. the minimum P_B is attained through the choice of an orthonormal transformation. Thus even under the relaxed conditions on S_0, the best power is achieved with orthonormal S_0.

Thus, regardless of A the best S_0 is a Karhunen-Loeve Transform of R_w, and the $\sigma^2_{e_{j,k}}$ equal the eigenvalues of R_w. Then from the definition of supermajorization in Definition 6.1 and Fact 5, it follows that the optimizing A must be such that the set of resulting eigenvalues of R_w weakly supermajorize all possible sets of attainable eigenvalues. As V_c is unitary in (3.12), the eigenvalues of R_w are the same as those of

$$\begin{aligned}
\Omega(A) &= \Lambda_c^{-1}\left[\begin{array}{cc} I_M & A\end{array}\right]\left[\begin{array}{c} U_0^H \\ U_1^H\end{array}\right] R_v \left[\begin{array}{cc} U_0 & U_1\end{array}\right]\left[\begin{array}{c} I_M \\ A^H\end{array}\right]\Lambda_c^{-1} \\
&= \Lambda_c^{-1}\left[\begin{array}{cc} I_M & A\end{array}\right]\left[\begin{array}{cc} U_0^H R_v U_0 & U_0^H R_v U_1 \\ U_1^H R_v U_0 & U_1^H R_v U_1\end{array}\right]\left[\begin{array}{c} I_M \\ A^H\end{array}\right]\Lambda_c^{-1} \\
&= \Lambda_c^{-1}\left[U_0^H R_v U_0 + U_0^H R_v U_1 A^H + A U_1^H R_v U_0 + A U_1^H R_v U_1 A^H\right]\Lambda_c^{-1} \qquad (4.47)
\end{aligned}$$

Now observe that as R_v is positive definite, and $U=[U_0\,U_1]$ is unitary,

$$\left[\begin{array}{c} U_0^H \\ U_1^H\end{array}\right] R_v \left[\begin{array}{cc} U_0 & U_1\end{array}\right] = \left[\begin{array}{cc} U_0^H R_v U_0 & U_0^H R_v U_1 \\ U_1^H R_v U_0 & U_1^H R_v U_1\end{array}\right] \qquad (4.48)$$

is positive definite. Thus, each of the matrices $U_1^H R_v U_1$, $U_0^H R_v U_0$ and $U_0^H R_v U_0 - U_0^H R_v U_1\left(U_1^H R_v U_1\right)^{-1} U_1^H R_v U_0$, must be positive definite and nonsingular. Direct verification shows that because of (4.47),

$$\begin{aligned}
\Omega(A) &= \Lambda_c^{-1}\Big\{U_0^H R_v U_0 - U_0^H R_v U_1\left(U_1^H R_v U_1\right)^{-1} U_1^H R_v U_0 \\
&+ \left[U_0^H R_v U_1\left(U_1^H R_v U_1\right)^{-1} + A\right] U_1^H R_v U_1\left[A^H + \left(U_1^H R_v U_1\right)^{-1} U_1^H R_v U_0\right]\Big\}\Lambda_c^{-1}.
\end{aligned}$$

Define

$$Q_1 = \Lambda_c^{-1}\left[U_0^H R_v U_0 - U_0^H R_v U_1\left(U_1^H R_v U_1\right)^{-1} U_1^H R_v U_0\right]\Lambda_c^{-1} \qquad (4.49)$$

and

$$Q_2 = \Lambda_c^{-1}\left[U_0^H R_v U_1\left(U_1^H R_v U_1\right)^{-1} + A\right] U_1^H R_v U_1\left[A^H + \left(U_1^H R_v U_1\right)^{-1} U_1^H R_v U_0\right]\Lambda_c^{-1}. \qquad (4.50)$$

Clearly Q_1 is positive definite and Q_2 is positive semidefinite. Only Q_2 depends on A. Defining $\lambda_i(\Omega(A))$ as the eigenvalues of $\Omega(A)$, from Lemma 6.1, and Fact 1,

$$\begin{aligned} \{\lambda_i(\Omega(A))\}_{i=1}^M &\prec \{\lambda_i(Q_1)+\lambda_i(Q_2)\}_{i=1}^M \\ \Rightarrow \{\lambda_i(\Omega(A))\}_{i=1}^M &\prec^W \{\lambda_i(Q_1)+\lambda_i(Q_2)\}_{i=1}^M. \end{aligned}$$

Since $\lambda_i(Q_2) \geq 0$, from Fact 3

$$\{\lambda_i(Q_1)+\lambda_i(Q_2)\}_{i=1}^M \prec^W \{\lambda_i(Q_1)\}_{i=1}^M. \tag{4.51}$$

Thus, from Fact 2

$$\{\lambda_i(\Omega(A))\}_{i=1}^M \prec^W \{\lambda_i(Q_1)\}_{i=1}^M. \tag{4.52}$$

Thus the optimizing A is one which forces $Q_2 = 0$, i.e.

$$A = -U_0^H R_v U_1 \left(U_1^H R_v U_1\right)^{-1}. \tag{4.53}$$

This is independent of S_0 and the optimum bit rate allocations $b_{i,j}$. Instead it is determined exclusively by R_v, provided by the second order statistics of $v(k)$, and U_i provided by the SVD of the blocked channel-equalizer combination matrix $\mathbf{C}(z)$. The resulting value of R_w is

$$R_w = V_c \Lambda_c^{-1} \left[U_0^H R_v U_0 - U_0^H R_v U_1 \left(U_1^H R_v U_1\right)^{-1} U_1^H R_v U_0\right] \Lambda_c^{-1} V_c^H. \tag{4.54}$$

To summarize, the optimizing A is obtained directly using (4.53) with the channel characteristics supplying U_i and the second order statistics of $v(k)$ supplying R_v. This gives R_w from (4.54). S_0 is then provided by the eigenvectors of R_w permuted so that with $\sigma_{e_{j,k}}^2$ the eigenvalues of R_w, an optimum arrangement characterized by Lemma 4.6 is attained. This gives the requisite $\sigma_{e_{j,k}}^2$ and (4.16) gives the optimum bit allocations $b_{j,k}$.

It is interesting to note that the solution of A is identical to that given in [7] for the single user case. Modulo the permutation required to enforce the optimum rearrangement requirement, the optimizing S_0 is also the same as for the single user case. Thus, even though the optimum bit rate allocations differ in the single and multiuser settings, the transceiver itself is identical.

To summarize, we showed that there is a conceptual separation between the three selections, i.e. the optimizing A is determined exclusively by R_v, provided by the knowledge of the interference and channel-equalizer characteristics; S_0 is determined entirely by A and the channel-equalizer characteristics; $\mathcal{I}_k$ are determined entirely by R_e, in turn provided by S_1 and S_0, and the bit allocations are determined once the above quantities are found. Further as noted in the Introduction, we showed that without loss of generality, the optimizing S_0, G_0 are unitary.

5 Simulation results

In this section, we compare the transmitting power of the DFT based DMT under no optimum bit allocation and optimum bit allocation with an optimum unitary transceiver. We assume the equalized-channel to be $C(z) = 1 + 0.5z^{-1}$, and a noise source $v(n)$ whose power spectral density is shown in fig. 3. We assume the DMT system supports two user services. Both services employ QAM modulation schemes, and the target rates for the two users are 600 Kbps and 1 Mbps respectively. The (i, j) on the x-axis of the plot indicates that user 1 and 2 were respectively allocated i, j number of channels. The plot shows that there is a 10 dB saving in transmit power with our design over the DFT based DMT under optimum bit allocation, and a 14 dB improvement over the conventional DMT with no optimum bit allocation.

6 Conclusions

In this paper, an optimum bit allocation strategy and design of a general biorthogonal DMT multicarrier transceiver system employing zero padding redundancy were presented, for minimizing the transmit power when different users with varied QoS requirements are supported and are assigned potentially different number of subchannels. We showed that no gains in transmit power can be obtained by considering biorthogonal transceivers over orthogonal transceivers. Our results also showed that should the channel/interference remain invariant after the initial connection is estab-

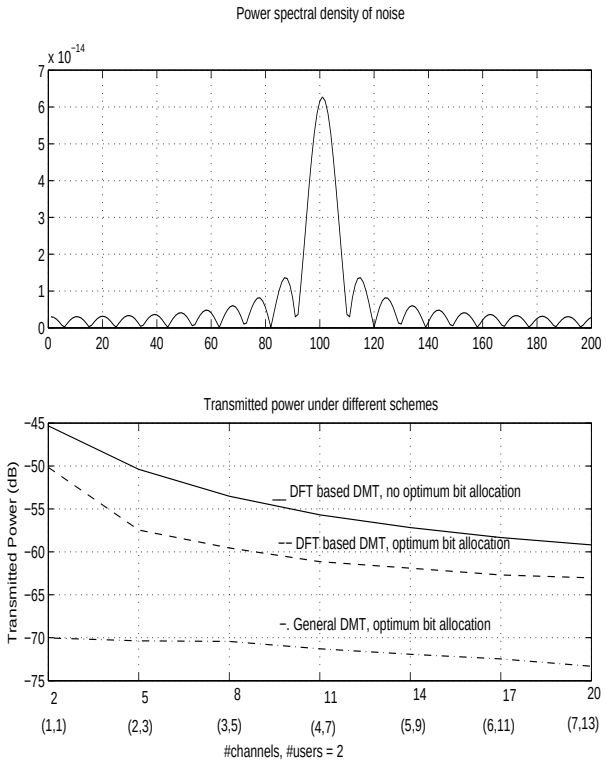

Figure 3: Comparison of transmit power levels.

lished, then only bit loading and subchannel selection need be updated in response to changing traffic needs. The optimum transceiver itself depends *only on the channel and interference conditions and not on the QoS requirements.* Indeed to within a permutation of subchannels, the optimum transceiver obtained here is identical to that obtained in [7], [11].

Appendix

Relevant results from the theory of majorization are stated. First consider the definition of majorization.

Definition 6.1 [Definition of majorization] *Consider the following two sequences* $\mathbf{x} = \{x_1, \ldots, x_n\}$ *and* $\mathbf{y} = \{y_1, \ldots, y_n\}$ *with the ordering* $x_i \geq x_{i+1}$ *and* $y_i \geq y_{i+1}$. *Then we say that* $\mathbf{y}$ *majorizes* $\mathbf{x}$*, denoted as* $\mathbf{x} \prec \mathbf{y}$*, if the following holds with equality*

at $k = n$

$$\sum_{i=1}^{k} x_i \leq \sum_{i=1}^{k} y_i, \quad 1 \leq k \leq n. \tag{6.55}$$

We say that $\mathbf{y}$ *weakly supermajorizes* $\mathbf{x}$*, denoted* $\mathbf{x} \prec^W \mathbf{y}$*, if*

$$\sum_{i=j}^{n} x_i \geq \sum_{i=j}^{n} y_i, \quad 1 \leq j \leq n. \tag{6.56}$$

We also have the following facts.

Fact 1 *If* $\mathbf{x} \prec \mathbf{y}$*, then* $\mathbf{x} \prec^W \mathbf{y}$*.*

Fact 2 *If* $\mathbf{x} \prec^W \mathbf{y}$ *and* $\mathbf{y} \prec^W \mathbf{z}$*, then* $\mathbf{x} \prec^W \mathbf{z}$*.*

Fact 3 *Suppose* $\mathbf{a} = \{a_1, \ldots, a_n\}$*,* $a_i \geq 0$*, then* $(\mathbf{x} + \mathbf{a}) \prec^W \mathbf{x}$*.*

One of the examples of majorization in matrix theory is the comparison between the diagonal elements and eigenvalues of a Hermitian matrix. The following is a general result that holds for Hermitian matrices.

Fact 4 *If* H *is an* $n \times n$ *Hermitian matrix with diagonal elements* $\{h_1, \ldots, h_n\} = \mathbf{h}$*, and eigenvalues* $\{\lambda_1, \ldots, \lambda_n\} = \lambda$*, then* $h \prec \lambda$ *on* R^n*.*

The following Lemma gives a comparison of eigenvalues of matrices and sums of matrices.

Lemma 6.1 *Consider two* $M \times M$ *Hermitian matrices* Q_1 *and* Q_2*. Suppose the eigenvalues of* Q_1*,* Q_2 *and* $Q_1 + Q_2$ *are respectively* $\lambda_i(Q_1)$*,* $\lambda_i(Q_2)$*, and* $\lambda_i(Q_1 + Q_2)$*,* $\lambda_i(\cdot) \geq \lambda_{i+1}(\cdot)$*. Then*

$$\{\lambda_i(Q_1 + Q_2)\}_{i=1}^{M} \prec \{\lambda_i(Q_1) + \lambda_i(Q_2)\}_{i=1}^{M}.$$

Functions that preserve the ordering of majorization are said to be Schur convex. Note the trivial fact that a function ϕ is Schur convex if and only if $-\phi$ is Schur concave. The following defines Schur concave functions.

Definition 6.2 [Definition of Schur concavity] *A real valued function* $\phi(\mathbf{z}) = \phi(z_1, \ldots, z_n)$ *defined on a set* $\mathcal{A} \subset R^n$ *is said to be Schur concave on* $\mathcal{A}$ *if*

$$\mathbf{x} \prec \mathbf{y} \quad on\ \mathcal{A} \quad \Rightarrow \quad \phi(\mathbf{x}) \geq \phi(\mathbf{y}).$$

ϕ *is strictly Schur concave on* $\mathcal{A}$ *if strict inequality* $\phi(\mathbf{x}) > \phi(\mathbf{y})$ *holds when* $\mathbf{x}$ *is not a permutation of* $\mathbf{y}$.

A useful condition for verifying if a given function ϕ is Schur concave is now considered. The following theorem results in a test for strict Schur concavity.

Theorem 6.1 *Let* $\phi(\mathbf{z})$ *be a scalar real valued function defined and continuous on* $\mathcal{D} = \{(z_1, \ldots, z_n) : z_1 \geq \ldots \geq z_n\}$, *and differentiable on the interior of* $\mathcal{D}$. *Then* $\phi(\mathbf{z})$ *is Schur concave on* $\mathcal{D}$ *if* $\frac{\partial \phi(\mathbf{z})}{\partial z_k}$ *is increasing in* k.

Fact 5 *Suppose* $\phi(\mathbf{z})$ *satisfies the conditions of Theorem 6.1. Then* $\phi(\mathbf{x}) > \phi(\mathbf{y})$ *whenever* $\mathbf{x} \prec^W \mathbf{y}$.

References

[1] S. Akkarakaran and P.P. Vaidyanathan, "Filterbank optimization with convex objectives and the optimality of principal component forms", *IEEE Transactions on Signal Processing*, pp 100-114, Jan 2001.

[2] J.S. Chow, J.C. Tu, J.M. Cioffi, "A discrete multitone transceiver system for HDSL applications", *IEEE Journal on Selected Areas in Communications*, pp 895-908, Aug 1991.

[3] L.M.C. Hoo, J. Tellado and J.M. Cioffi, "Discrete dual QoS loading algorithms for multicarrier systems ", *IEEE International Conference on Communications*, pp 796-800, 1999.

[4] R.A. Horn, C.R. Johnson, *Matrix Analysis*, Cambridge University Press, 1999.

[5] D. Kivanc and H. Liu, "Subcarrier allocation and power control for OFDMA", *IEEE Journal on Selected Areas in Communications*, To appear.

[6] B. S. Krongold, K. Ramchandran and D. L. Jones, "Computationally Efficient Optimal Power Allocation Algorithms for Multicarrier Communication Systems", *IEEE Transactions on Communications*, pp 23-27, Jan 2000.

[7] Y.-P. Lin and S.-M. Phoong, "Perfect discrete multitone modulation with optimal transceivers", *IEEE Transactions on Signal Processing*, pp 1702 -1711, June 2000.

[8] Y.-P. Lin and S.-M. Phoong, "Optimal ISI-free DMT transceivers for distorted channels with colored noise", *IEEE Transactions on Signal Processing*, pp 2702 -2712, Nov 2001.

[9] A. W. Marshall and I. Olkin, *Inequalities: Theory of Majorization and its applications*, Academic Press, 1979.

[10] B. Muquet, Z. Wang, G.B. Giannakis, M. de Courville and P. Duhamel, "Cyclic prefixing or zero padding for wireless multicarrier transmissions?", *IEEE Transactions on Communications*, pp 2136-2148, Dec 2002.

[11] A. Pandharipande and S. Dasgupta, "Optimal transceivers for DMT based multiuser communication", *IEEE International Conference on Acoustics, Speech, and Signal Processing*, pp 2369 -2372, 2001. Also *IEEE Transactions on Communications*, accepted for publication.

[12] J.G. Proakis, *Digital Communications*, McGraw-Hill, Third Edition, 1995.

[13] A. Scaglione, S. Barbarossa and G.B. Giannakis, "Filterbank transceivers optimizing information rate in block transmissions over dispersive channels", *IEEE Transactions on Information Theory*, pp 1019-1032, Apr 1999.

[14] A. Scaglione, P. Stoica, S. Barbarossa, G.B. Giannakis and H. Sampath, "Optimal designs for space-time linear precoders and decoders", *IEEE Transactions on Signal Processing*, pp 1051-1064, May 2002.

[15] T. Starr, J.M. Cioffi and P. Silverman, *Understanding Digital Subscriber Line Technology*, Prentice Hall, 1998.

[16] P.P. Vaidyanathan, Y.-P. Lin, S. Akkarakaran and S.-M. Phoong, , "Discrete multitone modulation with principal component filter banks", *IEEE Transactions on Circuits and Systems I: Fundamental Theory and Applications*, pp 1397-1412, Oct 2002.

[17] C. Y. Wong, R.S. Cheng, K.B. Lataief and R.D. Murch, "Multiuser OFDM with adaptive subcarrier, bit, and power allocation", *IEEE Journal on Selected Areas in Communication*, pp 1747-1758, Oct 1999.

AN IMPROVED FEEDBACK SCHEME FOR DUAL CHANNEL IDENTIFICATION IN WIRELESS COMMUNICATION SYSTEMS

Honghui Xu[1]*, Soura Dasgupta*[1]*, and Zhi Ding*[2]

[1]Department of Electrical & Computer Engineering
The University of Iowa
Iowa City, IA-52242, USA.
hoxu, dasgupta@engineering.uiowa.edu

[2]Department of Electrical & Computer Engineering
University of California
Davis, CA 95616, USA.
zding@ece.ucdavis.edu

ABSTRACT

In an earlier paper we had presented a novel dual channel identification approach for mobile wireless communication systems. Unlike traditional channel estimation methods that rely on training symbols, this approach used a bent-pipe feedback mechanism requiring the mobile station (MS) to send portions of its received signal back to the Base Station (BS) for wireless channel identification. Using a filter-bank decomposition concept, we introduced an effective algorithm for identifying both the forward and the reverse channels based only on this feedback information. This new method permits transfer of computational burden from the MS to the resource rich BS and leads to significant savings in bandwidth consuming training signals. This paper proposes a more informative feedback method leading to significant performance improvement over our earlier scheme.

1. INTRODUCTION

Two important tasks in mobile wireless communications systems are channel estimation, and compensation aided by frequent transmission of training signals. In most future cellular systems the forward link, carrying data from Base Stations (BS) to a Mobile (MS), will support higher data rates than the reverse link. Consequently, the estimation and compensation of the Forward Link Channel (FLC) requires more resources and longer training sequences than that of the Reverse Link Channel (RLC). Equally, the current practice is to assign the compensation and estimation of the FLC entirely to the MS, which generally has less computational reserves than the BS.

To permit the resource rich BS to share in the compensation of the FLC, and to reduce the bandwidth consuming training of the FLC, in [2] we proposed a new approach to the estimation and compensation of the FLC in mobile wireless communication systems using a novel *bent pipe feedback* mechanism. In principle, this feedback mechanism enables the BS to estimate and compensate both the FLC the RLC, without any training signals on either link or resort to blind estimation techniques. While practical realities temper these expectations, as we demonstrated in [2], this idea has significant advantages.

Specifically, the approach of [2] requires that the MS feed back to the BS a portion of the received signal, over the time slot conventionally reserved for RLC training. Clearly, this permits the BS to estimate the Roundtrip Channel (RTC). *However, the key novelty of our approach lies in the following discovery: By feeding back only a portion, rather than the entire received signal, one empowers the BS to identify both the FLC and the RLC from the roundtrip feedback signal alone.* This novel channel feedback does not require high speed reverse links and naturally accommodates asymmetric data link structures, and structures where the RLC and FLC have different carrier frequencies. Furthermore, no additional training signals are necessary for estimating the RLC at the BS, though some training for synchronization will still be needed.

As the BS will miss changes in the FLC that occur within feedback latency, the MS must estimate and compensate the residual ISI in the channel dynamics the BS cannot compensate. Over reasonable distances and mobile speeds these changes are modest enough to make the partially precompensated FLC dynamics relatively mild. Thus, a 5km roundtrip causes a feedback delay of 16.67 μs, a time span over which the FLC undergoes little change. This is underscored by the fact that in GSM each data frame has a duration of 557 μs, and training occurs only once per data frame. Thus the channel variation within the resolution of this delay occurs mainly because of Doppler effect. Yet a vehicle traveling at 100km/hr suffers a maximum Doppler shift of 55 Hz in the cellular band; a shift not large enough to cause drastic changes in the FLC characteristics over latencies of tens of microseconds. Thus the residual ISI that must be equalized at the receiver will be significantly milder leading to the need for much shorter training sequences on the FLC. Given that no training for estimation is needed on the RLC, and that feedback data occupies the RLC training slot used in conventional communication, this implies substantial savings in the bandwidth devoted to the overall training, and a siginficant transfer of the FLC compensation/estimation burden to the BS. Simulations presented in [2] support this contention. This scheme also permits the use of such adaptive coding at the BS as has been advocated by several authors [3]- [6].

The scheme of [2] is preliminary in nature. One of its disadvantages is that it fails to make as efficient a use of the feedback slot as is desirable. In particular a large fraction of the feedback slot carries zero samples that do not contain useful information about the FLC. The key contribution of this paper is to formulate a *more informative feedback scheme that carries more information about the FLC leading to improved FLC estimation.*

2. THE FEEDBACK SCHEME

For the most part in this paper we assume that the ratio of the data rates supported on the FLC and RLC is M/L, with $M > L$. Later

Supported by NSF grants ECS-9970105, CCR-9973133 and 999620.

we will comment on how to accomodate the case of $M \leq L$. In fig. 1 $H(z)$ and $G(z)$ are the discrete time baseband models of the FLC and RLC respectively, $w_i(n)$ are the noise sequence at their output, $x(n)$ and $y(n)$ are respectively the data sequence transmitted and received by the BS. The samples $s_1(n)$, received at the MS are rate converted by the N-branch rate convertor, [1] that generates L samples for every M samples at its input, i.e. effects a rate conversion by a factor of L/M. The sequence $s_2(n)$ is retransmitted over the RLC over the slots usually reserved for RLC training: $u(k)$ models the interference caused by the normal RLC data because of imperfect synchronization.

In this arrangement $N \leq L < M$. Effectively, over sample lengths of L, $s_2(n)$ contains N out of every M samples of $s_1(n)$, and has in addition $L - N$ zeros. The scheme in [2] uses *only the top branch of this arrangement*, i.e. has $N = 1$. Consequently in [2] out of every L-symbol feedback slot only one sample contains the data received at the MS, with the remaining $L - 1$ symbols being zero samples. Thus in [2] the available feedback slot is under utilized as far as information exchange is considered. This causes important information to be unnecessarily discarded, reducing the ability to track time variations, resulting in larger residual ISI in the FLC compensated on the basis of the estimate at the BS. As we will demonstrate in Section 4, the more sophisticated rate convertor with $N = L$, leads to improved performance.

Consider the M and L fold type I and II polyphase decompositions of $H(z)$ and $G(z)$ respectively, i.e. $H(z) = \sum_{i=0}^{M-1} E_i(z^M) z^{-i}$ and $G(z) = \sum_{i=0}^{L-1} R_i(z^L) z^{-(L-i-1)}$. Then, [1], absent noise and interference, Fig. 1 can be transformed into Fig. 2, where $\mathbf{R}(z)$ and $\mathbf{E}(z)$ are respectively, left and right pseudocirculant matrices given by

$$\mathbf{R}(z) = \begin{pmatrix} R_0(z) & R_1(z) & \cdots & R_{N-1}(z) \\ R_1(z) & R_2(z) & \cdots & R_N(z) \\ \vdots & \vdots & \vdots & \vdots \\ R_{L-1}(z) & z^{-1}R_0(z) & \cdots & z^{-1}R_{N-2}(z) \end{pmatrix} \quad (1)$$

and $\mathbf{E}(z)$=

$$\begin{pmatrix} E_0(z) & E_1(z) & \cdots & E_{M-1}(z) \\ z^{-1}E_{M-1}(z) & E_0(z) & \cdots & E_{M-2}(z) \\ \vdots & \vdots & \vdots & \vdots \\ z^{-1}E_{M-N+1}(z) & z^{-1}E_{M-N+2} & \cdots & E_{M-N} \end{pmatrix}. \quad (2)$$

Define

$$E(z) = [E_0(z), \cdots, E_{M-1}(z)] \quad (3)$$

$$R(z) = [R_0(z), \cdots, R_{L-1}(z)]^T. \quad (4)$$

Define in Fig.2 $\mathbf{Y}(\mathbf{z}) = [Y_1(z), \cdots, Y_L(z)]^T$ and $\mathbf{X}(\mathbf{z}) = [X_1(z), \cdots, X_M(z)]^T$ where $X_i(z)$ and $Y_i(z)$ are the z-transform of $x_i(n)$ and $y_i(n)$. Then we have the following relation

$$\mathbf{Y}(\mathbf{z}) = \mathbf{R}(z)\mathbf{E}(z)\mathbf{X}(\mathbf{z}). \quad (5)$$

Since $X_i(z)$ and $Y_i(z)$ are known to BS, the round trip channel $\mathbf{R}(z)\mathbf{E}(z)$ can be estimated. The question is, under what conditions can one extract $H(z)$ and $G(z)$ from $\mathbf{R}(z)\mathbf{E}(z)$. Clearly the best one can hope for is to estimate $\mathbf{R}(z)$ and $\mathbf{E}(z)$ to within a scaling constant and common delays among the $E_i(z)$ and $R_i(z)$. In the case of [2], such an extraction is possible if either (not necessarily both) of the following conditions apply.

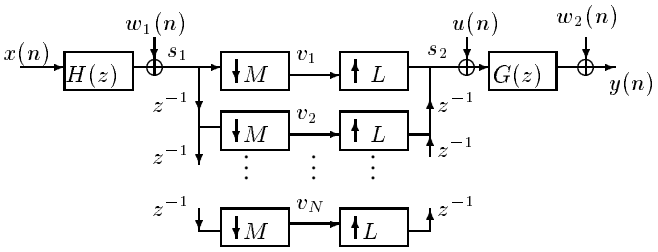

Fig. 1. System model of improved scheme: Rate changer with N branches.

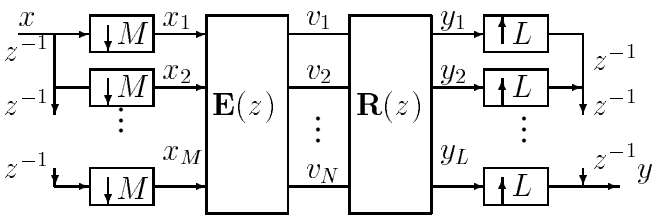

Fig. 2. Polyphase Representation.

Assumption 1 *The greatest common divisor (gcd) of the set of polynomials $R_i(z)$ is a pure delay z^{-d} (d integer). Further their maximum order l_R is known.*

Assumption 2 *The gcd of set of the set of polynomials $E_i(z)$ is a pure delay z^{-d} (d integer). Further their maximum order l_E is known.*

To see why, observe that in the setting of [2], i.e. $N = 1$, (5) is replaced by $\mathbf{Y}(\mathbf{z}) = R(z)E(z)\mathbf{X}(\mathbf{z})$. Thus the *rank-1* matrix $R(z)E(z)$ can be estimated. Observe the k-th row of $R(z)E(z)$ is simply, $R_k(z)[E_0(z), \cdots, E_{M-1}(z)]$. Under Assumption 2, the gcd of the elements of this row provides to within a delay and scaling, $R_k(z)$ and hence also $E_i(z)$ and $H(z)$. Similar unraveling is possible should Assumption 1 hold.

Observe in the setting of this paper the rank-1 matrix $R(z)E(z)$ is not directly available. Yet in the next two sections, we show that under either Assumption 1 or 2, $H(z)$ and $G(z)$ can be obtained to within a scaling and delay from the the roundtrip dynamics captured by $\mathbf{R}(z)\mathbf{E}(z)$.

3. PROOF OF IDENTIFIABILITY

In this section we show that $E(z)$ is identifiable to within a scaling constant, from $\mathbf{R}(z)\mathbf{E}(z)$, when $M > L \geq N$, and assumption 2 holds with the common delay d among the E_i equalling zero. In section 3.3, we discuss the case where this common delay is nonzero. The knowledge of $E(z)$ provides $H(z)$. A similar result can be formulated when assumption 1 holds or when $L \geq M > N$ or when $L = M > N$. *Thus even the case of $L = M$ can be captured.* In each case the selection of N ensures that some received signal is discarded and $s_2(n) \neq s_1(n-k)$.

3.1. Definitions and notations

For an $M \times N$ polynomial matrix $A(z) = \sum_{i=0}^{l} A(i)z^{-l}$, where l is the degree of $A(z)$, define the $mM \times (l+m)N$ generalized

Sylvester matrix of $A(z)$ as

$$\mathcal{T}_m(A) = \begin{pmatrix} A(0) & \cdots & A(l) & & \\ & \ddots & \ddots & \ddots & \\ & & A(0) & \cdots & A(l) \end{pmatrix}. \quad (6)$$

For the $r \times Mm$ matrix $B = [B(0), \cdots, B(m-1)]$, define

$$\mathcal{P}_{m,M}(B) = \sum_{i=0}^{m-1} B(i) z^{-i}. \quad (7)$$

where $B(i)$ and $\mathcal{P}_{m,M}(B)$ have dimension $r \times M$. Note that $\mathcal{P}_{m,M}(B)$ is a function of z.

Define an $M \times M$ polynomial matrix $Q_M(z)$ as

$$Q_M(z) = \begin{pmatrix} \mathbf{0}_{(M-1)\times 1} & \mathbf{I}_{M-1} \\ z^{-1} & \mathbf{0}_{1\times(M-1)} \end{pmatrix} \quad (8)$$

where $\mathbf{I}_{M-1}$ denotes $(M-1) \times (M-1)$ identity matrix; $\mathbf{0}_{m\times n}$ denotes the $m \times n$ zero matrix.

3.2. Identifiability

With $\mathbf{C}(z) = \mathbf{R}(z)\mathbf{E}(z)$,

$$\mathcal{T}_m(\mathbf{C}^T) = \mathcal{T}_m(\mathbf{E}^T)\mathcal{T}_{l_E+1+m}(\mathbf{R}^T) \quad (9)$$

Whenever $G(z)H(z) \neq 0$, $\mathcal{T}_m(\mathbf{R}^T)$ and $\mathcal{T}_m(\mathbf{E})$ are full rank for all intgers $m > 0$. Hence $\mathcal{T}_m(\mathbf{C}^T)$ and $\mathcal{T}_m(\mathbf{E}^T)$ have identical left nullspaces. Thus the knowledge of $\mathbf{C}(z)$ provides the left nullspace of $\mathcal{T}_m(\mathbf{E}^T)$. The following theorem shows that the left null space of $\mathcal{T}_m(\mathbf{E}^T)$ under assumption 2 provides $H(z)$ to within a scaling.

Theorem 1 *Suppose $E(z)$ and $\mathbf{E}(z)$ are defined in (3) and (2) respectively and assumption 2 is in force, with $d = 0$ and $M > L \geq N$. Then for any integer $m > Nl_E + N - 1$, $\mathcal{T}_m(\mathbf{E}^T)$ has a nontrivial left null space. Suppose B is a matrix whose rows span the left nullspace of $\mathcal{T}_m(\mathbf{E}^T)$. Let*

$$\mathbf{B}(z) = [(\mathcal{P}_{m,M}(B))^T, \cdots, Q_M^{N-1}(\mathcal{P}_{m,M}(B))^T]. \quad (10)$$

Consider an M-dimensional nonzero polynomial row vector $\hat{E}(z)$ with degree l_E. Then

$$\mathcal{T}_1(\hat{E})\mathcal{T}_{l_E}(\mathbf{B}) = 0 \text{ iff } \hat{E}(z) = cE(z) \quad (11)$$

where c is a nonzero constant.

Thus indeed the left null space of $\mathcal{T}_{l_E}(\mathbf{B})$, constructed from the left nullspace of $\mathcal{T}_m(\mathbf{C}^T)$, provides $E(z)$ to a scaling.

3.3. A Subspace Algorithm

Assume assumption 2 holds with $d = 0$. Suppose the signals $x(n)$, $u(n)$, $w_1(n)$ and $w_2(n)$ are zero mean, white and mutually uncorrelated. In view of the noise free model of (5), and the knowledge of $x(n)$ and $y(n)$ at the BS, a standard least squares scheme provides an estimate of $\mathcal{T}_m(\mathbf{C}^T)$ and hence its SVD:

$$\mathcal{T}_m(\mathbf{C}^T) + \mathcal{N} = (V_s\ V_n) \begin{pmatrix} \Sigma_s & 0 \\ 0 & \Sigma_n \end{pmatrix} \begin{pmatrix} W_s^H \\ W_n^H \end{pmatrix} \quad (12)$$

Find B whose rows span the left nullspace of $\mathcal{T}_m(\mathbf{C}^T)$, where $m > Nl_E + N - 1$, and construct $\mathbf{B}(z)$ defined in (10). Because of the assumption of lack of correlation between $x(n)$ and the noise and interference, B is provided by V_n. Then solving for $\mathcal{T}_1(\hat{E})$ as the eigenvector corresponding to the smallest eigenvalue of $\mathcal{T}_{l_E}(\mathbf{B})\mathcal{T}_{l_E}(\mathbf{B})^H$, where $(\cdot)^H$ indicates transpose conjugate, provides $E(z)$. Since $\mathcal{T}_{l_R+1}(\mathbf{E})$ has full row rank one finds $G(z)$ also to a scaling constant, using

$$\mathcal{T}_1(\mathbf{R}) = \mathcal{T}_1(\mathbf{C})(\mathcal{T}_{l_R+1}(\mathbf{E}))^\dagger.$$

If $E_i(z)$ have a common delay then this manifests in certain columns of $\mathcal{T}_m(\mathbf{C}^T)$ being zero. Then applying the above procedure on the matrix with these zero columns removed provides $H(z)$ and $G(z)$ to within a scaling and a delay.

4. SIMULATIONS

We present two simulation examples. The first example shows the basic performance of the scheme in this paper relative to that of [2]. The second example illustrates the reduction of training levels needed on the FLC when channel parameters change with time.

4.1. Simulation I

In the simulation, FLC and RLC are generated from two delayed raised-cosine pulse $C(t, \alpha)$, where α is the roll-off factor. $C(t, \alpha)$ is limited in 8T for FLC and in 6T for RLC. The FLC and RLC have the respective analog models: $0.3C(t, 0.25) + 0.8C(t - T/2, 0.25)$ and RLC $= 0.5C(t, 0.10) + 0.6C(t - T/3, 0.10)$. We use downsampling factor $M = 3$ and upsampling factor $L = 2$ and $N = L$. Noises $w_1(n)$ and $w_2(n)$ are zero mean and have the same variance. The input signal $x(n)$ is i.i.d BPSK. To obtain a performance measure of channel estimation, we define the normalized root-mean-square error (NRMSE) as

$$\text{NRMSE} = \frac{1}{\| h \|_2} \sqrt{\frac{1}{M_t} \sum_{i=1}^{M_t} \| \hat{h}_{(i)} - h \|_2^2} \quad (13)$$

where M_t is the number of Monte Carlo runs; h is the actual channel and $\hat{h}_{(i)}$ is the i estimation. In our simulation $M_t = 100$. In each run 600 symbols are used. *We call the scheme in [2] old scheme and the scheme in this paper new scheme.* Fig. 3 shows NRMSE versus input SNR, where input SNR is defined as

$$\text{Input SNR} = 10 \log 10\text{E}(x^2(n))/\text{E}(w_1^2(n)) \quad (14)$$

A zero-forcing preequalizer is constructed for FLC and a post equalizer for the RLC, on the basis of the FLC and RLC estimates. Both are housed at the BS. Equalizer SNR for the FLC, is computed using the signal power at the FLC input. For RLC, it uses the signal power at the equalizer output. BER versus equalizer SNR is displayed in Fig. 4, where the input symbol is BPSK signal. Both figures show the performance improvement due to the more informative feedback of this paper.

4.2. Simulation II: Reduced training for a time varying channel

We use COST-207 Typical Urban(TU) [7] model with 100 echo paths, BPSK data and maximum Doppler frequency 55Hz. We assume the channels to be quasistatic, i.e., time-invariant in one frame and time-variant from frame to frame. The receive filters

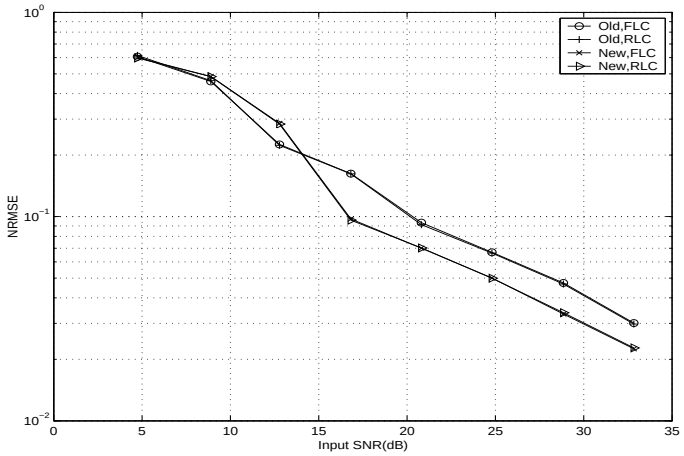

Fig. 3. NRMSE versus input SNR for both schemes

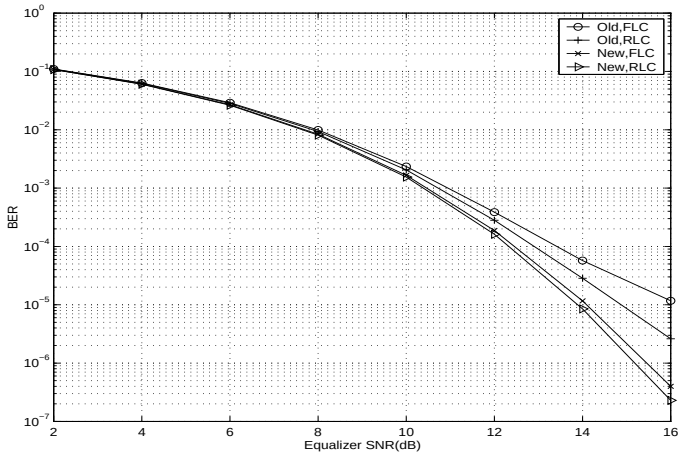

Fig. 4. BER versus equalizer SNR for both schemes.

for FLC and RLC are raised cosine functions with roll-off factors 0.2 and 0.1 respectively. The FLC sustains a data rate of 1 Mbps, and the RLC supports 0.667 Mbps. We use downsampling factor $M = 3$ and upsampling factor $L = 2$. The schemes with $N = 1$ and $N = 2$ are called old scheme and new scheme respectively. In both cases we compare two settings:

(a) Training aided equalization of FLC at the MS and of the RLC at the BS, with no feedback.

(b) No training on the RLC, but instead sending feedback data of the same length as the RLC training data in (a). A precompensator, obtained by the new scheme or the old scheme is used on the FLC and is augmented by a post-equalizer estimated at the receiver using reduced training.

Methods in (a) and (b) use the same signal power at the FLC input. Fig. 5 shows n_b/n_t versus input SNR for methods in (a) and (b) to achieve the same BER. Here n_t is the length of the FLC training sequence used in (a) and n_b the length of training used in (b), so that the same FLC BER is obtained in both cases. As is evident in Fig. 5, in order to achieve the same BER as the conventional method, the new scheme needs less training data and thus saves more bandwidth than the old scheme when input SNR$>$ 6dB. By way of further comparison we note that at 18dB SNR, while the training sequence length in [2] is 30% of (a), the length for the new scheme is only 15%, i.e. half that needed by [2].

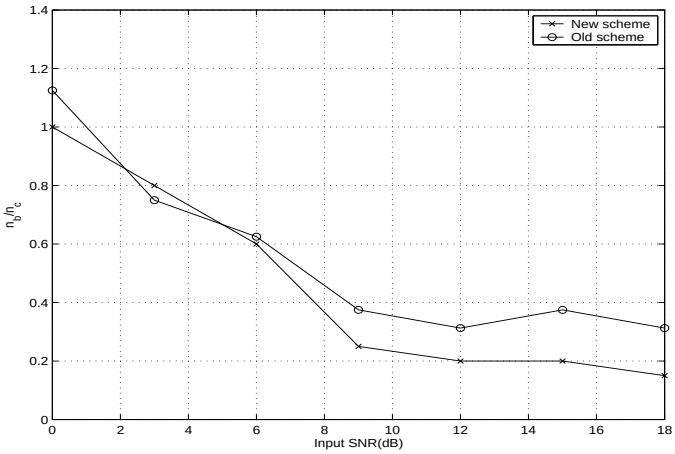

Fig. 5. n_b/n_t versus SNR at the same BER.

5. CONCLUSION

In this paper, a bent pipe multi-branch feedback scheme is used to estimate FLC and RLC from RTC. By exploiting the properties of the nullspace of pseudocirculant matrices, the identifiability result and unravelling method are derived for this improved scheme. Since this improved scheme uses more information from FLC, we get performance improvement compared to the scheme in [2].

6. REFERENCES

[1] P. P. Vaidyanathan, *Multirate Systems and Filter Banks*, Prentice Hall, 1992.

[2] H. Xu, S. Dasgupta and Z. Ding, "A novel channel identification method for fast wireless communication systems communications", *Proc. of ICC*, vol.8, pp. 2443 -2448, 2001. Submitted to *IEEE Transactions on Communications*.

[3] R. W. Heath, Jr. and A. Paulraj, "A Simple Scheme for Transmit Diversity using Partial Channel Feedback," *Proc. of 32nd Asilomar Conf. on Signals, Systems and Computers*, pp.1073-8, Pacific Grove, CA, 1998.

[4] L.M.C. Hoo, J. Tellado, J.M. Cioffi, "Discrete dual QoS loading algorithms for multicarrier systems", *IEEE International Conference on Communications*, pp 796-800, 1999.

[5] J. Zhang, A. Sayeed and B. Van Veen, "Optimal transceiver design for selective wireless broadcast with channel sttae estimation", in *Proceedings of ICASSP*, May 2002, Orlando, Fla.

[6] D. L. Goeckel, "Adaptive Coding for Fading Channels using Outdated Channel Estimates", *IEEE Transactions on Communications*, Vol. 47, pp. 844-855, June 1999.

[7] P.Hoeher, "A statistical discrete-time model for the WSSUS multipath channel", *IEEE Trans. on Vehicular Technology*, VT-41(4):461-468, April 1992.

Complete Characterization of Channel Resistant DMT with Cyclic Prefix

Soura Dasgupta and Ashish Pandharipande*

Abstract

In this paper, we provide a complete characterization of Discrete Multitone Transmission (DMT) systems that employ a cyclic prefix redundancy, and can be equalized by a bank of one tap equalizers in each subchannel, for almost all values of channel parameters. We show that amomg all possible FIR transmitting and receiving filters of arbitrary order, such channel resistant transmission requires (a) that the receive filters be matched to the transmit filters, and (b) that to within a scaling and delay, the transmit and receive filters have IDFT and DFT coefficients. Thus we prove that, should cyclic prefix be applied, only trivial variants of traditional DFT based DMT systems are channel resistant.

EDICS: SPL.COM

*Department of Electrical and Computer Engineering, The University of Iowa, Iowa City, IA-52242, USA. Email: dasgupta@engineering.uiowa.edu and pashish@engineering.uiowa.edu. This work was supported by US Army contract, DAAAD19-00-1-0534, and NSF grants ECS-9970105 and CCR-9973133.

1 Introduction

Discrete multitone (DMT) modulation, depicted in fig. 1 is a standard in many wireline and wireless applications,[1]. An M-point block transformation, $A(z)$ is applied to M-parallel data streams, followed by a parallel to serial conversion (block P to S). For an FIR channel with transfer function,

$$H(z) = \sum_{i=0}^{\kappa} h_i z^{-1}, \tag{1.1}$$

a *cyclic prefix* redundancy of length κ is added by the CPI block, and is removed by the CPR block. Thus each M-block of $v(n)$ is converted to an N-block of $s(k)$, $N = \kappa + M$, by prepending the last κ samples of the block. After CPR, one performs serial to parallel conversion (StoP block) , and the inverse block transformation, $B(z)$. The overall system has the equivalent description of fig. 2. In traditional DMT $A(z)$ is a block IDFT operation, and $B(z)$ is a block DFT operation, i.e. with W the M-point DFT matrix having ik-th element

$$[W]_{ik} = e^{-j\frac{2\pi(i-1)(k-1)}{M}}, \quad A(z) = W^H \text{ and } B(z) = W. \tag{1.2}$$

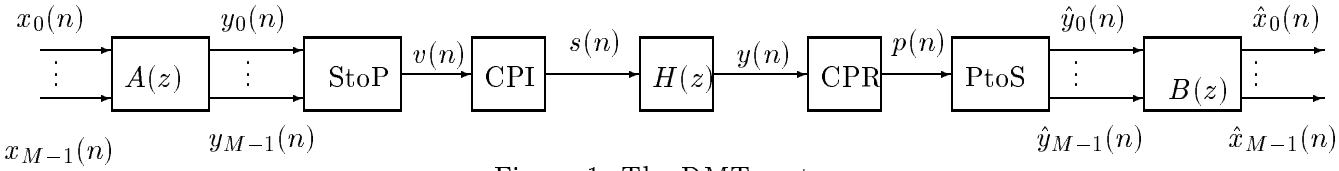

Figure 1: The DMT system.

Under (1.2), $F_i(z)$ and $G_i(z)$ are mutually matched, respectively causal and anticausal of degree $M-1$ with coefficients of $F_i(z)$ being the cefficients of the i-th column of W^H. This leads to considerable spectral overlap between the subchannels. Cyclic prefix and (1.2) ensure that

$$X(n) = [x_0(n), \cdots, x_{M-1}(n)]^T \text{ and } \hat{X}(n) = [\hat{x}_0(n), \cdots, \hat{x}_{M-1}(n)]^T \quad \hat{X}(n) = \Delta(h_0, \cdots, h_\kappa)X(n) \tag{1.3}$$

with diagonal, $\Delta(h_0, \cdots, h_\kappa)$ nonsingular for almost all h_i barring those for which $H(z)$ has a unit circle zero at an M-th root of unity. Thus, for almost all channels of order no greater than κ, one tap equalizer at each subchannel output ensures ISI removal. We call such a system *Channel Resistant DMT*.

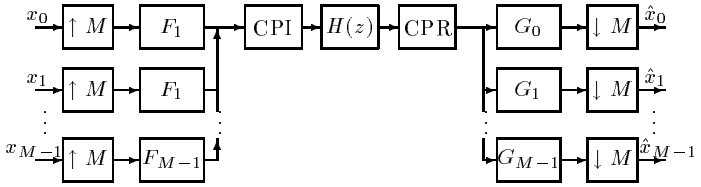

Figure 2: A multicarrier system with cyclic prefix

More general orthogonal block transforms, with zero padding redundancy, and precoding are in [2]-[6]. Improved spectral separation through longer $F_i(z)$ and $G_i(z)$, is advocated in [7]. Given the prevalence of

cyclic prefix redundancy in practical systems, and the issues raised in [7], we ask whether there are longer length $F_i(z)$ and $G_i(z)$ that together with cyclic prefix redundancy, ensure channel resistance? We thus characterize all $M \times M$ FIR

$$A(z) = \sum_{i=-p_1}^{p_2} A_i z^{-i} \text{ and } B(z) = \sum_{i=-q_1}^{q_2} B_i z^{-i} \tag{1.4}$$

such that with cyclic prefix redundancy, and $H(z)$ as in (1.1), (1.3) holds with diagonal $\Delta(h_0, \cdots, h_\kappa)$ nonsingular for almost all h_i. We show that all such $A(z)$, $B(z)$ yield $F(z)\, G(z)$, that are mutually matched to within complex scaling constants, and are identical to their counterparts yielded by the conventional DMT, to within scaling constants and delays. Thus channel resistance with cyclic prefix is incompatible with greater spectral separation.

2 Formulation

In fig. 1 successive M-blocks of $v(n)$ and $p(n)$ and N-blocks of $r(n)$ and $s(n)$ obey, [2]:

$$\mathbf{v}(n) = [v(Mn), \cdots, v(Mn-M+1)]^T = [y_0(n), \cdots, y_{M-1}(n)]^T = A(z)X(n) \tag{2.5}$$

$$\mathbf{s}(n) = [s(Nn), \cdots, s(Nn-N+1)]^T = \begin{bmatrix} 0 & & I_\kappa \\ & I_M & \end{bmatrix} \mathbf{v}(n) \tag{2.6}$$

$$\mathbf{r}(n) = [r(Nn), \cdots, r(Nn-N+1)]^T = \begin{bmatrix} h_0 & z^{-1}h_{N-1} & z^{-1}h_{N-2} & \cdots & z^{-1}h_1 \\ h_1 & h_0 & z^{-1}h_{N-1} & \cdots & z^{-1}h_2 \\ \vdots & \vdots & \vdots & \vdots & \vdots \\ h_{N-1} & h_{N-2} & \cdots & h_1 & h_0 \end{bmatrix} \mathbf{s}(n) \tag{2.7}$$

$$\mathbf{p}(n) = [p(Mn), \cdots, p(Mn-M+1)]^T = \begin{bmatrix} 0 & I_M \end{bmatrix} \mathbf{r}(n) \quad \hat{X}(n) = B(z)\mathbf{p}(n) \tag{2.8}$$

Define circulant(η) to be the square circulant matrix with first row η. Then, [2], one has

$$\mathcal{H} = \text{circulant} \begin{bmatrix} h_0 & 0 & \ldots & 0 & h_\kappa & \ldots & h_1 \end{bmatrix}, \quad \hat{X}(n) = B(z)\mathcal{H}A(z)X(n). \tag{2.9}$$

with $\mathcal{H}$ $M \times M$. Further we note, that because of (2.5) and (2.8), fig. 1 is equivalent to fig. 2 with

$$[F_0(z), \cdots, F_{M-1}(z)] = \left[1, z^{-1}, \ldots, z^{-(M-1)}\right] A(z^M), \; [G_0(z), \cdots G_{M-1}(z)]^T = \left[1, z, \cdots z^{(M-1)}\right] B^T(z^M). \tag{2.10}$$

Channel resistance then requires that with diagonal, $\Delta(h_0, \cdots, h_\kappa)$ nonsingular for almost all h_i,

$$B(z)\mathcal{H}A(z) = \Delta(h_0, \cdots, h_\kappa). \tag{2.11}$$

Observe with the $M \times M$ circulant shift matrix

$$J = \text{circulant}\left[\begin{array}{cccc} 0 & 1 & \dots & 0 \end{array}\right], \qquad \mathcal{H} = h_0 I + \sum_{i=1}^{k} J^{M-i} h_i. \tag{2.12}$$

Thus (2.11) requires that with diagonal Δ_i and at least one Δ_i nonsingular

$$B(z)A(z) = \Delta_0 \text{ and } \forall 1 \le i \le \kappa \quad B(z)J^{M-i}A(z) = \Delta_i. \tag{2.13}$$

3 The Main Result

The following Lemma is useful.

Lemma 3.1 *Suppose two $M \times M$ nonsingular matrices $\hat{B}$ and $\hat{A}$ are such that both $\hat{B}\hat{A}$ and $\hat{B}J^{M-1}\hat{A}$ are diagonal. Then for some permutation matrix P and diagonal matrices D_B and D_A, $\hat{B} = D_B P W^H$ and $\hat{A} = W P^T D_A$.*

Proof: As $\hat{B}\hat{A}$ is diagonal, the expression for $\hat{B}$ ensures that for $\hat{A}$. Call $\bar{A}_i$ the $M \times (M-1)$ matrix comprising all but the i-th column of $\hat{A}$ and $b_i = [b_{i1}, \cdots, b_{iM}] \neq 0$ the i-th row of $\hat{B}$. As $\text{rank}(\bar{A}_i) = M-1$,

$$\left[\begin{array}{c} b_i \\ b_i J^{M-1} \end{array}\right] \bar{A}_i = 0 \Rightarrow \text{rank}\left(\left[\begin{array}{c} b_i \\ b_i J^{M-1} \end{array}\right]\right) = 1.$$

Thus for some $\alpha_i \neq 0$, $[b_{i1}, \cdots, b_{iM}] = \alpha_i [b_{i2}, \cdots, b_{iM}, b_{i1}]$. Thus, for $1 \le li < M$, $b_{il} = \alpha_i b_{i,l+1}$ and $b_{i1} = \alpha_i b_{iM}$. Thus $\alpha_i^M = 1$ and $b_i = b_{i1}[1, \alpha_i \cdots, \alpha_i^{M-1}]$. ∎

In (2.13) as at least one Δ_i is nonsigular, $B(z)$, $A(z)$ are nonsigular. Thus from Lemma 3.1, for almost all z, $B(z) = D_B(z)P(z)W^H$ and $A(z) = WP^T(z)D_A(z)$, with $D_B(z)$, $D_A(z)$ diagonal and $P(z)$ a permutation matrix at almost all z. Observe, that for D_i nonzero, diagonal and P_i, P permutations, and D a diagonal matrix, $D_1P_1 + D_2P_2 = DP$ iff $P_1 = P_2$. Thus $P(z) = P$ is constant. Further, from (1.2), $D_A(z) = \sum_{i=-p_1}^{p_2} D_{Ai} z^{-i}$ and $D_B(z) = \sum_{i=-q_1}^{q_2} D_{Bi} z^{-i}$. Further $D_B(z)D_A(z) = \Delta_0$. It is readily seen that that the product of two, two sided scalar polynomials $a(z)$ and $b(z)$ is a constant iff for some l, $a(z) = a_l z^l$ and $b(z) = b_{-l} z^{-l}$. Thus, as $D_B(z)$ and $D_A(z)$ are diagonal, for some constant nonsingular, diagonal Λ_A and Λ_B and $\mathcal{Z} = \text{ diag } \{z^{i_1}, \cdots, z^{i_M}\}$

$$B(z) = \Lambda_B \mathcal{Z} P W^H \text{ and } A(z) = W P^T \mathcal{Z}^{-1} \Lambda_A. \tag{3.14}$$

As $W^H \mathcal{H} W$ is always diagonal, this is also sufficient for (2.11), with $\Delta(h_0, \cdots, h_\kappa)$ nonsingular unless $H(z)$ has a zero at an M-th root of unity. Call the filters for the tradional DMT $\hat{F}_i(z)$ and $\hat{G}_i(z)$, i.e.

$$\left[\hat{F}_0(z), \cdots, \hat{F}_{M-1}(z)\right] = \left[1, z^{-1}, \dots, z^{-(M-1)}\right] W^H, \ \left[\hat{G}_0(z), \cdots \hat{G}_{M-1}(z)\right]^T = \left[1, z, \cdots z^{(M-1)}\right] W^T. \tag{3.15}$$

Then, because of (2.10) and (3.14), we have the following main result.

Theorem 3.1 *Under (1.4) (2.11) holds for all h_i with $\Delta(h_0, \cdots, h_\kappa)$ nonsingular unless $H(z)$ has a zero at an M-th root of unity, iff the following two conditions hold. (i) With $\hat{F}_i(z)$ as in(3.15), for some complex $\alpha_i \neq 0$, integer k_i and permutation P, $[F_0(z), \cdots, F_{M-1}(z)] = [\alpha_0 z^{Mk_0} \hat{F}_0(z), \cdots, \alpha_{M-1} z^{Mk_{M-1}} \hat{F}_{M-1}(z)]P$; and (ii) for some complex $\beta_i \neq 0$, $G_i(z) = \beta_i F_i^*(1/z)$.*

Consequently, the level of specral overlap between the subchannels is the same as in traditional DMT.

4 Conclusions

We have shown that all channel resistant DMT systems are trivial variants of the DFT based system, as long as cyclic redundancy is employed. This stands in contrast to the results of [6], [3] where more general DMT systems under precoding are shown to be channel resistant.

References

[1] J.S. Chow, J.C. Tu and J.M. Cioffi, "A discrete multitone transceiver system for HDSL applications", *IEEE Journal on Selected Areas in Communications*, pp 895-908, Aug 1991.

[2] Y. Lin, and S. Phoong, "Perfect discrete multitone modulation with optimal transceivers", *IEEE Transactions on Signal Processing*, pp 1702 -1711, June 2000.

[3] A. Scaglione, G. B. Giannakis, and S. Barbarossa, "Redundant Filterbank Precoders and Equalizers", *IEEE Transactions on Signal Processing*, SP-47:1988-2022, July 1999.

[4] A. Pandharipande and S. Dasgupta, "Optimum DMT based transceivers for multiuser communications", in *Proc. ICASSP*, 2001, Salt Lake City, Utah.

[5] P.P. Vaidyanathan, "Filter Banks in Digital Communications", *IEEE Ccts and Sys Mag*, Mar. 2001.

[6] X.-G. Xia, "New precoding for intersymbol interference cancellation using nonmaximally decimated Multirate Filterbanks with ideal FIR equalizers", *IEEE Trans. Signal Processing*, pp 2431-2441, 1997.

[7] S.D. Sandberg and M.A. Tzannes, "Overlapped discrete multitone modulation for high speed copper wire communications", *IEEE Journal on Selected Areas in Communications*, pp 1571-1585, Dec 1995.

[8] P.P. Vaidyanathan, *Multirate Systems and Filter Banks*, Prentice Hall, 1992.

A NEW ALGORITHM FOR OPTIMUM BIT LOADING

Manish Vemulapalli[1], *Soura Dasgupta*[1], *and Ashish Pandharipande*[2]

[1]Department of Electrical & Computer Engineering
The University of Iowa
Iowa City, IA-52242, USA.
mvemulap, dasgupta@engineering.uiowa.edu

[2]Department of Electrical & Computer Engineering
University of Florida
Gainesville, FL 32611-6130, USA.
ashish@dsp.ufl.edu

ABSTRACT

In this paper we present an efficient bitloading algorithm that applies to both subband coding and multicarrier communication. The goal is to effect an optimal distribution of positive integer bit values among various subchannels to achieve a minimum distortion error variance for subband coding and transmitted power for multicarrier communications. Existing algorithms in the literature grow with the total number of bits that must be distributed. The novelty of our algorithm lies in the fact that its complexity is independent of the total number of bits to be allocated.

1. INTRODUCTION

An important problem in both subband coding and multicarrier communications is bitloading. Specifically, for an N-subchannel system in these problems reduce to general problem of finding b_k to

$$\text{Minimize: } P(b_1,..,b_N)=\sum_{k=1}^{N}\phi_k(b_k) \tag{1}$$

$$\text{Subject to : } \sum_{k=1}^{N} b_k = B, b_k \in \{0,1,...B\}, \tag{2}$$

where ϕ_k is a convex function, and B is a positive integer. In subband coding

$$\phi_k(b_k)=\alpha_k 2^{-2b_k} \tag{3}$$

where α_k is determined by the signal variance in the k-th subchannel, [1] and $P(b_1,..,b_N)$ is the average distortion variance, and b_k is the bits assigned to the k-th subchannel. Further α_k increases with increasing signal variance. In multicarrier systems

$$\phi_k(b_k)=\alpha_k 2^{b_k} \tag{4}$$

where α_k reflect target performance, and channel and interference conditions experienced in the k-th subchannel, [11], [12] and $P(b_1,..,b_N)$ is the total transmitted power. Higher values of α_k reflects more adverse subchannel conditions and/or stringent performance goals; b_k is the the number of bits assigned to each symbol in the cognizant subchannel.

It is recognized that for general convex functions $\phi_k(\cdot)$, the above constrained minimization grows in complexity with the size of B. Since B can be large, it is important to formulate algorithms for which the complexity bound is *independent of B.* The principle contribution of this paper is to show that if one works with the special case of (4), then such an algorithm is indeed feasible. *The algorithm we provide in this paper though formulated in the context of (4), can be trivially modified to accomodate both (3), and indeed a general function*

$$\phi_k(b_k)=\alpha_k a^{\eta b_k} \tag{5}$$

To place this work in context we note the presence of several bit loading algorithms in the literature. These include, [3], [4], [6], [8], [10]. The two most advanced and recent are [10] and [3]. The complexity of [10] grows as $O(N\log(N))$ with the number of subchannels, but linearly with B. On the other hand [3] provides a *suboptimal solution* with complexity $O(N)$. Strictly speaking its complexity does not grow with B, as it restricts the maximum number of bits to be assigned to any subchannel to some B^*. Instead the complexity grows with B^*. The assumption of small B^* is certainly problematic in subband coding, and even in communications settings when certain subchannels experience deep fades. In such a case efficiency may demand that large number bits be assigned to subchannels with more favorable conditions. A still another contributor to the complexity of [3] is the dynamic range of α_i, which again comes into play in the presence of deep fades. All other algorithms have run times that increase with B.

By contrast, we provide an *exact solution* to (1, 2), under (4), whose complexity has an upper bound that is determined *only by N* and is in fact $O(N\log N)$. The role of B is only to induce cyclic fluctuations in the precise number of computations, and neither B nor the dynamic range of α_k, affects the upper bound of the run time.

The paper is organized as follows. Section 2 recaps a result from [13], that is specialized in this paper to formulate the algorithm given in section 3. The complexity and proof of correctness are provided in Sections 4 and 5, respectively. Section 6 gives simulations comparing the run time of this algorithm with those of [10] and [3].

2. A GENERAL RESULT

We now present a general result from [13] that solves (1), (2) for arbitrary convex $\phi_k(\cdot)$. This result is specialized to the cases of (3) and (4) in subsequent sections. Denote for $k=1,...,N, x=1,...,B$,

$$\delta_k(x)=\phi_k(x)-\phi_k(x-1). \tag{6}$$

The ϕ_k's being convex, it follows that

Supported by ARO contract DAAD19-00-1-0534 and NSF grants ECS-9970105, ECS-0225432 and CCR-9973133. Pandharipande was with the Department of Electrical and Computer Engineering, the University of Iowa, Iowa City, IA-52242, USA when this work was partially completed.

$$\delta_k(1) < \delta_k(2) < ... < \delta_k(B), \forall k. \quad (7)$$

Let S denote the set of smallest B elements of

$$\tau = \{\delta_k(x) : k = 1, ..., N, x = 1, ..., B\}$$

The following lemma from [13], gives an optimum solution to (1), (2).

Lemma 1 *The optimal solution* $\mathbf{b}^* = [b_1^*, ..., b_N^*]^T$ *to problem (1), (2), is defined as follows*

$$b_k^* = \begin{cases} 0 & : \quad \delta_k(1) \notin S \\ B & : \quad \delta_k(B) \in S \\ y & : \quad \delta_k(y) \in S, \delta_k(y+1) \notin S \end{cases}$$

In essence this lemma provides a conceptual framework for solving (1), (2). Specifically, construct S, and for each k, determine the largest integer argument b_k for which $\delta_k(b_k)$ is in S. For general convex functions ϕ_k the complexity of all known solutions grows with B. In the rest of the paper we show by example of (4) that the result when specialized to (4) leads to an algorithm that does not depend on B. A trivial modification of this algorithm can be formulated for (3), and indeed (5) and is omitted.

3. PROPOSED LOADING ALGORITHM

In the special case of (4), one finds that,

$$\delta_k(x) = \alpha_k 2^{x-1}. \quad (8)$$

The first step of the algorithm requires ordering the α_i, and can be accomplished in $O(N \log N)$ steps. Henceforth assume without sacrificing generality that:

$$\alpha_1 \leq \alpha_2 \leq .. \leq \alpha_N. \quad (9)$$

Define the sequence:

$$l_i = \lceil \log_2(\frac{\alpha_i}{\alpha_1}) \rceil, i = 1, 2, ..., N \quad (10)$$

with $l_{N+1} = \infty$, where $\lceil a \rceil$ is the smallest integer greater than or equal to a. The significance of the integers l_i is explained by Lemma 2

Lemma 2 *With* l_i *defined in (10),*

$$\alpha_1 2^{l_i - 1} < \alpha_i \leq \alpha_1 2^{l_i},$$

i.e.

$$\delta_1(l_i) < \delta_i(1) \leq \delta_1(l_i + 1).$$

Proof: From (10) we have $l_i = \lceil \log_2(\frac{\alpha_i}{\alpha_1}) \rceil$. The definition of the ceiling function gives us the following result,

$$l_i - 1 < \log_2(\frac{\alpha_i}{\alpha_1}) \leq l_i.$$

Hence the result. ■

Then the proposed algorithm for solving (1), (2) under (4) is given below. It assumes that the ordering implicit in (9), has already occurred, and assigns b_i bits to the i-th subchannel.

Proposed algorithm

Step-1: Find the smallest k such that

$$R_k = \sum_{i=1}^{k-1} (l_k - l_i) \geq B \quad (11)$$

Then

$$b_i = 0 \quad \forall i \in \{k, k+1, \cdots, N\}. \quad (12)$$

Step-2: Find

$$\Delta = B - R_{k-1} \quad (13)$$

$$r = \Delta \bmod (k-1) \quad (14)$$

$$q = \Delta \text{div} (k-1) \quad (15)$$

Step-3: Find the r smallest elements of the set

$$\{\delta_1(l_{k-1} - l_1), \delta_2(l_{k-1} - l_2), \cdots, \delta_{k-1}(0)\}. \quad (16)$$

In particular, with l_{j_i} such that with $l_{j_i} \in \{1, 2, \cdots, k-1\}$,

$$\delta_{j_i}(l_{k-1} - l_{j_i}) \leq \delta_{j_{i+1}}(l_{k-1} - l_{j_{i+1}}), \quad (17)$$

call

$$J = \{j_1, j_2, ..., j_r\}. \quad (18)$$

If $r = 0$, J is empty.

Step-4: For all $i \in \{1, 2, \cdots, k-1\}$,

$$b_{j_i} = \begin{cases} l_{k-1} - l_i + q + 1 & \text{if} \quad i \in J, \\ l_{k-1} - l_i + q & \text{else.} \end{cases} \quad (19)$$

4. COMPLEXITY

Observe that the complexity inplicit in achieving (9) is $O(N \log N)$. Determination of k so that (11) holds requires at most $2N$ operations, *regardless of B*. Indeed one has, with

$$\rho_1 = 0$$

$$\rho_n = \rho_{n-1} + l_n,$$

$$R_n = (n-1)l_n - \rho_{n-1}.$$

The only impact that B has in the complexity of determining k is that for sufficiently small B, $k < N$ and the number of computations is further reduced to $2(k-1)$.

Determining the ranking manifest in (17) is detrmined only by r and k, and is

$$O(r \log(k-1)) \leq O((N-1) \log(N-1)).$$

Determination of r requires 2 operations, independent of B. B does affect the precise value of r, which however is no greater than $N-1$.

Thus the overall complexity, is bounded by $O(N \log(N))$, with B playing no role in the determination of this bound. The only effect that B has on the overall complexity is to cause fluctuations in the precise number of operations, within a range that is independent of B. To recap, these fluctuations occur when:

- For small B, $k < N$, and finding k requires only $2(k-1)$ operations.
- As B changes r fluctuates between 0 and $N-1$, and the number of operations required to determine the smallest r elements of the set in (16) changes.

5. PROOF FOR CORRECTNESS

We now show that the algorithm in section 3 does indeed solve (1), (2), under (4). In view of Lemma 1 it suffices to show that the set

$$S^* = \{\delta_1(1), \cdots, \delta_1(b_1), \delta_2(1), \cdots, \delta_2(b_2), \ldots, \delta_{k-1}(b_{k-1})\}, \tag{20}$$

is such that

$$S^* = S,$$

defined in section 2. This in turn requires the demonstration of the following facts.

(A) $|S^*| = |S| = B$, where $|\cdot|$ represents the cardinality of its argument.

(B) For all $i, j \in \{1, 2, \cdots, N\}$,

$$\delta_i(b_{i+1}) \geq \delta_j(b_j).$$

The first theorem proves (A).

Theorem 1 *With b_i defined in (11-19), $|S^*| = B$.*

Proof: Since $b_i = 0$ for all $i \in \{k, k+1, \cdots, N\}$, we need to show that

$$\sum_{i=1}^{k-1} b_i = B.$$

From (11-19) we have that

$$\begin{aligned}
\sum_{i=1}^{k-1} b_i &= \sum_{i \in J} b_i + \sum_{i \in \{\{1,\cdots,k-1\}-J\}} b_i \\
&= r(q+1) + (k-1-r)q + \sum_{i=1}^{k-1}(l_{k-1} - l_i) \\
&= \Delta + R_{k-1} \\
&= B.
\end{aligned}$$

■

To prove (B) we need an additional Lemma.

Lemma 3 *With l_i, k and q as in (10-15),*

$$q \begin{cases} \leq l_k - l_{k-1} & \text{if } r = 0 \\ < l_k - l_{k-1} & \text{if } r \neq 0 \end{cases}$$

Proof: From (11-15)

$$\begin{aligned}
(k-1)q + r &\leq R_k - R_{k-1} \\
&= \sum_{i=1}^{k}(l_k - l_i) - \sum_{i=1}^{k-1}(l_{k-1} - l_i) \\
&= (k-1)(l_k - l_{k-1}).
\end{aligned}$$

Hence the result. ■

We now prove (B) for the case where $r = 0$.

Theorem 2 *Consider (10-19). Suppose $r = 0$. Then (B) above holds.*

Proof: For all $i \in \{2, \cdots, k-1\}$, from Lemma 2, we have:

$$\delta_i(b_i) = \alpha_i 2^{l_{k-1} - l_i + q - 1} \leq \alpha_1 2^{l_{k-1} + q - 1} = \delta_1(b_1), \tag{21}$$

as $l_1 = 0$. Thus $\delta_1(b_1)$ is the largest member of S^* in (20).

From Lemma 2, for all $i \in \{1, \cdots, k-1\}$,

$$\delta_i(b_i + 1) = \alpha_i 2^{l_{k-1} - l_i + q} > \alpha_1 2^{l_{k-1} + q - 1} = \delta_1(b_1). \tag{22}$$

Further, as (12) holds, we have from Lemmas 2 and 3 that for all $i \in \{k, k+1, \cdots, N\}$,

$$\delta_1(b_1) = \alpha_1 2^{l_{k-1} + q - 1} \leq \alpha_1 2^{l_k - 1} < \alpha_k = \delta_k(1). \tag{23}$$

In view of (21), (22) and (23), prove the result. ■

Finally we prove (B) for the case where $r \neq 0$.

Theorem 3 *Consider (10-19). Suppose $r \neq 0$. Then (B) above holds.*

Proof: With the indices j_i defined in (17), we first show that

$$\delta_{j_r} \geq \delta_i(b_i) \quad \forall i \in \{1, \cdots, k-1\}. \tag{24}$$

In view of (17) this is clearly true for $i \in J$. Now consider $p \in \{\{1, \cdots, k-1\} - J\}$. Because of (19) and Lemma 2,

$$\begin{aligned}
\delta_p(b_p) &= \alpha_p 2^{l_{k-1} - l_p + q - 1} \\
&\leq \alpha_1 2^{l_{k-1} + q - 1} \\
&< \alpha_{j_1} 2^{l_{k-1} - l_{j_1} + q} \\
&= \delta_{j_1}(b_{j_1}) \\
&\leq \delta_{j_r}(b_{j_r}),
\end{aligned}$$

where the last inequality follows from (17).

For all $i \in \{\{1, \cdots, k-1\} - J\}$, (17, 18) demonstrate that

$$\delta_i(b_i + 1) \geq \delta_{j_r}(b_{j_r}). \tag{25}$$

Further, from Lemma 2 for all $i \in J$,

$$\delta_i(b_i + 1) = \alpha_i 2^{l_{k-1} - l_i + q + 1} > \alpha_1 2^{l_{k-1} + q} \geq \delta_{j_r}(b_{j_r}).$$

Then the result is proved by observing from Lemma 3 that

$$\begin{aligned}
\delta_{j_r}(b_{j_r}) &= \alpha_{j_r} 2^{l_{k-1} - l_{j_r} + q} \\
&\leq \alpha_{j_r} 2^{l_{k-1} - l_{j_r} - 1} \\
&\leq \alpha_1 2^{l_k - 1} \\
&< \alpha_k = \delta_k(1).
\end{aligned}$$

■

6. SIMULATIONS

A comparison of the performance of the algorithms of [10] and [3] and the proposed algorithm with respect to the number of computations required is shown in the figures 1 and 2, for the cases where $N = 32$ and $N = 64$, respectively. In implementing [3], which is a suboptimal algorithm, the maximum number of bits, B^* that any channel can be assigned is kept at B.

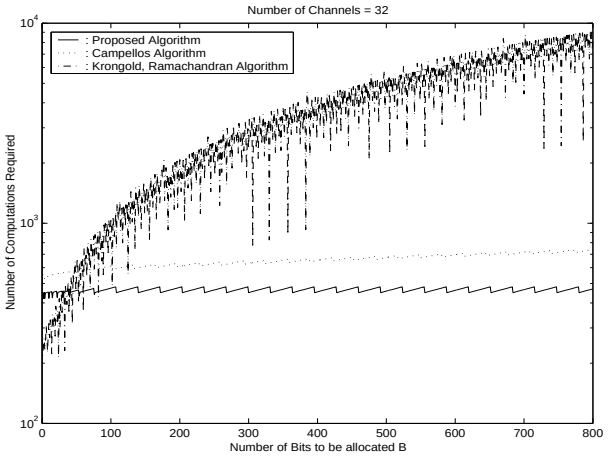

Fig. 1. Runtime comparisions of the three algorithms for N=32

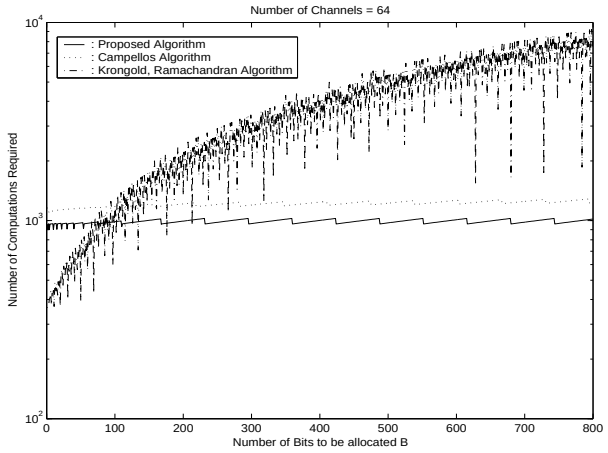

Fig. 2. Runtime comparisions of the three algorithms for N=64

Number of computations needed for each algorithm to converge to the optimal solution was calculated by assuming that addition, subtraction, div, mod, multiplication or division of two numbers would need one computation as would the logical comparisons between two decimal numbers. The results show that the algorithm described in [3] is linear with respect to B while the algorithm in [10] needs large number of computations to converge as B grows. The number of computations needed for the proposed algorithm is independent of the change in B the minor variations seen are attributed to the facts that for small B, k in (11) is small, reducing the number of computations slightly, and cyclic fluctuations induced by the variation in r (see (14)) between 0 and $N-1$. the sorting algorithm whose convergence depends on the input vector) and the difference in the runtimes becomes very significant for large B. Further the proposed algorithm out performs that of [3], even when B is small, and even in [3] $B = B^*$ will be chosen. This is largely because of the fact that the run time in [3] grows with the dynamic range of α_k.

7. CONCLUSIONS

We presented an optimum bit loading algorithm with a run time of $O(N \log N)$ which is more efficient than the ones existing in the literature, in that its complexity does not depend on the total number of bits to be allocated. The improvement in performance is very significant if B is large when compared to N.

8. REFERENCES

[1] S. Akkarakaran and P.P. Vaidyanathan, "Discrete multitone communication with principal component filter banks", *IEEE International Conference on Communications*, pp 901-905, 2001.

[2] A.N. Barreto and S. Furrer, "Adaptive bit loading for wireless OFDM systems", *IEEE International Symposium on Personal, Indoor and Mobile Radio Communications*, pp 88-92, 2001.

[3] J. Campello, "Practical bit loading for DMT", *IEEE International Conference on Communications*, pp 801-805, 1999.

[4] P.S. Chow, J.M. Cioffi and J.A.C. Bingham, "A practical discrete multitone transceiver loading algorithm for data transmission over spectrally shaped channels", *IEEE Transactions on Communications*, pp 773-775, 1995.

[5] T.H. Cormen, C.E. Leiserson, R.L. Rivest and C. Stein, *Introduction to Algorithms*, MIT Press and McGraw-Hill, Second Edition, 2001.

[6] R.F.H. Fischer and J.B. Huber, "A new loading algorithm for discrete multitone transmission", *IEEE Global Telecommunications Conference*,pp 724-728, 1996.

[7] Z. Galil and N. Megiddo, "A Fast Selection Algorithm and the Problem of Optimal Distribution of Effort", *Journal of the ACM*, pp 58-64, Vol 41, 1979.

[8] D. Hughes-Hartogs, "Ensemble Modem Structure for Imperfect Transmission Media", US Patent No.4679227 (July1987), 4731816 (March 1988), 4833706 (May1989).

[9] N. Katoh, T. Ibaraki and H. Mine, "A polynomial time algorithm for the resource allocation problem with a convex objective function", *Journal of Operational Research Society*, pp 449-455, Vol 30, 1979.

[10] B. S. Krongold, K. Ramchandran and D. L. Jones, "An efficient algorithm for optimal margin maximization in multicarrier communication systems", *IEEE Global Telecommunications Conference*, pp 899-903, 1999.

[11] Y.-P. Lin and S.-M. Phoong, "Perfect discrete multitone modulation with optimal transceivers", *IEEE Transactions on Signal Processing*, pp 1702-1711, June 2000.

[12] A. Pandharipande and S. Dasgupta, "Optimal transceivers for DMT based multiuser communication", *IEEE International Conference on Acoustics, Speech, and Signal Processing*, pp 2369 -2372, 2001. Also *IEEE Transactions on Communications*, accepted for publication.

[13] Toshihide Ibaraki and Naoki Katoh, *Resource Allocation Problems: algorithmic approaches*, MIT press, Cambridge, Massachusetts, 1988.